# Recombinant Expression, Purification and Characterization of Human Hyaluronidases

Dissertation
zur Erlangung des Doktorgrades der Naturwissenschaften (Dr. rer. nat.)
der Naturwissenschaftlichen Fakultät IV – Chemie und Pharmazie –
der Universität Regensburg


vorgelegt von
**Edith Hofinger**
aus Regenstauf

2007

Die vorliegende Arbeit entstand in der Zeit von April 2003 bis März 2007 unter der Leitung von Herrn Prof. Dr. A. Buschauer und Herrn Prof. Dr. G. Bernhardt am Institut für Pharmazie der Naturwissenschaftlichen Fakultät IV – Chemie und Pharmazie – der Universität Regensburg.

Das Promotionsgesuch wurde eingereicht im März 2007.

Tag der mündlichen Prüfung: 30. März 2007

| | | |
|---|---|---|
| Prüfungsausschuss: | Prof. Dr. S. Elz | (Vorsitzender) |
| | Prof. Dr. A. Buschauer | (Erstgutachter) |
| | Prof. Dr. G. Bernhardt | (Zweitgutachter) |
| | Prof. Dr. R. Gschwind | (Prüfer) |

“It doesn't matter if you fall down as long as you pick something up from the floor when you get up.”

*Efraim Racker*

# Danksagung

An dieser Stelle möchte ich mich bedanken bei:

Herrn Prof. Dr. A. Buschauer für die Möglichkeit an diesem interessanten Projekt arbeiten zu dürfen sowie für seine wissenschaftlichen Anregungen und seine konstruktive Kritik bei der Durchsicht dieser Arbeit.

Herrn Prof. Dr. G. Bernhardt für seine wissenschaftliche Anleitung, seine stetige Unterstützung beim Lösen experimenteller Probleme, sein Interesse am Fortgang der Experimente und für die kritische Durchsicht dieser Arbeit.

Herrn Prof. Dr. Rudolph (Institut für Biotechnologie, Martin-Luther Universität Halle-Wittenberg) für die Bereitstellung der Top10 und BL21(DE3)*RIL* Bakterien und des pET15b Vektors, für viele fachlichen Ratschläge sowie für die Möglichkeit im August/September 2004 in seiner Arbeitsgruppe Proteinfaltungsversuche durchzuführen.

Herrn Prof. Dr. M. Stubbs und Frau B. Epler (Institut für Biotechnologie, Martin-Luther Universität Halle-Wittenberg) für die Durchführung der Kristallisationsexperimente.

Herrn Dr. habil. H. Lilie (Institut für Biotechnologie, Martin-Luther Universität Halle-Wittenberg) für die Messung und Auswertung der analytischen Ultrazentrifugation und der CD-Spektren.

Frau Prof. Dr. Männel und Frau V. Runza (Lehrstuhl für Immunologie, Medizinische Fakultät, Universität Regensburg) für die Bereitstellung der DS-2 Zellen, des pCoHygro Vektors und des pMT/BiP/V5-HisA Vektors.

Herrn Dr. J. Oschmann für seine engagierte Betreuung während der Fermentation und der Faltungsexperimente am Institut für Biotechnologie, Martin-Luther Universität Halle-Wittenberg.

Frau S. Bollwein für die zuverlässige Durchführung der CE-Analytik.

Herrn Dr. H.-J. Wittmann für die Entwicklung der Programme zur Berechnung der Fragmentverteilungen.

den Mitarbeitern der analytischen Abteilung der Fakultät für die Aufnahme von ESI-Massenspektren.

der Arbeitsgruppe von Herrn Prof. R. Deutzmann (Fakultät für Biochemie, Genetik und Mikrobiologie, Universität Regensburg) für die N-terminale Peptidsequenzierung.

Herrn M. Jedrzejas für die Bereitstellung der pdb-Datei der Modellstruktur des human Hyal-1.

Frau M. Luginger und Frau S. Heinrich für die Hilfe bei allen organisatorischen Fragen.

Peter Richthammer für seine stets gutgelaunte Unterstützung bei technischen Problemen aller Art.

Frau Dr.  J. Hoechstetter und Herrn Dr. A. Botzki für die Einführung in das Hyaluronidase-Thema.

meinen studentischen Hilfskräften Sabine Weitensteiner, Christian Muhr und Erika Martina für ihre engagierte Mitarbeit im Labor.

meinen Laborkollegen Christine Müller, Lydia Schneider und Erich Schneider für ihre Hilfsbereitschaft und die heitere Atmosphäre im Labor.

allen Mitgliedern des Lehrstuhls für ein hervorragendes Arbeitsklima.

meinen Kollegen und Freunden Manuela Menke, Hendrik Preuss, Ralf Ziemek, Stephan Braun, Martin Spickenreither, Christian Horn, Christine Müller und Patrick Igel für viele anregende Diskussionen, aber auch für eine unterhaltsame und fröhliche Zeit in Regensburg.

dem Graduiertenkolleg 760 der DFG für die finanzielle und wissenschaftliche Förderung.

allen meinen Freunden und meiner Familie, auf deren Unterstützung ich mich jederzeit verlassen konnte.

# Contents

# Chapter 1

# Introduction

## 1.1. Hyaluronic acid

### *1.1.1. Structure and properties*

Hyaluronic acid (HA), also known as hyaluronan or hyaluronate, is a high molecular weight polysaccharide of the extracellular matrix. Commonly, hyaluronan is known as a lubricant responsible for the viscoelastic properties of tissue fluids and as a stabilizing and hydrating component of soft connective tissue. The term hyaluronic acid originates from the material used for the first isolation of hyaluronic acid by Meyer and Palmer (Meyer and Palmer 1934), namely the vitreous humor (hyaloid) of the eyes, and uronic acid as a constituent.

The chemical structure of hyaluronic acid is simple: a linear, negatively charged, unsulfated polymer composed of repeating disaccharide units linked by β-1,4 glycosidic bonds. Each disaccharide unit consists of D-glucuronic acid (GlcUAc) and N-acetyl-D-glucosamine (GlcNAc) connected by a β-1,3 glycosidic bond (Weissmann and Meyer 1954) **(Fig. 1.1)**.

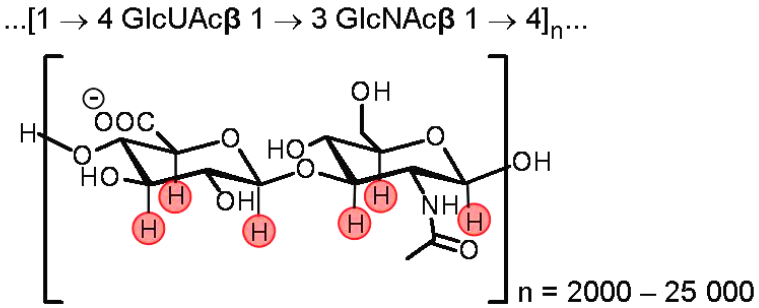


**Fig. 1.1** Hyaluronic acid is built of alternating units of D-glucuronic acid (GlcUAc) and N-acetyl-D-glucosamine (GlcNAc). Axial H-atoms, marked in red, contribute to the hydrophobic patches in the polysaccharide. (Modified from Hascall and Laurent 1997).

The polymer comprises, depending on the source, 2,000 – 25,000 disaccharide units, which corresponds to a molecular mass of $10^6$ – $10^7$ Da and a length of 2 – 25 µm. The carboxyl groups of the glucuronic acid ($pK_a$ = 3 – 4) (Hascall and Laurent 1997) cause the high negative charge of the polymer under physiological conditions.

Hyaluronic acid is a member of the family of glycosaminoglycans (GAGs) along with chondroitin-, keratan- and dermatane sulfate, heparin and heparin sulfate. These linear polysaccharides are generally composed of repeating disaccharide units of an uronic acid, D-glucuronic acid (GlcUAc) or L-iduronic acid (IdoAc), and an amino sugar, either N-acetyl-D-glucosamine (GlcNAc) or N-acetyl-D-galactosamine (GalNAc). Hyaluronic acid is an exception insofar as it is the only GAG, which is not covalently modified during its synthesis, especially not sulfated. Furthermore, in contrast to the other GAGs HA is not synthesized as a proteoglycan, i.e. covalently linked to a core protein, but is transferred during its synthesis directly through the plasma membrane into the extracellular space (Taylor and Gallo 2006).

Although the structure of hyaluronan is rather simple, the specific arrangement of the functional groups within the macro-molecule accounts for its unusual properties. In solution HA adopts an extended, hydrogen-bonded structure with a twist of 180° between each of the disaccharide units (Scott 1998) (**Fig. 1.2.a**). This tape-like, two-fold helix exhibits extensive hydrophobic patches due to the accumulation of axial H-atoms (**Fig. 1.1**) on alternating sides of the helix extending over almost three carbohydrate units.

In solution the hydrophobic interactions and H-bonds that can form between HA chains are counteracted by electrostatic repulsion of the carboxyl groups. Nuclear magnetic resonance and rotary shadowing electron-microscopy revealed honeycomb-like meshworks with neighboring HA chains arranged in an antiparallel fashion in very dilute solutions (1 µg/mL) (Scott 1998, Scott and Heatley 2002). However, the interactions responsible for aggregation are under physiological conditions insufficient for the formation of a specific tertiary structure. Moreover, hyaluronan is believed to be organized in a porous, dynamic network, resembling an expanded random coil with reversible formation and breakdown of tertiary structures (Sheehan and Almond 2001).

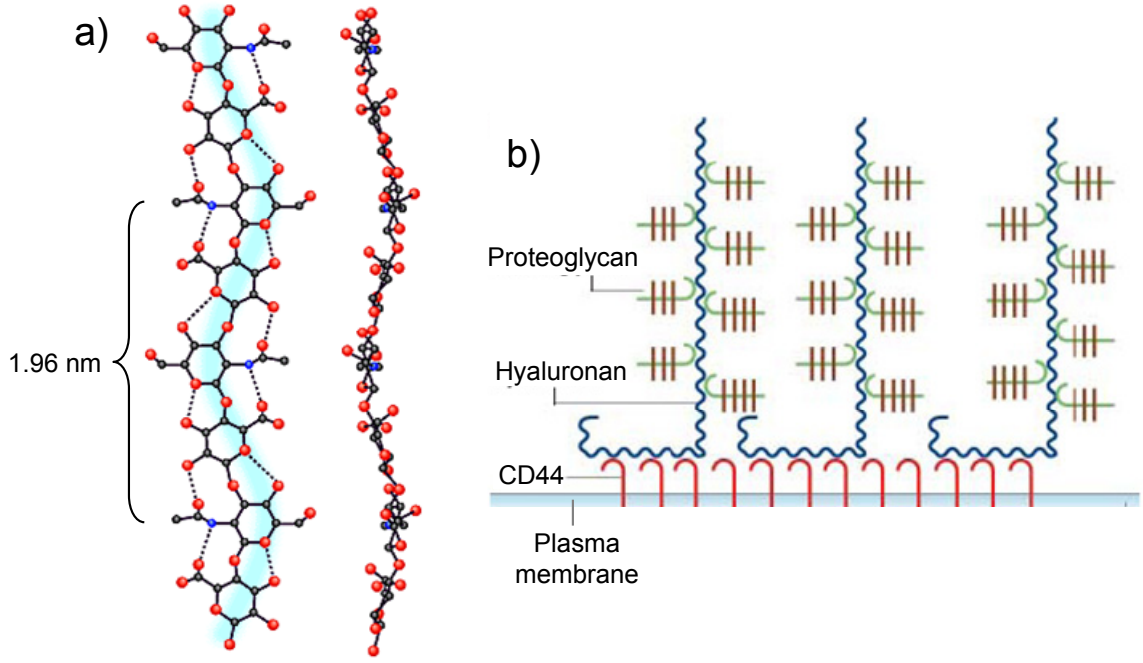


**Fig. 1.2** a) Models of the extended, two-fold hyaluronan helix with hydrogen bonds (dotted lines) between the neighboring carbohydrate units. The models are shown at right angles to each other. (Modified from Scott 1998). b) Representation of HA attached to the cell membrane by the hyaluronan receptor CD44. The repulsion of the negatively charged proteoglycans connected to the HA chains supports the extended structure of HA. (Modified from Toole 2004).

This dynamic meshwork provides the basis for the viscoelastic and hydrating properties of hyaluronan. Between the HA chains a huge amount of water can be trapped, which can be withdrawn upon application of an external pressure causing the resilience and malleability of substances like synovial joint fluids (Toole 2004). Dependent on the hydrodynamic volume molecules can move through the pores formed by the HA network, thus forming a diffusion barrier for some molecules. The constant re-organization of HA chains facilitates cell migration and tissue remodelling due to the creation of highly hydrated zones separating the cells from each other (Toole 2001).

In the extracellular matrix the HA chains are non-covalently connected to multiple proteoglycans, which repel each other due to their high negative charge and thereby facilitate the extended structure of the HA chain. The interaction between hyaluronan and the proteoglycans is fostered by the link protein (Hardingham 1998). Additionally, hyaluronan can be tethered to the cell surface through receptors such as CD44 (Knudson et al. 1993) or through retention to the hyaluronate synthases located in the plasma membrane (Heldin and Pertoft 1993) (**Fig. 1.2.b**).

### *1.1.2. Occurrence and metabolism*

Hyaluronan is found in the extracellular matrix of all vertebrates and in the capsule of some bacteria such as *Streptococcus* and *Pasteurella*. Extraordinarily high concentrations of hyaluronan occur in rooster comb (7.5 mg/mL), in the synovial fluid (3 – 4 mg/mL), in umbilical cord (3 mg/mL), in the vitreous humor of the eye (0.2 mg/mL), and in the skin (0.5 mg/mL. Both, the dermis and the epidermis of the skin, accommodate the largest amount of hyaluronan in the body (7 – 8 g, referring to ca. 50 % of the total HA in the body) (Prehm 2002). In cartilage hyaluronan binds a large number of chondroitin sulfate proteoglycans called aggrecans, and thus forms huge aggregates of several hundred million Dalton (Hardingham 1998).

Hyaluronan is a rapidly metabolized macromolecule with one third of the whole hyaluronan present in the human body (ca. 15 g) being turned-over every day (Stern 2004). The synthesis of HA differs, as mentioned above, distinctly from the synthesis of other GAGs: one of the three multipass transmembrane proteins, HA synthase-1, -2 or -3, extrudes the nascent HA chain from the reducing end through the plasma membrane into the extracellular space (Prehm 1984, Prehm 2006). In contrast to that, other GAGs are synthesized in the Golgi body from the non-reducing end, and are covalently linked to a protein.
This mechanism of HA synthesis applies to vertebrates and *Streptococci*, the HA polymerization in *Pasteurella*, however, proceeds by a different mechanism (Prehm 2002). The synthesis of the HA chain on the surface of the intracellular membrane enables the unrestricted extension of the polymer reaching up to 25,000 disaccharide units, a size impossible to be synthesized intracellularly (Stern 2004).

The high molecular weight HA chains are released from the synthases by dissociation or radical degradation (Prehm 1990), but stay in contact with the plasma membrane through interactions with cell surface receptors such as CD44 (Knudson et al. 1993) and, possibly, the membrane-anchored hyaluronidase Hyal-2 (**Fig. 1.2.b**). The concentration of HA in a tissue is maintained constant by balancing of the synthesis by catabolism. As proposed by Csoka et al. (Csoka et al. 2001) high molecular weight HA might be cleaved by the hyaluronidase Hyal-2 on the cell surface into fragments of ca. 20 kDa and internalized while still bound to Hyal-2. The endocytotic vesicles then fuse with lysosomes providing the optimum pH conditions for the further degradation of the HA fragments through the action of the hyaluronidase Hyal-1. In addition to the hyaluronidases, two exoglycosidases, β-glucuronidase and β-N-

acetylglucosaminidase, contribute to the catabolism of HA in lysosomes. Stern (Stern 2003) suggested the existence of a specialized mini organelle for the location of the HA metabolism, the so called hyaluronasome, similar to the glycogen granule.

### *1.1.3. Physiological and pathophysiological role of hyaluronan*

The functions of hyaluronan directly originating from its physicochemical properties are well-known: it acts as a lubricant and shock absorber, regulates water balance and osmotic pressure and occurs as a structure forming molecule in the vitreous humor of the eye, in Wharton's jelly and in joint fluids. Besides these functions, that are long known, hyaluronic acid was found to interact with other GAGs (Turley and Roth 1980) and a multitude of specific HA-binding proteins, referred to as hyaladherins (Day 2001). The hyaladherins can be divided according to their function into three groups: the hyaluronan-binding proteins responsible for the organization of the extracellular matrix, like the link protein and aggrecan (Hardingham 1998), cell-surface receptors of HA with CD44 (Knudson and Knudson 1999) and RHAMM (Turley and Harrison 1999) being the best known ones, and intracellular hyaladherins. Since HA has also been detected intracellularly in proliferating cells (Evanko and Wight 1999) these HA-binding proteins within the cell, e.g. the intracellular variant of RHAMM, P-32, Cdc37 and IHABP4, gain importance (Evanko and Wight 2001).

The diversity of interactions of hyaluronan is reflected in the great range of processes influenced by the polysaccharide. These processes are all involved in cell motility, cell migration and changes in cell-cell- and cell-matrix-adhesion. HA participates in many fundamental processes such as embryological development and morphogenesis (Toole 2001), wound healing (Longaker et al. 1991), inflammation (Weigel et al. 1986, Taylor and Gallo 2006), angiogenesis (Liu et al. 1996) and tumor progression (Paiva et al. 2005, Boregowda et al. 2006).

The size of the hyaluronan molecules plays a crucial role in the biological activity of the polysaccharide (**Fig. 1.3**). High molecular weight HA chains can provide hydrated pathways for the invasion and migration of cells due to their space-filling properties (Toole 2001). A hyaluronan-rich pericellular zone separates cells from each other and from matrix components, and protects cells from lymphocytes and viruses (Laurent and Fraser 1992). Thus, high molecular weight hyaluronan with a molecular weight of more than 500 kDa was

described as anti-inflammatory (Wang et al. 2006), immunosuppressive (Delmage et al. 1986) and anti-angiogenic (Feinberg and Beebe 1983).

HA chains with a molecular weight of 10 – 500 kDa, referred to as low molecular weight hyaluronan, exhibit effects directly opposing the functions of high molecular weight HA (**Fig. 1.3**) (Asari 2005). These low molecular weight HA fragments are angiogenic (West et al. 1985) and stimulate inflammation, cellular infiltration and extracellular matrix degradation by induction of cytokines (El Maradny et al. 1997, Noble 2002) and chemokines (McKee et al. 1996).

While most of the functions described for low molecular weight HA were also observed with HA fragments smaller than 25 disaccharide units, these oligosaccharides show additional activities, e.g. the activation of Hsp72 and suppression of cell death under stress conditions (Xu et al. 2002). These effects are presumably related to size-dependent binding to specific receptor molecules.

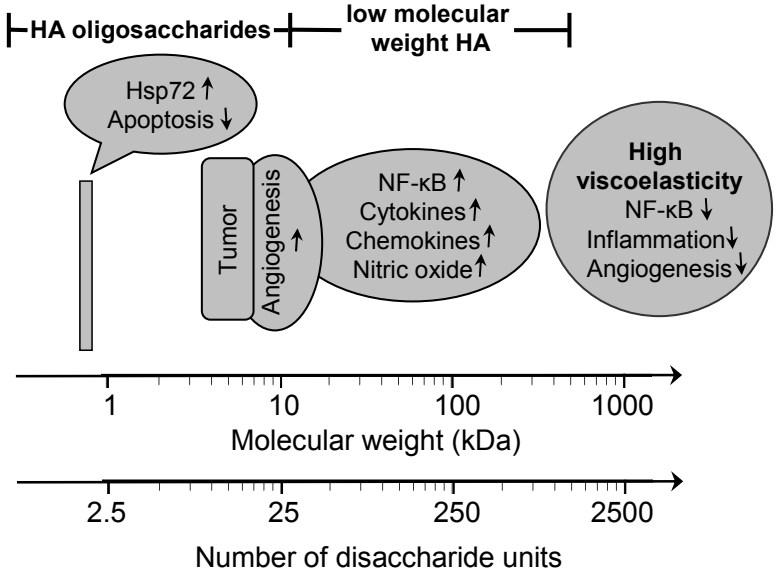


**Fig. 1.3** Hyaluronan changes its biological activity depending on its size. (Modified from Asari 2005).

## 1.2. The six human hyaluronidase subtypes

According to their catalytic mechanism Meyer classified three major families of hyaluronidases (Meyer 1971). The hyaluronidases of the first group, endo-β-N-acetylglucosaminidases, including vertebrate hyaluronidases, catalyze the hydrolysis of the β-1,4 glycosidic bond. The second group, termed β-eliminases or lyases, include bacterial hyaluronidases and catabolize HA in a β-elimination of the β-1,4 glycosidic bond, thereby introducing an unsaturated bond in position 4 of glucuronic acid. The third group of

hyaluronidases comprises endo-β-glucuronidases found in parasites like leeches and in some crustaceans.

As this work focuses on the production and characterization of human hyaluronidases the following section will provide an overview of the characteristic features of the vertebrate-type hyaluronidases with special focus on the human hyaluronidases.

### *1.2.1. Properties of mammalian hyaluronidases*

Mammalian hyaluronidases (E.C. 3.2.1.35) belong, according to the Carbohydrate Active Enzyme Database (CAZY) (Coutinho and Henrissat 1999), to the glycoside hydrolase family 56. They cleave the β-1,4 glycosidic bond of hyaluronic acid by hydrolysis in a non-processive endolytic process producing tetrasaccharides as the major final reaction products (Stern and Jedrzejas 2006). The process of degradation differs essentially between mammalian hyaluronidases and bacterial hyaluronate lyases. Lyases degrade HA after an initial endolytic cleavage step in a processive, exolytic fashion, thereby separating only one disaccharide unit from the reducing end of the HA chain at a time (Li et al. 2000, Li and Jedrzejas 2001). The degradation of HA by mammalian hyaluronidases, however, occurs in a random fashion with each endolytic cleavage step being accompanied by a new binding event at a random position within the HA chain (Stern and Jedrzejas 2006).

In addition to the degradation of HA, vertebrate-like hyaluronidases are capable of catabolizing chondroitin, chondroitin-4-sulfate (ChS A), chondroitin-6-sulfate (ChS C) and dermatan sulfate (ChS B) as alternative substrates (Meyer and Rapport 1952). The conversion of these alternative substrates, however, is much slower than the degradation of HA.

Furthermore, mammalian hyaluronidases exhibit not only hydrolytic activity but also transglycosidase activity (Weissmann 1955). During transglycosylation a HA fragment of at least one disaccharide unit is transferred from the non-reducing end of one oligosaccharide chain to the non-reducing end of another (Weissmann 1955, Highsmith et al. 1975, Takagaki et al. 1994) (**Fig. 1.4**).

Using bovine testicular hyaluronidase preparations transglycosylation was observed to be favored at neutral pH values and low ionic strength (Gorham et al. 1975, Saitoh et al. 1995). The transglycosylation activity provides the potential ability to cross-link different GAG chains as proven *in vitro* by Saitoh et al. (Saitoh et al. 1995).

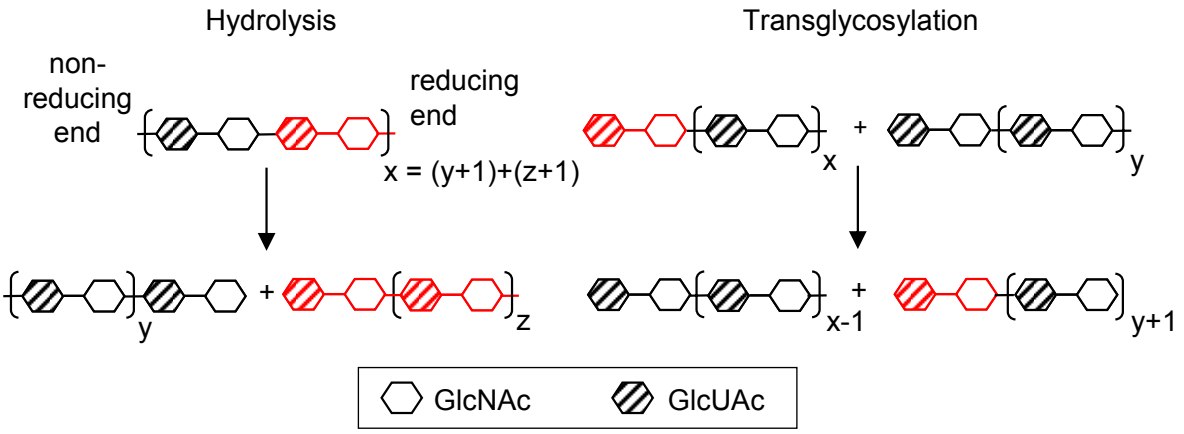


**Fig. 1.4** Schematic presentation of the reactions catalyzed by mammalian hyaluronidases. Glycosidic residues are represented with symbols as indicated in the legend. The oligosaccharide chains are shown in the direction from the non-reducing terminus (left) to the reducing terminus (right). Transglycosylation is shown for one disaccharide unit marked in red, but can also occur with larger fragments.

### *1.2.2. Structural features and catalytic mechanism of human hyaluronidases*

As no crystal structure of a mammalian hyaluronidase is available yet, information about the catalytic mechanism and the structure of human hyaluronidases can merely be transferred from the crystal structures of vertebrate-like hyaluronidases, being the bee venom hyaluronidase (1FCQ.pdb) (Markovic-Housley et al. 2000) and the wasp venom hyaluronidase (2ATM.pdb) (Skov et al. 2006).

Bee venom hyaluronidase (BVH) and wasp venom hyaluronidase both consist of a single domain with a $(\beta/\alpha)_7$ topology similar to the classical $(\beta/\alpha)_8$ TIM-barrel found in many glycosyl hydrolases (Henrissat et al. 1995). The barrel formed by seven β-sheets is surrounded by seven α-helices and contains a large substrate binding groove (ca. 30 Å x 10 Å) perpendicular to the barrel axis (Markovic-Housley et al. 2000). A hyaluronan hexasaccharide, presumably the minimum substrate for BVH, fits into the dimensions of the binding cleft as concluded from the structure of BVH co-crystallized with a HA tetrasaccharide (1FCV.pdb).

Based on the gene sequence six human hyaluronidase subtypes were identified with a sequence identity of ca. 40 %: Hyal-1, Hyal-2, Hyal-3, Hyal-4, PH-20 and a pseudogene, Phyal1 (Csoka et al. 2001). In contrast to BVH the human hyaluronidases contain at least one additional domain of 120 – 150 amino acids C-terminally to the catalytic domain (**Fig. 1.5**). Within the hyaluronidase catalytic domain the sequence identity between the human hyaluronidases and BVH averages 30 %.

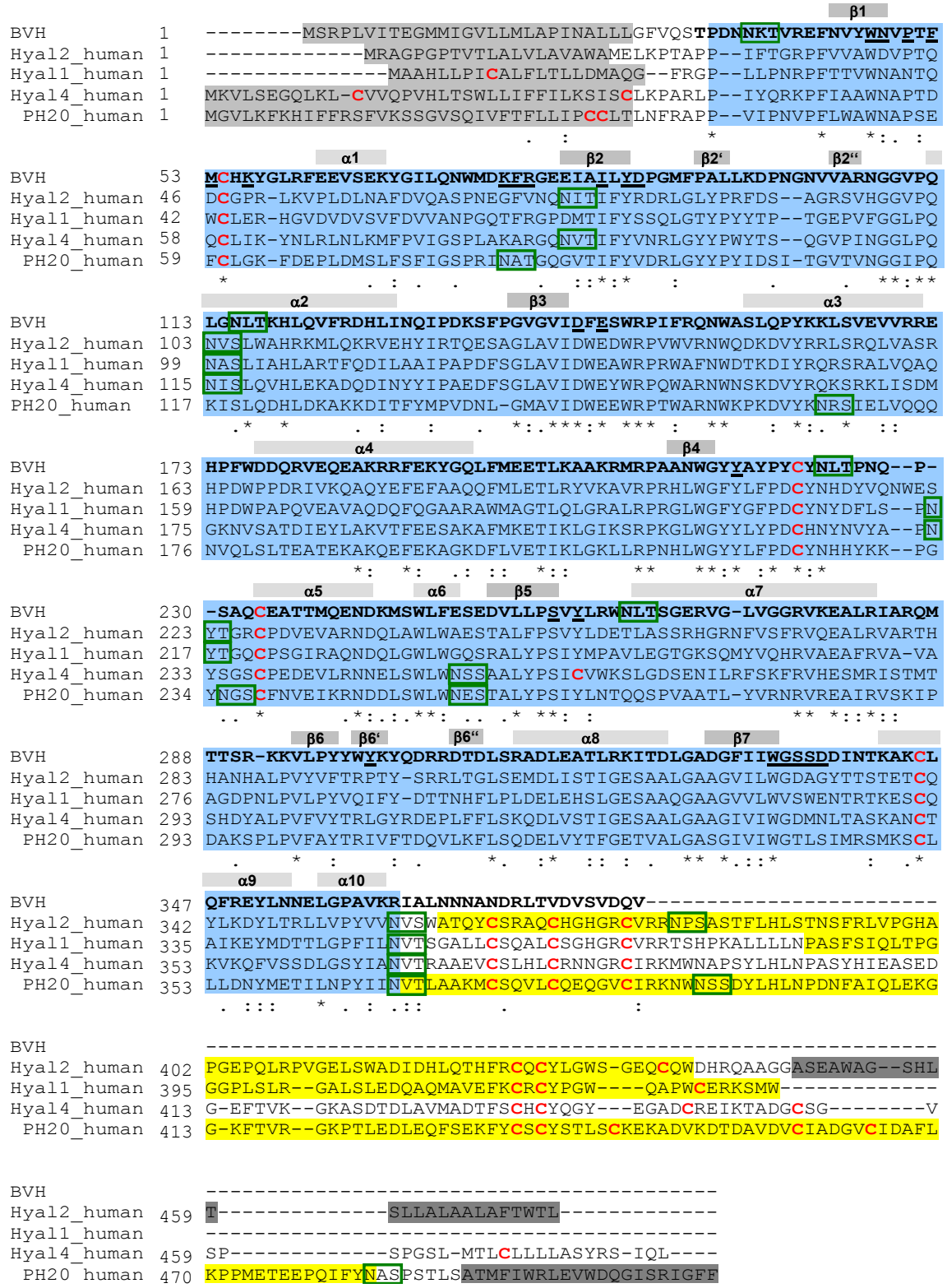


**Fig. 1.5** Sequence alignment of BVH (Swiss-Prot code: Q08169) with the human hyaluronidases Hyal-1 (Q12794), Hyal-2 (Q12891), Hyal-4 (Q9UL99) and PH-20 (Q8TC30). Domains are marked according to their potential function: signal peptide (light grey), catalytic domain (blue), C-terminal domain with various function (yellow) and GPI-anchoring signal peptides (dark grey). C residues are marked in red, potential N-glycosylation sites with green boxes and the residues of the active site of the BVH are underlined (Botzki 2004). The secondary structural elements indicated above each line were inserted according to the crystal structure of BVH (1FCQ.pdb, the sequence crystallized is printed bold). The alignment was generated with ClustalW and the symbols ., : and * refer to the similarity code used by the alignment program (Chenna et al. 2003).

The occurrence of few gaps in the sequence alignment as well as the conservation of residues in the active site and of four cysteine residues linked by disulfide bridges in BVH indicate a similar structural organization of the enzymes (**Fig. 1.5**). Fold recognition studies revealed a significantly higher structural similarity than expected from the amino acid sequence enabling the construction of 3D model structures of the human hyaluronidases (Jedrzejas and Stern 2005) and bovine PH-20, which exhibits a sequence identity of 65 % to human PH-20 (Botzki et al. 2004). The overall model structures of the human hyaluronidases resemble each other closely with the typical barrel-shaped catalytic domain exhibiting a broad binding groove for the substrate and a linker region connecting the catalytic domain to the C-terminal domain (Jedrzejas and Stern 2005).

In all hyaluronidases the binding groove is lined by electropositive and hydrophobic residues favoring the binding of substrate molecules with electronegative and hydrophobic patches such as HA and ChS. Model structures of the C-terminal domains were predicted by an *ab initio* approach due to missing similarity to any of the known 3D structures and are therefore rather unreliable. A common feature found in all human hyaluronidase models is the formation of a separate C-terminal domain connected to the catalytic domain by a flexible linker (Jedrzejas and Stern 2005). The C-terminal domains, which exhibit - except for the presence of an extraordinarily high amount of C residues - low similarity to each other, are speculated to be involved in either facilitating the HA binding, positioning of the substrate or in disruption of non-covalent interactions of substrate chains (Jedrzejas and Stern 2005, Stern and Jedrzejas 2006).

Although the structure of the human hyaluronidases remains speculative, the catalytic mechanism for the degradation of hyaluronic acid is very likely to follow the double-displacement mechanism derived from the X-ray structure of BVH co-crystallized with a HA tetrasaccharides (1FCV.pdb) (Markovic-Housley et al. 2000).

The active site is located approximately in the middle of the binding groove with E145 (BVH numbering in **Fig. 1.5**) being the only residue that participates in the catalytic mechanism. The surrounding amino acids D143, Y216, Y259 and W333 (BVH numbering in **Fig. 1.5**) that are highly conserved in the human hyaluronidases contribute to the positioning of the substrate moiety (Markovic-Housley et al. 2000, Jedrzejas and Stern 2005). Intriguingly, Y259, which is otherwise strictly conserved in the human hyaluronidases, is replaced in Hyal-4 by C163 indicating a specialized function of Hyal-4 (**Fig. 1.5**) (Jedrzejas and Stern 2005, Stern and Jedrzejas 2006).

Generally, glycosidases utilize two acid amino acids for cleavage of the glycosidic bond, one acting as an acid/base catalyst and one as a nucleophile. The mechanism of the hyaluronidases is an exception insofar as only a single carboxylate of the enzyme acts as an acid/base catalyst and the substrate itself acts as the nucleophile (Markovic-Housley and Schirmer 2002).

The substrate-assisted mechanism shown in **Fig. 1.6** is initiated by distortion of the GlcNAc residue in position -1* to a $^{1,4}$B-boat conformation (A). This positioning enables the nucleophilic attack of the N-acetyl group on the anomeric C-atom and the formation of the oxazolinium ion intermediate (B). Simultaneously, E145 donates its proton to the sugar chain in position +1 resulting in the release of the first reaction product. The covalent intermediate (B) is subsequently hydrolyzed by exchange of the reaction product in position +1 by a water molecule. The hydrolysis thus results in retention of the configuration of the anomeric C-atom at the reducing end of GlcNAc (Markovic-Housley and Schirmer 2002).

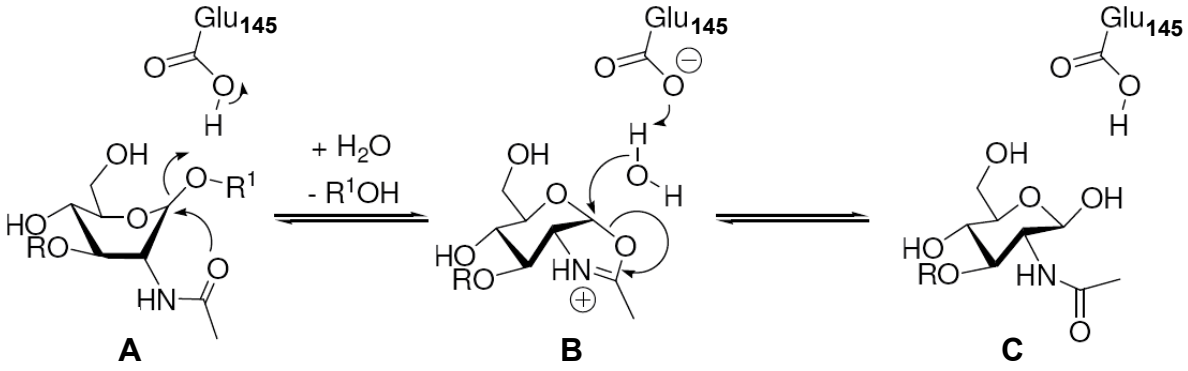


**Fig. 1.6** Double-displacement mechanism of bee venom hyaluronidase. The GlcNAc residue of the HA disaccharide bound in position -1 (Davies et al. 1997) forms a boat conformation (A), Glu145 acts as a acid/base catalyst and the carbonyl group of the N-acetyl-moiety acts as a nucleophile. The intermediate is an oxazolinium ion (B), that is subsequently hydrolyzed to form the reaction product (C). (Modified from Markovic-Housley and Schirmer 2002).

### *1.2.3. Subtype specific differences*

The sequence similarity between the six subtypes of human hyaluronidases varies between 33 and 42 % (Stern and Jedrzejas 2006). The genes coding for the hyaluronidase subtypes are clustered on two different chromosomes: *hyal-1*, *-2* and *-3* are clustered on chromosome 3p21.3, *hyal-4*, *ph-20* and *phyal1* on chromosome 7q31.3 (Csoka et al. 2001).

PH-20, also termed SPAM1 (sperm adhesion molecule 1), was the first hyaluronidase identified by its function as a "spreading factor" in testicular extracts (Duran-Reynalds 1929).

* According to the convention for labelling of an enzymatic substrate the position at the non-reducing end of the sugar chain is numbered with –n and at the reducing end with +n. Enzymatic cleavage occurs between -1 and +1 (Davies et al., 1997).

The major role of PH-20 is to facilitate penetration of the sperm through the HA-rich matrix of the oocyte. It thereby occurs as a multifunctional protein in a membrane-anchored and in a soluble isoform (Cherr et al. 2001) (cf. Chapter 6). Commercially available PH-20 preparations from bovine testes have been used for many years for experimental and therapeutic purposes, e.g. in orthopedia, ophthalmology and internal medicine (Baumgartner and Moritz 1988, Spruss et al. 1995, Menzel and Farr 1998, Muckenschnabel et al. 1998).

Hyal-1, which is alternatively named LUCA-1 (lung cancer protein 1), and Hyal-2, termed LUCA-2, represent the two major hyaluronidases in somatic tissue. Hyal-1 is an acid-active, soluble haluronidase found in lysosomes, in plasma and in urine with a high specific enzymatic activity (cf. Chapter 5). In contrast to Hyal-1, the catalytic activity of Hyal-2, a GPI-anchored hyaluronidase, is discussed controversially ranging from no hyaluronidase activity at all to the degradation of high molecular weight HA to fragments of 20 kDa and smaller fragments at various pH values. Yet, hints accumulate that the main function of Hyal-2 might not be the degradation of hyaluronic acid (cf. Chapter 7).

Hyal-3 was found to be expressed ubiquitously with extraordinarily high expression patterns detected in mammalian testis and bone marrow (Stern and Csoka 2000). The stem-cell like state of these cell types indicates a role of Hyal-3 in embryogenesis and stem-cell regulation (Csoka et al. 2001). The catalytic properties of Hyal-3 are currently unknown (Stern and Jedrzejas 2006).

Hyal-4 is probably a GPI-anchored protein like PH-20 and Hyal-2 and is exclusively expressed in muscle and placenta. It was proposed to be the first vertebrate chondroitinase with no activity against HA (Csoka et al. 2001). However, experimental evidence is still lacking, and the only hint for a specialized function of Hyal-4 is the presence of a C residue (C163) in a position close to the active site and strictly conserved in other hyaluronidases (cf. **Fig. 1.5**).

The pseudogene, *phyal-1*, is transcribed, yet the mRNA contains an internal stop codon resulting in preliminary abortion of translation. However, translation of *phyal1* into an active enzyme might occur in other species (Stern 2003).

Furthermore, MGEA5, a cytoplasmic β-N-acetylglucosaminidase, was described to exhibit an additional hyaluronidase activity (Comtesse et al. 2001). However, no sequence similarity could be found between the six human hyaluronidases and MGEA5.

### *1.2.4. Relevance of hyaluronidases in the development of cancer*

There is no doubt about the involvement of both hyaluronan and the catabolizing enzymes, the hyaluronidases, in tumor development and progression. However, data about the effects of hyaluronidases on cancer growth, progression, spread and outcome are controversial.

Hyal-1 and Hyal-2 can in some cases like in tobacco-related lung cancers and cancers of the upper airways function as tumor suppressor genes (Frost et al. 2000, Chang 2002), but were in other types of tumors described as oncogenes (Novak et al. 1999, Lokeshwar et al. 2001, Lokeshwar et al. 2005). Hyal-2 is assumed to be responsible for the strong oncogenic potential of Jaagsiekte sheep retrovirus as it acts as the cell surface receptor for the virus (Rai et al. 2001).

PH-20 was expressed in a series of malignant tumors, e.g. breast, prostate and laryngeal cancers and also in cell lines derived from melanomas, glioblastomas and colon carcinomas (for review see Stern 2005).

Abnormalities in the deposition of HA have been found in the stroma surrounding tumors indicating an aberrant HA metabolism. However, the contribution of stromal HA to the tumor mass varies significantly dependent on the kind of tumor. In the course of tumor progression the HA metabolism is also very likely to change dependent on the different stages of initiation, growth and metastasis (Stern 2005). At the initial stage of tumor formation high molecular weight HA can provide hydrated pathways for cell migration and diffusion of nutrients. If supply by diffusion becomes insufficient low molecular weight HA fragments (**Fig. 1.3**) produced through the action of Hyal-2 could promote angiogenesis (West et al. 1985). This phenomenon of the angiogenic switch (Folkman 2002) could account for some of the anomalies described in literature.

The situation is severely complicated by the fact that HA is under normal conditions turned-over quickly and abnormalities in the concentration of HA can reflect aberrations both in the anabolic and in the catabolic pathways. Furthermore, the hyaluronidase activity is controlled in the tissue by biological inhibitors that are hardly characterized (Mio and Stern 2002).

In addition to the effects mediated by the degradation products of HA, GPI-anchored hyaluronidases (PH-20, Hyal-2 and, presumably Hyal-4) themselves can participate in signal transduction events. As shown for PH-20 the interaction between HA and a hyaluronidase can increase intracellular $Ca^{2+}$ levels resulting in an amplification of the zona-pellucida induced acrosome reaction (Sabeur et al. 1998, Cherr et al. 2001). The interaction of signaling molecules like Src-family tyrosine kinases with GPI-anchored proteins appears to take place in glycosphingolipid-cholesterol microdomains, so called "lipid rafts" (Kasahara and Sania 2000). Within these membrane domains aggregation and cross-linking of GPI-anchored proteins, e.g. upon binding to hyaluronic acid, are supposed to trigger intracellular signaling events (Cherr et al. 2001).
Although rather little is known about the oncogenic potential of PH-20, Hyal-2 was shown to mediate transformation of fibroblasts by virus-induced disturbance of the interaction between Hyal-2 and RON receptor tyrosine kinase (Danilkovitch-Miagkova et al. 2003).

Many of the contradictory data accumulated during the last years could be resolved if the differential functions of the hyaluronidase subtypes and the interactive pathways of the HA catabolism were better understood.

## 1.3. References

Asari A. (2005). Novel functions of hyaluronan oligosaccharides. http://www.glycoforum.gr.jp/science/hyaluronan/HA12a/HA12aE.html

Baumgartner G., Moritz A. *Hyaluronidase: Anwendungen in der Onkologie.* Springer-Verlag. Wien, Berlin, Heidelberg. (1988).

Boregowda R., Appaiah H., Siddaiah M., Kumarswamy S., Sunila S., Thimmaiah K.N., Mortha K.K., Toole B., Banerjee S. (2006). Expression of hyaluronan in human tumor progression. *J. Carcinog.* **5**: 2-10.

Botzki A. (2004). Structure-based design of hyaluronidase inhibitors. *Doctoral thesis*. University of Regensburg. http://www.opus-bayern.de/uni-regensburg/volltexte/2004/378/

Botzki A., Rigden D.J., Braun S., Nukui M., Salmen S., Hoechstetter J., Bernhardt G., Dove S., Jedrzejas M.J., Buschauer A. (2004). L-Ascorbic Acid 6-Hexadecanoate, a Potent Hyaluronidase Inhibitor: X-ray structure and molecular modelling of enzyme-inhibitor complexes. *J. Biol. Chem.* **279**: 45990-45997.

Chang N.S. (2002). Transforming growth factor-beta1 blocks the enhancement of tumor necrosis factor cytotoxicity by hyaluronidase Hyal-2 in L929 fibroblasts. *BMC Cell Biol.* **3**: 8-17.

Chenna R., Sugawara H., Koike T., Lopez R., Gibson T.J., Higgins D.G., Thompson J.D. (2003). Multiple sequence alignment with the Clustal series of programs. *Nucleic Acids Res.* **31**: 3497-3500.

Cherr G.N., Yudin A.I., Overstreet J.W. (2001). The dual functions of GPI-anchored PH-20: hyaluronidase and intracellular signaling. *Matrix Biol.* **20**: 515-25.

Comtesse N., Maldener E., Meese E. (2001). Identification of a Nuclear Variant of MGEA5, a Cytoplasmic Hyaluronidase and a [beta]-N-Acetylglucosaminidase. *Biochem. Biophys. Res. Commun.* **283**: 634-640.

Coutinho P.M., Henrissat B. Carbohydrate-active enzymes: an integrated database approach. (http://www.cazy.org). *in: Recent Advances in Carbohydrate Bioengineering*. H.J. Gilbert, G. Davies, B. Henrissat and B. Svensson ed. The Royal Society of Chemistry. Cambridge. (1999): pp. 3 - 12.

Csoka A.B., Frost G.I., Stern R. (2001). The six hyaluronidase-like genes in the human and mouse genomes. *Matrix Biol.* **20**: 499-508.

Danilkovitch-Miagkova A., Duh F.M., Kuzmin I., Angeloni D., Liu S.L., Miller A.D., Lerman M.I. (2003). Hyaluronidase 2 negatively regulates RON receptor tyrosine kinase and mediates transformation of epithelial cells by jaagsiekte sheep retrovirus. *Proc. Natl. Acad. Sci. U. S. A.* **100**: 4580-4585.

Davies G.J., Wilson K.S., Henrissat B. (1997). Nomenclature of sugar-binding subsites in glycosyl hydrolases. *Biochem. J.* **321**: 557-559.

Day A.J. (2001). Understanding hyaluronan - protein interactions. http://www.glycoforum.gr.jp/science/hyaluronan/HA16/HA16E.html

Delmage J.M., Powars D.R., Jaynes P.K., Allerton S.E. (1986). The selective suppression of immunogenicity by hyaluronic acid. *Ann. Clin. Lab. Sci.* **16**: 303-310.

Duran-Reynalds F. (1929). The effects of extracts of certain organs from normal and immunized animals on the infecting power of vaccine virus. *J. Exp. Med.* **50**: 327-340.

El Maradny E., Kanayama N., Kobayashi H., Hossain B., Khatun S., Liping S., Kobayashi T., Terao T. (1997). The role of hyaluronic acid as a mediator and regulator of cervical ripening. *Hum. Reprod. Update* **12**: 1080-1088.

Evanko S.P., Wight T.N. (1999). Intracellular localization of hyaluronan in proliferating cells. *J. Histochem. Cytochem.* **47**: 1331-1341.

Evanko S.P., Wight T.N. (2001). Intracellular hyaluronan. http://www.glycoforum.gr.jp/science/hyaluronan/HA20/HA20E.html

Feinberg R.N., Beebe D.C. (1983). Hyaluronate in vasculogenesis. *Science* **220**: 1177-1179.

Folkman J. (2002). Role of angiogenesis in tumor growth and metastasis. *Semin. Oncol.* **29**: 15-18.

Frost G.I., Mohapatra G., Wong T.M., Csoka A.B., Gray J.W., Stern R. (2000). HYAL1LUCA-1, a candidate tumor suppressor gene on chromosome 3p21.3, is inactivated in head and neck squamous cell carcinomas by aberrant splicing of pre-mRNA. *Oncogene Res.* **19**: 870-877.

Gorham S.D., Olavesen A.H., Dodgson K.S. (1975). Effect of ionic strength and pH on the properties of purified bovine testicular hyaluronidase. *Connect. Tissue Res.* **3**: 17-25.

Hardingham T.E. (1998). Cartilage: aggrecan - link protein - hyaluronan aggregates. http://www.glycoforum.gr.jp/science/hyaluronan/HA05/HA05E.html

Hascall V.C., Laurent T.C. (1997). Hyaluronan: structure and physical properties. http://www.glycoforum.gr.jp/science/hyaluronan/HA01/HA01E.html

Heldin P., Pertoft H. (1993). Synthesis and Assembly of the Hyaluronan-Containing Coats around Normal Human Mesothelial Cells. *Exp. Cell Res.* **208**: 422-429.

Henrissat B., Callebaut I., Fabrega S., Lehn P., Mornon J.-P., Davies G. (1995). Conserved catalytic machinery and the prediction of a common fold for several families of glycosyl hydrolases. *Proc. Natl. Acad. Sci. U. S. A.* **92**: 7090-7094.

Highsmith S., Garvin J.H., Jr, Chipman D.M. (1975). Mechanism of action of bovine testicular hyaluronidase. Mapping of the active site. *J. Biol. Chem.* **250**: 7473-7480.

Jedrzejas M.J., Stern R. (2005). Structures of vertebrate hyaluronidases and their unique enzymatic mechanism of hydrolysis. *Proteins.* **61**: 227-238.

Kasahara K., Sania Y. (2000). Functional roles of glycosphingolipids in signal transduction via lipid rafts. *Glycoconj. J.* **17**: 153-162.

Knudson W., Bartnik E., Knudson C.B. (1993). Assembly of pericellular matrices by COS-7 cells transfected with CD44 lymphocyte-homing receptor genes. *Proc. Natl. Acad. Sci. U. S. A.* **90**: 4003-4007.

Knudson W., Knudson C.B. (1999). The hyaluronan receptor, CD44. http://www.glycoforum.gr.jp/science/hyaluronan/HA10/HA10E.html

Laurent T.C., Fraser J.R.E. (1992). Hyaluronan. *FASEB J.* **6**: 2397-2404.

Li S., Jedrzejas M.J. (2001). Hyaluronan binding and degradation by Streptococcus agalactiae hyaluronate lyase. *J. Biol. Chem.* **276**: 41407-41416.

Li S., Kelly S., Lamani E., Ferraroni M., Jedrzejas M. (2000). Structural basis of hyaluronan degradation by Streptococcus pneumoniae hyaluronate lyase. *EMBO J.* **19**: 1228-1240.

Liu D., Pearlman E., Diaconu E., Guo K., Mori H., Haqqi T., Markowitz S., Willson J., Sy M.S. (1996). Expression of hyaluronidase by tumor cells induces angiogenesis in vivo. *Proc. Natl. Acad. Sci. U. S. A.* **93**: 7832-7837.

Lokeshwar V.B., Cerwinka W.H., Lokeshwar B.L. (2005). HYAL1 Hyaluronidase: A Molecular Determinant of Bladder Tumor Growth and Invasion. *Cancer Res.* **65**: 2243-2250.

Lokeshwar V.B., Rubinowicz D., Schroeder G.L., Forgacs E., Minna J.D., Block N.L., Nadji M., Lokeshwar B.L. (2001). Stromal and epithelial expression of tumor markers hyaluronic acid and HYAL1 hyaluronidase in prostate cancer. *J. Biol. Chem.* **276**: 11922-11932.

Longaker M.T., Chiu E.S., Adzick N.S., Stern M., Harrison M.R., Stern R. (1991). Studies in fetal wound healing. V. A prolonged presence of hyaluronic acid characterizes fetal wound fluid. *Ann. Surg.* **213**: 292-296.

Markovic-Housley Z., Miglinerini G., Soldatova L., Rizkallah P., Müller U., Schirmer T. (2000). Crystal Structure of Hyaluronidase, a Major Allergen of Bee Venom. *Structure* **8**: 1025-1035.

Markovic-Housley Z., Schirmer T. Structural evidence for substrate assisted catalytic mechanism of bee venom hyaluronidase, a major allergen of bee venom. *in: Carbohydrate Bioengineering: Interdisciplinary Approaches.* T.T. Teeri, B. Svensson, H.J. Gilbert and T. Feizi ed. RCS. London. (2002). pp. 19-27.

McKee C.M., Penno M.B., Cowman M., Burdick M.D., Strieter R.M., Bao C., Noble P.W. (1996). Hyaluronan (HA) Fragments Induce Chemokine Gene Expression in Alveolar Macrophages. The Role of HA Size and CD44. *J. Clin. Invest.* **98**: 2403-2413.

Menzel E.J., Farr C. (1998). Hyaluronidase and its substrate hyaluronan: biochemistry, biological activities and therapeutic uses. *Cancer Lett.* **131**: 3-11.

Meyer K. Hyaluronidases. *in: The Enzymes.* P.D. Boyer ed. Academic Press. New York, London. (1971). **5**: pp. 307-320.

Meyer K., Palmer J.W. (1934). The polysaccharide of the vitreous humor. *J. Biol. Chem.* **107**: 629-634.

Meyer K., Rapport M.M. (1952). Hyaluronidases. *Adv. Enzymol. Relat. Areas Mol. Biol.* **13**: 199-236.

Mio K., Stern R. (2002). Inhibitors of the hyaluronidases. *Matrix Biol.* **21**: 31-37.

Muckenschnabel I., Bernhardt G., Spruss T., Buschauer A. (1998). Pharmacokinetics and tissue distribution of bovine testicular hyaluronidase and vinblastine in mice: an attempt to optimize the mode of adjuvant hyaluronidase administration in cancer chemotherapy. *Cancer Lett.* **131**: 71-84.

Noble P.W. (2002). Hyaluronan and its catabolic products in tissue injury and repair. *Matrix Biol.* **21**: 25-29.

Novak U., Stylli S.S., Kaye A.H., Lepperdingerm G. (1999). Hyaluronidase-2 Overexpression Accelerates Intracerebral but not Subcutaneous Tumor Formation of Murine Astrocytoma Cells. *Cancer Res.* **59**: 6246-6250.

Paiva P., Van Damme M.-P., Tellbach M., Jones R.L., Jobling T., Salamonsen L.A. (2005). Expression patterns of hyaluronan, hyaluronan synthases and hyaluronidases indicate a role for hyaluronan in the progression of endometrial cancer. *Gynecol. Oncol.* **98**: 193-202.

Prehm P. (1984). Hyaluronate is synthesized at plasma membranes. *Biochem. J.* **220**: 597-600.

Prehm P. (1990). Release of hyaluronate from eukaryotic cells. *Biochem. J.* **267**: 185-189.

Prehm P. Hyaluronan. *Biopolymers. Polysaccharides I: Polysaccharides from prokaryotes.* A. Steinbüchel, E.J. Vandamme and S. DeBaets ed. Wiley-VCH. Weinheim. (2002). **5**: 379-406.

Prehm P. (2006). Biosynthesis of hyaluronan: direction of chain elongation. *Biochem. J.* **398**: 496-473.

Rai S.K., Duh F.-M., Vigdorovich V., Danilkovitch-Miagkova A., Lerman M.I., Miller A.D. (2001). Candidate tumor suppressor HYAL2 is a glycosylphosphatidylinositol (GPI)-anchored cell-surface receptor for jaagsiekte sheep retrovirus, the envelope protein of which mediates oncogenic transformation. *Proc. Natl. Acad. Sci. U. S. A.* **98**: 4443-4448.

Sabeur K., Cherr G.N., Yudin A.I., Overstreet J.W. (1998). Hyaluronic acid enhances induction of the acrosome reaction of human sperm through interaction with the PH-20 protein. *Zygote* **6**: 103-111.

Saitoh H., Takagaki K., Majima M., Nakamura T., Matsuki A., Kasai M., Narita H., Endo M. (1995). Enzymic Reconstruction of Glycosaminoglycan Oligosaccharide Chains Using the Transglycosylation Reaction of Bovine Testicular Hyaluronidase. *J. Biol. Chem.* **270**: 3741-3747.

Scott J.E. (1998). Secondary and tertiary structures of hyaluronan in aqueous solution. Some biological consequences.
http://www.glycoforum.gr.jp/science/hyaluronan/HA02/HA02E.html

Scott J.E., Heatley F. (2002). Biological properties of hyaluronan in aqueous solution are controlled and sequestered by reversible tertiary structures, defined by NMR spectroscopy. *Biomacromolecules* **3**: 547-553.

Sheehan J., Almond A. (2001). Hyaluronan: Static, hydrodynamic and molecular views.
http://www.glycoforum.gr.jp/science/hyaluronan/HA21/HA21E.html

Skov L.K., Seppala U., Coen J.J., Crickmore N., King T.P., Monsalve R., Kastrup J.S., Spangfort M.D., Gajhede M. (2006). Structure of recombinant Ves v 2 at 2.0 Angstrom resolution: structural analysis of an allergenic hyaluronidase from wasp venom. *Acta Crystallogr. D. Biol. Crystallogr.* **62**: 595-604.

Spruss T., Bernhardt G., Schönenberger H., Schiess W. (1995). Hyaluronidase significantly enhances the efficacy of regional vinblastine chemotherapy of malignant melanoma. *J. Cancer Res. Clin. Oncol.* **121**: 193-202.

Stern R. (2003). Devising a pathway for hyaluronan catabolism: are we there yet? *Glycobiology* **13**: 105R-115.

Stern R. (2004). Hyaluronan catabolism: a new metabolic pathway. *Eur. J. Cell Biol.* **83**: 317-325.

Stern R. (2005). Hyaluronan Metabolism: a major paradox in cancer biology. *Pathol. Biol.* **53**: 372-382.

Stern R., Csoka A.B. (2000). Mammalian hyaluronidases. http://www.glycoforum.gr.jp/science/hyaluronan/HA15/HA15E.html

Stern R., Jedrzejas M.J. (2006). Hyaluronidases: Their Genomics, Structures, and Mechanism of Action. *Chem. Rev.* **106**: 818-839.

Takagaki K., Nakamura T., Izumi J., Saito H., Endo M. (1994). Characterization of hydrolysis and transglycosylation by testicular hyaluronidase using ion-spray mass spectrometry. *Biochemistry* **33**: 6503-6507.

Taylor K.R., Gallo R.L. (2006). Glycosaminoglycans and their proteoglycans: host-associated molecular patterns for initiation and modulation of inflammation. *FASEB J.* **20**: 9-22.

Toole B.P. (2001). Hyaluronan in morphogenesis. *Semin. Cell Dev. Biol.* **12**: 79-87.

Toole B.P. (2004). Hyaluronan: from extracellular glue to pericellular cue. *Nature Rev. Cancer.* **4**: 528-539.

Turley E.A., Harrison R. (1999). RHAMM, a member of the hyaladherins. http://www.glycoforum.gr.jp/science/hyaluronan/HA11/HA11E.html

Turley E.A., Roth S. (1980). Interactions between the carbohydrate chains of hyaluronate and chondroitin sulphate. *Nature* **283**: 268-271.

Wang C.T., Lin Y.T., Chiang B.L., Lin Y.H., Hou S.M. (2006). High molecular weight hyaluronic acid down-regulates the gene expression of osteoarthritis-associated cytokines and enzymes in fibroblast-like synoviocytes from patients with early osteoarthritis. *Osteoarthritis Cartilage* **14**: 1237-1247.

Weigel P.H., Fuller G.M., LeBoeuf R.D. (1986). A model for the role of hyaluronic acid and fibrin in the early events during the inflammatory response and wound healing. *J. Theor. Biol.* **119**: 219-234.

Weissmann B. (1955). The transglycosylative action of testicular hyaluronidase. *J. Biol. Chem.* **216**: 783-794.

Weissmann B., Meyer K. (1954). The structure of hyalobiuronic acid and of hyaluronic acid from umbilical cord. *J. Am. Chem. Soc.* **76**.

West D.C., Hampson I.N., Arnold F., Kumar S. (1985). Angiogenesis induced by degradation products of hyaluronic acid. *Science* **228**: 1324-1326.

Xu H., Ito T., Tawada A., Maeda H., Yamanokuchi H., Isahara K., Yoshida K., Uchiyama Y., Asari A. (2002). Effect hyaluronan oligosaccharides on the expression of heat shock proteins. *J. Biol. Chem.* **277**: 17308-17314.

# Chapter 2

# Scope and objectives

Hyaluronan is recently gaining increasing importance in many areas of cell biology, oncology and immunology. Yet the knowledge about the synthetic and catabolic pathways involved in the control of hyaluronic acid maintenance is limited. This is in part due to the lack of in-depth information on the catabolizing enzymes, the hyaluronidases. Human hyaluronidases have been isolated from human tissue and fluids in very low quantities insufficient for enzymatic and structural characterization studies. Therefore, the aim of this thesis was the recombinant production of human hyaluronidases, the establishment of efficient purification strategies and the identification of biochemical and enzymatic properties of these hardly characterized enzymes.

As a first approach, the human hyaluronidases Hyal-1, Hyal-2, Hyal-4 and PH-20 were intended to be produced in *E. coli* as expression system and, if necessary, refolded *in vitro*. The presence of several cysteine residues probably all linked by disulfide bridges in the native hyaluronidases indicated the formation of inclusion bodies in the reducing cytoplasm of standard *E. coli* strains. However, *in vitro* folding systems have been intensively improved during the last years providing general strategies for the folding of unknown proteins. Alternatively, the use of *E. coli* strains optimized for the production of disulfide-linked proteins in the cytoplasm was planned to be tested for the expression of human hyaluronidases.

Insect cells have previously proven to be suitable for the expression of recombinant bee venom hyaluronidase, an enzyme with significant homology to the human hyaluronidases. Therefore, *Drosophila* Schneider-2 cells were suggested as a eukaryotic expression system with the ability to introduce mammalian-like glycosylation patterns.

Biochemical characterization studies with respect to the pH-dependent activity of the human hyaluronidases against the natural substrate, hyaluronic acid, and other glycosaminoglycans as alternative substrates should provide further insight into the specific functions of the human hyaluronidase subtypes. The degradation of HA should be followed by various hyaluronidase activity assay systems including colorimetric, turbidimetric, viscosimetric and electrophoretic techniques in order to gain more detailed information about the subtype specific differences of the catalytic process.

The unique properties of hyaluronic acid as a macro-molecular substrate complicate the observation of enzyme kinetics in terms of Michaelis-Menten kinetics. Therefore, kinetic parameters were intended to be determined by the conversion of the suspected minimum substrate, the hyaluronic acid hexasaccharide. Oligosaccharides comprising one to four [GlcUAc(β1-3)GlcNAc(β1-4)] units were to be produced enzymatically and separated in a preparative scale by size exclusion chromatography.
A capillary zone electrophoresis (CZE) method was to be established for a qualitative and quantitative separation of hyaluronic acid oligosaccharide mixtures produced through the time-dependent action of different hyaluronidase subtypes. Analysis of these oligosaccharide mixtures produced by the hyaluronidases can provide important information about the affinity of low molecular weight compounds towards the binding pocket of hyaluronidases. Furthermore, the transglycosylation catalyzed in addition to the hydrolysis of hyaluronic acid fragments could be studied in detail by this method.

The production of catalytically active human hyaluronidases in recombinant expression systems was planned as a basis for enzymological and biophysical studies of these poorly characterized enzymes. Furthermore, the hyaluronidases can be used for the development of specific inhibitors, which can be employed, for example, as pharmacological tools.

# Chapter 3

# Heterologous expression of the human hyaluronidases PH-20, Hyal-1, Hyal-2 and Hyal-4 in bacteria

## 3.1. Introduction

In consequence of the sequencing of the human genome in 2003 (Rogers 2003), databases containing human gene sequences as well as cDNA libraries are available nowadays. This enables the heterologous production of any human protein in host organisms like bacteria, yeast, insect cells or mammalian cells. The *E. coli* system, being the most convenient and best characterized recombinant expression system, is often the first choice, due to its easy handling, the fast production of high amounts of protein and the possibility for scaling-up (Graumann and Premstaller 2006).

The great evolutionary distance between human and bacterial protein transcription and translation causes several problems. However, those have mainly been overcome in the past years by selective improvement of bacterial strains. Exemplarily: insertion of additional tRNAs for codons rarely used in *E. coli* improves expression of proteins utilizing these codons, stringent control of basal expression levels enables the production of toxic proteins, deficiencies in proteases like *lon* and *ompT* reduce the intracellular degradation of foreign proteins (for review see Terpe 2006).

The major disadvantage of bacterial expression systems is the absence of post-translational modifications like glycosylations, disulfide bridge formation or lipid modifications (palmitoylation, myristoylation). This often leads to misfolding of mammalian proteins and the formation of insoluble, inactive protein aggregates, so called inclusion bodies (IBs)

(Baneyx and Mujacic 2004). Production of disulfide-bonded, soluble proteins can sometimes be achieved by secretion of the protein into the periplasm (Georgiou and Segatori 2005) or in the cytoplasm of glutathione reductase/thioreductase-deficient bacterial strains (Bessette et al. 1999).

If post-translational modifications are known to influence the activity of the protein of interest, eukaryotic expression systems are generally preferred. While the expression in yeast (*Saccharomyces cerevisiae*, *Pichia pastoris*) is also easy and fast, the glycosylation pattern introduced by normal yeast strains differs to a great extent from the glycosylation in mammals (Sethuraman and Stadheim 2006). Insect cells (Sf9, DS-2) are an alternative for mammalian cell lines due to their relatively simple cultivation, fast growth and the production of high amounts of protein with a glycosylation pattern similar to human proteins (Schmidt 2004). Among mammalian expression systems CHO (chinese hamster ovary) cells are the most common ones (Schmidt 2004). For reasons of completeness cell-free translation systems should be mentioned, which have evolved during the last years as promising tools for the production of proteins difficult to access with "*in vivo"* expression systems (Yoshihiro et al. 2006).

The choice of the expression system depends on the characteristics of the foreign protein. The primary structures of the human hyaluronidases Hyal-1, Hyal-2, Hyal-4 and PH-20 contain four and five cysteine residues, respectively, within the hyaluronidase domain and 6 – 8 cysteine residues in the C-terminal domain (cf. Chapter 1). Due to the localization of hyaluronidases in the extracellular matrix or in lysosomes these cysteine residues are assumed to be at least partially linked by disulfide bridges. The strict conservation of the four cysteine residues within the catalytic domain in all human hyaluronidases indicates disulfide linkage similar to the one in bee venom hyaluronidase (Markovic-Housley et al. 2000). Hyal-4 contains an additional cysteine residue (C263) within the hyaluronidase domain with yet unknown function and oxidation state.

Although the human hyaluronidases were expected to form IBs due to the presence of disulfide bridges, they were expressed in the cytoplasm of *E. coli* BL21(DE3)*RIL* and in Rosetta-gami™(DE3), a glutathione reductase/thioreductase-deficient strain. The formation of IBs can be advantageous for the production of very high quantities of heterologous protein (exceeding 50 % of the total cell protein) with minimal impurities (Baneyx and Mujacic

2004). However, complete denaturation, solubilization and re-folding are necessary to gain catalytically active protein (Jaenicke and Rudolph 1989).

## 3.2. Materials and Methods

### *3.2.1. Enzymes, chemicals and standard techniques*

Primers were synthesized by MWG Biotech AG, Ebersberg, Germany. DNA sequencing was performed by Entelechon, Regensburg, Germany. Restriction enzymes, dNTPs, T4 ligase, RNase A, polymerases and respective buffers were purchased from Fermentas, St. Leon-Rot, Germany. Lysozyme and CIP (calf intestine alkaline phosphatase) were from Roche Diagnostics, Mannheim, Germany. Antibiotics, IPTG (isopropylthiogalactoside) and dimethylamminobenzaldehyde (DMAB) were purchased from Sigma-Aldrich, Munich, Germany. Substances for microbiological experiments (tryptone, yeast extract, agar) and cetyltrimethylammoniumbromide (CTAB) were purchased from Roth, Karlsruhe, Germany. BTH (Neopermease®) was a gift from Sanabo, Vienna, Austria. BSA was purchased from Serva, Heidelberg, Germany, and all other chemicals were from Merck, Darmstadt, Germany.

### *3.2.2. Amplification of hyaluronidase cDNAs by PCR*

Clones carrying cDNA sequences of the human hyaluronidases *hyal-1*, *hyal-2*, *hyal-4* and *ph-20* were purchased as I.M.A.G.E. clones (Lennon et al. 1996) from RZPD (Deutsches Ressourcenzentrum für Genomforschung GmbH, Berlin, Germany) (**Tab. 3.1**).

**Tab. 3.1** cDNAs of human hyaluronidases from arrayed cDNA libraries as purchased by RZPD.

| cDNA | RZPD clone I.D. | Library vector | Tissue |
|---|---|---|---|
| *ph-20* | IMAGp998N231077Q3 | pBluescriptR | testis |
| *hyal-1* | IRAKp961O1779Q2 | pCMV-SPORT 6.0 | stomach, colon, kidney |
| *hyal-2* | IMAGp958H01139Q2 | pOTB7 | kidney |
| *hyal-4* | IMAGp998G15205Q3 | pT7T3d-PacI | spleen |

All cDNAs were completely sequenced using standard primers (T7, sp6) and specific internal primers if necessary. The hyaluronidase cDNAs were analyzed for a signal peptidase cleavage site by the program SignalP 3.0 (Bendtsen et al. 2004). Signal peptides identified thereby were not included in the following cloning steps. Each of the four hyaluronidase subtypes was

cloned as a truncated (short, S) and full-length variant (long, L). Fragments were amplified by PCR with primers containing additional restriction sites for *Nde*I and *Bam*HI (**Tab. 3.3** and **Tab. 3.4**). The general PCR reaction mixture used is shown in **Tab. 3.2**, while conditions with respect to the annealing temperature and the $MgSO_4$ concentration were optimized for each reaction separately (**Tab. 3.3** and **Tab. 3.4**).

**Tab. 3.2** PCR reaction mixture for amplification of *ph-20*, *hyal-1*, *hyal-2* and *hyal-4* cDNAs for cloning into pET15b.

| | |
|---|---|
| 4 µL | Template DNA (25 µg/mL) |
| 2 µL | Forward primer (25 µM) |
| 2 µL | Reverse primer (25 µM) |
| 5 µL | *Pfu* reaction buffer containing 15 mM $MgSO_4$ (10 x) |
| 5 µL | dNTP Mix (2 mM/dNTP) |
| 1 µL | *Pfu* DNA-polymerase (2.5 U/µL) |
| x µL | $MgSO_4$ (25 mM) |
| ad 50 µL | $H_2O$ |

**Tab. 3.3** PCR primers (5'-3'-direction) for cloning of different hyaluronidase variants into *Nde*I and *Bam*HI restriction sites of pET15b. Underlined sequences indicate these restriction sites within the primers, bold letters indicate additionally introduced stop codons. $MgSO_4$ refers to the final concentration in the PCR reaction mixture and $T_a$ indicates the annealing temperature.

| **Hyaluro-nidase** | **Forward primer** | **Reverse primer** | **$MgSO_4$** | **$T_a$** |
|---|---|---|---|---|
| PH-20/S | CGAGTGTCATATGCTG AATTTCAGAG | ACTGGATCC**TTA**CATTTT GGCTGCTAG | 2.5 mM | 59.5 °C |
| PH-20/L | | ATCGGATCCTCAGAAGA AACCAATTC | 2.0 mM | 58.0 °C |
| Hyal-1/S | CTTAATTCATATGTTT AGGGGCCCCTTGC | TAAGGATCC**TTA**GAGAA GGGCCCCACTG | 2.5 mM | 59.5 °C |
| Hyal-1/L | | TAAGGATCCTCACCACA TGCTCTTCCG | 2.0 mM | 58.0 °C |

| | | | | |
|---|---|---|---|---|
| Hyal-2/S | TAGAATTGCATATGG AGCTCAAGCCC | AATGGATCC**TCA**ATATT GGGTGGCCC | 1.5 mM | 59.5 °C |
| Hyal-2/L | | ATAGGATCCCTACAAGG TCCAGGTAAAG | 2.0 mM | 60.5 °C |

The PCR was performed in a Mastercycler gradient Thermocycler (Eppendorf, Wesseling-Berzdorf, Germany) and comprised the following steps:
1) 5 min, 90 °C, 2) 30 s, 95 °C, 3) 30 s, $T_a$, 4) 1 min/kb PCR-product, 72 °C 5) 30 cycles repeating step 2)-4), 6) 5 min, 72 °C.
PCR-fragments were analyzed by agarose gel electrophoresis (cf. 3.2.10) and purified either directly from the PCR mix using a PCR Purification Kit (Quiagen, Hilden, Germany) or, if side products were identified by gel electrophoresis, by excision of the relevant band from the gel and subsequent purification from the agarose gel slice (QIAEX II Purification Kit, Quiagen, Hilden, Germany). All DNA purifications were performed according to the manufacturer's instructions.

### *3.2.3. Overlap extension PCR of hyal-4 cDNA*

For insertion of a G227C mutation the *hyal-4* cDNA was amplified by overlap extension PCR. In the first step PCR reactions I and II were performed under the conditions summarized in **Tab. 3.2** with pT3T7D/*hyal-4* as template DNA and primers shown in **Tab. 3.4**.

**Tab. 3.4** PCR primers (5'-3'-direction) for the amplification of hyal-4 cDNA in the first PCR step of an overlap extension PCR. Additionally introduced *Nde*I and *Bam*HI restriction sites are underlined and new stop codons are printed bold.

| | **Hyaluronidase subtype** | **Forward primer** | **Reverse primer** |
|---|---|---|---|
| PCR I | Hyal-4/S and Hyal-4/L | CTGGATCATATGCTAAAA CCTGCTCGAC | CAAGGGATTTCCAGACAC AGATAGAAGG |
| PCR II | Hyal-4/S | CCTTCTATCTGTGTCTGG AAATCCCTTG | ATTGGATCC**TCA**TACCTC AGCAGCTCTG |
| PCR II | Hyal-4/L | | GATGGATCCTCACAACTG AATGCTTCG |

All reactions were performed at an annealing temperature of 58 °C and a $MgSO_4$ concentration of 1.5 mM. PCR products were analyzed by agarose gel electrophoresis and extracted from the gel. The conditions of the subsequent overlap extension PCR are shown in **Tab. 3.5**.

**Tab. 3.5** Overlap extension PCR for amplification of Hyal-4/S and Hyal-4/L with a G227C mutation.

| | |
|---|---|
| 12 µL | Gel extract PCR I (from 2 x 50 µL PCR reaction I) |
| 12 µL | Gel extract PCR II (from 2 x 50 µL PCR reaction II) |
| 10 µL | Forward primer PCR I |
| 10 µL | Reverse primer PCR II |
| 10 µL | *Pfu* reaction buffer containing 15 mM $MgSO_4$ (10 x) |
| 10 µL | dNTP mix (2 mM/dNTP) |
| 2.5 µL | *Pfu* polymerase (1 U/µL) |
| Ad 100 µL | $H_2O$ |

The overlap extension reaction was achieved by the following thermocycle:
1) 5 min, 90 °C, 2) 1 min, 95 °C, 3) 1 min, 50 °C, 4) 1 min, 72 °C, 5) 25 cycles repeating steps 2) – 4), 6) 5 min, 72 °C.
The final PCR products were purified by gel extraction (cf. 3.2.2).

### *3.2.4. Restriction digest and ligation of PCR fragments and pET15b*

For sub-cloning the vector pET15b (Novagen®, Merck, Darmstadt, Germany) and the PCR products were both digested with *Nde*I and *Bam*HI. The first restriction step was performed in a reaction mixture containing 2 µL of plasmid DNA (1.0 mg/mL) and 20 µL of purified PCR product, respectively, 8 µL of 10 x Y+/TANGO™ buffer, 3 µL of *Nde*I (10 U/µL). Then water was added to reach a final volume of 40 µL. After incubation at 37 °C overnight 1 µL of *Bam*HI (10 U/µL) was added and the digestion was continued for 1 h. To avoid self-ligation of the vector the DNA was additionally treated for 1 h at 37 °C with 0.05 U CIP per pmol DNA ends present in the reaction mixture. Enzymatic restriction and dephosphorylation of 3'-ends were stopped by 20 min incubation at 80 °C. Restriction digests were purified by agarose gel electrophoresis (cf. 3.2.2).
Ligation was performed in a total volume of 18 µL containing 50 – 150 ng of pET15b DNA and 5 – 10 times the molar amount of insert DNA. The reaction mixture was incubated for 5

min at 45 °C. Then 2 µL of 10 x ligase buffer containing ATP and 1 Weiss U of ligase were added on ice. After incubation overnight at 4 °C ligation was stopped by heating at 65 °C for 10 min. The ligation mixture was transformed into *E. coli* Top10 (Invitrogen, Karlsruhe, Germany) and colonies were screened for the ligation product by colony PCR (cf. 3.2.7). After preparation of the pET15b/hyaluronidase constructs the correctness of the inserts was confirmed by sequencing.

### *3.2.5. Generation of competent E. coli cells*

All competent *E. coli* strains used in this work were prepared by $CaCl_2$ treatment. 200 mL LB-medium (Luria-Bertani medium) were inoculated with 2 mL of an overnight culture of the respective *E. coli* strain and the culture was grown at 37 °C and 200 rpm until a cell density of $OD_{600}$ = 0.2 was reached. Bacteria were placed on ice for 10 min, centrifuged for 7 min (4,000 g, 4 °C) and resuspended in 32 mL of ice-cold, sterile $CaCl_2$-solution (60 mM $CaCl_2$, 15 % (v/v) glycerol, 10 mM PIPES, pH 7.0). After incubation on ice for 30 min the bacteria were again pelleted (5 min, 4,000 g, 4 °C) and resuspended in 6.4 mL of ice-cold $CaCl_2$-solution. This concentrated bacteria suspension was incubated in aliquots of 200 µL for 2 h on ice, frozen in liquid $N_2$ and stored at -80 °C until transformation.

### *3.2.6. Transformation of competent E. coli*

200 µL of freshly thawed competent *E. coli* cells were incubated with 5 ng of plasmid DNA or 10 µL of ligation mix (cf. 3.2.4) for 30 min on ice. A heat shock of 1.5 min at 42 °C was applied to allow DNA uptake by the cells. After 2 min on ice 1 mL of sterile SOC-medium (0.5 % (w/v) yeast extract, 2 % (w/v) trypton, 10 mM NaCl, 2.5 mM KCl, 10 mM $MgCl_2$, 10 mM $MgSO_4$, 20 mM glucose) was added and the bacteria were shaken for 45 min at 37 °C and 200 rpm. 20 - 50 µL of this suspension were plated on LB-agar plates containing 100 µg/mL of ampicillin. Colonies formed after incubation at 37 °C overnight.

### *3.2.7. Colony PCR for the selection of positive clones*

To check for clones containing the insert DNA 10 colonies were picked from an agar plate and transferred to 1 mL of LB-medium. Bacteria were grown for 2 h (37 °C, 200 rpm), pelleted (4,000 g, 3 min) and resuspended in 50 µL of water. Bacteria were lyzed by boiling for 5 min and used as a template for an analytical PCR reaction with primers hybridizing with vector sequences framing the multiple cloning site (T7 primers for pET15b) (**Tab. 3.6**).

The thermocycle was performed as follows:

1) 5 min, 90 °C, 2) 1 min, 94 °C, 3) 1 min, 50 °C, 4) 2 min, 72 °C, 5) 35 cycles repeating steps 2) – 4), 6) 6 min, 72 °C.

The complete PCR mixture was analyzed on a 1 % agarose gel.

**Tab. 3.6** PCR reaction mix for colony PCR of pET15b/*hyaluronidase* clones.

| | |
|---|---|
| 10 µL | Template (lysed bacteria) |
| 1 µL | T7 promotor primer (5 µM) |
| 1 µL | T7 terminator primer (5 µM) |
| 2 µL | dNTP mix (2 mM) |
| 2 µL | 10 x Taq reaction buffer with $MgCl_2$ |
| 3.8 µL | $H_2O$ |
| 0.2 µL | *Taq* polymerase (5 U/µL) |

### *3.2.8. Preparation of plasmid DNA from E. coli*

Small scale isolation of plasmid DNA ("Mini-prep") from *E. coli* was performed as follows:

4 mL of an overnight culture were centrifuged for 15 min at 3,000 rpm, the pellet was resuspended in 200 µL of GTE-buffer (1 % (w/v) glucose, 25 mM Tris/HCl, 10 mM EDTA, pH 7.5) supplemented with 5 µL of RNase A (10 mg/mL). After addition of 400 µL of freshly prepared "lysis buffer" (200 mM NaOH, 1 % (w/v) SDS) the solution was mixed by inverting several times and incubated on ice for exactly 5 min. Cell lysis was stopped by addition of 300 µL of 3 M potassium acetate and incubation on ice for 10 min. Cellular debris and chromosomal DNA were pelleted by 10 min centrifugation at 13,000 rpm. Plasmid DNA remaining in the supernatant was precipitated by addition of 1 mL of cold 70 % (v/v) ethanol. After incubation on ice for 30 min and centrifugation (10 min, 13,000 rpm at 4 °C) the plasmid DNA was washed once with 200 µL of ethanol. The resulting pellet was dried for ca. 15 min at RT and then solubilized in 50 µL of $H_2O$.

Large scale isolation ("Maxi-prep") of plasmid DNA was performed with a Quiagen Plasmid Purification Kit (Quiagen, Hilden, Germany) following the manufacturer's instructions.

Plasmid DNA concentrations and purity were determined photometrically. If the quotient $A_{280}/A_{260}$ was < 0.59, the DNA was considered to contain no protein impurities and the DNA concentrations were calculated by the following equation:

$$c(DNA) = 70 \cdot A_{260} - 40 \cdot A_{280} \quad \text{with c(DNA) in µg/mL.} \qquad \text{Eq.3.1}$$

### *3.2.9. Overnight cultures, glycerol stocks and LB-agar plates*

Bacterial overnight cultures were shaken for 12 – 15 h at 200 rpm in LB-medium containing the necessary antibiotics.

For long term storage of bacteria 850 µL of an overnight culture were added to 150 µL of sterile, 87 % (v/v) glycerol. This glycerol stock culture was stored at -80°C.

LB-agar plates were prepared by heating LB-agar (1 % (w/v) tryptone, 0.5 % (w/v) yeast extract, 1 % (w/v) NaCl, 1.35 % (w/v) agar, pH 7.0) under stirring until the agar was completely dissolved. Then the agar was cooled to 55 °C in a water bath before the appropriate antibiotics were added. Finally, 20 – 30 mL of agar were poured into a sterile culture plate, which was stored at 4 °C until use.

### *3.2.10. Agarose gel electrophoresis*

Agarose (Peqlab, Erlangen, Germany) was added to 50 mL of 1 x TBE-buffer (89 mM Tris, 89 mM boric acid, 2 mM EDTA) to achieve a final concentration of 1 % (w/v) and 1.7 % (w/v), respectively. Under stirring the agarose was completely melted at 80 °C, then 2 µL of ethidium bromide (10 mg/mL, Sigma-Aldrich, Munich, Germany) were added and the gel mixture was poured into a gel chamber (10 cm x 10 cm). After placing the comb the agarose was allowed to solidify at room temperature for 15 – 20 min. Then the gel was placed into the electrophoresis chamber filled with 1 x TBE-buffer.

All DNA samples were mixed with 10 x PCR loading buffer (Peqlab, Erlangen, Germany) to yield a final concentration of 1 x PCR loading buffer. 5 µL of GeneRuler$^{TM}$ DNA Ladder Mix (Fermentas, St. Leon-Rot, Germany) were added to 15 µL of water and 5 µL of 10 x PCR loading buffer. Gel pockets were filled with 25 µL of sample and electrophoresis was performed at 90 V for 1.5 h.

Gels were photographed in a Gel-Doc detection system (Bio-Rad, Munich, Germany) with an excitation wavelength of 254 nm. Data were analyzed using Quantity One quantification software, version 4.0.3. (Bio-Rad, Munich, Germany).

### *3.2.11. Hyaluronidase expression in E. coli BL21(DE3)RIL*

For protein expression *E. coli* BL21(DE3)*RIL* cells (Stratagene, Cedar Creek, USA) were transformed with the pET15b/*hyaluronidase* vectors. Hyaluronidase expression was achieved by inoculation of LB-medium supplemented with 100 µg/mL of ampicillin to an $OD_{600}$ of 0.15 with an overnight culture. For efficient protein expression it proved to be essential to use

overnight cultures containing freshly transformed bacteria and overnight culture incubation times of less than 15 h. Bacteria were grown for 2 – 3 h at 200 rpm and 37 °C until an $OD_{600}$ of 0.6 ± 0.5 was reached, then recombinant protein expression was induced by addition of 1 mM of IPTG (if not indicated otherwise). Generally, bacteria were harvested 3 – 4 h after induction of expression by centrifugation (30 min, 5,000 g, 4 °C). Cell pellets could be stored at -20 °C for a few months.

For total cell protein analysis by SDS-PAGE 1 mL of cell suspension was centrifuged (1 min, 13,000 rpm, 4 °C) and resuspended in 100 µL of 1 x PBS and 100 µL of 5 x SDS sample buffer (cf. 3.2.14). Cell lysis and complete denaturation of proteins was achieved by boiling of the samples for 15 min. To compare the total cell protein before and after induction with IPTG the samples were normalized with respect to cell density.

### *3.2.12. Hyaluronidase expression in Rosetta-gami™(DE3)*

The *E. coli* strain Rosetta-gami™(DE3) (Novagen®, Merck, Darmstadt, Germany) was transformed with the pET15b/*hyaluronidase* constructs. Expression and analysis of total cell protein was performed as described for *E. coli* BL21(DE3)*RIL* (cf. 3.2.11).

All media and agarose plates used for the growth of *E. coli* Rosetta-gami™(DE3) were supplemented with 15 µg/mL kanamycin, 12.5 µg/mL tetracycline and 34 µg/mL chloramphenicol.

### *3.2.13. Separation of soluble and insoluble cell fractions*

Bacterial pellets were resuspended in 1/10 of the original culture volume of bacterial lysis buffer (20 mM Tris/HCl, pH 7.5, 0.5 mg/mL lysozyme), e.g. 2 mL of lysis buffer were added to a pellet from 20 mL of bacterial culture. After incubation on ice for 1 h cell lysis was enhanced by sonication on ice (15 bursts, microtip, power level 4 – 5, 40 – 50 % duty, Branson-Sonifier B15, G. Heinemann, Schwäbisch-Gmünd, Germany). By centrifugation (30 min, 10,000 g, 4 °C) the suspension was separated into a supernatant with soluble proteins from the cytoplasm and an insoluble pellet containing fragments of membranes and insoluble proteins.

The pellet was washed twice with 20 mM Tris/HCl, pH 7.5, and pelleted after each washing step by centrifugation (5 min, 10,000 g, 4 °C). For SDS-PAGE the pellet was resuspended in 1 % (w/v) SDS, a sample was taken and mixed with an equal volume of 5 x SDS sample buffer (cf. 3.2.14) before boiling for 3 min at 100 °C.

### *3.2.14. Discontinuous SDS-PAGE*

12 % separation gel mixtures contained 2.1 mL of water, 1.5 mL of 1.5 M Tris/HCl, pH 8.8, 60 µL of 10 % (w/v) SDS and 2.4 mL of acrylamide/bisacrylamide (30 % solution, acrylamide/bisacrylamide = 29/1, Sigma-Aldrich, Munich, Germany) per gel. Polymerization was started by addition of 3 µL of N,N,N',N'-tetramethylethylenediamine (TEMED) and 40 µL of freshly prepared 10 % (w/v) ammonium peroxodisulfate (APS). The mixture was filled into gel chambers (10 x 10 x 0.8 cm) and covered with a layer of water-saturated isobutyl alcohol. After 15 – 20 min the gel was completely polymerized and the stacking gel was pipetted on top of the separation gel after the isobutyl alcohol had been washed away with water. 4 % stacking gel mixtures contained 1.8 mL of water, 0.75 mL of 0.5 M Tris/HCl, pH 6.8, 30 µL of 10 % (w/v) SDS and 0.4 mL of acrylamide/bisacrylamide (30 %, see above). 3 µL of TEMED and 10 µL of 10 % (w/v) APS were added to initiate polymerization.

Electrophoresis was performed in a PerfectBlue$^{TM}$ Double gel system Twin S (Peqlab, Erlangen, Germany) at 150 V for 1 – 1.5 h with the electrode chambers filled with 1x running buffer. 5 x running buffer contained 9 g Tris, 43.2 g glycine and 3 g SDS in 600 mL of water.

If not indicated otherwise protein samples were mixed with 0.2 – 0.5 volumes of 5 x SDS sample buffer (0.2 M Tris/HCl, pH 6.8, 10 % (w/v) SDS, 10 mM DTT, 20 % (v/v) glycerol, 0.05 % (w/v) bromphenol blue) and heated for at least 3 min at 100 °C.

Gels were analyzed with a Bio-Rad gel detection system (GS-710 Imaging Densitometer) using Quantity One quantification software, version 4.0.3. (Bio-Rad, Munich, Germany).

### *3.2.15. Turbidimetric hyaluronidase activity assay*

The turbidimetric hyaluronidase activity assay described by Di Ferrante (Di Ferrante 1956) was slightly modified for the 96-well plate format. The incubation mixture contained the following components:

31 µL of incubation buffer, 8 µL of BSA (0.2 mg/mL), 8 µL of HA (2 mg/mL), 13 µL of $H_2O$, 10 µL of sample containing the enzyme.

As incubation buffer McIlvaine's buffer (McIlvaine 1921) was used. The buffer was prepared by mixing solution A (0.2 M $NaH_2PO_4$, 0.1 M NaCl) and solution B (0.1 M citric acid, 0.1 M NaCl) in appropriate portions to adjust the required pH. In general a mixture containing the incubation buffer, BSA, HA and $H_2O$ was prepared and 60 µL of this mixture were pipetted into each well before addition of the sample.

The 96-well plates were incubated at 37 °C for a defined reaction time. Then high molecular weight HA was precipitated with 200 µL of alkaline CTAB solution (2.5 % (w/v) CTAB in

0.5 M NaOH) and the plates were incubated for 20 min at room temperature. The extent of precipitation was measured by the optical density at 580 and 355 nm, respectively, in a Tecan GENios Pro microtiter plate reader (Tecan, Crailsheim, Germany) with XFluorGeniosPro Software, version V.4.55. The plate was shaken in the reader for 10 s in the orbital mode and the OD was measured with 10 flashes in the centre of each well after a settle time of 2 s.

The optical density values given in the experimental section are mean values ± SEM (standard error of means) of triplicates.

### *3.2.16. Colorimetric hyaluronidase activity assay*

A detailed description of the colorimetric hyaluronidase activity assay is given in Chapter 4. Incubation buffers were identical to the buffers used in the turbidimetric activity assay (3.2.15).

## 3.3. Results and Discussion

### *3.3.1. Analysis of hyaluronidase cDNA sequences*

The sequences of the cDNA inserts derived from the arrayed cDNA libraries were only partially sequenced by the I.M.A.G.E. consortium yet. Therefore, all purchased cDNA sequences were compared to the hyaluronidase cDNA sequences in the Gene Bank (Benson et al. 2006).

The sequence of the *ph-20* cDNA was identified to be identical to BC026163 (Gene Bank Accession number). The ORF included in this cDNA codes for a protein registered as Q8TC30 in the Swiss-Prot/TrEMBL database (Swiss-Prot/TrEMBL, Boeckmann 2003), which is a PH-20 variant differing from the registered PH-20/SPAM-1 (HYAP_HUMAN, accession number P38567) in its C-terminal propeptide. As this propeptide most probably functions as the signal sequence for addition of a GPI-anchor (cf. Chapter 1) it is not supposed to influence enzymatic activity. However, analysis of the C-terminal sequence of Q8TC30 revealed no GPI-anchorage signal.

The cDNA of *hyal-1* showed 99 % sequence identity to BC035695. The two bases mutated in comparison to the reference sequence were located in the 3'-UTR and did not affect further recombinant protein expression experiments (cf. Appendix 1). The encoded protein sequence was identical to the database entry Q12794 (Hyal-1/LUCA-1).

The sequence of the *hyal-2* cDNA was identical to BC000692 coding for Q12891.

Putative *hyal-4* cDNA was compared to NM_012269. Three mutations were found within the ORF, but only one coded for an amino acid substitution while the other ones were silent mutations (cf. Appendix 1). The amino acid substitution would have resulted in an exchange of C227 in Hyal-4 (Q9UL99) by G227. This amino acid sequence is registered at Swiss-Prot as Q9Y6T9 (Gene Bank Acc. BC_104788 and BC_104790), however, no further information is available about this protein. Furthermore, the *hyal-4* cDNA was truncated at the 5'-end lacking the codons for the amino acids M1 and K2 (Q9UL99) at the N-terminal end. Both amino acids were located within the signal peptide and had therefore no effect on the recombinant expression experiments.

The complete ORFs coding for human PH-20, Hyal-1 and Hyal-2 were thus available for cloning into recombinant expression vectors. The C227G mutation in Hyal-4 was re-mutated during sub-cloning to the original C residue by overlap extension PCR in order to receive the coding sequence for human Hyal-4 as reported at the Swiss-Prot database.

### *3.3.2. Construction of pET15b/ph-20, pET15b/hyal-1 and pET15b/hyal-2*

Homology studies suggest the existence of several domains in the primary sequence of human hyaluronidases (cf. Chapter 1). At the N-terminus of the proteins a signal peptide sequence is responsible for the transport of the nascent peptide chain to the ER (endoplasmic reticulum). After insertion of the N-terminus into the ER the signal peptide is cleaved off and is therefore not present in the mature protein. Analysis of the N-terminal sequence of all hyaluronidases by neuronal networks and Hidden Markov Models confirmed the length of the signal peptides in PH-20, Hyal-1 and Hyal-2 (cf. Chapter 1.). For Hyal-4 a unique signal peptidase restriction site was found by both models. Signal peptides were not included in the recombinant hyaluronidases expressed in *E. coli*.

The hyaluronidase domain containing the active site is linked to the C-terminal domain by a short linker sequence. For construction of the short enzyme variants this linker was included, but not the following C-terminal domain with yet unknown function. The size of these short variants' PCR products was ca. 1.0 kb (**Fig. 3.1**).

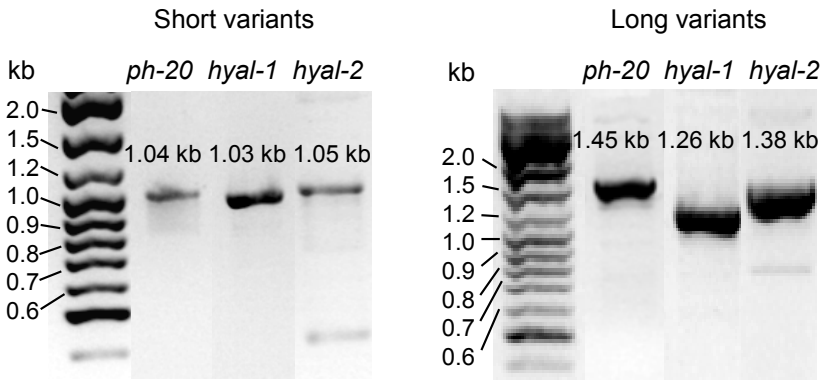


**Fig. 3.1** PCR products of short (left) and long constructs (right) of *ph-20*, *hyal-1* and *hyal-2*. After mixing with 10 x PCR loading buffer 5 µL of the original PCR mixtures of the short variants were applied to the gel and 10 µL of the original PCR mixtures of the long variants were applied to the gel.

The long variants comprised the whole cDNA except for the signal peptide. PH-20 and Hyal-2 are known to contain propeptides at the C-terminus, which are presumably cleaved off after linkage to a GPI-anchor. However, it is not clear whether these propeptides are necessary for proper folding of the protein in the ER, where the propeptide is still present. As several examples of folding enhancement by propeptides exist in literature (Hahm and Chung 2001, Rattenholl et al. 2001), the long variants of PH-20 and Hyal-2 were both cloned including the propeptide coding sequences. The resulting PCR products exhibited a size of ca. 1.4 kb. The PCR product of the long variant of Hyal-1 (Hyal-1/L) is shorter compared to PH-20 and Hyal-2 as this hyaluronidase lacks the propeptide for GPI-anchorage and contains a shorter C-terminal domain.

The PCR products were digested with *Bam*HI and *Nde*I and ligated into pET15b to yield the bacterial expression vectors pET15b/*ph-20*, pET15b/*hyal-1* and pET15b/*hyal-2* (**Fig. 3.2**). The expression vector pET15b is a 5.7 kb plasmid carrying at its expression site an N-terminal His-tag followed by a thrombin cleavage site and three cloning sites (*Nde*I, *Xho*I and *Bam*HI). The whole expression site is under control of a T7 promotor. Additionally, the plasmid contains the *amp*$^R$ and the *lacI* gene.

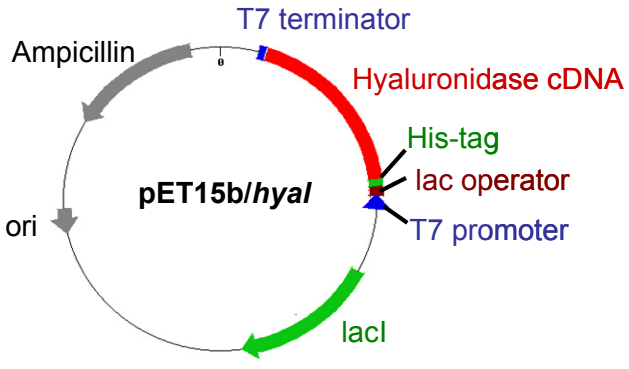


**Fig. 3.2** Plasmid map of the pET15b/*hyaluronidase* expression vector.

### *3.3.3. Construction of pET15b/hyal-4 expression vectors by overlap extension PCR*

Sequencing of cDNA clone IMAGp998G15205Q3 showed that this vector contained a cDNA coding for Hyal-4 with a C→G mutation at amino acid 227. This residue seems essential for a completely functional Hyal-4, therefore the codon GGT coding for G227 was mutated into TGT coding for C227 by overlap extension PCR (**Fig. 3.3**).

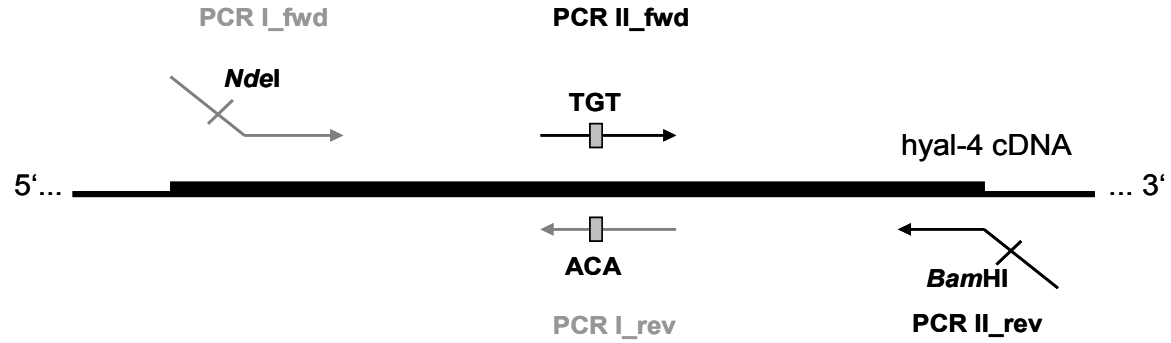


**Fig. 3.3** Schematic presentation of the amplification and mutation of *hyal-4* cDNA. Two separate PCR reactions, PCR I (primers shown in grey) and PCR II (primers shown in black) were performed in order to introduce a mutation (GGT → TGT) in the middle of the gene.

Primers were chosen as described for *ph-20*, *hyal-1* and *hyal-2* (3.3.2). As determined by primary sequence analysis Hyal-4 also contains a catalytic and a C-terminal domain. Therefore, a short variant comprising only the catalytic domain plus a putative linker at the C-terminus as well as a long variant comprising both domains were amplified (cf. **Tab. 3.7**). The reaction product of PCR I was identical for both variants while in PCR II a different reverse primer (PCR II_rev in **Fig. 3.3**) had to be used.

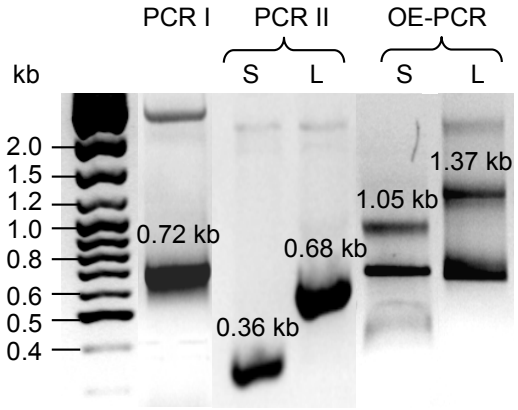


**Fig. 3.4** PCR products of the short (S) and long (L) variants of *hyal-4* during amplification and mutation by overlap extension PCR (OE-PCR). Each lane contained 20 µL of the PCR mixture.

Overlap extension PCR yielded for both the short and the long variant of *hyal-4* a PCR product of 1.05 and 1.37 kb, respectively (OE-PCR in **Fig. 3.4**), though the product still contained a high amount of the original PCR I product (0.72 kb). The high amount of PCR I product remaining in the mixture was probably due to inaccuracies in the amount of PCR I and II products used, as the DNA concentrations were estimated by comparison of the bands

on the gel with the amounts of DNA of the respective bands of the marker. However, as the products of the overlap extension PCR were purified from the gel the impurities did not impede the following cloning steps.

### *3.3.4. Expression of human hyaluronidases in E. coli BL21(DE3)RIL*

*E. coli* BL21(DE3)*RIL* were transformed with pET15b plasmids containing the human hyaluronidase cDNAs. **Tab. 3.7** gives an overview of the expected recombinant enzymes. *E. coli* BL21(DE3)*RIL* is a specialized protein expression strain with tRNAs for R, I and L codons rarely used in bacteria. The expression system is based on a T7-RNA polymerase encoded by the *E. coli* strain and controlled by a *lac* promoter, thus ensuring a tight and IPTG-inducible expression control of genes controlled by a T7 promotor.

**Tab. 3.7** Sequence length and molecular weight of recombinant hyaluronidases in the truncated (S) and full-length variants (L). The protein I.D. refers to the amino acid sequences described in the Swiss-Prot database (Boeckmann 2003).

| Hyaluronidase variant | Hyaluronidase amino acids | Complete sequence length | Molecular Weight | Protein I.D. (SwissProt) |
|---|---|---|---|---|
| PH-20/S | L36 - M375 | 361 aa | 39.3 kDa | Q8TC30 |
| PH-20/L | L36 - F511 | 497 aa | 56.7 kDa | |
| Hyal-1/S | F22 - L357 | 357 aa | 39.9 kDa | Q12794 |
| Hyal-1/L | F22 - W435 | 434 aa | 48.3 kDa | |
| Hyal-2/S | M21 - Y364 | 364 aa | 39.6 kDa | Q12891 |
| Hyal-2/L | M21 - L473 | 473 aa | 51.4 kDa | |
| Hyal-4/S | L35 - V375 | 362 aa | 41.1 kDa | Q9UL99 |
| Hyal-4/L | L35 - L480 | 467 aa | 52.7 kDa | |

All eight hyaluronidase subtypes were expressed in *E. coli* and the cell lysates were analyzed by SDS-PAGE. Comparison of cell lysates before and after induction of expression revealed the occurrence of a band increasing in intensity after induction (**Fig. 3.5**). Analysis of the molecular weight of the respective proteins indicated the expression of the recombinant enzymes with the molecular mass expected from the amino acid sequence (**Tab. 3.7**).

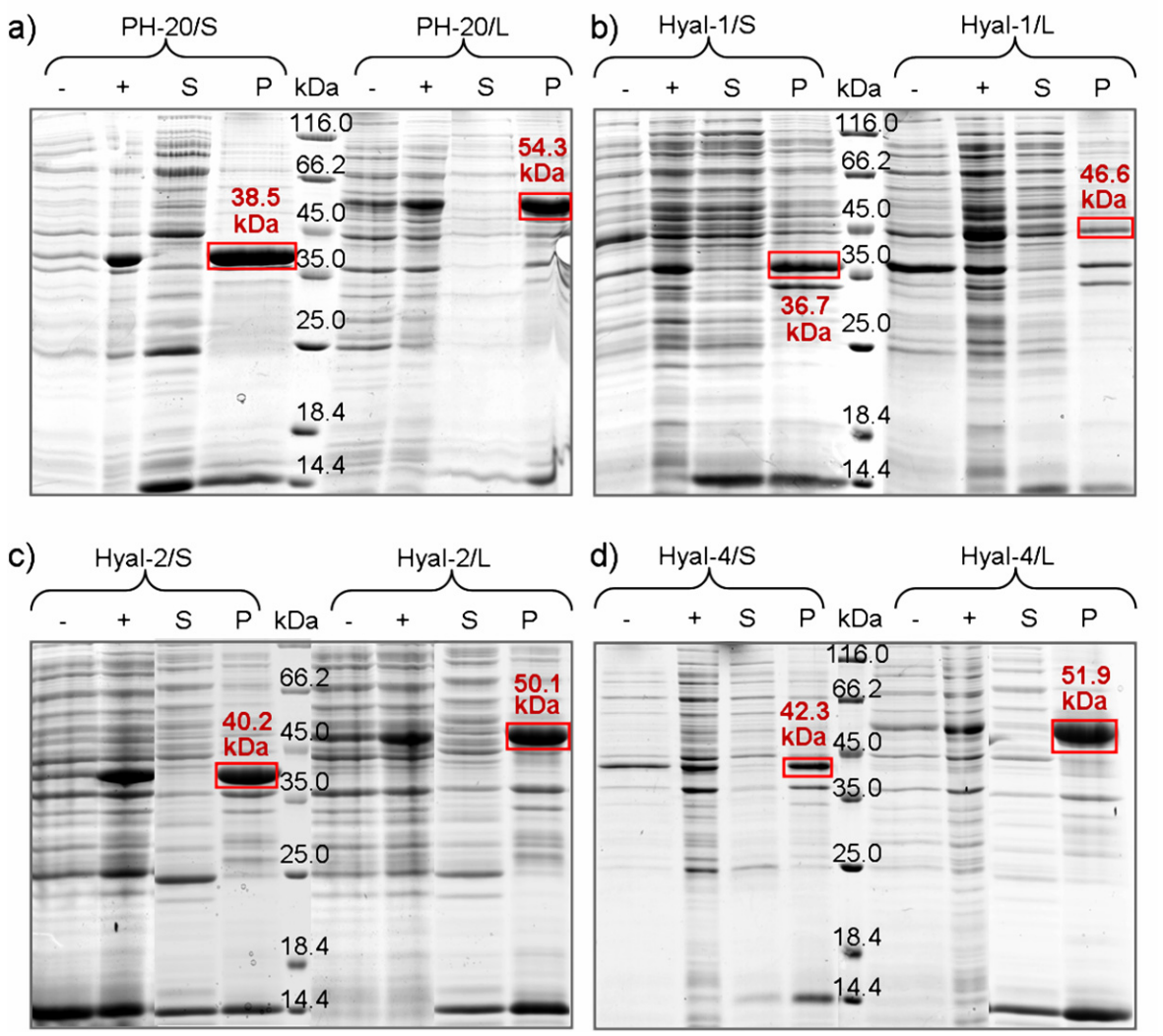


**Fig. 3.5** SDS-PAGE analysis of the cell lysates of *E. coli* BL21(DE3)*RIL*/pET15b/*hyaluronidase* before (-) and 3 – 4 h after induction of expression (+). Separation of the cell lysate into a soluble fraction (supernatant, S) and an insoluble fraction (pellet, P) proved the expression of human hyaluronidases as insoluble aggregates.
a) PH-20/S was determined to have a molecular mass of 38.5 kDa (theoretical: 39.3 kDa) and PH-20/L 54.3 kDa (theoretical: 56.7 kDa).
b) Hyal-1/S was determined to have a molecular mass of 36.7 kDa (theoretical: 39.9 kDa) and Hyal-1/L 46.6 kDa (theoretical: 48.3 kDa)
c) Hyal-2/S was determined to have a molecular mass of 40.2 kDa (theoretical: 39.6 kDa) and Hyal-2/L 50.1 kDa (theoretical: 51.4 kDa).
d) Hyal-4/S was determined to have a molecular mass of 42.3 kDa (theoretical: 41.1 kDa). Hyal-4/L was found on the SDS-PAGE at a molecular mass of 51.9 kDa (theoretical: 52.7 kDa).

Although the T7-controlled pET-expression system in *E. coli* is known to be a very tight system, low basal expression of some of the human hyaluronidases was observed (**Fig. 3.1**, e.g. PH-20/L and Hyal-4/S).

Furthermore, the strength of expression varied for the various subtypes and S/L variants, respectively. The level of expression of a recombinant protein can be influenced by the growth conditions or by the efficiency of translation due to the use of specific amino acid codons. Overall expression levels of the hyaluronidases calculated by densitometry varied

between 11 % (Hyal-4/S) and 42 % (Hyal-1/S) of the total cell protein. All recombinant hyaluronidases were exclusively found in the insoluble cell fraction, supporting the idea that most or all of the C residues are linked by disulfide bridges in the native hyaluronidases. The molecular masses calculated from the over-expressed proteins were found to be in accordance with the molecular masses calculated from the respective amino acid sequences (**Tab. 3.7**) within an error range of < 10 %.

The isolation of the IBs resulted in a partial purification effect due to the separation from soluble cell proteins. The content of recombinant enzyme determined by densitometric analysis of the SDS-PAGE reached up to 60 % of the protein present in the IBs, e.g. Hyal-4/L in **Fig. 3.5**.

### *3.3.5. Optimization of Hyal-1/L expression in E. coli BL21(DE3)RIL*

As the expression level of Hyal-1/L was found to be rather low compared to the other hyaluronidase subtypes (**Fig. 3.5**), experiments were performed with varying IPTG concentrations and induction times (**Fig. 3.6**).

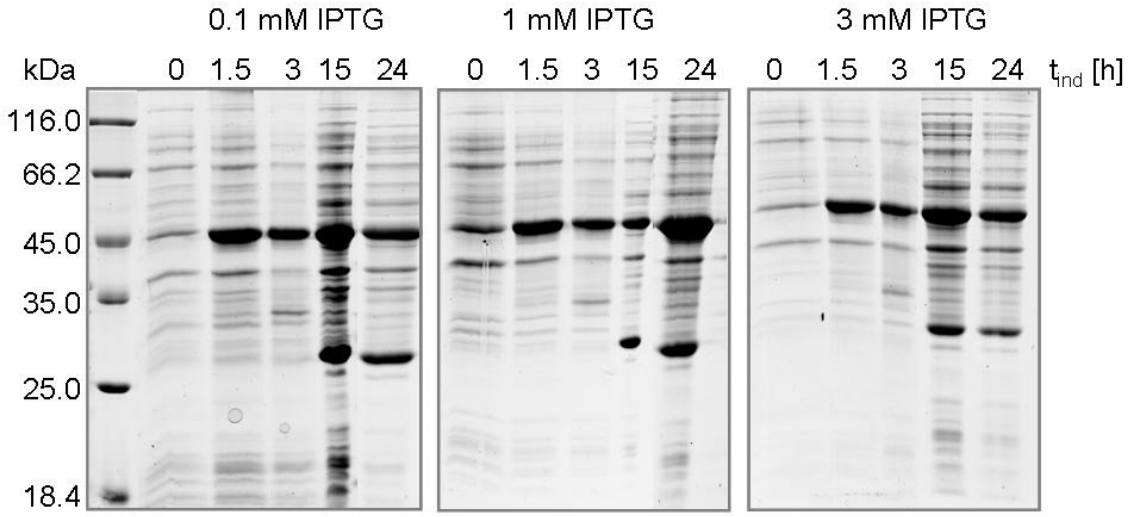


**Fig. 3.6** SDS-PAGE analysis of cell lysates of *E. coli* BL21(DE3)*RIL*/pET15b/*hyal-1/L* at various time points ($t_{ind}$) after induction of Hyal-1/L expression by IPTG at various concentrations.

Variations in the IPTG concentration used for the induction of expression did not influence the amount of recombinant protein significantly. Elongation of the periods of induction for more than 3 h resulted in an increased expression of low molecular weight impurities, mainly a protein of ca. 28 kDa (**Fig. 3.6**) possibly being a degradation product of the recombinant Hyal-1/L.

In comparison to the expression of Hyal-1/L observed in 3.3.4 the expression in the optimization experiments was much stronger due to the use of an overnight culture grown for only 10 h from a freshly transformed bacterial colony. In the experiments shown in 3.3.4 glycerol stocks were used for the preparation of overnight cultures, which were incubated for ca. 15 h. Therefore, standard expression of Hyal-1/L was performed with 1 mM IPTG and an induction time of 3 h. As the overnight culture conditions influenced the protein expression levels significantly overnight cultures were induced with colonies of freshly transformed bacteria and grown for < 12 h. The decrease in expression levels after long periods of incubation was probably due to depletion of ampicillin allowing the growth of bacteria lacking the pET15b plasmid.

Proteins expressed as insoluble, inactive aggregates are known to be hardly toxic for *E. coli* (Baneyx and Mujacic 2004), a problem that occurs rather often when working with soluble recombinant proteins. However, bacterial growth could be inhibited by the presence of insoluble aggregates of foreign protein expressed under control of the strong T7 promotor, which is, as shown above, not completely tight.

### *3.3.6. Expression of the human hyaluronidase subtypes in E. coli Rosetta-gami™(DE3)*

To allow for disulfide bond formation in the cytoplasm of bacteria *E. coli* strains have been developed, which are deficient in glutathione reductase and thioredoxin reductase. The *E. coli* strain Rosetta-gami™(DE3) exhibiting this deficiency additionally enhances the expression of proteins containing codons rarely used in bacteria.

Therefore, the human hyaluronidases were expressed in *E. coli* Rosetta-gami™(DE3) using the pET15b plasmid, which already proved high expression levels in *E. coli* BL21(DE3)*RIL*. Rosetta-gami™(DE3) grew much slower than other strains (24 h till colony formation on agar plates). As this bacteria strain contains several plasmids, e.g. for the expression of rare codons, growth was performed in the presence of multiple antibiotics (kanamycin, tetracycline, chloramphenicol), which possibly slows down bacterial growth. Nevertheless, expression of the foreign genes could be achieved 3 h after induction of expression (**Fig. 3.7**).

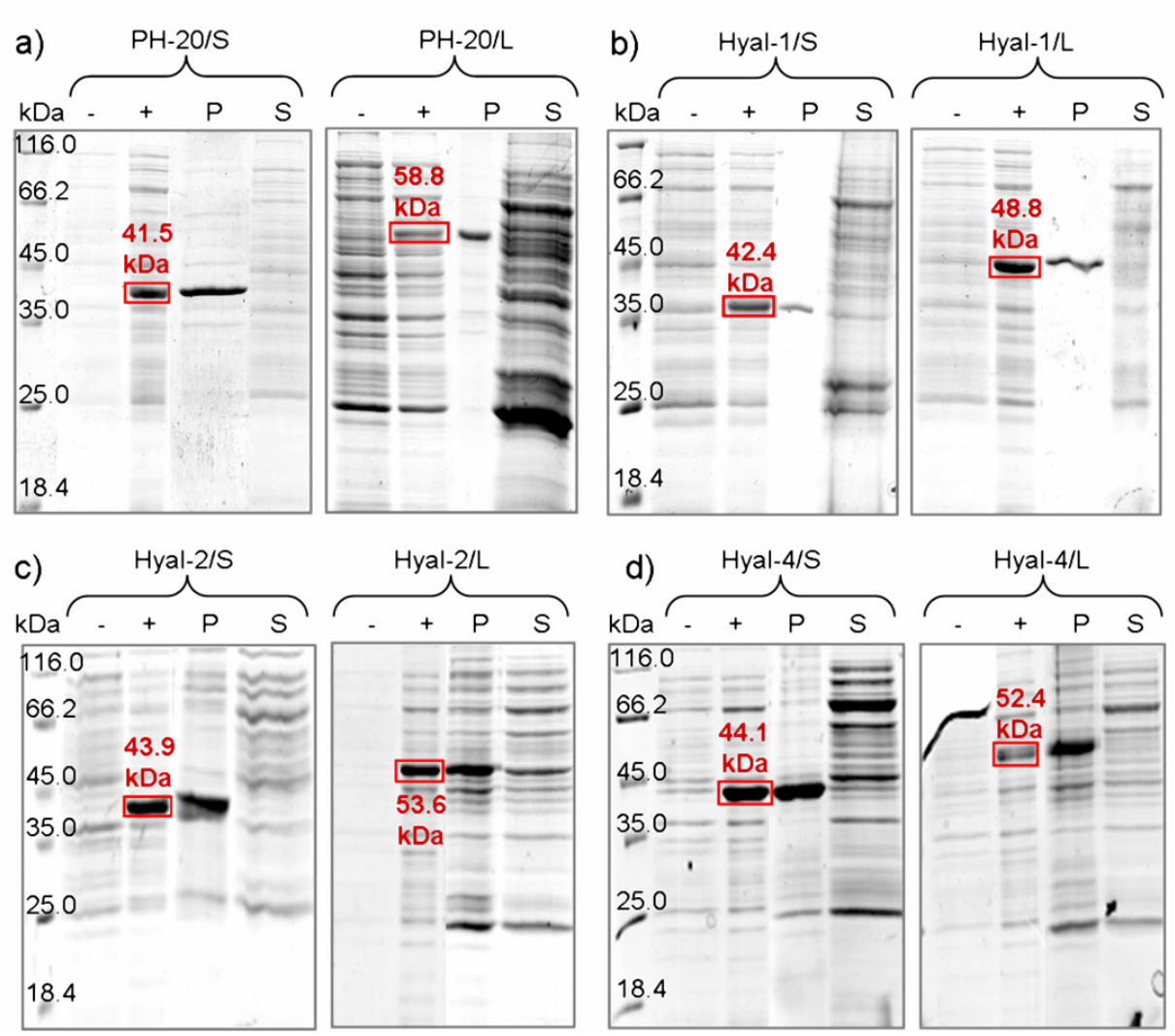


**Fig. 3.7** Recombinant expression of the long (L) and short (S) variants of the human hyaluronidases PH-20, Hyal-1, Hyal-2 and Hyal-4 in Rosetta-gami™(DE3). The SDS-PAGE analysis shows total cell lysates before (-) and 3 h after induction (+) as well as the soluble cell lysate fraction (supernatant, S) and the insoluble cellular fraction (pellet, P). Molecular masses of the proteins were calculated using the molecular weight markers.

Separation of the total cell lysates into soluble and insoluble fractions revealed that the main fraction of all hyaluronidases was found in the cell pellet. To investigate if any properly folded hyaluronidase was present in the soluble cell fraction the soluble cell fractions were assayed for hyaluronidase activity in the turbidimetric activity assay at pH 4.0 and 5.0, respectively (**Fig. 3.8**).

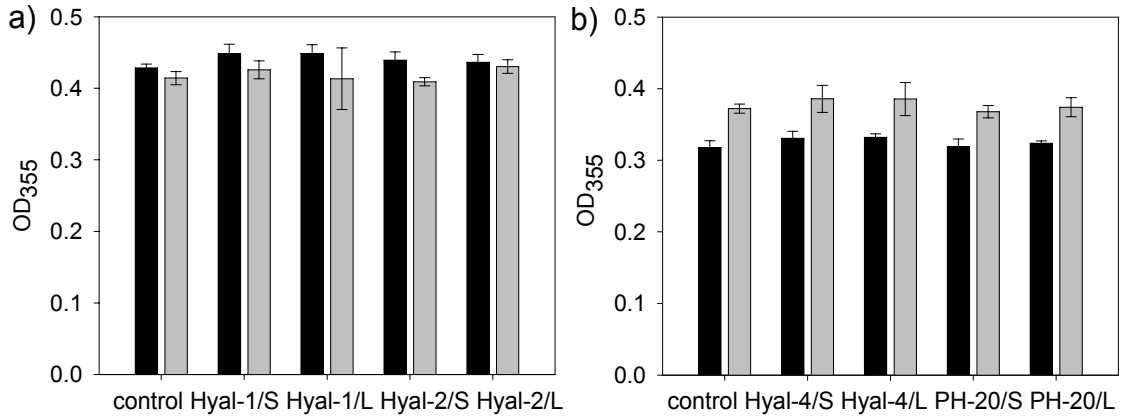


**Fig. 3.8** Turbidimetric hyaluronidase activity assay at pH 4.0 (a) and pH 5.0 (b) using soluble cell fractions from Rosetta-gami$^{TM}$(DE3)/pET15b/*hyaluronidase* as samples. Incubation was stopped after 0 (black bars) and 24 h incubation (grey bars) at 37 °C. As a control lysis buffer was treated identical to the samples.

As Hyal-1 and Hyal-2 are presumably acid active enzymes (Frost et al. 1997, Lepperdinger et al. 1998) they were assayed for hyaluronidase activity at pH 4.0. Bovine PH-20 is known to have an activity optimum at pH 5.0 – 6.0 in the turbidimetric assay (Hoechstetter 2005). Therefore, cell fractions containing human PH-20 were tested for hyaluronidase activity at pH 5.0. None of the soluble cell fractions showed hyaluronidase activity in the turbidimetric activity assay, i.e. turbidity was not found to be reduced after 24 h of incubation compared to the turbidity measured directly after addition of the sample to the assay system. Since not even the hyaluronidases with well known activity profiles (Hyal-1 and PH-20) showed any enzymatic activity, no further variations of pH or substrate were tested for Hyal-2 and Hyal-4.

The results obtained in the turbidimetric assay were confirmed in the colorimetric activity assay (data not shown), which revealed a significantly increased absorbance of 0.05 – 0.2 $A_{585}$ for the reference samples (incubation time 0). This observation could be explained by the presence of sugar moieties in the cytoplasm of bacteria reacting in the Morgan-Elson assay. However, no increase in the absorbance at 585 nm was observed after 24 h of incubation of HA with the soluble cell fractions.

## 3.4. Summary and conclusions

The human hyaluronidases PH-20, Hyal-1, Hyal-2 and Hyal-4 were expressed in *E. coli* as fusion proteins with an N-terminal His-tag. All enzymes were expressed in their whole length as well as in C-terminally truncated variants and were found to be expressed in high levels in *E. coli* BL21(DE3)*RIL*. The human hyaluronidases formed insoluble aggregates in the cytoplasm of the bacteria as anticipated from the presence of several disulfide bridges in the native hyaluronidases. During isolation of the inclusion bodies partial purification of the hyaluronidases could be achieved.
Furthermore, the *E. coli* strain Rosetta-gami$^{TM}$(DE3) facilitating the formation of disulfide bonds in the cytoplasm was tested for the expression of active hyaluronidases, but yielded only insoluble protein aggregates as well. Possibly, disulfide bridge formation in the cytoplasm was insufficient or incorrect, thus resulting in wrong folding of the hyaluronidases.

Since no active hyaluronidases could be expressed in the bacterial systems *in vitro* protein folding experiments were necessary to gain enzymatically active human hyaluronidases. Due to the absence of reliable activity assays for Hyal-2 and Hyal-4 folding experiments were attempted for Hyal-1 and PH-20 only as described in the following chapter.

## 3.5. References

Baneyx F., Mujacic M. (2004). Recombinant protein folding and misfolding in Escherichia coli. *Nat. Biotechnol.* **22**: 1399-1408.

Bendtsen J.D., Nielsen H., von Heijne G., Brunak S. (2004). Improved prediction of signal peptides: SignalP 3.0. *J. Mol. Biol.* **340**: 783-795.

Benson D.A., Karsch-Mizrachi I., Lipman D.J., Ostell J., Wheeler D.L. (2006). GenBank. *Nucleic Acids Res.* **34**: D16-20.

Bessette P.H., Aslund F., Beckwith J., Georgiou G. (1999). Efficient folding of proteins with multiple disulfide bonds in Escherichia coli cytoplasm. *Proc. Natl. Acad. Sci. U. S. A.* **96**: 13703-13708.

Boeckmann B., Bairoch, A., Apweiler, R., Blatter, M.-C., Estreicher, A., Gasteiger, E., Martin, M.J., Michoud, K., O'Donovan, C., Phan, I., Pilbout, S., Schneider, M. (2003). The SWISS-PROT protein knowledgebase and its supplement TrEMBL in 2003. *Nucleic Acids Res.* **31**: 365-370.

Di Ferrante N. (1956). Turbidimetric measurement of acid mucopolysaccharides and hyaluronidase activity. *J. Biol. Chem.* **220**: 303-306.

Frost G.I., Csoka T.B., Wong T., Stern R. (1997). Purification, Cloning, and Expression of Human Plasma Hyaluronidase. *Biochem. Biophys. Res. Commun.* **236**: 10-15.

Georgiou G., Segatori L. (2005). Preparative expression of secreted proteins in bacteria: status report and future prospects. *Curr. Opin. Biotechnol.* **16**: 538-545.

Graumann K., Premstaller A. (2006). Manufacturing of recombinant therapeutic proteins in microbial systems. *Biotechnol. J.* **1**: 164-186.

Hahm M.S., Chung B.H. (2001). Refolding and Purification of Yeast Carboxypeptidase Y Expressed as Inclusion Bodies in Escherichia coli. *Protein Expr. Purif.* **22**: 101-107.

Hoechstetter J. (2005). Characterisation of bovine testicular hyaluronidase and a hyaluronate lyase from Streptococcus agalactiae. *Doctoral thesis*. University of Regensburg. http://www.opus-bayern.de/uni-regensburg/volltexte/2005/519/

Jaenicke R., Rudolph R. Folding proteins. *in: Protein structure - a practical approach.* T.E. Creighton ed. IRL Press. Oxford. (1989). pp.191-223.

Lennon G.G., Auffray C., Polymeropoulos M., Soares M.B. (1996). The I.M.A.G.E. Consortium: an integrated molecular analysis of genomes and their expression. *Genomics* **33**: 151-152.

Lepperdinger G., Strobl B., Kreil G. (1998). HYAL2, a human gene expressed in many cells, encodes a lysosomal hyaluronidase with a novel type of specificity. *J. Biol. Chem.* **273**: 22466-22470.

Markovic-Housley Z., Miglinerini G., Soldatova L., Rizkallah P., Müller U., Schirmer T. (2000). Crystal Structure of Hyaluronidase, a Major Allergen of Bee Venom. *Structure* **8**: 1025-1035.

McIlvaine T.C. (1921). A buffer solution for colorimetric comparison. *J. Biol. Chem.* **49**: 183-186.

Rattenholl A., Lilie H., Grossmann A., Stern A., Schwarz E., Rudolph R. (2001). The pro-sequence facilitates folding of human nerve growth factor from Escherichia coli inclusion bodies. *Eur. J. Biochem.* **268**: 3296-3303.

Rogers J. (2003). The finished genome sequence of Homo sapiens. *Cold Spring Harb. Symp. Quant. Biol.* **68**: 1-11.

Schmidt F.R. (2004). Recombinant expression systems in the pharmaceutical industry. *Appl. Microbiol. Biotechnol.* **65**: 363-372.

Sethuraman N., Stadheim T.A. (2006). Challenges in therapeutic glycoprotein production. *Curr. Opin. Biotechnol.* **17**: 341-346.

Swiss-Prot/TrEMBL. ExPASy Proteomics Server. http://us.expasy.org.

Terpe K. (2006). Overview of bacterial expression systems for heterologous protein production: from molecular and biochemical fundamentals to commercial systems. *Appl. Microbiol. Biotechnol.* **72**: 211-222.

Yoshihiro S., Yutetsu K., Bei-Wen Y., So U., Takuya U. (2006). Cell-free translation systems for protein engineering. *FEBS J.* **273**: 4133-4140.

# Chapter 4

# *In vitro* folding experiments with the human hyaluronidases PH-20 and Hyal-1 expressed in *E. coli*

## 4.1. Introduction

Eukaryotic proteins over-expressed in *E. coli* often form insoluble, dense aggregates, so-called inclusion bodies (IBs) (Marston 1986). IBs consist almost exclusively of the over-expressed protein and can amount to more than 50 % of the total cell protein (Lilie et al. 1998). Proteins, such as the human hyaluronidases, which contain disulfide bridges, form IBs in the majority of cases if they are produced in the reducing cytoplasm of *E. coli* (Lilie et al. 1998, Tsumoto et al. 2004). As solubilization of IBs can only be achieved after complete denaturation of the protein (Lange and Rudolph 2005) great efforts have been undertaken to provide general methods for the renaturation of proteins from IB material under *in vitro* conditions.

Urea and guanidinium chloride (GdmCl) are the most frequently used denaturing (chaotropic) agents as they are assumed to keep proteins in a disordered, flexible and soluble state (Tsumoto et al. 2003) due to their preferential binding to the unfolded protein (Timasheff 1992, Bhuyan 2002). To bring the denatured proteins into a compact, properly folded conformation the denaturing agent is removed while the protein is transferred to an aqueous solvent (Tsumoto et al. 2003).

The concentration of the chaotropic agent can be reduced slowly as occurring during dialysis. Since the protein can adopt partially folded structures at medium denaturant concentrations,

this method is only applicable if the intermediate folding states are not prone to aggregation (De Bernadez Clark et al. 1999, Tsumoto et al. 2003). Otherwise the denatured protein can be folded by direct dilution of a concentrated, denatured protein solution in the folding buffer. Quick mixing results in a fast drop of the denaturant concentration and a collapse of the protein structure (Tsumoto et al. 2003), thus avoiding partially folded protein structures at intermediate denaturant concentrations. To keep aggregation low, even at higher protein concentrations, the protein is often added in several pulses or continuously (Vallejo and Rinas 2004). Another *in vitro* folding method is the matrix-assisted folding, i.e. the protein is bound to a solid support under denaturing conditions, and is folded while still bound to the matrix (Li et al. 2004). This technique can be used with a variety of protein tag fusions resistant to chaotropic agents, thus combining folding with purification (Vallejo and Rinas 2004). However, protein binding to the matrix can also cause sterical hindrance of the folding reaction (Tsumoto et al. 2003).

Folding of proteins *in vivo* is facilitated by chaperones (Deuerling and Bukau 2004), disulfide bridge isomerases (Frand et al. 2000) and small, polar molecules like sugars, salts and amino acids (Yancey et al. 1982). *In vitro* methods have been developed utilizing the same principles: chaperones or artificial chaperone systems supporting the folding process (Rozema 1996, Daugherty et al. 1998, Walter and Buchner 2002), disulfide shuffling systems allowing for rapid disulfide bridge exchanges (Wetlaufer 1984) and the use of stabilizing and solubilizing reagents, respectively, for the improvement of folding yields (De Bernadez Clark et al. 1999, Lange and Rudolph 2005).

For extracellular or membrane-anchored proteins the formation of correct disulfide bonds is often essential for proper folding. Oxidation of cysteine residues can be facilitated by air oxygen in the presence of $Cu^{2+}$ ions (Menzella et al. 2002) or by a disulfide shuffling system, consisting of low molecular weight thiols such as glutathione or C in their reduced and oxidized state (Wetlaufer 1984, Vallejo and Rinas 2004).

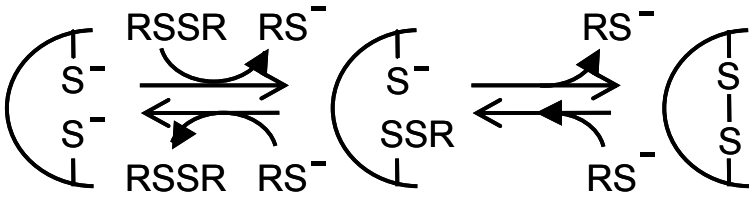


**Fig. 4.1** Principle of disulfide bridge formation in a protein facilitated by a disulfide shuffling system containing low molecular weight thiols in the reduced ($RS^-$) and oxidized state (RSSR). (Adapted scheme according to Jaenicke and Rudolph 1989)

At alkaline pH (pH > 8.0) the C residues of the protein can react with the disulfide shuffling system forming mixed disulfides and finally intramolecular cystines, which are supposed to be energetically favored, if the resulting protein structure is the native one (**Fig. 4.1**) (Lange and Rudolph 2005).

Protein folding can be supported by addition of low molecular weight compounds, so called co-solutes, either enhancing intra- and intermolecular interactions ("folding enhancer") or increasing the solubility of unfolded or partially folded protein structures ("aggregation suppressors") (Tsumoto et al. 2003). Among the variety of substances successfully used as folding aids, the amino acid arginine (Arg) is the most common one (De Bernadez Clark et al. 1999). Arginine is believed to reduce protein-protein interactions (Baynes et al. 2005, Reddy et al. 2005) possibly by preferential interactions with tyrosin residues (Tsumoto et al. 2004). However, the exact mechanism of action is not completely understood.
Further co-solutes suppressing aggregation are polymers (Cleland et al. 1992), detergents (Krause et al. 2002) and chaotropic agents at low concentrations (Orsini and Goldberg 1978). Contrarily, co-solutes like sugars (Arakawa and Timasheff 1982), polyols and some salts (Hofmann et al. 1995, Lange and Rudolph 2005) enhance the formation of the compact, native protein structure ("folding enhancers"), but also favor aggregation. Since the effects of the folding aids depend on specific changes in the excluded volume of the co-solutes and interactions with the protein surface (Schellman 2003), the properties of the protein of interest determine the use of the folding agents.

*In vitro* folding of an enzyme can be monitored easily in an appropriate activity assay. Therefore, *in vitro* folding of the human hyaluronidases expressed in *E. coli* (cf. Chapter 3) was performed with PH-20 and Hyal-1 due to the knowledge of the substrate and the availability of reliable activity assay systems (Gold 1982, Gmachl and Kreil 1993). *In vitro* folding of Hyal-2 and Hyal-4 was omitted due to the lack of information about the substrate and appropriate activity assays. Denatured bovine testicular hyaluronidase (BTH) was used as a reference to observe the refolding of a mammalian hyaluronidase.

## 4.2. Materials and Methods

### *4.2.1. Chemicals*

Wet yeast extract was purchased from OHLY (Deutsche Hefewerke, Hamburg, Germany). Hyaluronic acid from *Streptococcus zooepidemicus* was purchased from Aqua Biochem GmbH, Dessau, Germany. Lysozyme was from Boehringer Mannheim GmbH, Mannheim, Germany, Benzonase from Merck, Darmstadt, Germany. BTH (Neopermease®, 50 000 IU/mg, according to the supplier) was a gift from Sanabo, Vienna, Austria. BSA was purchased from Serva, Heidelberg, Germany, Cetyltrimethylammonium bromide (CTAB) and Tween 20 from Roth, Karlsruhe, Germany, and IPTG, *p*-dimethylaminobenzaldehyde (DMAB), GlcNAc and L-arginine · HCl (Arg) from Sigma, Munich, Germany. All other chemicals were from Merck, Darmstadt, Germany.

### *4.2.2. Fermentation of E. coli BL21(DE3)RIL/pET15b/hyal-1/L*

6 L of sterile complete medium (50 g/L wet yeast extract, 5.0 g/L glucose, 11 g/L $K_2HPO_4 \cdot 2\ H_2O$, 0.5 g/L $NH_4Cl$, 0.68 g/L $MgSO_4 \cdot 7\ H_2O$) containing 100 µg/mL of ampicillin were initiated by addition of 100 mL of *E. coli* BL21(DE3)*RIL*/pET15b/*hyal-1/L* overnight culture grown for 9 h in LB-medium with 100 µg/mL ampicillin. Fermentation was monitored by measuring cell density ($OD_{600}$), pH, temperature, pressure and glucose concentration. The pH was controlled by automatic addition of 10 % (v/v) $H_3PO_4$ and 10 % (v/v) KOH, respectively. At the beginning of the fermentation process the pH was adjusted to 7.5 to ensure a strong growth of bacteria in the presence of glucose. At an $OD_{600}$ of 22.2 (6 h after initiation) the glucose of the medium was depleted and the culture was fed for a further 1.5 h by addition of sterile feeding solution (30 % (w/v) wet yeast extract, 25 % (v/v) glycerol in water) at a flow rate of 2.5 mL/min. When feeding of the culture was started, the pH was adjusted to 6.5. 7.5 h after initiation of the culture, 1 mM IPTG (from a 1 M stock solution in water) was added to induce expression of Hyal-1/L. The bacteria were cultured for 4 h before the suspension was centrifuged (20 min, 6,000 g, 4 °C), and the pellets stored at -80 °C.

### *4.2.3. Isolation and solubilization of inclusion bodies (IBs)*

A bacterial pellet of 1 g (wet weight) was resuspended in 5 mL of 100 mM Tris/HCl, 1 mM EDTA, pH 7.0. After addition of 7.5 mg of lysozyme the suspension was kept on ice for 30 min. To support cell lysis the cells were sonicated on ice (microtip, power level 4 – 5, 40 – 50 % Duty, 3 times 15 s continuous mode, Branson-Sonifier B15, G. Heinemann, Schwäbisch-Gmünd, Germany). For pellets > 100 g a French press was used for cell lysis. Then 5 µL of

benzonase (25 U/mL) and 15 µL of 1 M $MgCl_2$ were added and the suspension incubated at room temperature for 30 min. After addition of 2.5 mL of 3 x TEN buffer (60 mM EDTA, 6 % Triton X-100, 1.5 M NaCl, pH 7.0), the mixture was incubated for 30 min on ice. Then the IBs were pelleted by centrifugation (15 min, 5,000 g, 4 °C) and washed twice with 15 mL of 100 mM Tris/HCl, 20 mM EDTA, pH 7.0. Resuspension of the dense protein aggregates was facilitated by the use of an ultraturrax.

After the last washing step the IB pellet was solubilized in denaturing buffer (8 M urea or 6 M GdmCl, 20 mM Tris/HCl, 1 mM EDTA, 50 mM DTT, pH 8.5) to gain a protein concentration of 5 – 10 mg/mL. Solubilization was supported by the use of an ultraturrax. The turbid reddish-brown solution was stirred overnight at room temperature and centrifuged (15 min, 5,000 g, 25 °C) to pellet insoluble membrane fragments. The supernatant was then dialyzed at 4 °C extensively against denaturing buffer without EDTA and DTT (MWCO 14,000).

### *4.2.4. Purification of human hyaluronidases by IMAC under denaturing conditions*

Hyal-1/L was purified by ion metal affinity chromatography (IMAC) with a $Ni^{2+}$ ion immobilized on nitrilotriacetic acid-agarose (NTA-agarose) (Quiagen, Hilden, Germany). The column was equilibrated with 20 mM Tris/HCl, 8 M urea, pH 8.5. After application of the sample the column was washed with 2 column volumes (CV) of 20 mM Tris/HCl, 8 M urea, pH 6.5. Elution was achieved by decreasing the pH of the buffer to 4.5. Fractions of 1 mL were collected and analyzed with respect to their protein concentration and by SDS-PAGE.

While high concentrations of urea do not interfere with SDS-PAGE analysis, GdmCl forms insoluble aggregates with SDS. Therefore, GdmCl was removed from the samples by the following procedure: the sample (maximum 100 µL) was mixed with water to obtain a final volume of 1 mL. Then 100 µL of 1 % (w/v) sodium deoxycholate were added, the sample was vortexed and 200 µL of 50 % (w/v) TCA were added. The turbid solution was mixed again thoroughly. Protein aggregates were pelleted by centrifugation (15 min, 12,000 g), washed once with 1 mL of acetone, and the pellet was dried. Proteins were then resuspended in 20 – 100 µL of SDS-sample buffer and prepared for SDS-PAGE (cf. Chapter 3).

For protein folding experiments the fractions containing recombinant hyaluronidase were combined and concentrated in centrifugal devices (MWCO 30,000, Millipore, Eschborn, Germany) until a protein concentration of 3 – 10 mg/mL was reached.

### *4.2.5. In vitro protein folding*

Folding experiments were performed by direct dilution of a concentrated protein sample in the folding buffer. The concentrated protein solution was added dropwise under intensive stirring to a degassed folding buffer. Basically, the folding buffer contained 20 mM Tris/HCl, 0.2 mg/mL BSA and 1 mM EDTA, pH 8.5. Further additives as well as variations in the basic buffer system are indicated for the respective experiments. The pH of the folding buffer was adjusted after addition of all additives. Aggregation could be observed immediately after dilution by measuring the optical density (OD) at 400 nm. Enzymatic activity assays (cf. 4.2.8 and 4.2.9) were performed at different time periods after initiation of the folding reaction.

Folding by air oxidation (Menzella et al. 2002) was tested by direct dilution of the protein solution in a buffer containing 100 mM Tris/HCl, 50 mM NaCl, 10 µM $CuSO_4$, pH 10, under intensive stirring at room temperature for 24 h.

As some folding additives were found to have a strong influence on the hyaluronidase activity assays, all samples underwent a buffer exchange into 100 mM Tris/HCl, 20 mM NaCl, pH 7.0, (for BTH and PH-20) or into 20 mM Tris/HCl, pH 7.5, (for Hyal-1) either by dialysis or by gel filtration (Sephadex G-25 NAP$^{TM}$ columns, GE Healthcare Bio-sciences AB, Uppsala, Sweden).

### *4.2.6. Determination of protein concentrations*

Protein concentrations were determined by the method of Bradford (Bradford 1976) using the Bio-Rad protein assay (Bio-Rad, Munich, Germany) with BSA as a standard substance. The assay was performed according to the supplier's instructions.

### *4.2.7. SDS-PAGE and Western blot*

SDS-PAGE was performed as described in Chapter 3. Western blotting was achieved in a Perfect-Blue "Semi-Dry" electro blot apparatus (Peqlab, Erlangen, Germany). As protein standard the peqGOLD Prestained Protein-Marker (Peqlab, Erlangen, Germany) was used. After electrophoresis the gel was equilibrated for 5 min in transfer buffer (25 mM Tris/HCl, pH 8.3, 192 mM glycine, 20 % (v/v) methanol), placed on top of a nitrocellulose membrane (0.2 µm, Peqlab, Erlangen, Germany) between 6 filter slides equilibrated in transfer buffer and blotted for 1.5 h at 10 mA/10 cm² of membrane.

Then, the membrane was blocked by shaking for 1 h in 5 % (w/v) fat-free milk powder solubilized in PBS. The membrane was washed 3 x 5 min in washing buffer (0.05 % (v/v) Tween 20 in PBS) and then incubated for 2 h with primary antibody (mouse anti-His IgG,

Dianova, Hamburg, Germany) diluted 2000-fold in 10 mL of washing buffer. The primary antibody was washed away (see above) and the membrane was incubated for 1 h with 5 µL of secondary antibody (biotinylated anti-mouse/rabbit IgG, Vector Laboratories, Burlingame, USA) in 10 mL of washing buffer.

After washing the membrane was incubated with a biotin/avidin/horseradish peroxidase (HRP) reaction kit (VECTASTAIN® ABC-kit Standard, Vector Laboratories, Burlingame, USA), which was prepared 30 min before use according to the manufacturer's instructions. After a further washing step the membrane was stained with DAB (diaminobenzidine) staining solution as described by the supplier (DAB kit, Vector Laboratories, Burlingame, USA). Brown bands occurred after 2 – 15 min. Excessive substrate was washed away with water and the dry membrane was scanned with a DAB/HRP filter on a Bio-Rad gel detection system (GS-710 Imaging Densitometer) using Quantity One quantification software, version 4.0.3. (Bio-Rad, Munich, Germany).

### *4.2.8. Turbidimetric hyaluronidase activity assay*

The turbidimetric hyaluronidase activity assay was performed as described in Chapter 3. All measurements were correlated to internal negative controls containing the same incubation mixtures as the samples, but buffer solution instead of enzyme. The buffer was chosen according to the buffer solution used for the solubilization of the respective enzyme. The optical density values given in the results and discussion section are mean values ± SEM (standard error of means) of triplicates.

For human PH-20 and BTH McIlvaine's buffer, pH 5.0, was used as an incubation buffer, for human Hyal-1 either McIlvaine's buffer, pH 4.0, or 0.1 M Na-formate, 0.1 M NaCl, pH 3.5, was used. McIlvaine's buffer was prepared by mixing solution A (0.2 M $NaH_2PO_4$, 0.1 M NaCl) and solution B (0.1 M citric acid, 0.1 M NaCl) in appropriate portions to adjust the required pH.

### *4.2.9. Colorimetric hyaluronidase activity assay (Morgan-Elson assay)*

The colorimetric assay based on the method described by Reissig et al. (Reissig et al. 1955) was performed according to Muckenschnabel et al. (Muckenschnabel et al. 1998). Degradation products of hyaluronic acid were quantified by the amount of GlcNAc formed at the reducing ends of the HA chains by measuring the absorbance of the Morgan-Elson reaction product at 585 nm (Muckenschnabel et al. 1998). Calibration curves were determined with GlcNAc under identical assay conditions.

According to the International Union of Biochemistry 1 unit (U) of hyaluronidase is defined as the enzymatic activity catalyzing the liberation of 1 µmol GlcNAc at the reducing ends of sugars per min under specified conditions, i. e. in a reaction mixture containing 50 µL of enzyme sample, 150 µL of $H_2O$, 100 µL of BSA (0.2 mg/mL), 100 µL of buffer (0.2 M Na-formate, 0.1 M NaCl, pH 3.68) and 50 µL of substrate (5 mg/mL of HA from rooster comb in $H_2O$). 0.1 mU (0.1 nmol GlcNAc/min) are approximately equivalent to 1 international unit (IE) (Muckenschnabel et al. 1998).

If buffer conditions varied from the conditions mentioned above, the enzymatic activity is given as µmol GlcNAc/min in the respective incubation mixture. During *in vitro* folding experiments the hyaluronidase activity was either referenced to the folding buffer volume (µmol GlcNAc·$min^{-1}$·$mL^{-1}$) or to the mass of protein present in the folding mixture (µmol GlcNAc·$min^{-1}$·$mg^{-1}$).

All incubation mixtures were prepared with HA from *S. zooepidemicus* and with the volumes described above. As incubation buffers McIlvaine's buffer at various pH and 0.1 M Na-formate, 0.1 M NaCl, pH 3.5, respectively, were used. Incubation buffers are indicated for each experiment.

## 4.3. Results and discussion

### *4.3.1. Refolding of bovine testicular hyaluronidase (BTH)*

To get an idea about *in vitro* folding of mammalian hyaluronidases, control experiments were performed with a commercially available bovine testicular hyaluronidase (BTH) preparation, Neopermease®. As shown previously, BTH consists of three proteins fractions with the 58 kDa fraction exhibiting the highest specific activity (Oettl et al. 2003). The specific activity of BTH was determined to be 2.5 µmol·$min^{-1}$·$mg^{-1}$, which is in accordance to the manufacturer's declaration (Oettl 2000). The pH optimum as well as optimum ionic strength in the buffer system are well known from previous experiments (Hoechstetter 2005), thus enabling the determination of hyaluronidase activity during folding experiments under optimized incubation conditions.

For refolding, BTH was treated identically to the IB material after the last washing step, i.e. BTH was completely reduced and denatured. Refolding was monitored by the regain of enzymatic activity in the turbidimetric hyaluronidase activity assay (**Fig. 4.2**).

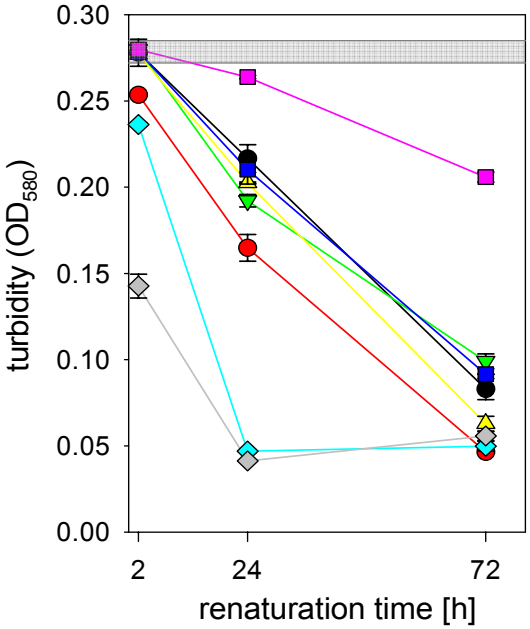


| | GSSG : GSH | Additives |
|---|---|---|
| ● | 1 mM : 10 mM | - |
| ● | 1 mM : 3 mM | - |
| ▽ | 10 mM : 1 mM | - |
| △ | 1 mM : 10 mM | 0.5 M Arg |
| ■ | 1 mM : 10 mM | 1.0 M Arg |
| ■ | 1 mM : 10 mM | 0.3 M $NaSO_4$ |
| ◆ | 1 mM : 3 mM | 0.2 mg/ml BSA |
| ◆ | 1 mM : 3 mM | 0.2 mg/ml BSA, 1.0 M Arg |

**Fig. 4.2** Refolding of 50 µg/mL BTH monitored by the regain of enzymatic activity in the turbidimetric activity assay after an incubation period of 1 h. The basic folding buffer was supplemented with a disulfide shuffling system (GSSG/GSH) and folding additives as indicated in the table. In the absence of enzymatic activity $OD_{580}$ was determined to be 0.279 ± 0.007, indicated by the grey area in the chart.

Though denaturation of BTH was only observed by the loss of enzymatic activity, the concentrations of denaturing and reducing agent (6 M GdmCl, 50 mM DTT) were assumed to result in a complete reduction of disulfide bridges as well as a complete destruction of tertiary structure (Jaenicke and Rudolph 1989).

A partial regain of activity could be observed in all folding buffers after at least 24 h (**Fig. 4.2**). The velocity of refolding was influenced more intensively by the stabilizing or solubilizing properties of the additives than by the GSSG/GSH ratio. BSA and Arg showed the best effects on the kinetics of refolding. Both additives support solubility and prevent aggregation and adhesion of proteins, respectively (Jaenicke and Rudolph 1989, Baynes et al. 2005). Addition of $NaSO_4$ exhibiting a "folding enhancer" effect (cf. 4.1) (Tsumoto et al. 2003) decreased the yield of active BTH significantly probably due to increased aggregation of folding intermediates. The best folding system containing 0.2 mg/mL BSA and 1.0 M Arg yielded ca. 80 % of the original activity.

As oxidation of disulfide bridges can be achieved by air oxygen with trace amounts of divalent cations catalyzing the process (Jaenicke and Rudolph 1989, Menzella et al. 2002), BTH was also assessed for refolding by air oxidation in the presence of $Cu^{2+}$. Without any further additives a regain of the activity of only 5 – 6 % of the original activity was observed, but if the air oxidation buffer was supplemented with 0.5 M Arg or 0.16 mg/mL gelatine a

regain of enzymatic activity of 24 % and 80 %, respectively, was achieved. These results confirmed the importance of solubilizing agents during refolding of BTH. The choice of the oxidation system seemed to be of minor importance.

### *4.3.2. In vitro folding experiments with PH-20/S and PH-20/L*

Inclusion bodies containing PH-20/S and PH-20/L were isolated from *E. coli* (cf. Chapter 3) and directly used for folding experiments. Folding was performed by direct dilution of a completely denatured and reduced protein solution containing 5 – 10 mg/mL PH-20/S and PH-20/L, respectively, in folding buffers supplemented with additives as used for BTH previously (De Bernadez Clark et al. 1999).

At different time points after initiation of the folding reaction samples were probed for their catalytic activity in the turbidimetric hyaluronidase activity assay with incubation periods between 1 – 24 h. Though a variety of disulfide shuffling systems (GSSG/GSH = 1 mM/10 mM to 10 mM/1 mM, air oxidation) and additives (Arg, BSA, gelatine, salts) was explored, no hyaluronidase activity could be observed for any of the PH-20 derivatives.

### *4.3.3. Preliminary folding experiments with Hyal-1/S and Hyal-1/L*

A first screening of folding conditions for Hyal-1/S and Hyal-1/L was performed in analogy to the refolding of BTH as described in 4.3.1. Samples of the folding mixture were dialyzed and monitored for hyaluronidase activity in the turbidimetric assay (**Fig. 4.3.b**). In contrast to Hyal-1/L, which showed hyaluronidase activity in the presence of 1.0 M Arg in the folding buffer, the C-terminally truncated Hyal-1 derivative, Hyal-1/S, exhibited no enzymatic activity in any of the folding buffer systems (**Fig. 4.3.a**).

Sequence analysis and comparison with the crystal structure of BVH (Markovic-Housley et al. 2000, Jedrzejas and Stern 2005) suggested an inferior role of the C-terminal domain in the catalytic action of the human hyaluronidases (cf. Chapter 1). Moreover, the short variant of the enzyme contains only four cysteine residues in contrast to ten cysteines in Hyal-1/L. If all cysteine residues are combined in a random fashion only three possible disulfide-linked protein isoforms exist theoretically for four cysteine residues (Hyal-1/S), while the ten cysteine residues present in Hyal-1/L provide 945 possible disulfide-bridged protein isoforms (Jaenicke and Rudolph 1989). Based on these preliminary considerations the truncated Hyal-1 variant (Hyal-1/S) was assumed to be better suitable for *in vitro* folding than the full-length

protein (Hyal-1/L). However, the absence of any Hyal-1/S activity indicates a role of the C-terminal domain in folding, stability or activity of the hyaluronidase.

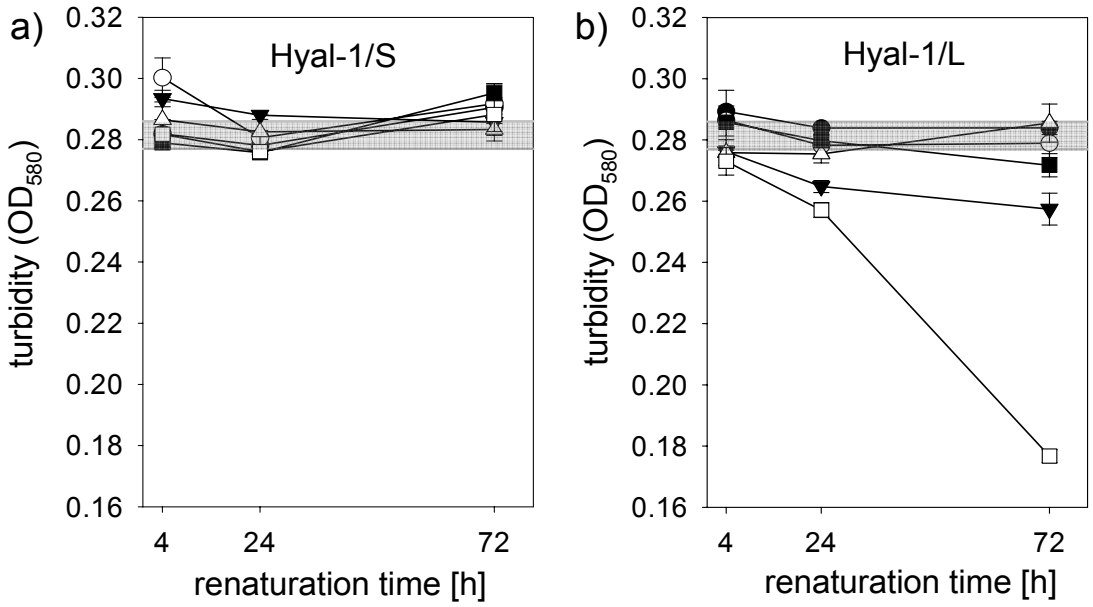


**Fig. 4.3** Variation of the GSSG/GSH ratio and Arg concentrations during folding experiments with Hyal-1/S (a) and Hyal-1/L (b). The folding mixtures contained 50 µg/mL of protein in folding buffer supplemented with the following additives: GSSG/GSH = 1 mM/10 mM (●); GSSG/GSH = 1 mM/3 mM (○); GSSG/GSH = 1 mM/10 mM, 0.5 M Arg (Δ); GSSG/GSH = 1 mM/10 mM, 1.0 M Arg (■); GSSG/GSH = 1 mM/3 mM, 1.0 M Arg (□); GSSG/GSH = 10 mM/1 mM, 1.0 M Arg (▼). Turbidimetric activity assays were performed after dialysis of the samples with an incubation time of 24 h. At zero enzymatic activity the $OD_{580}$ was 0.281 ± 0.005 as indicated by the grey area in the graph.

The folding reaction of Hyal-1/L was significantly influenced by the presence of Arg and the GSSG/GSH ratio of the disulfide shuffling system. The highest enzymatic activity was obtained in a buffer system containing 1.0 M Arg, 1 mM GSSG and 3 mM GSH. The same folding mixture did not enhance activity in the absence of Arg indicating the necessity of solubilizing agents for folding of hyaluronidases in accordance to the results obtained previously for BTH (cf. 4.3.1).

### *4.3.4. Ni-IMAC purification of Hyal-1/L*

Further optimization of the folding conditions was performed with Hyal-1/L purified by Ni-IMAC. Ni-IMAC is advantageous for the purification of IBs as it can be performed in the presence of high concentrations of denaturing agents (8 M urea or 6 M GdmCl). Completely denatured and reduced Hyal-1/L IB material was bound to a Ni-IMAC column and eluted by a decrease of pH (**Fig. 4.4.a**). Protonation of the His-tag at pH values below its $pK_A$ of 6.0 released the recombinant protein from the Ni-complex binding. Hyal-1/L was eluted at pH 4.5

occurring as the major protein band on the SDS-PAGE with a molecular weight of 48 kDa (**Fig. 4.4.b**).

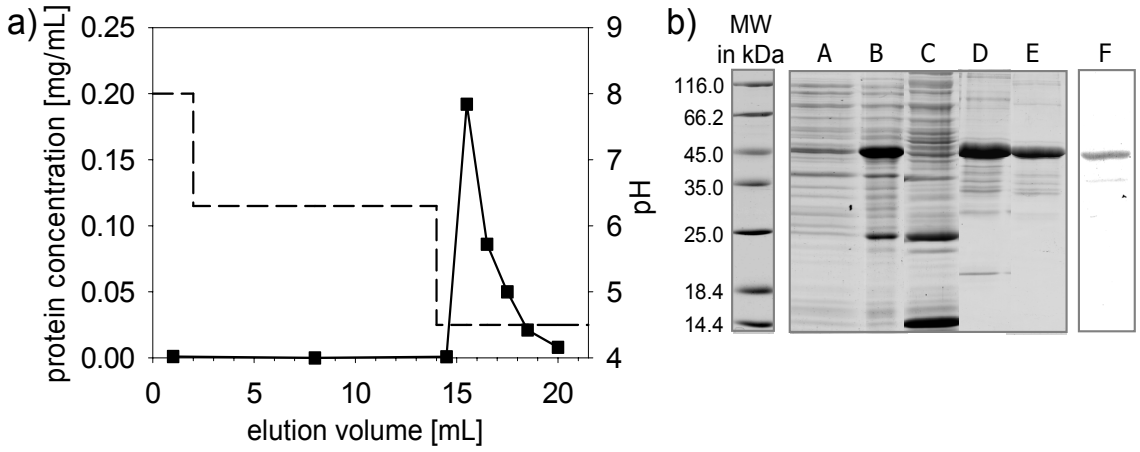


**Fig. 4.4** a) Elution profile of Ni-IMAC (CV 5 mL) purification of Hyal-1/L from IB material as followed by the protein concentration (solid line). All purification steps were performed in 20 mM Tris, 6 M urea with pH values as indicated (dashed line). b) SDS-PAGE analysis of the isolation and purification of Hyal-1/L from *E. coli* BL21(DE3)*RIL*. A) total cell lysate before induction; B) cell lysate 5 h after induction with 1 mM IPTG; C) cytoplasmic fraction; D) insoluble fraction; E) eluate (pH 4.5) of the Ni-IMAC purification; F) Western blot of sample E with anti-His-IgG.

The purification effect achieved by Ni-IMAC was rather low (**Fig. 4.4.b**), but the IBs already showed reasonable purity in SDS-PAGE analysis before purification. No major effects on the folding yield could be seen for Ni-IMAC purified protein in comparison to unpurified IB material. Hyal-1/L was purified either from normal bacterial cultures of from fermented bacteria. Generally, ca. 10 mg of Ni-IMAC purified protein were obtained per g bacterial pellet (wet weight).

### *4.3.5. Influence of the denaturing agent on the aggregation of Hyal-1/L*

Solubilization of IBs was usually performed by addition of 8 M urea or 6 M GdmCl, respectively. Generally, GdmCl is preferred as denaturing agent due to its stronger denaturing properties compared to urea (De Bernadez Clark et al. 1999). Additionally, urea tends to decompose at high pH values into ammonium and cyanate, which can cause side chain modifications of the protein (Stark et al. 1960).

However, if Hyal-1/L was denatured in GdmCl aggregation in the folding mixture was much more pronounced than when folding was performed with urea-denatured Hyal-1/L (**Fig. 4.5**). Surprisingly, the choice of urea instead of GdmCl as denaturing agent prevented aggregation almost completely even at higher protein concentrations, while the addition of 1 M Arg hardly influenced turbidity (**Fig. 4.5**).

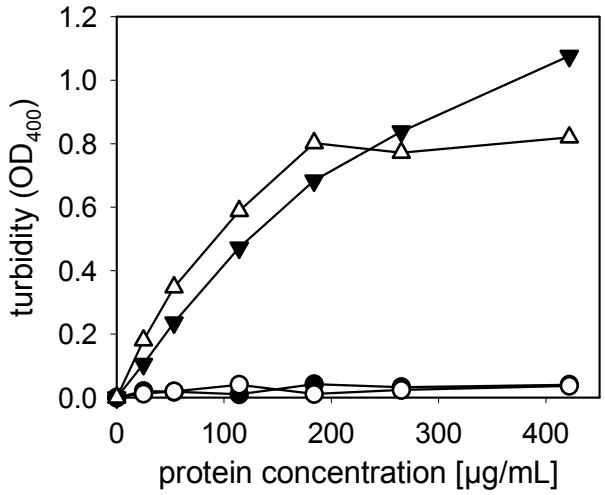


**Fig. 4.5** Aggregation during *in vitro* folding was followed by measuring the turbidity at 400 nm in the folding mixture during addition of Hyal-1/*E. coli* solubilized in 8 M urea (circles) or 6 M GdmCl (triangles). Black symbols show dilution in a folding buffer supplemented with 1 M Arg, white symbols represent a folding mixture without Arg.

Thus, the advantageous effect of Arg on hyaluronidase folding observed by enzymatic activity (cf. 4.3.3) could not be ascribed to the inhibition of aggregation, at least not at a macroscopic scale.

### *4.3.6. Optimization of Hyal-1/L folding conditions*

Initial folding experiments (4.3.3) yielded best *in vitro* folding of Hyal-1/L in a folding buffer system containing 100 mM Tris/HCl, 1 mM EDTA, 0.2 mg/mL BSA, 1 M Arg, 1 mM GSSG and 3 mM GSH at pH 8.5. Based on the successful folding principle established in the initial experiments (**Fig. 4.6**) the folding buffer system as well as the "desalting" methods and buffers were optimized.

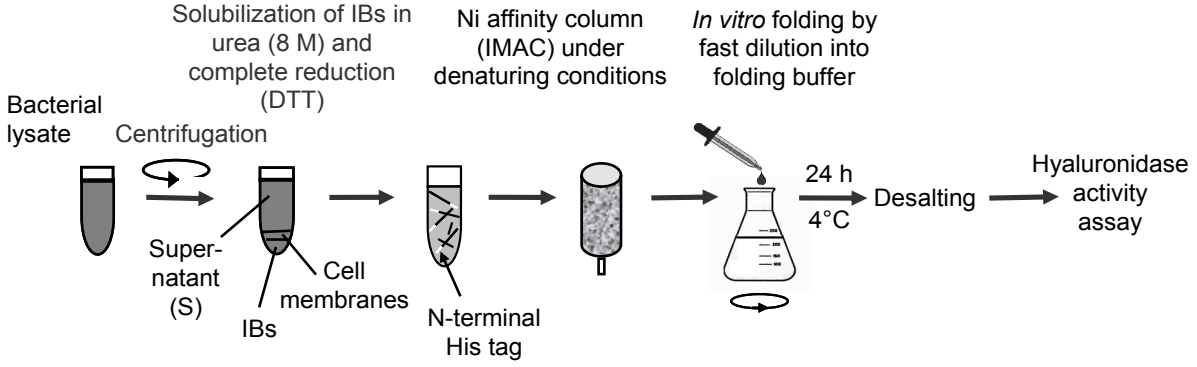


**Fig. 4.6** Schematic presentation of purification and *in vitro* folding of Hyal-1/L expressed in *E. coli*. Folding was monitored by measurement of the hyaluronidase activity after "desalting" of the sample by gel filtration or dialysis.

For further optimization the GSSG content of the folding buffer was increased while the Arg concentration was kept high (0.5 – 1.0 M). **Fig.4.7** shows a strong dependency of the Hyal-1/L folding reaction on the composition of the disulfide shuffling system as observed previously in the preliminary experiments (cf. 4.3.3).

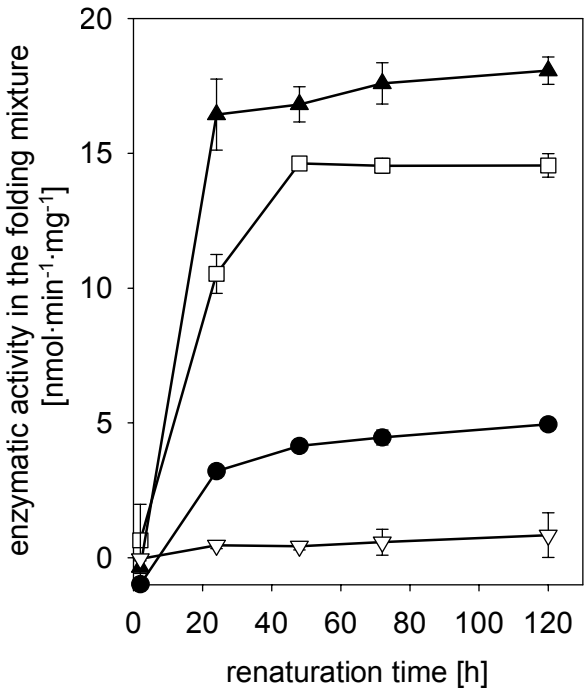


**Fig. 4.7** Folding kinetics monitored via the hyaluronidase activity over 120 h. At t = 0 Ni-IMAC purified, urea-denatured Hyal-1/L was diluted 40-fold in basic folding buffers containing the following additives: GSSG/GSH = 1 mM/3 mM, 0.5 M Arg (●); GSSG/GSH = 1 mM/3 mM, 1 M Arg (□); GSSG/GSH = 1 mM/1 mM, 1 M Arg(▲); GSSG/GSH = 0.3 mM/3 mM, 1 M Arg (▽). The final Hyal-1/L concentration was 50 µg/mL. Enzymatic activity was measured after buffer exchange in the colorimetric hyaluronidase assay using McIlvaine's buffer, pH 4.0, as incubation buffer. Enzymatic activities are mean values ± SEM of three incubation mixtures.

When the folding reaction was monitored over 120 h both, the velocity of the folding reaction and the maximum activity values, were obviously dependent on the GSSG/GSH ratio. The highest enzymatic activity was obtained already 24 h after initiation of the folding reaction in a buffer system containing a 1/1 ratio of GSSG/GSH and 1 M Arg.

Disulfide shuffling is also depending on the degree of deprotonation of C residues in the protein of interest (cf. 4.1). As the $pK_a$ value of C residues in a protein depends on the close environment, a variation of pH values during the folding reaction can influence the amount of C residues available for disulfide bridge formation (Jaenicke and Rudolph 1989).

Variation of the pH between 7.5 and 9.5 during the folding reaction did not influence the efficiency of folding of Hyal-1/L. However, EDTA and BSA were proven to be essential for efficient folding of Hyal-1/L (**Fig. 4.8**). The necessity of EDTA indicates either the presence of metalloproteases, which partially degrade Hyal-1/L during the folding reaction (24 h), or a high sensitivity of Hyal-1/L towards metal ions.

BSA was added to the folding mixture to avoid adhesion of proteins to the surface of the reaction vessel and for stabilization (Jaenicke and Rudolph 1989). Hyaluronidases are known to have a tendency for surface adhesion and are therefore often used in combination with BSA (Gold 1982, Oettl 2000).

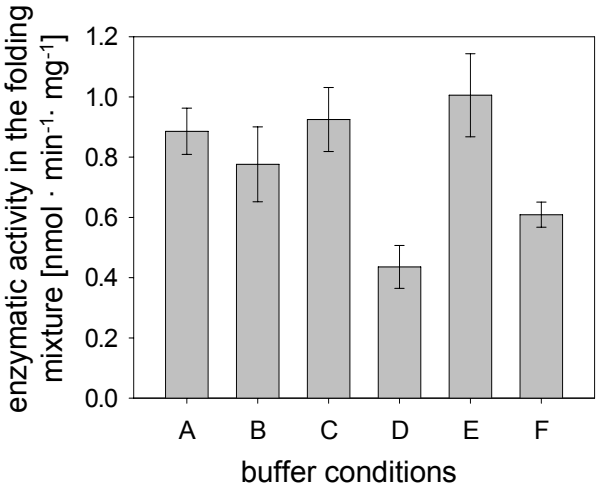


Buffer conditions

| | GSSG : GSH | Additives | pH |
|---|---|---|---|
| **A** | 1 mM : 1 mM | BSA, EDTA | 7.5 |
| **B** | 1 mM : 1 mM | BSA, EDTA | 8.5 |
| **C** | 1 mM : 1 mM | BSA, EDTA | 9.5 |
| **D** | 1 mM : 1 mM | EDTA | 8.5 |
| **E** | 4 mM : 4 mM | BSA, EDTA | 8.5 |
| **F** | 1 mM : 1 mM | BSA | 8.5 |

**Fig. 4.8** Variation of the pH and the additives BSA and EDTA in the folding mixture of Hyal-1/L. Folding was performed by 20-fold dilution of a urea-denatured Hyal-1/L solution in 100 mM Tris/HCl, 1.0 M Arg with additives and pH as indicated. Enzymatic activity in the folding mixture was determined 24 h after initiation of the folding reaction as described in **Fig.4.7**. Enzymatic activities are mean values ± SEM of three incubation mixtures.

However, the use of high concentrations of BSA with a molecular weight of 66 kDa during the folding reaction poses the problem of an additional protein impurity. BSA does not interfere with hyaluronidase activity assays, but disturbs biophysical characterization studies. Therefore, it was tried, if BSA can be excluded from the folding buffer at higher protein concentrations. As shown in **Tab. 4.1** BSA is essential for activity at protein concentrations < 100 µg/mL, but does not influence enzymatic activity at higher protein concentrations (≥ 200 µg/mL) if urea is used as denaturing agent.

**Tab. 4.1** Enzymatic activity in the folding mixture in nmol GlcNAc · $min^{-1}$ · $mg^{-1}$ determined after 24 h of renaturation in the colorimetric activity assay using McIlvaine's buffer, pH 4.0. Folding was achieved by 40-fold dilution of completely denatured Hyal-1/L IBs in basic folding buffer supplemented with 1 mM GSH, 1 mM GSSG and 1.0 M Arg. The chaotropic agents indicate the denaturing reagents (6 M GdmCl and 8 M urea, respectively), the concentrations in µg/mL refer to the protein concentrations in the folding mixtures.

| | | enzymatic activity [nmol·$min^{-1}$·$mL^{-1}$] | |
|---|---|---|---|
| **Folding conditions** | | **- BSA** | **+ BSA** |
| GdmCl | 50 µg/mL | 0.0 | 3.0 |
| | > 100 µg/mL | 0.0 | 0.0 |
| Urea | 50 µg/mL | 0.0 | 4.0 |
| | 200 µg/mL | 4.9 | 5.0 |

A comparison of the enzymatic activities obtained in **Fig. 4.7** and in **Fig. 4.8** revealed an almost 20-fold lower specific enzymatic activity (nmol GlcNAc · $min^{-1}$ · $mg^{-1}$) in the same buffer system (1 mM GSSG, 1 mM GSH, 1 M Arg in the basic folding buffer and a renaturation period of 24 h). This difference can be explained by a higher concentration of

urea in the folding buffer used in **Fig. 4.8** due to a lower dilution factor of the denatured protein solution.

### *4.3.7. Variation of the reducing conditions and pulse experiments*

As aggregation was observed during removal of DTT from the completely reduced and denatured Hyal-1/L by dialysis, folding of Hyal-1/L was determined in the presence of very low DTT concentrations (0.5 mM DTT instead of 50 mM). In this "low reductive system" Hyal-1/L was reduced by addition of 0.5 mM DTT during denaturation in 8 M urea. Residual DTT was not removed from the protein solution, but was oxidized in the folding reaction by addition of GSSG.

To compare both systems, Hyal-1/L IB material was folded at various protein concentrations using a disulfide shuffling system of 1 mM GSSG/1 mM GSH in the standard system and 1.5 mM GSSG/0.5 mM GSH in the low reductive system, respectively, while all other compounds of the folding buffer were kept constant (**Fig. 4.9**).

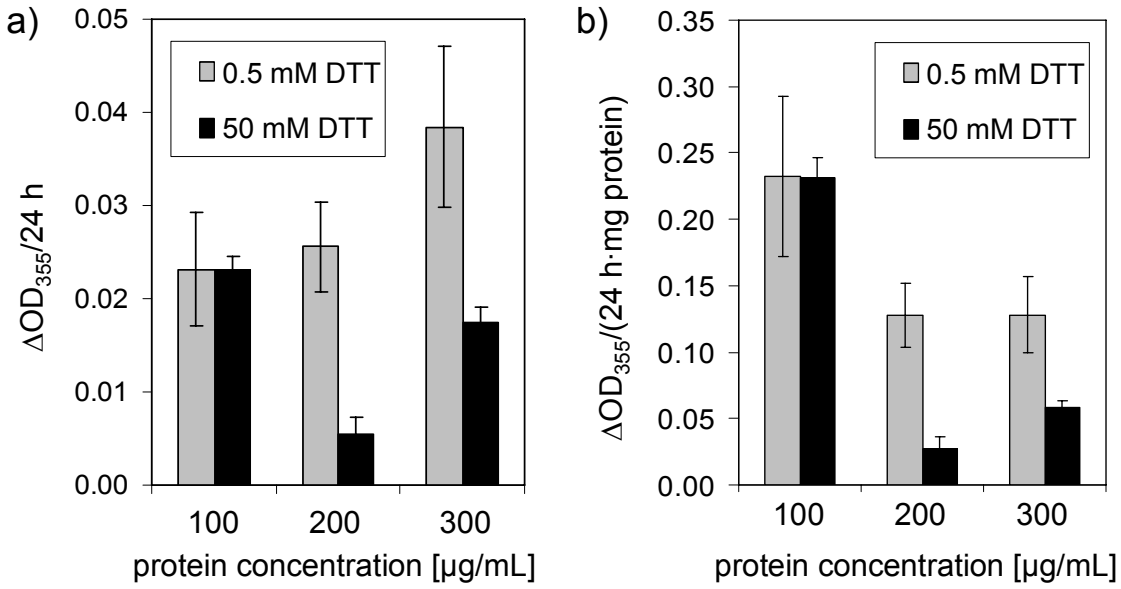


**Fig. 4.9** Comparison of Hyal-1/L activity after folding in the standard system (50 mM DTT) and in the "low reductive (0.5 mM DTT) system" at increasing protein concentrations as determined in the turbidimetric activity assay. Samples were "desalted" after 24 h folding reaction by gel filtration and the enzymatic activity was determined in the turbidimetric assay using 0.1 M Na-formate, 0.1 M NaCl, pH 3.5, as incubation buffer. a) Enzymatic activity is shown as $\Delta OD_{355}$, i.e. $OD_{355}$ (zero activity) - $OD_{355}$ (sample), measured after 24 h incubation in the activity assay. b) Enzymatic activity is shown as $\Delta OD_{355}$ after 24 h incubation time and per mg protein present in the folding mixture.

While in the "low reductive system" (0.5 mM DTT) an increase in the total activity ($\Delta OD_{355}$/24 h) was observed with increasing protein concentrations, concentrations > 100 µg/mL resulted in a lower activity in the standard folding system using 50 mM DTT (**Fig.**

**4.9.a**). However, when taking the yield of active protein per mg denatured protein used for folding ($\Delta OD_{355}$/(24h · mg protein)) into account, the best folding yield was obtained at a protein concentration of 100 µg/mL in both systems (**Fig. 4.9.b**).

Since the "low reductive folding system" (0.5 mM DTT) seemed to be more effective at higher protein concentrations, pulse experiments were performed in this system using various protein concentrations (**Fig. 4.10**).

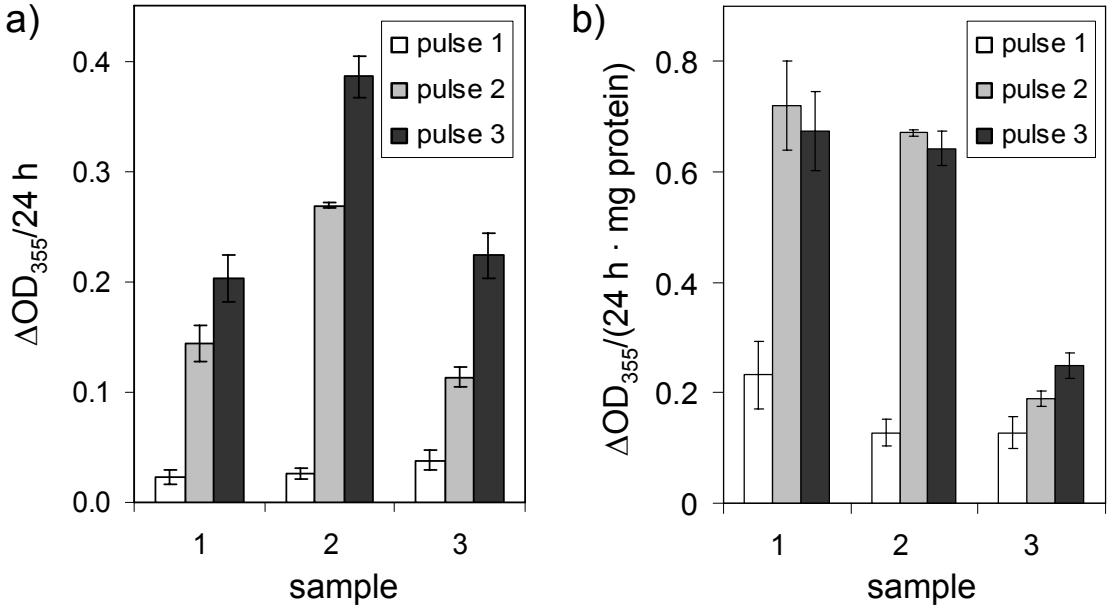


**Fig. 4.10** Folding of Hyal-1/L in the "low reductive system (0.5 mM DTT)" with protein pulses set every 24 h. Each sample was pulsed 3 times with the same protein concentration: sample 1: 100 µg/mL, sample 2: 200 µg/mL, sample 3: 300 µg/mL. Aliquots of 1 mL were taken after an incubation time of 24 h, "desalted" by gel filtration and the enzymatic activity determined in the turbidimetric assay using 0.1 M Na-formate, 0.1 M NaCl, pH 3.5, as incubation buffer. a) Enzymatic activity is shown as $\Delta OD_{355}$, i.e. $OD_{355}$(zero activity)-$OD_{355}$(sample), measured after 24 h incubation in the activity assay. b) Enzymatic activity is shown as $\Delta OD_{355}$ after 24 h incubation time and per mg protein present in the folding mixture.

In the pulsed folding experiments the highest activity ($\Delta OD_{355}$/24 h) as well as the highest yield in activity per mg of protein ($\Delta OD_{355}$/(24h · mg protein)) was achieved with protein pulses of 200 µg/mL (**Fig. 4.10**). Interestingly, the activity ($\Delta OD_{355}$/24 h) measured after pulse 2 increased at all concentrations more than 2-fold compared to pulse 1, although the protein concentration was only twice as high as after pulse 1 (**Fig. 4.10.a**). Furthermore, the system pulsed three times with 100 µg/mL (sample 1/pulse 3) seemed to be much more efficient both in activity ($\Delta OD_{355}$/24 h) and in the yield of active protein ($\Delta OD_{355}$/(24 h · mg protein)) than the sample pulsed once with 300 µg/mL (sample 3/pulse 1), although both samples contained the same protein concentration. A similar effect can be observed when comparing sample 2/pulse 3 and sample 3/pulse 2, which both contained 600 µg/mL of protein, but differed significantly in the resulting activity (**Fig. 4.10**).

Since no BSA was present in these folding mixtures, the observed differences in activity could be due to adhesion of Hyal-1/L to surfaces of the reaction vessels at low protein concentrations, especially if no protein was present in the folding mixture before. However, at higher protein concentrations (300 µg/mL) aggregation limited protein folding resulting in lower yields of activity per mg of protein.

In summary, the use of several pulses with low protein concentrations was found to be superior in both active protein yield and total activity compared to the addition of the same amount of protein in a single pulse.

### *4.3.8. Theoretical considerations based on the Hyal-1 structure*

Proteins exhibiting a strong tendency for aggregation in aqueous buffer systems often contain hydrophobic patches. However, analysis of the hydrophobicity of Hyal-1/L by the algorithm of Kyte and Doolittle (Kyte and Doolittle 1982) revealed an even distribution of hydrophobic and hydrophilic amino acids within the primary sequence.

Homology models of Hyal-1, e.g. Gl15147354 in MODBASE (Pieper et al. 2004), comprise merely the catalytic domain as they are based on the crystal structure of the BVH (Markovic-Housley et al. 2000). In BVH charged amino acids (D, E, K, R) are distributed equally on the complete protein surface (**Fig. 4.11.a** and **c**). The Hyal-1 model based on the crystal structure of the BVH exhibits an equal distribution of charged residues on the side of the enzyme containing the large binding groove for the substrate (**Fig. 4.11.b**). However, at the "backside", i.e. at the side not directly in contact with the substrate, the Hyal-1 model as well as the other human hyaluronidase models exhibits an area of hydrophobic amino acids exposed to the surface (Fehler! Verweisquelle konnte nicht gefunden werden.**.d**). Jedrzejas and Stern (Jedrzejas and Stern 2005) postulated the existence of a flexible linker between the catalytic domain and the C-terminal domain, nevertheless, the C-terminal domain could be in contact with the catalytic domain covering the hydrophobic surface otherwise exposed to the aqueous environment.

This hydrophobic surface area, albeit only based on the model structure, could explain the failure in the production of catalytically active, C-terminally truncated hyaluronidase Hyal-1 (see above) and PH-20 derivatives (Gmachl and Kreil 1993, Arming et al. 1997) missing the complete C-terminal domain.

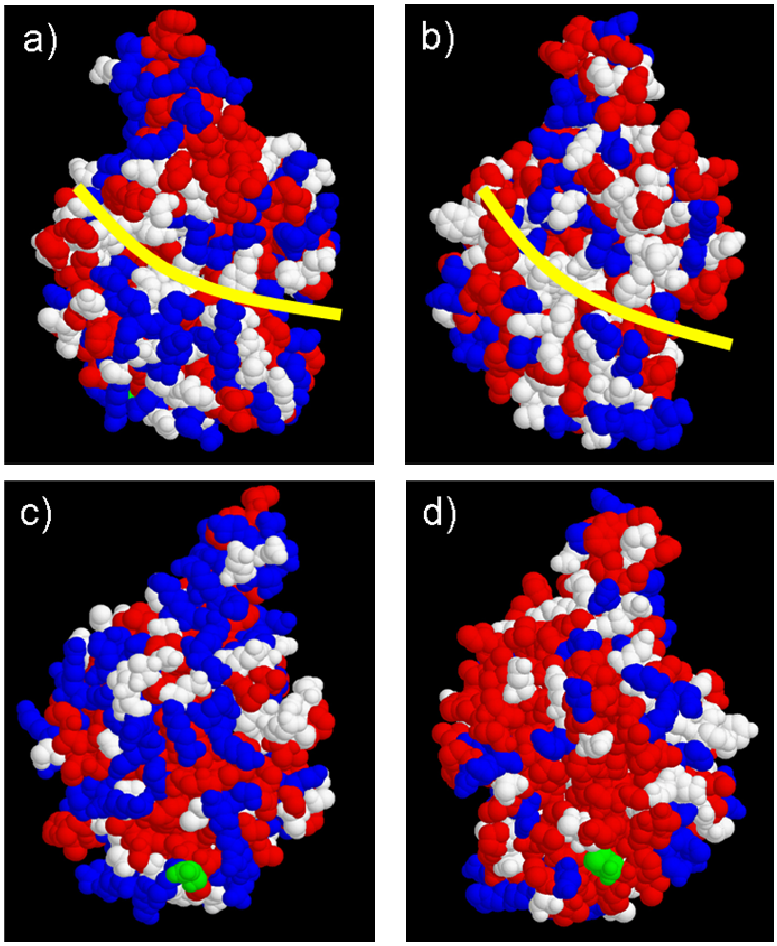


**Fig. 4.11** Comparison of the crystal structure of BVH (1FCQ.pdb) and a model of Hyal-1 (Gl15147354 from MODBASE (Pieper et al. 2004)) in respect of the distribution of charged (D, E, K, R shown in blue) and hydrophobic (F, L, I, V shown in red) amino acids exposed on the surface. a) HA binding side of BVH; b) HA binding side of the Hyal-1 model structure; c) "backside" of BVH; d) "backside" of Hyal-1. The putative position of the HA chain is highlighted in yellow, the C-terminal amino acid in green. Structures were visualized using Rasmol 2.6 (Massachusetts, USA).

Further investigation of the primary sequence of Hyal-1/L revealed the presence of a high amount of charged residues (15 %). Uversky proposed a systematic explanation for the tendency of proteins to form stable intermediates during the unfolding process based on the ratio of the mean net charge (number of charged amino acids at pH 7 per total number of amino acids) to the mean hydrophobicity (sum of hydrophobicity values calculated by the Kyte and Doolittle algorithm per total number of amino acids) (Uversky 2002). In this model proteins with both low to medium net charge and low hydrophobicity tend to form stable intermediates, while proteins with a high overall hydrophobicity tend to unfold without any intermediates rather independent on their net charge (**Fig.4.12**). As the mean net charge of Hyal-1/L is extraordinarily high (0.15) compared to the proteins observed by Uversky Hyal-1/L is positioned in a range with medium hydrophobicity (0.45) and a very high net charge, i.e. in a region of intermediate-forming proteins if the diagram is being extrapolated to higher mean net charge values. BVH, which was described in literature (Soldatova et al. 1998) to be

refolded *in vitro* at very low efficiencies, was found to have an even higher mean net charge at similar hydrophobicity values compared to Hyal-1/L.

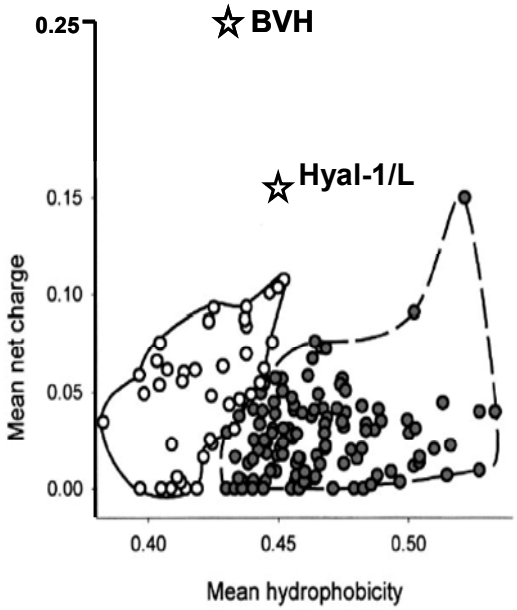


**Fig. 4.12** Mean net charge plotted against the mean hydrophobicity of a protein. Open symbols represent proteins forming stable intermediates during unfolding, while the filled symbols show proteins forming no intermediates during unfolding. BVH and Hyal-1 are shown as stars. The scheme was modified from Uversky 2002.

The extremely high overall charge of hyaluronidases could provide an explanation for the influence of the kind of denaturing agent on the extent of aggregation occurring during *in vitro* folding (cf. 4.3.5). In contrast to urea, GdmCl is a charged molecule and electrostatic interactions with amino acids of the protein surface could cause GdmCl to stay in close proximity to Hyal-1/L. During subsequent *in vitro* folding by fast mixing with folding buffer urea could spread equally in the folding buffer, while GdmCl might remain partially bound to the highly charged protein and might thus stabilize intermediates prone to aggregation.

Although the effects discussed above can explain the phenomena observed during *in vitro* folding of Hyal-1/L the theory is to be considered as speculative. One could imagine also other effects causing the different sensitivity of Hyal-1/L towards urea and GdmCl, e.g. the weaker denaturing ability of urea compared to GdmCl.

## 4.4. Summary and conclusions

*In vitro* folding of hyaluronidases could be monitored by observation of the enzymatic activity, although not directly in the folding buffer. The samples had to undergo a buffer exchange to avoid interferences with enzymatic activity assays due to the presence of folding additives.

*In vitro* folding experiments with PH-20 (PH-20/S and PH-20/L) yielded no active protein in contrast to Hyal-1/L. Possibly, folding of PH-20 is more complex than folding of Hyal-1 because of the larger size of the C-terminal domain (8.4 kDa in Hyal-1, 17.4 kDa in PH-20), the existence of two additional C residues in the C-terminal domain and the presence of the propeptide in PH-20. Although the propeptide is known to be removed after anchorage of PH-20 to the membrane via a GPI-anchor, its function during protein folding remains unclear.

The C-terminally truncated variant of Hyal-1, Hyal-1/S, was expected to be folded more efficiently and more easily than the full-length enzyme, Hyal-1/L, due to the smaller size of the enzyme on the one hand and the presence of less C residues on the other hand. Usually, small proteins tend to fold faster than larger ones and the number of possible disulfide-bridged protein isoforms increases significantly with the number of cysteine residues (3 possibilities for 4 C, 945 for 10 C) (Jaenicke and Rudolph 1989).
However, during *in vitro* folding experiments only Hyal-1/L was found to exhibit hyaluronidase activity. The failure to produce C-terminally truncated hyaluronidase derivatives might be explained by the close contact of the catalytic domain and the C-terminal domain in human hyaluronidases (cf. 4.3.8).
Folding of Hyal-1/L was to a great extent dependent on the disulfide shuffling system indicating the necessity of the correct formation of disulfide bonds in the native protein. Control experiments using BTH showed a preference of hyaluronidases for solubilizing agents, especially Arg, and a negative effect of folding enhancers like ammonium sulfate. Arg is a common folding additive, however, its mechanism of folding support could not be elucidated up to now (Tsumoto et al. 2004, Baynes et al. 2005). Presumably, it facilitates solubilization of folding intermediates without the denaturing effect of chaotropic salts (Lilie et al. 1998, Mayer and Buchner 2004). In the case of Hyal-1/L Arg could not inhibit aggregation during folding of GdmCl-denatured Hyal-1/L. Folding of GdmCl-denatured Hyal-1/L yielded low quantities of active enzyme only at low protein concentrations

independent of the disulfide shuffling system and the presence of Arg. Contrarily, folding of urea-denatured Hyal-1/L resulted in less aggregates and allowed the use of higher protein concentrations.

Taken together, *in vitro* folding of Hyal-1/L yielded enzymatically active protein, albeit with a low specific hyaluronidase activity (0.11 U/mg) and at low yields. A detailed comparison of the properties of *in vitro* folded Hyal-1/L and the same enzyme expressed in a eukaryotic expression system is given in the following chapter.
Due to the insufficient results achieved with PH-20 and Hyal-1 folding experiments with Hyal-2 and Hyal-4 were omitted. In addition, for these hardly characterized hyaluronidases monitoring of folding poses a major problem since no appropriate and reliable activity assays exist.

## 4.5. References

Arakawa T., Timasheff S.N. (1982). Stabilization of protein structure by sugars. *Biochemistry* **21**: 6536-6544.

Arming S., Strobl B., Wechselberger C., Kreil G. (1997). In vitro mutagenesis of PH-20 hyaluronidase from human sperm. *Eur. J. Biochem.* **247**: 810-814.

Baynes B.M., Wang D.I., Trout B.L. (2005). Role of arginine in the stabilization of proteins against aggregation. *Biochemistry* **44**: 4919-4925.

Bhuyan A.K. (2002). Protein Stabilization by Urea and Guanidine Hydrochloride. *Biochemistry* **41**: 13386-13394.

Bradford M.M. (1976). A rapid and sensitive method for the quantitation of microgram quantities of proteins utilizing the principle of protein-dye binding. *Anal. Biochem.* **72**: 248-254.

Cleland J.L., Builder S.E., Swartz J.R., Winkler M., Chang J.Y., Wang D.I. (1992). Polyethylene glycol enhanced protein refolding. *Biotechnology (N.Y.)* **10**: 1013-1019.

Daugherty D.L., Rozema D., Hanson P.E., Gellman S.H. (1998). Artificial Chaperone-assisted Refolding of Citrate Synthase. *J. Biol. Chem.* **273**: 33961-33971.

De Bernadez Clark E., Schwarz E., Rudolph R. (1999). Inhibition of aggregation side reactions during in vitro protein folding. *Methods Enzymol.* **309**: 217-236.

Deuerling E., Bukau B. (2004). Chaperone-assisted folding of newly synthesized proteins in the cytosol. *Crit. Rev. Biochem. Mol. Biol.* **39**: 261-277.

Frand A.R., Cuozzo J.W., Kaiser C.A. (2000). Pathways for protein disulphide bond formation. *Trends Cell Biol.* **10**: 203-210.

Gmachl M., Kreil G. (1993). Bee venom hyaluronidase is homologous to a membrane protein of mammalian sperm. *Proc. Natl. Acad. Sci. U. S. A.* **90**: 3569-3573.

Gold E.W. (1982). Purification and properties of hyaluronidase from human liver. *Biochem. J.* **205**: 69-74.

Hoechstetter J. (2005). Characterisation of bovine testicular hyaluronidase and a hyaluronate lyase from Streptococcus agalactiae. *Doctoral thesis*. University of Regensburg. http://www.opus-bayern.de/uni-regensburg/volltexte/2005/519/

Hofmann A., Tai M., Wong W., Glabe C.G. (1995). A Sparse Matrix Screen to Establish Initial Conditions for Protein Renaturation. *Anal. Biochem.* **230**: 8-15.

Jaenicke R., Rudolph R. Folding proteins. *in: Protein structure - a practical approach.* T.E. Creighton ed. IRL Press. Oxford. (1989). pp. 191-223.

Jedrzejas M.J., Stern R. (2005). Structures of vertebrate hyaluronidases and their unique enzymatic mechanism of hydrolysis. *Proteins.* **61**: 227-238.

Krause M., Rudolph R., Schwarz E. (2002). The non-ionic detergent Brij 58P mimics chaperone effects. *FEBS Lett.* **532**: 253-255.

Kyte J., Doolittle R.F. (1982). A simple method for displaying the hydropathic character of a protein. *J. Mol. Biol.* **157**: 105-132.

Lange C., Rudolph R. Production of recombinant proteins for therapy, diagnostics, and industrial research by in vitro folding. *in: Protein Folding Handbook*. J. Buchner and T. Kiefhaber ed. Wiley-VCH. Weinheim. (2005). **2**: pp. 1245-1280.

Li M., Su Z.-G., Janson J.-C. (2004). In vitro protein refolding by chromatographic procedures. *Protein Expr. Purif.* **33**: 1-10.

Lilie H., Schwarz E., Rudolph R. (1998). Advances in refolding of proteins produced in E. coli. *Curr. Opin. Biotechnol.* **9**: 497-501.

Markovic-Housley Z., Miglinerini G., Soldatova L., Rizkallah P., Müller U., Schirmer T. (2000). Crystal Structure of Hyaluronidase, a Major Allergen of Bee Venom. *Structure* **8**: 1025-1035.

Marston F.A. (1986). The purification of eukaryotic polypeptides synthesized in Escherichia coli. *Biochem. J.* **240**: 1-12.

Mayer M., Buchner J. Refolding of inclusion body proteins. *in: Molecular Diagnosis of infectious diseases.* J. Decker, Reischl, U. ed. Humana Press. Totowa. (2004). **94**: pp. 239-245.

Menzella H.G., Gramajo H.C., Ceccarelli E.A. (2002). High recovery of prochymosin from inclusion bodies using controlled air oxidation. *Protein Expr. Purif.* **25**: 248-255.

Muckenschnabel I., Bernhardt G., Spruss T., Dietl B., Buschauer A. (1998). Quantitation of hyaluronidases by the Morgan-Elson reaction: comparison of the enzyme activities in the plasma of tumor patients and healthy volunteers. *Cancer Lett.* **131**: 13-20.

Oettl M. (2000). Biochemische Charakterisierung boviner testikulärer Hyaluronidase und Untersuchungen zum Einfluß von Hyaluronidase auf das Wachstum von Tumoren. *Doctoral thesis*. University of Regensburg.

Oettl M., Hoechstetter J., Asen I., Bernhardt G., Buschauer A. (2003). Comparative characterization of bovine testicular hyaluronidase and a hyaluronate lyase from Streptococcus agalactiae in pharmaceutical preparations. *Eur. J. Pharm. Sci.* **18**: 267-277.

Orsini G., Goldberg M.E. (1978). The renaturation of reduced chymotrypsinogen A in guanidine HCl. Refolding versus aggregation. *J. Biol. Chem.* **253**: 3453-3458.

Pieper U., Eswar N., Braberg H., Madhusudhan M.S., Davis F., Stuart A.C., Mirkovic N., Rossi A., Marti-Renom M.A., Fiser A., Webb B., Greenblatt D., Huang C., Ferrin T., Sali A. (2004). MODBASE, a database of annotated comparative protein structure models, and associated resources. *Nucleic Acids Res.* **32**: D217-D222.

Reddy K., Ravi C., Lilie H., Rudolph R., Lange C. (2005). L-Arginine increases the solubility of unfolded species of hen egg white lysozyme. *Protein Sci.* **14**: 929-935.

Reissig J., Strominger J., Leloir L. (1955). A modified colorimetric method for the estimation of N-Acetylamino sugars. *J. Biol. Chem.* **217**: 959-966.

Rozema D., Gellman, S. H. (1996). Artificial chaperone-assisted refolding of denatured-reduced lysozyme: modulation of the competition between renaturation and aggregation. *Biochemistry* **35**: 15760-15771.

Schellman J.A. (2003). Protein Stability in Mixed Solvents: A Balance of Contact Interaction and Excluded Volume. *Biophys. J.* **85**: 108-125.

Soldatova L.N., Crameri R., Gmachl M., Kemeny D.M., Schmidt M., Weber M., Mueller U.R. (1998). Superior biologic activity of the recombinant bee venom allergen hyaluronidase expressed in baculovirus-infected insect cells as compared with Escherichia coli. *J. Allergy Clin. Immunol.* **101**: 691-8.

Stark G.R., Stein W.H., Moore S. (1960). Reactions of the Cyanate Present in Aqueous Urea with Amino Acids and Proteins. *J. Biol. Chem.* **235**: 3177-3181.

Timasheff S.N. (1992). Water as ligand: preferential binding and exclusion of denaturants in protein unfolding. *Biochemistry* **31**: 9857-9864.

Tsumoto K., Ejima D., Kumagai I., Arakawa T. (2003). Practical considerations in refolding proteins from inclusion bodies. *Protein Expr. Purif.* **28**: 1-8.

Tsumoto K., Umetsu M., Kumagai I., Ejima D., Philo J.S., Arakawa T. (2004). Role of Arginine in Protein Refolding, Solubilization, and Purification. *Biotechnol. Prog.* **20**: 1301-1308.

Uversky V.N. (2002). Cracking the folding code. Why do some proteins adopt partially folded conformations, whereas other don't? *FEBS Lett.* **514**: 181-183.

Vallejo L., Rinas U. (2004). Strategies for the recovery of active proteins through refolding of bacterial inclusion body proteins. *Microb. Cell Fact.* **3**: 11-23.

Walter S., Buchner J. (2002). Molekulare Chaperone: zelluläre Maschinen für die Proteinfaltung. *Angew. Chem.* **114**: 1142-1158.

Wetlaufer D.B. (1984). Nonenzymatic formation and isomerization of protein disulfides. *Methods Enzymol.* **107**: 301-304.

Yancey P.H., Clark M.E., Hand S.C., Bowlus R.D., Somero G.N. (1982). Living with water stress: evolution of osmolyte systems. *Science* **217**: 1214-1222.

# Chapter 5

# Purification and characterization of human Hyal-1 expressed by DS-2 cells

## 5.1. Introduction

The major amount of hyaluronan in somatic tissues is assumed to be degraded by Hyal-1 in combination with Hyal-2, and, to a minor extent, PH-20 (Stern 2005). While Hyal-2 and PH-20 are both linked to the cell-membrane by a glycosylphosphatidylinositol-(GPI-)anchor, Hyal-1 is a soluble, acid active lysosomal enzyme (Gold 1982). Acid active hyaluronidase has been isolated and purified from plasma, serum and liver, but characteristics as well as molecular sizes of the proteins isolated varied: 57 kDa for plasma hyaluronidase (Frost et al. 1997), 72 kDa for serum hyaluronidase (Afify et al. 1993) and 76 kDa for human liver hyaluronidase (Gold 1982). Although only plasma hyaluronidase has been identified as a gene product of *hyal-1* (Frost et al. 1997), the hyaluronidases isolated from serum and liver also show typical properties of Hyal-1. In urine an additional protein binding to Hyal-1 antibodies was described by Csoka et al. (Csoka et al. 1997) with a molecular mass of 45 kDa. This second, enzymatically active Hyal-1 isoform was supposed to be a truncated form of the 57 kDa isoform with an interior part of the protein missing. However, function and mechanism of this truncation are unknown.

Modulation of Hyal-1 expression has been observed in a genetic disorder, called mucopolysaccharidosis IX (Triggs-Raine et al. 1999), and in a number of malignant tumors. Based on the identification of the *hyal-1* gene in a region of major deletions in tobacco-related bronchial carcinoma the gene was originally called *LUCA-1* (lung cancer protein – 1) before the protein was correlated to its function as a hyaluronidase (Hosoe et al. 1994, Wei et al. 1996). During the last years it became obvious that *hyal-1* functions not only as a tumor

suppressor gene (TSG) as observed in lung cancer, but can also promote tumor growth and aggressiveness in prostate and bladder cancer (Lokeshwar et al. 2001, Franzmann et al. 2003). Hyal-1 in human urine has therefore been investigated for its potential as a marker protein for malignant urogenital cancers (Posey et al. 2003, Lokeshwar et al. 2005, Aboughalia 2006). However, information on the role of Hyal-1 in cancer progression remain controversial, possibly due to the fact that several different mechanisms control the activity of Hyal-1 *in vivo*, e.g. the control of *hyal-1* expression on the DNA as well as on the RNA level (Lokeshwar et al. 2002, Stern 2005) and the existence of inhibitors of hyaluronidase activity (Mio and Stern 2002).
Isolation of Hyal-1 from human sources has been hampered by the extremely low amounts of the enzyme present in the plasma and by the instability of the hyaluronidase during the purification process. As no in-depth characterization of the enzyme has been carried out only limited information on the enzymatic properties of Hyal-1 is available.

Human Hyal-1 was expressed in prokaryotic expression systems as described in Chapter 3 and 4. Although human Hyal-1 was refolded *in vitro* to an active conformation, the yield of active protein as well as the specific enzymatic activity were extremely low. Therefore, *Drosophila* Schneider-2 (DS-2) cells (Schneider 1972) were selected as an alternative eukaryotic expression system. As shown previously for bee venom hyaluronidase (BVH) (Soldatova et al. 1998), insect cells seem to be appropriate for the expression of hyaluronidases.
DS-2 cells are immortalized, undifferentiated, embryonic *Drosophila melanogaster* cells with the ability to integrate up to 400 copies of an expression cassette into the genome (Deml and Wagner 1998). They are easy to cultivate and are especially suited for the expression of secreted proteins as they grow in serum-free medium.

## 5.2. Materials and Methods

### *5.2.1. Vectors, cells, enzymes and chemicals*

*Drosophila* Schneider-2 cells (DS-2 cells), pCoHygro and pMT/BiP/V5-HisA were kindly provided by V. Runza (Institute of Immunology, Faculty of Medicine, University of Regensburg, Germany). Materials for subcloning were described in Chapter 3.
Hyaluronic acid from *Streptococcus zooepidemicus* was purchased from Aqua Biochem GmbH, Dessau, Germany. Chondroitin 4-sulfate (A) from bovine trachea, chondroitin 6-

sulfate (C) from shark cartilage and chondroitin sulfate B from porcine intestinal mucosa were from Sigma, Munich, Germany. Chondroitinase ABC from *Proteus vulgaris* with an activity of 0.35 U/mg on chondroitin sulfate C was also purchased from Sigma, Munich, Germany. ChS A and ChS C contained impurities of the respective other GAG of up to 30 % as indicated by the supplier.

Triton X-100 was from Roth, Karlsruhe, Germany. Hygromycin was from A.G. Scientific Inc., San Diego, USA. All other chemicals were of HPLC or analytical grade and were purchased from Merck, Darmstadt, Germany.

### *5.2.2. Subcloning of hyal-1 cDNA in the insect cell expression vector pMT/Hygro*

By combination of pMT/BiP/V5-HisA and pCoHygro (both designed by Invitrogen, Karlsruhe, Germany) a new expression vector for DS-2 cells - pMT/Hygro - was generated. To obtain this vector, pMT/BiP/V5-HisA and pCoHygro were both cleaved with *Acc*I and *Sap*I, the respective fragments were purified by agarose gel electrophoresis and ligated after dephosphorylation of the 5' ends of pMT/BiP/V5-HisA. Restriction digest was performed in a single step using 4 U of *Sap*I and 10 U of *Acc*I per µg of plasmid DNA in 1 x NEB4 buffer (New England Biolabs, Frankfurt a. M., Germany). The mixture was incubated for 2 h at 37 °C.

Human *hyal-1* cDNA was amplified by PCR (**Tab. 5.1** and **Tab. 3.2**) using the IRAKp961O1779Q2 plasmid (**Tab. 3.1**) as template, digested with *Sma*I and *Not*I and ligated into pMT/Hygro, which had been digested with the same enzymes and dephosphorylated at the 5' ends.

**Tab. 5.1** PCR primers (5'-3'-direction) for cloning of *hyal-1/S* and *hyal-1/L* into *Sma*I and *Not*I restriction sites of pMT/Hygro. Underlined sequences indicate these restriction sites within the primers. $MgSO_4$ refers to the final concentration in the PCR reaction mixture and $T_a$ indicates the annealing temperature used for the PCR reaction.

| Hyaluronidase | Forward primer | Reverse primer | $MgSO_4$ | $T_a$ |
|---|---|---|---|---|
| Hyal-1/S | ATCTATTCCCGGGTT | ATTATATCGCGGCCG CCCGAGAAGGGCCCC | 2.5 mM | 80.0 °C |
| Hyal-1/L | TAGGGGCCCCTTGC | ATTATATCGCGGCCG CCACATGCTCTTCC | 1.5 mM | 80.0 °C |

The restriction digest was performed in two steps: *Sma*I digested the DNA in 1 x Y+/TANGO™ during 1 h incubation at 30 °C, then *Not*I was added, the buffer concentration

increased to 2 x Y+/TANGO™ and digestion continued for 2 h. A detailed description of all cloning steps is given in Chapter 3.

### *5.2.3. DS-2 cell culture conditions and storage*

DS-2 cells were grown in serum-free Insect-XPRESS™ medium (Cambrex Bio Science, Copenhagen, Denmark) at 27 ± 1 °C in normal atmosphere. Adherent cultures were grown in 25-cm² culture flasks (Nunc, Wiesbaden, Germany) for sub-culturing and small-scale expression experiments. For sub-culturing cells were serially passaged every 3 – 4 days. The semi-adherent, nearly confluent cells were removed from the bottom of the flask by tapping and the resulting suspension was diluted 5 – 6-fold with fresh medium. Suspension cultures were used for large-scale protein expression experiments, and were shaken at 135 rpm at 27 ± 1 °C.

For long term storage cells were grown to a density of 10 – 20 · $10^6$ cells/mL, centrifuged (3 min, 1,000 g, 4 °C), resuspended in the same volume of 1 x sterile PBS, centrifuged again and resuspended in the same volume of freezing medium (45 % fresh medium, 45 % conditioned medium containing 10 % DMSO). The cell suspension was split into aliquots of 1 mL and cooled down slowly for the storage in liquid nitrogen. For revival the DS-2 cells were quickly thawed and 1 mL of the cell suspension was diluted in 5 mL of fresh medium. After 2 – 4 h of incubation at normal growth conditions the medium was completely exchanged by fresh medium to remove residual DMSO.

Cells were routinely monitored for mycoplasma contaminations by PCR using the VenorGEM™ mycoplasma detection kit (Minerva Biolab, Berlin, Germany).

### *5.2.4. Transfection of DS-2 cells*

DS-2 wild type cells were transfected with pMT/Hygro/*hyal-1* using Lipofectamin™ 2000 CD (Invitrogen, Karlsruhe, Germany) and FuGENE® 6 (Roche Applied Sciences, Mannheim, Germany) as transfection reagents. DS-2 cells were seeded in 6-well plates at a cell density of 1 · $10^6$ cells/mL one day before transfection. Transfections were performed according to the manufacturers' instructions.

### *5.2.5. Expression of Hyal-1/S and Hyal-1/L in transiently transfected DS-2 cells*

Transiently transfected cells were screened for heterologous protein expression by induction with 0.5 mM sterile $CuSO_4$ (stock solution 100 mM) 24 h after transfection. At various time points after induction samples of the cell medium were analyzed by Western blotting and enzymatic activity assays, respectively.

### *5.2.6. Expression of Hyal-1/L in stably transfected DS-2 cells*

For selection of stably transfected DS-2/pMT/Hygro/*hyal-1/L* cells the medium was exchanged 24 h after transfection against fresh medium supplemented with 300 µg/mL hygromycin. The selection medium was subsequently changed every 3 – 4 days till the hygromycin resistant cells were confluent, then passaging was continued in the presence of hygromycin as described for the wild type cells.

For induction of protein expression 0.5 mM sterile $CuSO_4$ was added to a suspension culture at a cell density of $1.5 – 2.0 \cdot 10^6$ cells/mL. Ten days after induction the cells were harvested by centrifugation (1,500 g, 15 min, 4 °C) and the medium was used for isolation of Hyal-1/L.

### *5.2.7. Purification of Hyal-1/L from DS-2 cell medium*

After addition of 1 mM EDTA and 0.1 % (v/v) Triton X-100 to the medium Hyal-1/L was precipitated by 30 % saturation of the medium with ammonium sulfate. The suspension was incubated on ice for 1 h before the precipitate was pelleted by centrifugation (20,000 g, 60 min, 10 °C). The pellet was solubilized in 1/10 of the original medium volume of 50 mM Na-phosphate, 0.1 % Triton X-100, pH 6.0. After stirring overnight at 4 °C insoluble protein aggregates were removed by centrifugation (20,000 g, 60 min, 4 °C), and the clear supernatant was loaded on CM (Carboxymethyl)-Sephadex C-50 (Amersham Biosciences, Uppsala, Sweden) packed in a 26/20 column (40 mL column volume (CV), Amersham Biosciences, Uppsala, Sweden) and equilibrated in 50 mM Na-phosphate, 0.1 % Triton X-100, pH 6.0. The column was washed with 2 CV of equilibration buffer before Hyal-1/L was eluted by a linear gradient from 0 – 0.5 M NaCl increasing over 10 CV. After elution the column was washed with 2 CV of equilibration buffer supplemented with 1 M NaCl. Cation exchange chromatography was performed at a flow rate of 1 mL/min and a detector wavelength of 280 nm. Fractions of 8 mL were collected automatically. Protein purification was performed with an ÄKTA FPLC device and a Frac-950 fraction collector using UNICORN$^{TM}$ v5.10 software (GE Healthcare Bio-Sciences AB, Uppsala, Sweden) for data analysis.

The pH of the elute was carefully adjusted to 6.3 with 1 M NaOH and the fractions exhibiting hyaluronidase activity were pooled. The sample was then loaded on a HisTrap$^{TM}$ FF column (3 x 5 mL CV, GE Healthcare Bio-Sciences AB, Uppsala, Sweden) equilibrated in 50 mM Na-phosphate, 0.5 M NaCl, 0.1 % Triton X-100, pH 6.8. The column was washed with 2 CV of equilibration buffer and elution was achieved in three steps: firstly, the pH of the equilibration buffer was decreased to pH 4.5 (elute 1), secondly, the $Ni^{2+}$ ions were eluted

together with Hyal-1/L by washing with 10 CV of 50 mM Na-phosphate, 0.5 M NaCl, 50 mM EDTA, pH 6.0 (elute 2). In the third step the residual Hyal-1/L was eluted by addition of 0.1 % Triton X-100 to the elution buffer 2 (elute 3). Ni-IMAC was performed at a flow rate of 0.5 mL/min. Fractions of 1 mL were collected manually and pooled after determination of their specific enzymatic activity. Pure samples were dialyzed against 50 mM Na-phosphate, 0.5 M NaCl, 1 mM EDTA, pH 6.0. Enzyme purity was confirmed by SDS-PAGE.
All buffers used during the purification process were vacuum-degassed and filtrated through a 0.45 µm filter (Millipore, Eschborn, Germany).

### *5.2.8. SDS-PAGE and Western blot*

For SDS-PAGE and Western blotting the protocols described in Chapter 4 were followed. As primary antibody Anti-V5-IgG (Sigma, Munich, Germany) diluted 2000fold in 10 mL of washing buffer was used, the secondary antibody was identical to the one used in Chapter 4.

### *5.2.9. Zymography*

Substrate gel electrophoresis was performed according to the method described by Cherr et al. (Cherr et al. 1996). In brief, SDS polyacrylamide gels were prepared as described in Chapter 3 with the separating gel supplemented with 67 µg/mL hyaluronic acid. Generally protein samples were prepared by mixing with 0.25 volumes of 5 x SDS sample buffer (cf. 3.2.14) without DTT and were not boiled prior to electrophoresis.
After electrophoresis SDS was removed from the gel by washing with a 2.5 % (v/v) Triton X-100 solution for 30 min, a short incubation period in water and washing with incubation buffer (see below) for 30 min. Then, the gel was equilibrated with incubation buffer for 2 – 24 h at 37 °C. The incubation buffer was chosen to achieve maximum enzymatic activity, i.e. in the case of Hyal-1/L 0.1 M Na-formate, 0.1 M NaCl, pH 3.5 were used.
To visualize regions of hyaluronan digest the gels were stained in 0.5 % alcian blue in 7 % acetic acid for 1 h, destained in 7 % acetic acid and counterstained with Coomassie Brilliant Blue G-250 (Serva, Heidelberg, Germany).

### *5.2.10. Detection of glycoproteins by PAS staining of gels*

For detection of glycoproteins SDS-PA gels were stained by the periodic acid – Schiff (PAS) technique with Schiff's reagent purchased from Sigma, Munich, Germany, following the procedure described by Zacharius et al. (Zacharius et al. 1969).

### *5.2.11. Deglycosylation of Hyal-1/L expressed in DS-2 cells*

4 µg of partially purified Hyal-1/L (0.6 U/mg) were incubated with 0 – 2 U N-glycosidase F (Roche, Mannheim, Germany) for 4 h at 37 °C in 100 µL of 50 mM Na-phosphate, 10 mM EDTA, pH 6.0. 20 µL of each sample were used for Western blotting and 50 µL were analyzed in the colorimetric hyaluronidase activity assay.

### *5.2.12. N-terminal sequencing of Hyal-1/L*

10 µg of purified Hyal-1/L were precipitated by methanol-chloroform-precipitation (Wessel and Flügge 1984) and solubilized in 300 µL of milli-Q water. After lyophilization the protein was N-terminally sequenced by Edman degradation (Edman and Begg 1967). Sequencing was performed at the laboratory of Prof. Dr. Deutzmann at the Institute of Biochemistry, Microbiology and Genetics, University of Regensburg, Germany, in a Procise® Protein Sequencing System 492 with phenylthiohydantoin amino acid analyzer (Applied Biosystems, Foster City, USA).

### *5.2.13. Colorimetric hyaluronidase activity assay*

The assay was performed as described in Chapter 4. The following incubation mixtures were used:

Incubation mixture A: 150 µL of water, 100 µL of BSA (0.2 mg/mL), 100 µL of 0.1 M formic acid/Na-formate, pH 3.5, 50 µL of HA (5 mg/mL), 50 µL of sample.

Incubation mixture B: 150 µL of water, 100 µL of BSA (0.2 mg/mL), 100 µL of McIlvaine's buffer, 50 µL of HA (5 mg/mL), 50 µL of sample.

McIlvaine's buffer was adjusted to the desired pH by mixing solution A (0.2 M $Na_2HPO_4$/0.1 M NaCl, solution) and B (0.1 M citric acid/0.1 M NaCl).

### *5.2.14. Turbidimetric hyaluronidase activity assay*

A detailed description of the turbidimetric activity assay is given in Chapter 3.

Incubation mixture A: 31 µL of 0.1 M formic acid/Na-formate, pH 3.5, 8 µL of BSA (0.2 mg/mL), 8 µL of HA (2 mg/mL), 13 µL of $H_2O$, 10 µL of sample.

Incubation mixture B: 15 µL of McIlvaine's buffer (cf. 5.2.13), 15 µL of BSA (0.2 mg/mL), 8 µL of HA (5 mg/mL), 22 µL of water, 10 µL of sample.

If further additives were used in the assay, water was replaced by the additive solubilized in water.

### *5.2.15. Chondroitinase activity assays*

Chondroitinase activity was determined by the colorimetric and the turbidimetric method, respectively, (cf. 5.2.13 and 5.2.14) substituting HA by chondroitin sulfate A, B or C.
Absorbance spectra of the Morgan-Elson reaction products were measured in a Cary 100 UV-Vis Spectrophotometer (Varian, Darmstadt, Germany).

### *5.2.16. Determination of protein concentrations*

Protein concentrations were determined by the bicinchoninic acid (BCA) assay (Smith et al. 1985) using BSA as standard because of the presence of detergents in the protein samples. The assay was performed by mixing 70 µL of the BCA working solution described by Smith et al. (Smith et al. 1985) with 70 µL of sample. Absorbance was quantified after 1 h of incubation at 60 °C at 580 nm in a microplate reader (Tecan Deutschland GmbH, Crailsheim, Germany) applying 10 flashes per well.

### *5.2.17. MALDI-TOF MS*

MALDI-TOF MS was carried out on a GSG/future linear MALDI-TOF mass spectrometer (GSG Mess- und Analysengeräte GmbH, Bruchsal, Germany). For sample preparation the GSG/SPA sample preparation system was used. 1 µL of pure Hyal-1 (1.3 µM in 0.5 mM Na-phosphate, 5 mM NaCl, pH 6.0) was mixed with 1 µL of matrix solution (10 mg of 2,5-dihydroxybenzoic acid dissolved in 1 mL of methanol/water (50 : 50)). 1 µL of the mixture was applied to the mesa and allowed to dry. Spectra were acquired in the positive ion mode over an m/z range of 400 – 100,000 Da.

### *5.2.18. Biophysical characterization*

CD spectroscopy and analytical ultracentrifugation were performed by Dr. H. Lilie at the Institute of Biotechnology, Martin-Luther University Halle-Wittenberg, Germany. For the analysis a purified sample of Hyal-1 (10 U/mg, 0.5 mg/mL) solubilized in 50 mM Na-phosphate, 0.5 M NaCl, 1 mM EDTA, pH 6.0 was used. CD spectra were measured in 0.1 mm cuvettes on a Jasco 710 spectropolarimeter (Jasco, Gross-Umstadt, Germany) at a scan speed of 50 nm/min and a temperature of 20 °C. Spectra were measured 20 times, averaged and corrected for contributions of the buffer. Secondary structure elements were calculated by the program CDNN based on a neuronal network trained with 30 spectra of proteins with a known crystal structure (Böhm et al. 1992).

Analytical ultracentrifugation was performed in a Beckmann Optima XL-A centrifuge and a 50Ti rotor. Sedimentation equilibrium measurements (absorption at 230 nm and 280 nm) were carried out at 10,000 rpm and 20 °C. After 60 h of centrifugation the apparent molecular mass was calculated using the software provided by Beckman Instruments (Palo Alto, USA).

Crystallization was performed by B. Epler and Dr. M. Stubbs at the Institute of Biotechnology, Martin-Luther University Halle-Wittenberg, Germany. High-throughput screening of crystallization conditions was performed using 9.5 mg/mL purified Hyal-1 in the presence of 0.1 % (v/v) Triton X-100 and 6.9 mg/mL purified Hyal-1 in the absence of Triton X-100. Both enzymes were solubilized in 50 mM Na-phosphate, 0.5 M NaCl, 1 mM EDTA, pH 6.0. For screening of crystallization conditions the CrystalScreen$^{TM}$ kit 1 and 2 (Hampton Research, Aliso Viejo, USA) and the Basic Crystallization kit (Sigma, Munich, Germany) were used.

## 5.3. Results and discussion

### *5.3.1. Construction of pMT/Hygro*

Originally, the DS-2 cell system for the heterologous expression of proteins designed by Invitrogen (Karlsruhe, Germany) utilizes two cotransfected vectors for the selection of transfected cells, one carrying the foreign gene in a cloning/expression region (pMT/BiP/V5-HisA) and one carrying the hygromycin resistance gene (pCoHygro). To avoid the necessity to transfect a cell with both vectors pMT/Hygro was designed as a combination of the hygromycin containing region from pCoHygro and the essential regions of pMT/BiP/V5-HisA. The *Acc*I and *Sap*I cleavage sites were found to be positioned in both vectors in a fortunate way to enable the vector combination described above. Digestion of pMT/BiP/V5-HisA with *Acc*I and *Sap*I resulted in the removal of only 0.3 kb from the 3.6 kb vector (**Fig. 5.1**, lane A and B), while pCoHygro was cleaved into two fragments of similar length (2.1 and 2.4 kb) (**Fig. 5.1**, lane C and D). Isolation of the 2.1 kb fragment carrying the hygromycin resistance was only possible after prolonged agarose gel electrophoresis. Prior to transformation of *E. coli* Top10 cells, the 3.3 kb pMT/BiP/V5-HisA fragment and the 2.1 kb pCoHygro fragment were isolated from the gel, ligated, and the resulting plasmids were screened for the correct construct. The identity of the plasmid pMT/Hygro was confirmed by sequencing.

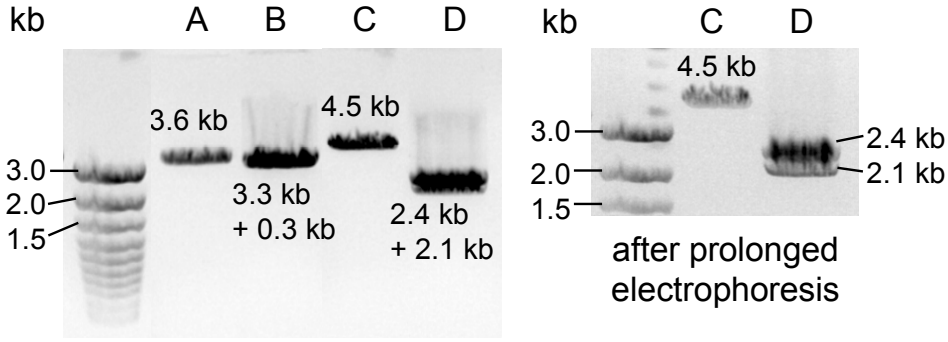


**Fig. 5.1** Agarose gel electrophoresis of pMT/BiP/V5-HisA and pCoHygro after restriction digest. A) pMT/BiP/V5-HisA linerarized with *Acc*I. B) pMT/BiP/V5-HisA digested with *Acc*I and *Sap*I. C) pCoHygro linearized with *Acc*I. D) pCoHygro digested with *Acc*I and *Sap*I.

### *5.3.2. Construction of pMT/Hygro/hyal-1/S and pMT/Hygro/hyal-1/L*

A truncated (S) and a full-length (L) *hyal-1* cDNA variant were cloned into pMT/Hygro by specific amplification of the respective fragments by PCR (**Fig. 5.2**), restriction digest using *Sma*I and *Not*I and ligation into pMT/Hygro digested with the same enzymes.

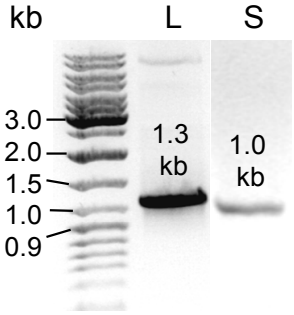


**Fig. 5.2** PCR products of *hyal-1/S* (S) and *hyal-1/L* (L) analyzed by agarose gel electrophoresis. Each lane contained 5 µL of the PCR mixture and 1 µl of 10 x PCR loading buffer.

Hyal-1/L and Hyal-1/S were expected to be targeted to the ER and the extracellular compartment due to an exchange of the mammalian signal sequence for an insect cell signal peptide (BiP). The full-length (L) as well as the truncated (S) variant of Hyal-1 were both fused C-terminally to a His-tag and a V5 epitope. Expression of the recombinant proteins was controlled by a metallothionein promotor ($P_{metallothionein}$), a regulatory element originally inducing expression of proteins protecting the cell against heavy metal ion effects. A schematic view of the insect cell expression vector is given in **Fig. 5.3**.

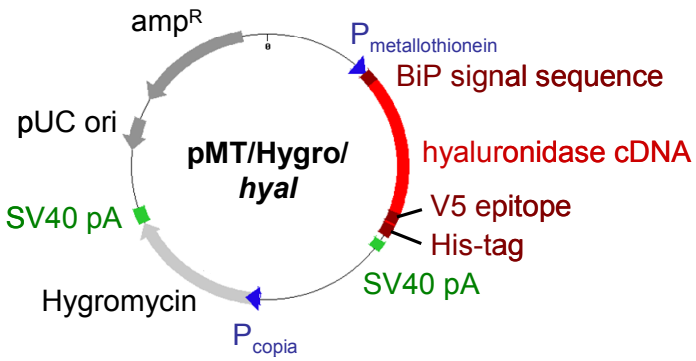


**Fig. 5.3** DS-2 cell expression vector pMT/Hygro with hyaluronidase cDNA (*hyal*) located in the multiple cloning/expression site.

### *5.3.3. Expression of Hyal-1/S and Hyal-1/L in DS-2 cells*

5.3.3.1. Transient expression of Hyal-1/S and Hyal-1/L in DS-2 cells

To investigate if the hyaluronidases were expressed by the DS-2 cells in the expected way protein expression was induced directly after transfection of the DS-2 cells with the pMT/Hygro/*hyal-1*/S and pMT/Hygro/*hyal-1*/L, respectively. The presence of the recombinant enzymes in the medium was confirmed by Western blot analysis using an anti-V5-antibody (**Fig. 5.4**).

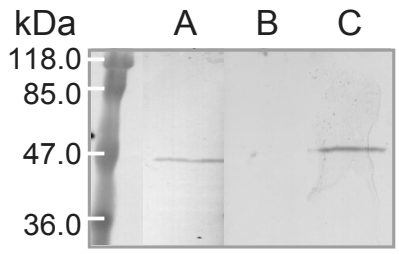


**Fig. 5.4** Western blot analysis of 30 µL of DS-2 cell medium 6 d after induction of transient expression of Hyal-1/S (A) and Hyal-1/L (C). Lane B contained induced wild type DS-2 cell medium. Anti-V5-IgG was used as primary antibody and biotinylated anti-mouse-IgG as secondary antibody. Detection of the antibody binding was achieved by HRP/DAB staining.

No cross reactivity with any wild type protein in the medium was observed (**Fig. 5.4**, lane B). Transfected DS-2 cells expressed a ca. 46 kDa protein (Hyal-1/S) and a ca. 51 kDa protein (Hyal-1/L), respectively, reacting with the primary antibody (**Fig. 5.4**, lane A and C). The molecular mass calculated from the amino acid sequence was 42.0 kDa (Hyal-1/S) and 50.5 kDa (Hyal-1/L), respectively. Variations in the molecular mass of the heterologous proteins can be caused by post-translational modifications of the proteins in the eukaryotic expression system, but also by the inaccuracy of the pre-stained Western blot standard proteins.

Hyaluronidase activity was subsequently determined for both Hyal-1/S and Hyal-1/L in the medium and in the complete cell lysate. However, neither the medium nor the complete cell lysate of DS-2 cells expressing Hyal-1/S contained any hyaluronidase activity. DS-2 cells transfected with pMT/Hygro/*hyal-1/L* exhibited 9 d after induction of expression a hyaluronidase activity of 0.6 nmol GlcNAc · $min^{-1}$ · $mL^{-1}$ cell suspension in the medium and an activity of 0.03 nmol GlcNAc · $min^{-1}$ · $mL^{-1}$ cell suspension in the complete cell lysate. The medium and complete cell lysate of wild-type DS-2 cells did not exhibit any hyaluronidase activity under identical assay conditions.

The presence of hyaluronidase activity in the cell lysate of transfected cells might be due to the fact that Hyal-1 is a lysosomal enzyme (Gold 1982). Although no simple consensus sequence exists for the transport of proteins to lysosomes, a structural motif in the three-dimensional structure of lysosomal proteins is supposed to be responsible for the sorting of

the majority of proteins to lysosomes via the mannose-6-phosphate receptor (Ni et al. 2006). Possibly, the human sequence motif for protein transport to lysosomes is, at least partially, recognized by insect cells, resulting in an accumulation of recombinant Hyal-1/L not only in the extracellular compartment, but also in lysosomes.

The low hyaluronidase activity in the medium indicates that the transfection efficiency was rather low. After selection of hygromycin-resistant DS-2 cells and optimization of growth and expression conditions (see below) ca. 450 nmol GlcNAc · $min^{-1}$ · $mL^{-1}$ cell suspension could be achieved in the medium 10 d after induction.

5.3.3.2. Stable expression of Hyal-1/L in DS-2 cells

For production of Hyal-1/L in a larger scale (up to 6 L) some parameters of the DS-2 cell expression system were explored in order to improve the yields of recombinant protein.

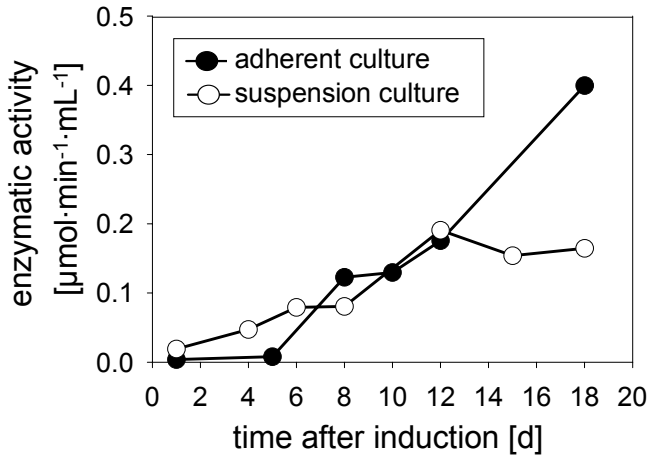


**Fig. 5.5** Hyal-1/L activity in the medium of stably transfected DS-2 cells depending on the time period after induction. Activity was determined by the colorimetric hyaluronidase activity assay (incubation mixture A) for cells grown in flasks (adherent culture, open circles) and for cells grown in suspension (filled circles). Cultures were initiated with 1.5 · $10^6$ cells/mL 24 h before induction.

As it is inconvenient to grow large quantities of adherent cells, DS-2 cells were grown in suspension and the enzyme yields (measured via the enzymatic activity in the medium) were compared to cells grown adherently in culture flasks (**Fig. 5.5**). After 10 – 12 d of induction expression levels were very similar for both cultures. While the enzymatic activity in the medium increased further in the adherent culture, the activity in the suspension culture medium remained at a constant level. Therefore, for suspension cultures an induction period of 10 – 12 d was chosen.

Furthermore, enzymatic activity depended on cell density (**Fig. 5.6**). Ten days after induction of expression the yield in recombinant hyaluronidase was similar, when initial cell densities were ≥ 2 · $10^6$ cells/mL, but dropped significantly at lower initial cell densities. DS-2 cells are known to be density sensitive, but cell growth should not be impeded at cell densities exceeding 0.5 · $10^6$ cells/mL (as declared by the supplier). However, for protein expression experiments it seemed to be advantageous to keep the initial cell density as high as possible (**Fig. 5.6**).

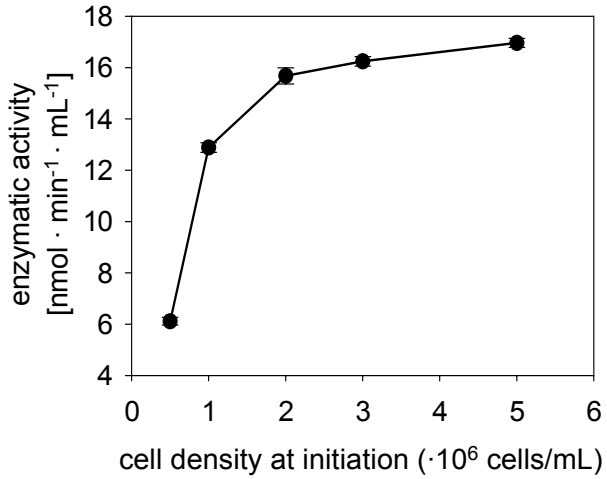


**Fig. 5.6** Hyal-1/L activity in the medium of stably transfected DS-2 cells depending of the cell density at the time of initiation of the cell culture. Expression was induced 24 h after initiation. The cells were cultivated in suspension for 10 d before the activity in the medium was determined by the colorimetric hyaluronidase activity assay using incubation mixture A.

During optimization experiments a range of different Hyal-1/L yields was observed in dependence on the sub-culturing stage of the transfected cells. This might be due to depletion of transfected DS-2 cells from the culture and deterioration of hygromycin solutions. Best expression yields with ca. 450 nmol GlcNAc · $min^{-1}$ · $mL^{-1}$ activity in the medium (colorimetric assay, incubation mixture A) were observed 10 - 12 d after induction of early passages of stably transfected DS-2 cells seeded at cell density of at least 2 · $10^6$ cells/mL. Hygromycin in the expression culture influenced expression yields only to a minor extent (data not shown) and was thus excluded from larger suspension culture volumes.

### *5.3.4. Purification of Hyal-1/L from DS-2 cell medium*

5.3.4.1. Ammonium sulfate precipitation

In order to reduce the sample volume Hyal-1/L was in the first purification step precipitated in the DS-2 cell medium by ammonium sulfate.

Ammonium sulfate precipitation was performed in the presence of 1 mM EDTA and 0.1 % Triton X-100. An initial precipitation experiment revealed that the main fraction of Hyal-1 activity was found in the ammonium sulfate precipitate at 30 % saturation (**Fig. 5.7**). At 40 % saturation Hyal-1 activity was still found in the precipitate, however, at this concentration a strong increase in aggregation was observed in the medium indicating the co-precipitation of other proteins in the medium.

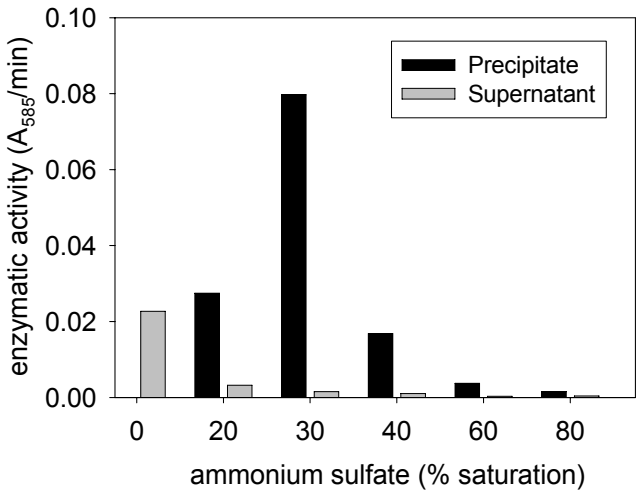


**Fig. 5.7** Precipitation of Hyal-1/L at increasing ammonium sulfate concentrations. $(NH_4)_2SO_4$ was added to DS-2/pMT/Hygro/*hyal-1/L* medium 10 d after induction of expression. The solution was stirred for 15 min on ice, proteins were precipitated at 12,000 g (10 min) and the precipitate solubilized in 50 mM Na-phosphate, 0.5 M NaCl, 0.1 % Triton X-100, pH 7.8 to yield a 10-fold concentration of the sample.

This precipitation step reduced the sample volume by a factor of 10. Precipitation of Hyal-1/L by ammonium sulfate was advantageous for concentration of the sample, but unfortunately resulted also in a loss of total Hyal-1/L due to incomplete solubility of the precipitated protein in solubilization buffer.

5.3.4.2. Ion exchange chromatography

As a primary step of the purification procedure Hyal-1/L (pI = 7.3, calculated from the amino acid sequence) was bound to a cation exchange chromatography column (CM-Sephadex) at pH 6.0. At pH values above pH 6.3 Hyal-1/L started to form aggregates due to approximation to the pI.

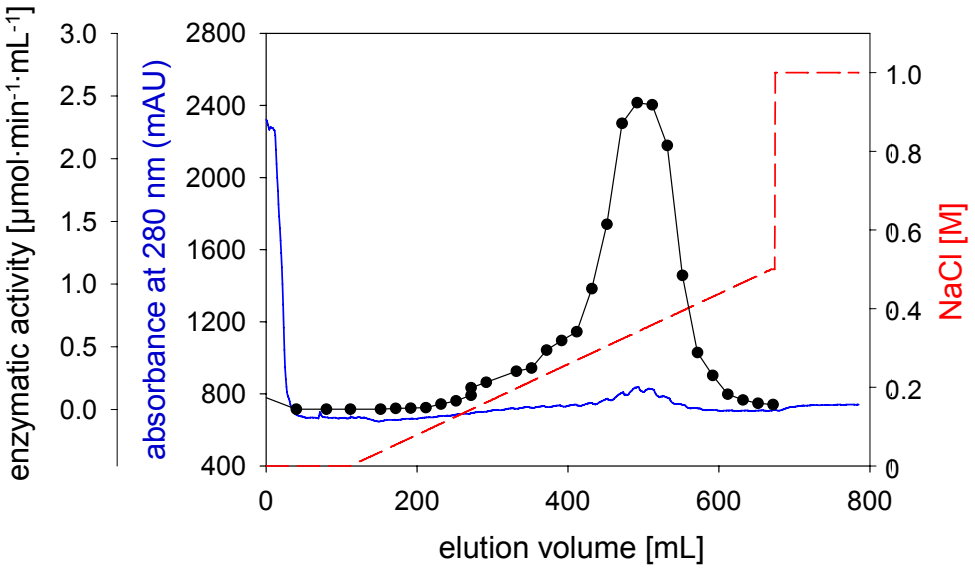


**Fig. 5.8** Elution profile of Hyal-1/L bound to a CM-Sephadex cation exchange column (CV 37 mL). The absorbance (solid, blue line) was followed at 280 nm and the enzymatic activity (black circles) was measured in fractions of 8 mL in the colorimetric hyaluronidase activity assay using 0.1 M formic acid/Na-formate, 0.1 M NaCl, pH 3.5, as incubation buffer. Elution was achieved at increasing NaCl concentrations (dashed, red line).

At pH 6.0 91 % of the enzymatic activity of Hyal-1/L bound to the CM-Sephadex material. Elution was achieved by application of a linear NaCl gradient. Hyal-1/L eluted at NaCl concentrations of 0.3 – 0.4 M as a broad single peak (**Fig. 5.8**) yielding 83 % of the activity bound to the column.

Alternatively, Hyal-1/L was assayed with respect to binding to an anion exchange chromatography column (Q-Sepharose) at pH 8.0. Though the protein bound with very high affinity (98 % binding of Hyal-1/L activity), the enzyme was neither eluted by increasing NaCl concentrations (up to 1.0 M) nor by a decrease in pH to pH 4.5. Elution was finally achieved by addition of 1.0 M arginine, possibly due to the solubilizing properties of this amino acid (cf. Chapter 4) (data not shown).
As anion exchange chromatography seemed to pose more problems than the cation exchange chromatography, and additionally, Hyal-1/L is known to exhibit its activity at acid pH, purification by CM-Sephadex at pH 6.0 was favored.

5.3.4.3. IMAC purification

The fusion to a C-terminal His-tag allowed for the purification of Hyal-1/L via IMAC. In the course of the previous purification steps $Cu^{2+}$ ions present in the medium of the insect cells were separated from the protein by addition of EDTA. Therefore, Hyal-1/L eluted from the cation exchange chromatography column was bound under slightly acidic conditions (pH 6.8) and after addition of 0.2 M NaCl to a Ni-IMAC. A strong tendency for aggregation of the Hyal-1/L sample was observed at pH values above pH 6.5, thus the pH of the sample was adjusted to 6.3 for binding, while the pH of the equilibration buffer was kept at pH 6.8 to allow for sufficient deprotonation of the His residues. This enabled a reasonable binding affinity of Hyal-1/L (70 % of the original activity) with minimum deficiencies during pH adjustment.

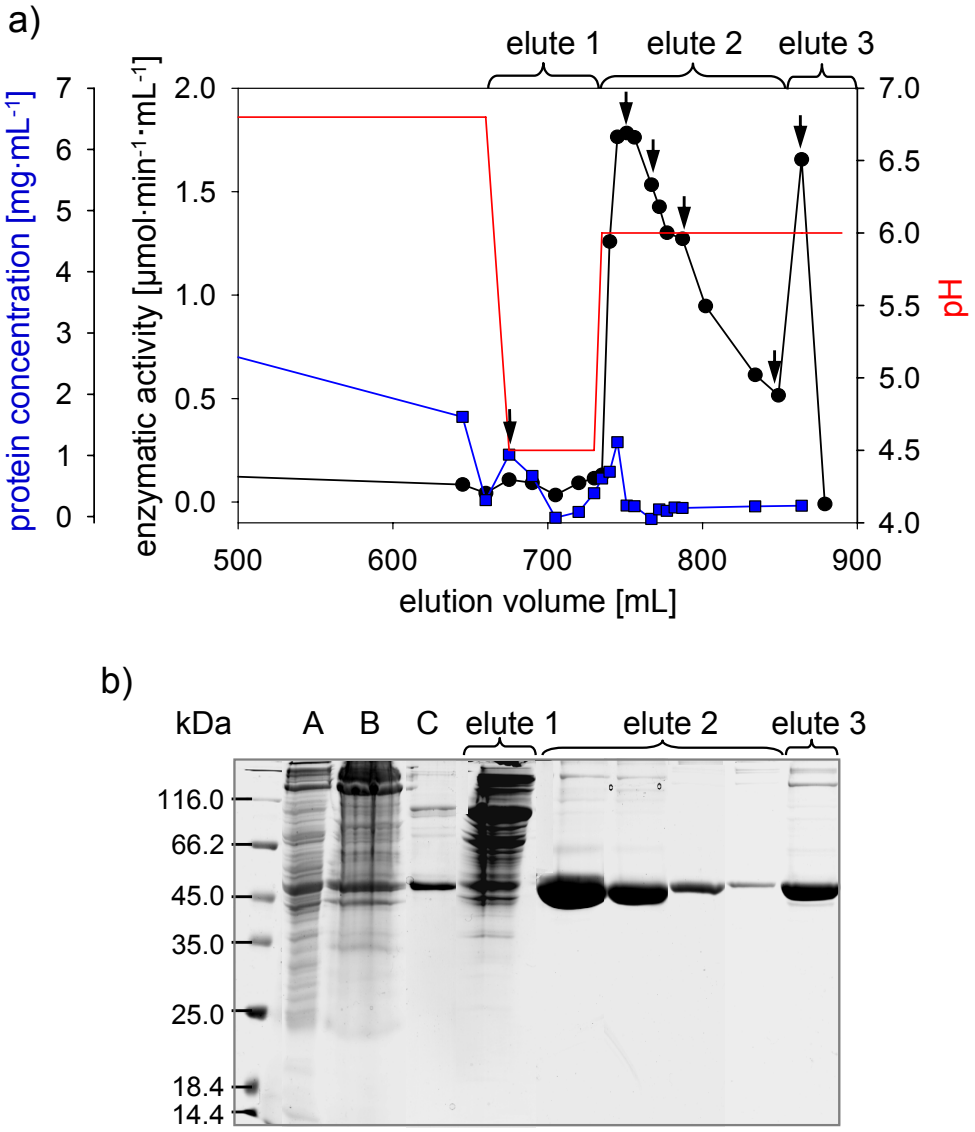


**Fig. 5.9** Ni-IMAC purification (3 x 5 mL CV) of Hyal-1/L subsequent to ammonium sulfate precipitation and cation exchange chromatography. a) The elution profile of the Ni-IMAC shows the washing with equilibration buffer (pH 6.8), elution by a decrease of the pH (elute 1), elution by addition of EDTA at pH 6.0 (elute 2) and elution with EDTA in the presence of Triton X-100 (elute 3). The protein concentration is represented by the blue squares, the enzymatic activity by black circles and the pH by the solid red line. b) SDS-PAGE analysis of the Hyal-1/L purification procedure. Each lane contained 30 µL of sample and 6 µL of 5 x SDS sample buffer. A) DS-2/pMT/Hygro/*hyal-1/L* medium, 11 d after induction; B) ammonium sulfate precipitate after solubilization; C) Hyal-1/L after cation exchange chromatography; elute 1) – elute 3) refer to fractions of the Ni-IMAC marked with an arrow in a). The fractions were applied to the gel in the sequence of elution.

A wide variety of binding buffers as well as elution methods was tested to gain sufficient purity of the protein in combination with high elution yields. Standard procedures, e.g. purification by the Protino® Ni-ion purification kit (Macherey-Nagel, Düren, Germany) and binding in the presence of low concentrations (10 – 20 mM imidazole) failed due to insufficient binding (maximum 30 % of the initial activity). Furthermore, binding of Hyal-1/L

in the $CuSO_4$-supplemented medium directly to chelating Sepharose resulted in very weak binding of the enzyme.

In the absence of imidazole in the binding buffer a high amount of impurities was bound to the Ni-IMAC column, but could be eluted by washing with binding buffer at pH 4.5 (**Fig. 5.9**). Normally, a decrease in the pH to values below pH 6.0 is supposed to elute the His-tagged protein as well. However, in the case of Hyal-1/L only a minor fraction of the His-tagged protein was eluted at pH 4.5 and in the presence of high concentrations of imidazole (data not shown), while the main amount of Hyal-1/L could be gained only after elution of the $Ni^{2+}$ ions with EDTA. As shown in **Fig. 5.9.b** Hyal-1/L eluted by EDTA occurred on the SDS-PAGE as a single band of 54 kDa with minimal impurities.

In the absence of Triton X-100 in the elution buffer (elute 2 in **Fig. 5.9.a**) Hyal-1/L eluted extremely slowly from the column material even after elution of the $Ni^{2+}$ ions. Addition of Triton X-100 enabled a faster and more concentrated elution of Hyal-1/L (elute 3 in **Fig. 5.9.a**). During the whole purification procedure Triton X-100 had to be added to the buffers to avoid adhesion of Hyal-/L to column materials as well as to centrifugal devices. However, Triton X-100 can not be removed from the protein completely and disturbed photometric analyses of Hyal-1/L.

Observations during optimization of the purification of Hyal-1/L suggest that the recombinant protein binds to the Ni-IMAC column via the His-tag, albeit not exclusively. The extraordinarily slow elution even in the absence of $Ni^{2+}$ ions indicates a high affinity of the hyaluronidase itself to the column material, i.e. to Sepharose (cross-linked agarose) resulting in a retardation of Hyal-1/L in respect of the $Ni^{2+}$ ions.

Although protein purification column materials like Sepharose are designed to exhibit only minimum protein binding affinity, the special properties of the hyaluronidases strongly impede the protein purification methods. Possibly, the structural relationship of agarose to the natural substrate, hyaluronic acid, caused the unexpected binding affinity of Hyal-1/L to the Ni-IMAC column material. A similar, extraordinarily high binding affinity of Hyal-1/L was observed upon binding to Q-Sepharose (cf. 5.3.4.2), but not to CM-Sephadex. Presumably, Sephadex (cross-linked dextran) exhibits fewer interactions with the hyaluronidase than Sepharose.

### *5.3.5. Characteristics of Hyal-1/L, expressed by DS-2 cells, in comparison to Hyal-1/L, expressed in E. coli*

In the following chapter Hyal-1/L, expressed in *E. coli* and refolded *in vitro*, is referred to as Hyal-1/*E. coli* and Hyal-1/L, expressed in DS-2 cells, as Hyal-1/DS-2. Due to missing enzymatic activity no characterization experiments were performed with Hyal-1/S.

The schematic representation of the primary structures in **Fig. 5.10** visualizes the differences between BVH, human Hyal-1, Hyal-1, expressed in *E. coli* (Hyal-1/*E. coli*), and Hyal-1, expressed in insect cells (Hyal-1/DS-2).

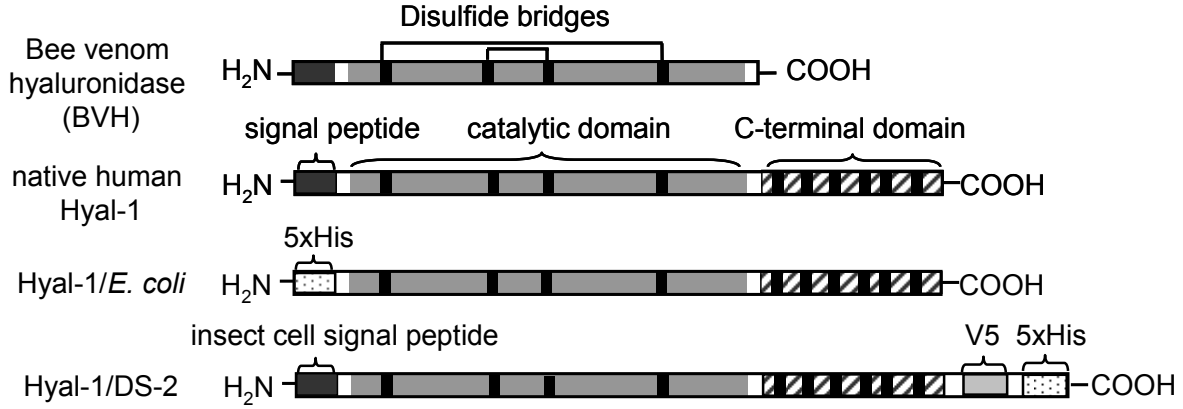


**Fig. 5.10** Diagrammatic representation of the primary structures of bee venom hyaluronidase (BVH), human Hyal-1 precursor, Hyal-1/*E. coli* and Hyal-1/DS-2. Domains are marked according to their function and C residues are shown as narrow black boxes. Disulfide bridge linkage is only known for BVH. The function of the C-terminal domain is unknown, but the sequence shows significant similarity to EGF domains.

#### 5.3.5.1. pH profiles

The pH profile of a hyaluronidase is a characteristic feature differing for each of the hyaluronidase subtypes. Human Hyal-1 is known to be an acid active enzyme with maximum catalytic activity at pH 3.5 – 4.0 (Gold 1982, Afify et al. 1993, Csoka et al. 1997, Frost et al. 1997). The pH profiles of Hyal-1/*E. coli* and Hyal-1/DS-2 resemble closely the profile of human plasma hyaluronidase reported by Muckenschnabel et al. (Muckenschnabel et al. 1998), which was measured under comparable assay conditions (**Fig. 5.11.a**). The pH profile of Hyal-1/DS-2 was shifted slightly to higher pH values with an optimum at pH 4.0 instead of pH 3.5 possibly due to effects of the buffer present in the enzyme samples.

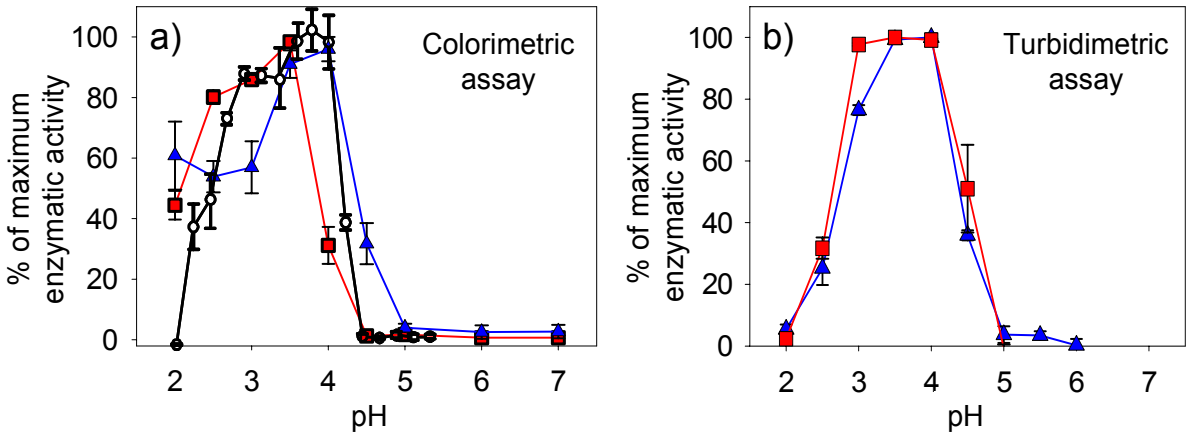


**Fig. 5.11** pH profiles of *in vitro* folded Hyal-1/*E. coli* (red squares) and Hyal-1/DS-2 (blue triangles). Black circles indicate the pH profile of human plasma hyaluronidase as determined by Muckenschnabel et al. (Muckenschnabel et al. 1998). Activities were determined in the colorimetric activity assay (a) using incubation mixture B and the turbidimetric activity assay (b) using incubation mixture B. Maximum hyaluronidase activity was normalized to 100 % for each Hyal-1 derivative. Activity values are mean values ± SEM of three incubation mixtures.

Hyaluronidase activity profiles were also measured in the turbidimetric activity assay to determine, if the pH optima of Hyal-1 were dependent on the type of assay as described previously for the pH profiles of BTH (Hoechstetter et al. 2001, Hoechstetter 2005). However, the turbidimetric and the colorimetric activity assay yielded nearly identical pH profiles for both recombinant enzymes, Hyal-1/*E. coli* and Hyal-1/DS-2, (**Fig. 5.11.b**), indicating the absence of pH dependent variations in the degradation mechanism (cf. Chapter 8).

5.3.5.2. NaCl sensitivity

For human hyaluronidase isolated from liver and plasma an inhibitory effect of NaCl at concentrations exceeding 100 mM has been reported (Gold 1982, Afify et al. 1993). Indeed, colorimetric determination of Hyal-1 activity at pH 3.5 with increasing NaCl concentration (0 - 1 M) revealed an inhibition of the hyaluronidase activity by NaCl (**Fig. 5.12**). However, Hyal-1/*E. coli* was already inhibited at concentrations > 50 mM, while Hyal-1/DS-2 showed an optimum of hyaluronidase activity at 100 mM NaCl with a fast drop in activity at concentrations > 100 mM. At 1 M NaCl the activity of both enzymes was completely inhibited. Without NaCl the activity of Hyal-1/DS-2 decreased by ca. 40 % compared to the optimum concentration of 100 mM, while the activity of Hyal-1/*E. coli* remained at its maximum even without any NaCl present.

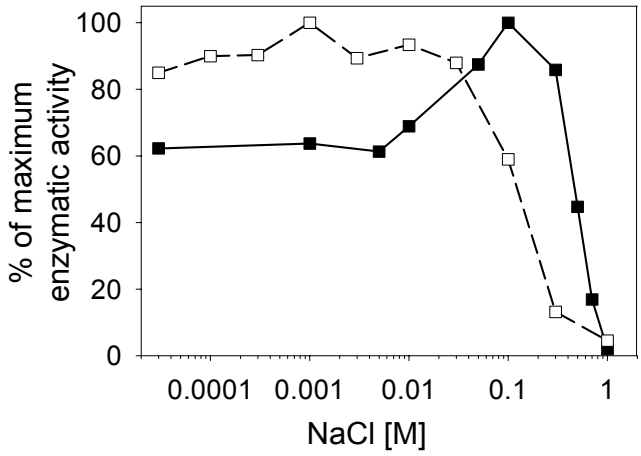


**Fig. 5.12** NaCl sensitivity of Hyal-1/*E. coli* (white squares) and Hyal-1/DS-2 (black squares) determined in the colorimetric activity assay (incubation mixture A).

The effects of ionic strength on hyaluronidase activity have often been ascribed to the ability of the substrate, hyaluronic acid, to interact with cations (Vercruysse et al. 1999, Oettl 2000). Alterations in the ionic strength could thus cause the formation or disruption of tertiary structures of hyaluronan, thereby influencing the contact regions available for the catabolizing enzymes.

Apparently, the differences in the sensitivity towards NaCl of Hyal-1/*E. coli* and Hyal-1/DS-2 can not merely be explained by the influence of the ionic strength on the hyaluronic acid as the catalytic site of the enzymes, and therefore, the mode of interaction with the substrate is supposed to be very similar for both enzymes. Since the inhibitory effects of NaCl were found to be reversible, one could imagine an influence of NaCl on the solubility of the enzymes in addition to the effects on the hyaluronic acid conformation. As solubility can be influenced by protein glycosylation this would provide a possible explanation for the differences in the NaCl sensitivities of the enzymes expressed in *E. coli* and in insect cells.

5.3.5.3. Sensitivity towards denaturing agents

During *in vitro* folding experiments with Hyal-1/*E. coli* a differential effect of GdmCl and urea on the solubility of the enzyme was observed (cf. Chapter 4, 4.2.). Therefore, the stability of Hyal-1/*E. coli* was determined in the presence of increasing concentrations of both denaturing agents by measuring the enzymatic activity (**Fig. 5.13**). Compared with urea as denaturing agent, a decrease in activity occurred at much lower GdmCl concentrations (50 % residual activity at 0.7 M GdmCl and 3 M urea, respectively). Even when taking the 1.5-fold stronger denaturing ability of GdmCl into consideration, the difference between the two denaturing agents is extraordinarily high. Hyal-1/DS-2 exhibited a similar behavior as Hyal-1/*E. coli* but with a slightly higher stability in both denaturing agents. Interestingly, the activity of Hyal-1/*E. coli* increased at concentrations up to 1.5 M urea in the reaction mixture, possibly due to an increased solubility of the enzyme.

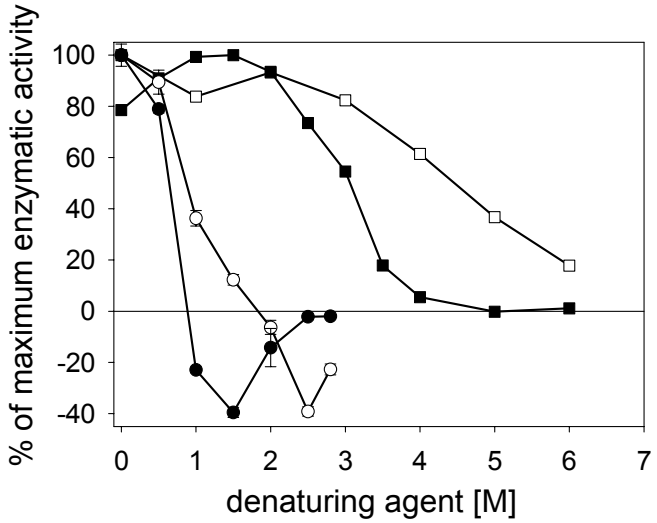


**Fig. 5.13** Dependency of hyaluronidase activity on increasing concentrations of urea (squares) and GdmCl (circles). Curves represented with open symbols were measured using Hyal-1/DS-2, curves with black symbols were measured using Hyal-1/*E. coli*. Urea dependencies were determined in the colorimetric activity assay (incubation mixture A), GdmCl dependencies in the turbidimetric activity assay (incubation mixture A). Maximum hyaluronidase activity was normalized to 100 % for each curve separately.

Activity curves were measured in the turbidimetric assay for GdmCl-dependence and in the colorimetric assay for urea-dependence due to disturbance of the alternative assay systems by the denaturing agents. References containing buffer instead of enzyme solution were subtracted for each concentration separately.

5.3.5.4. Effect of metal ions on the activity of Hyal-1/DS-2

Except for the influence of NaCl no other ionic effects have been described for human Hyal-1 yet. Therefore, a variety of divalent cations known to occur either as cofactors ($Ca^{2+}$, $Mg^{2+}$, $Zn^{2+}$) or as impurities in enzyme preparations ($Fe^{2+}$, $Ni^{2+}$, $Cu^{2+}$) were tested for their influence on Hyal-1/DS-2 activity at two different concentrations (10 mM and 100 mM) (**Fig. 5.14**).

The hyaluronidase activity was referenced to the activity in the presence of 100 mM of NaCl, the optimum NaCl concentration as determined in 5.3.5.2. To assure a minimum ionic strength of 100 mM the 10 mM mixtures were supplemented with 90 mM of NaCl. Although the ionic strength in the incubation mixtures was increased up to 4-fold compared to the reference ionic strength (100 mM), a maximum decrease of 10 – 15 % was expected as a result of the ionic strength (cf. 400 mM NaCl in **Fig. 5.12**).

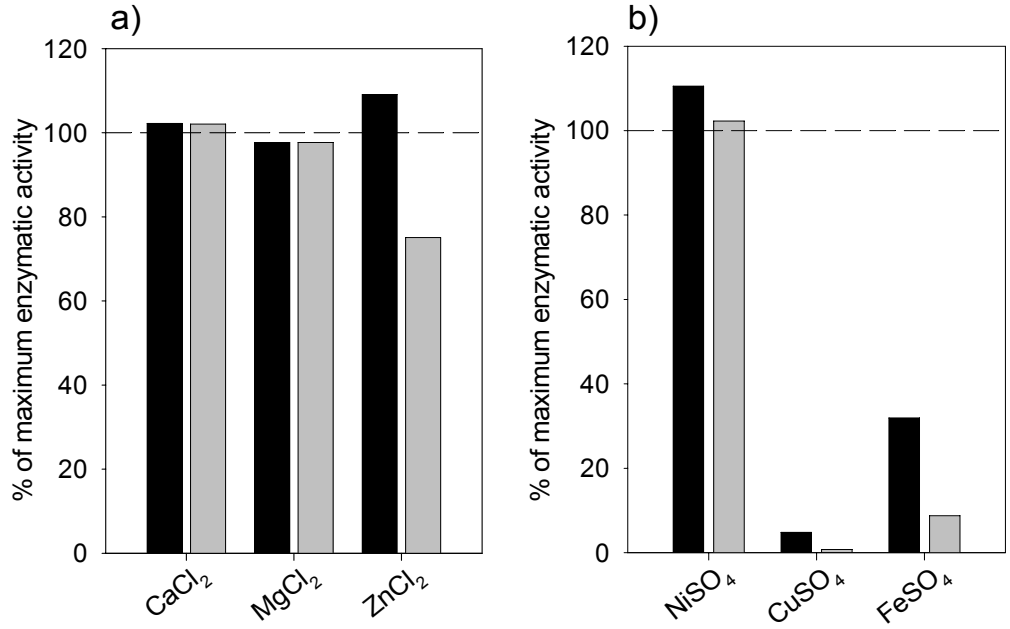


**Fig. 5.14** Influence of metal ions on the activity of Hyal-1/DS-2 as determined in the colorimetric activity assay (incubation mixture A) for 10 mM (black bars) and 100 mM (grey bars) of the salts indicated. Hyaluronidase activity at 100 mM NaCl was set as 100 %, incubation mixtures containing 10 mM of salt additive were supplemented with 90 mM NaCl.
a) Comparison to ionic strengths of 120 mM (10 mM salt additive, black) and 300 mM (100 mM salt additive, grey). b) Comparison to ionic strengths of 130 mM (10 mM salt additive, black) and 400 mM (100 mM salt additive, grey).

Compared to the enzymatic activity in the presence of 100 mM NaCl (100 %) only $NiSO_4$ and $ZnCl_2$ at low concentrations (10 mM) revealed a minor stimulation (≤ 10 %) of the Hyal-1/DS-2 activity. Strong inhibition (65 % - 98 %) was observed in the presence of 10 mM and 100 mM $FeSO_4$ and $CuSO_4$. As $Ni^{2+}$ from Ni-IMAC and $Cu^{2+}$ ions from the induction of expression were present during the purification of Hyal-1/DS-2 the effects of these ions were of special interest. However, induction of Hyal-1 expression in DS-2 cells was achieved by very low concentrations of $CuSO_4$ (0.5 mM). $Ni^{2+}$ ions occurred only in trace amounts due to leakage from the Ni-IMAC. Obviously, Hyal-1/DS-2 does not depend on any metal ion as a cofactor, but is inhibited by mM concentrations of $Cu^{2+}$ and $Fe^{2+}$.

5.3.5.5. Analysis of protein glycosylation

To confirm the presence of glycosidic modifications purified Hyal-1/L from both expression systems was stained after SDS-PAGE using the periodic acid-Schiff (PAS) technique. As expected, Hyal-1/*E. coli* did not react with Schiff´s reagent, while Hyal-1/DS-2 formed a pink band on the gel indicating the presence of glycosidic residues (**Fig. 5.15**).

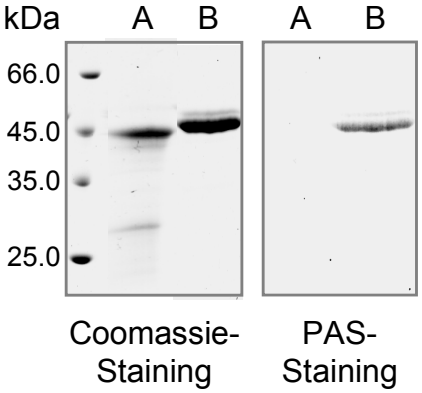


**Fig. 5.15** Analysis of glycosylation of Hyal-1/*E. coli* and Hyal-1/DS-2 by SDS-PAGE and PAS staining. After scanning the gel was additionally stained with Coomassie. A) Hyal-1/*E. coli* purified from IBs. B) Hyal-1/DS-2 purified from the medium of insect cells.

The amino acid sequence of Hyal-1/DS-2 contains three potential N-glycosylation sites (consensus sequence N-X-T/S) and no O-glycosylation sites as determined by the ExPASy NetOGlyc 3.1 tool (Julenius et al. 2005). When Hyal-1/DS-2 was deglycosylated under native conditions by incubation with increasing amounts of N-glycosidase F (PNGase F) a second band was detected in the Western blot with a molecular mass reduced by ca. 3 - 4 kDa compared to the untreated control sample (0 units N-glycosidase F) (**Fig. 5.16**). Although deglycosylation could not be followed to completion, a 40 % reduction of enzymatic activity could be observed in the colorimetric activity assay when about half of the protein present on the western blot was deglycosylated.

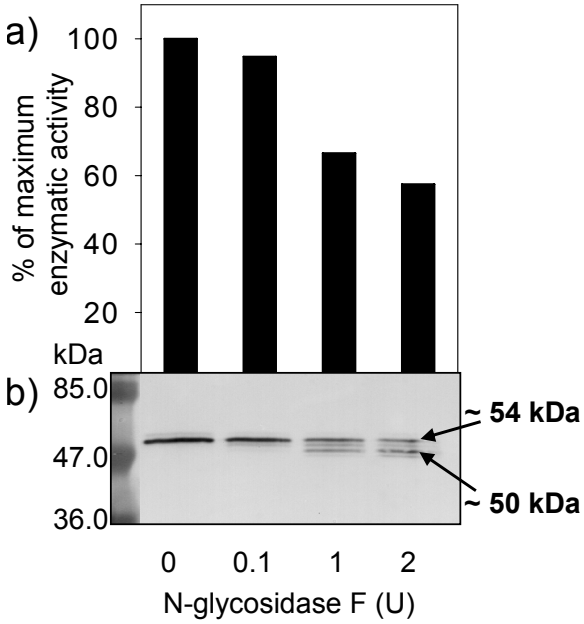


**Fig. 5.16** Partial deglycosylation of Hyal-1/DS-2 (4 µg, 0.6 U/mg) by incubation of the enzyme with increasing amounts of N-glycosidase F for 4 h at 37 °C in 50 mM Na-phosphate, 10 mM EDTA, pH 6.0. A) Measurement of Hyal-1 activity in a colorimetric assay, using 0.1 Na-formate, 0.1 NaCl, pH 3.5 as incubation buffer. B) Western Blot analysis of Hyal-1/DS-2 using anti-V5-IgG as primary antibody and HRP/DAB for subsequent staining.

The molecular mass of 54.2 kDa of Hyal-1/DS-2 was additionally confirmed by MALDI-MS. Thus, the glycosidic residues attached to the protein comprise a molecular mass of 4 kDa since the molecular mass expected from the amino acid sequence was 50.5 kDa.

5.3.5.6. Analysis of the catalytically active enzyme fraction

Hyal-1/DS-2 was analyzed for its catalytic activity on a zymography gel. Intriguingly, the activity of Hyal-1/DS-2 was hardly impeded by boiling for 5 min in the presence of reducing agents and 2 % SDS, indicating an extremely high stability of the recombinant enzyme (**Fig. 5.17**). In the absence of DTT the enzymatic activity remained undisturbed even after 10 min of boiling with SDS.

Surprisingly, the zymography showed two bands of ca. 53 and ca. 64 kDa as proteins exhibiting hyaluronidase activity at acid pH (**Fig. 5.17**). Since this observation is contradictory to the single protein band observed after purification of Hyal-1/DS-2 on the SDS-PAGE (**Fig. 5.9**), further experiments were performed to assure the existence of Hyal-1/L as a homogenous protein species.

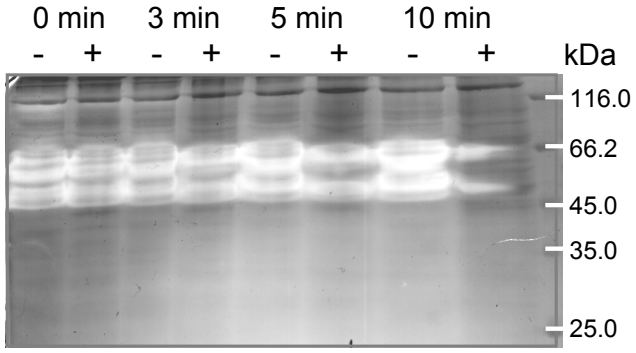


**Fig. 5.17** Zymography of Hyal-1/L expressed in DS-2 cells in the presence (+) and in the absence (-) of DTT. Samples contained 40 µl of DS-2 cells medium collected 10 d after induction of expression of Hyal-1/L. All samples were mixed with 10 µl of SDS sample buffer with or without DTT to achieve a final SDS concentration of 2 % and boiled for the times indicated above each pair of lanes. The gel was stained with Alcian blue and Coomassie.

Considering previous reports on the existence of two human hyaluronidase Hyal-1 isoenzymes of 45 kDa and 57 kDa in urine (Csoka et al. 1997), the question arose if Hyal-1 expressed in DS-2 cells might also be cleaved endoproteolytically as suggested for the isoenzymes in urine. Therefore, purified Hyal-1/L was N-terminally sequenced by Edman degradation and the identity of Hyal-1/L was confirmed as a protein with a homogenous N-terminal sequence. The N-terminus RSPWPGFRGPLLPNR is in accordance to the sequence expected from the amino acid sequence coded by pMT/Hygro/*hyal-1/L* after cleavage of the insect cell signal peptide (cf. Appendix 2).

Analysis of the purified protein on an SDS-PAGE in the presence and in the absence of DTT revealed a significant change in the electrophoretic mobility of Hyal-1/DS-2, depending on the absence or presence of the reducing agents (**Fig. 5.18**). In the absence of DTT Hyal-1/DS-2 was detected as a protein band with an apparent molecular weight of ca. 66 kDa, i.e. corresponding to one of the protein bands observed in the zymography. After reduction with DTT Hyal-1/DS-2 exhibited a molecular weight of ca. 54 kDa, which is in accordance with the molecular mass determined previously (5.3.4.3).

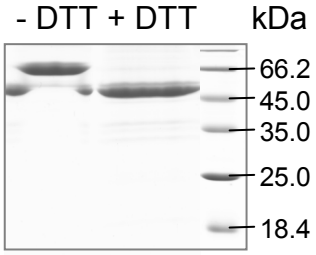


**Fig. 5.18** SDS-PAGE of purified Hyal-1/DS-2 in the absence (- DTT) and in the presence of reducing agents (+ DTT). 20 µl of enzyme were mixed with 5 µl SDS sample buffer, with or without DTT, and boiled for 3 min at 100 °C.

Apparently, the detection of Hyal-1/DS-2 as two distinct protein bands on the zymography gel was due to partial reduction of the protein during electrophoresis pretending the presence of two different proteins with hyaluronidase activity. This effect was mainly observed in unpurified protein samples with a high enzymatic activity.

### *5.3.6. Biophysical characterization of Hyal-1/DS-2*

5.3.6.1. CD spectroscopy

To gain initial information on the structural elements of Hyal-1 CD spectra were recorded in the range between 195 and 260 nm (**Fig. 5.19**). Automatic analysis of the secondary structure elements revealed 36 % α-helix, 8 % antiparallel β-sheets, 8 % parallel β-sheets, 16 % beta-turns and 31 % random coil.

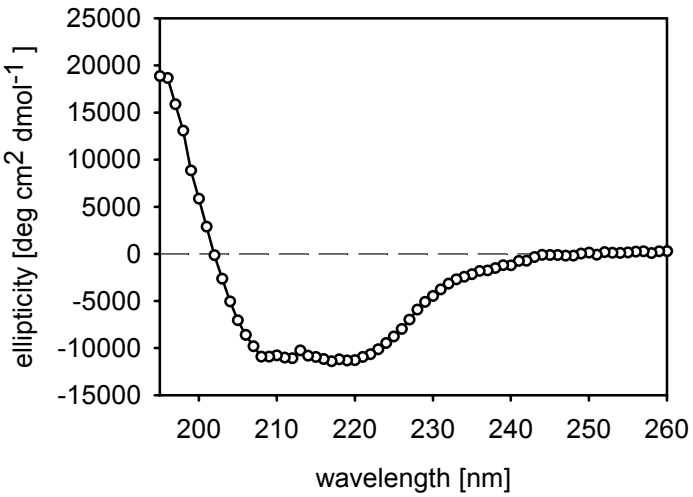


**Fig. 5.19** CD spectrum of 0.5 mg/mL Hyal-1 solubilized in 50 mM Na-phosphate, 0.5 M NaCl, 1 mM EDTA, pH 6.0.

The determined data are in good agreement with the $(\beta/\alpha)_7$ fold found in the crystal structure of BVH (1FCV.pdb). In BVH 32 % of the amino acid residues participate in α-helices, 13 % in β-sheets and 55 % are not assigned to any of the two secondary structure elements, i.e. they exhibit a random coil or turn structure (Botzki 2004).

The human Hyal-1 model structure (Jedrzejas and Stern 2005) comprising both, the catalytic and the C-terminal domain, exhibits 41 % α-helices, 9 % β-sheets and 50 % turn and random coil structures. The model of human Hyal-1 is – except for the percentage in β-sheets –

roughly in accordance with the CD-spectrum of Hyal-1. Since the model of the C-terminal domain was predicted by an *ab initio* approach (Jedrzejas and Stern 2005), deviations between the model structure and experimental data could be due to changes in the secondary structure of the C-terminal domain. Furthermore, it should be noted that except for the percentage of α-helix the calculated percentage of the other secondary structures is rather imprecise (personal communication by Dr. H. Lilie).

5.3.6.2. Analytical ultracentrifugation

As mentioned previously (5.3.5.5) the molecular mass of Hyal-1/DS-2 determined by SDS-PAGE and MALDI-MS was 54.2 kDa, with the protein component comprising 50.5 kDa and the glycosidic component comprising 3.7 kDa.

The molecular mass of Hyal-1/DS-2 was calculated from the sedimentation equilibrium considering a partial specific volume of 0.726 cm³/g, which was calculated from the partial specific volume of the protein fraction (0.735 cm³/g) and the carbohydrate fraction (0.610 cm³/g). Intriguingly, a molecular mass of 93.8 ± 1.3 kDa was determined from the sedimentation equilibrium at a protein concentration of 0.5 mg/mL (**Fig. 5.20**).

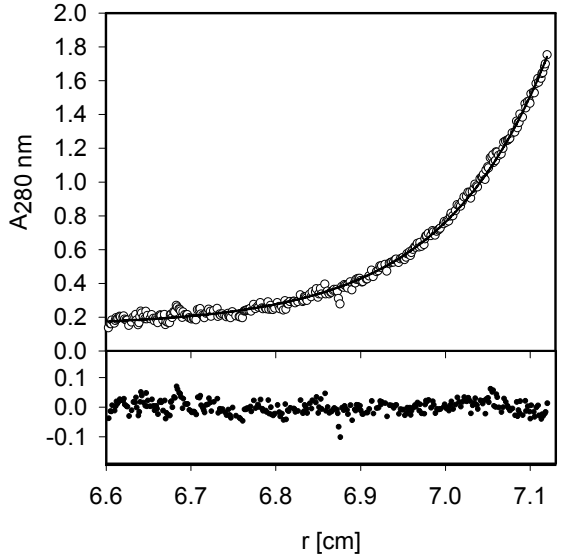


**Fig. 5.20** Sedimentation equilibrium observed after 60 h of centrifugation for 0.5 mg/mL Hyal-1/DS-2 solubilized in 50 mM Na-phosphate, 0.5 M NaCl, 1 mM EDTA, pH 6.0. The plot given at the bottom shows the difference between the experimental data and the calculated curve.

The average molecular mass of 94 kDa indicates the existence of Hyal-1/DS-2 as a dimer. The difference between the expected molecular mass of a Hyal-1/DS-2 dimer (108 kDa) and the one determined by analytical ultracentrifugation might be a result of the presence of low concentrations of monomer in the solution (personal communication by Dr. H. Lilie).

Unfortunately, the quantification of the average molecular mass in dependence of the protein concentration failed presumably due to the presence of low molecular weight compounds in the protein sample disturbing the baseline at lower protein concentrations. However, a shift in

the molecular weight towards a lower average molecular mass could be observed at decreasing protein concentrations indicating the existence of a monomer – dimer equilibrium. Determination of the molecular mass by analytical gel filtration was impossible because of interference of Hyal-1/DS-2 with the stationary phase resulting in a strongly asymmetric elution profile of the enzyme and a shift to longer retention times pretending a lower molecular mass (ca. 10 kDa) compared to the molecular weight standard proteins (data not shown).

5.3.6.3. Crystallization experiments

A variety of crystallization conditions was screened, but mainly resulted in the formation of Hyal-1/DS-2 aggregates. Few crystals were obtained, which either consisted merely of salt, were unstable during handling (**Fig. 5.21.a**) or too small for x-ray analysis (**Fig. 5.21.b**).

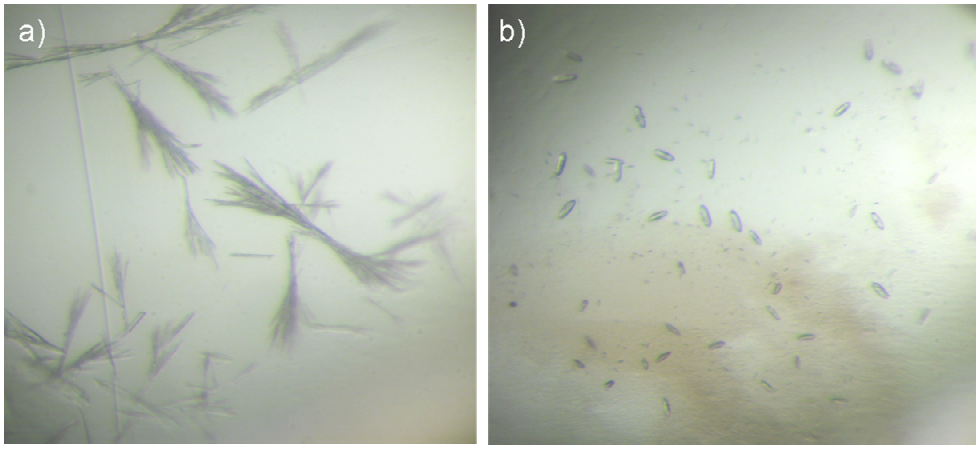


**Fig. 5.21** Crystals formed during crystallization experiments with Hyal-1/DS-2 in various buffers. (Photographed by B. Epler, Institute of Biotechnology, Martin-Luther University Halle-Wittenberg, Halle (Saale), Germany).

No significant differences in the formation of crystals were observed for Hyal-1 solubilized in the absence and in the presence of Triton X-100. A tendency of crystal formation was found to occur under two major conditions: firstly, using 0.2 M calcium chloride hexahydrate, 0.1 M Tris, pH 8.5 and precipitating agent PEG 4000 and hexanediol, respectively; secondly using 0.2 M zinc acetate, 0.1 M sodium cacodylate, pH 6.5 and precipitating agent PEG 8000 and PEG 4000, respectively (personal communication by B. Epler).

Since crystals were inappropriate for x-ray analysis a fine screening of crystallization conditions is in progress.

### *5.3.7. Substrate specificity of Hyal-1/DS-2*

Like all other hyaluronidases known up to date the human hyaluronidases are expected to accept not only HA but also other glycosaminoglycans as substrates (Stern and Jedrzejas 2006). Due to the availability of human hyaluronidases in very low quantities the degradation of alternative substrates has never been studied in detail.

A common alternative substrate recognized by vertebrate hyaluronidases is chondroitin sulfate, a polysaccharide consisting of β1→4 linked disaccharide units of sulfated β-D-GalNAc and β-D-GlcUAc residues linked by β1→3 glycosidic bonds (**Fig. 5.22**). Chondroitin sulfate B, also known as dermatan sulfate, additionally contains β-D-IdoAc instead of β-D-GlcUAc.

Chondroitin sulfates are important components of proteoglycans in the human body, e.g. of aggrecan, neurocan and brevican, and play an important role in inflammation (Taylor and Gallo 2006). They often occur together with HA and are thus accessible for hyaluronidases as well. In humans the hyaluronidase Hyal-4 is the only enzyme speculated to be a pure chondroitinase (cf. Chapter 1), while the other human hyaluronidases degrade ChS at a much slower rate than HA.

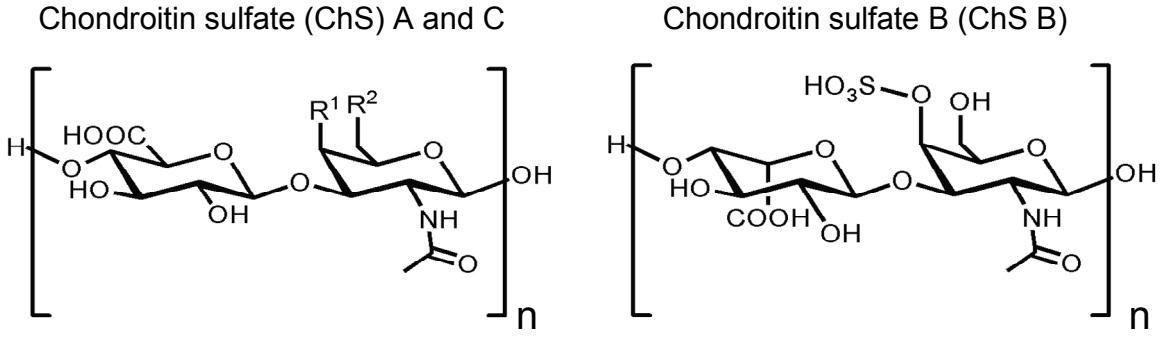


| | **R¹** | **R²** |
|---|---|---|
| **ChS A** | $OSO_3H$ | OH |
| **ChS C** | OH | $OSO_3H$ |

**Fig. 5.22** Structures of chondroitin sulfate A, B and C.

5.3.7.1. Chondroitinase activity assays

Due to the high structural similarity between ChS and HA the standard hyaluronidase activity assay systems used were tested for their ability to follow the degradation process of ChS. The turbidimetric assay is based on the precipitation of high molecular weight (> 6 – 8 kDa) hyaluronan fragments with quaternary ammonium salts. Degradation of hyaluronic acid results in a decrease in the turbidity (OD), which can be approximated by a linear fit for the initial degradation phase (**Fig. 5.23**). All chondroitin sulfates were found to precipitate with

CTAB in the turbidimetric assay, enabling the measurement of ChS degradation by this assay procedure.

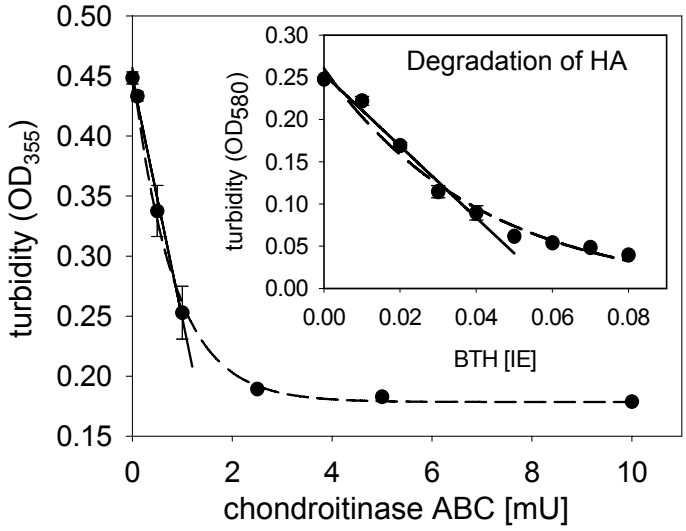


**Fig. 5.23** Degradation of ChS C by chondroitinase ABC from *Proteus vulgaris* followed in the turbidimetric activity assay at 355 nm (incubation mixture B, pH 7.0). Inset: degradation of hyaluronic acid by BTH followed in the turbidimetric activity assay at 580 nm (incubation mixture B, pH 4.0).

Yamagata et al. (Yamagata et al. 1968) detected the degradation products of bacterial chondroitinases by a colorimetric assay (Morgan-Elson assay). Since no reference substance was available for the quantification of the degradation products of ChS, the absorption spectra of the Morgan-Elson products originating from the degradation products of ChS A, ChS B and ChS C were compared to the spectrum of the Morgan-Elson reaction product formed with GlcNAc.

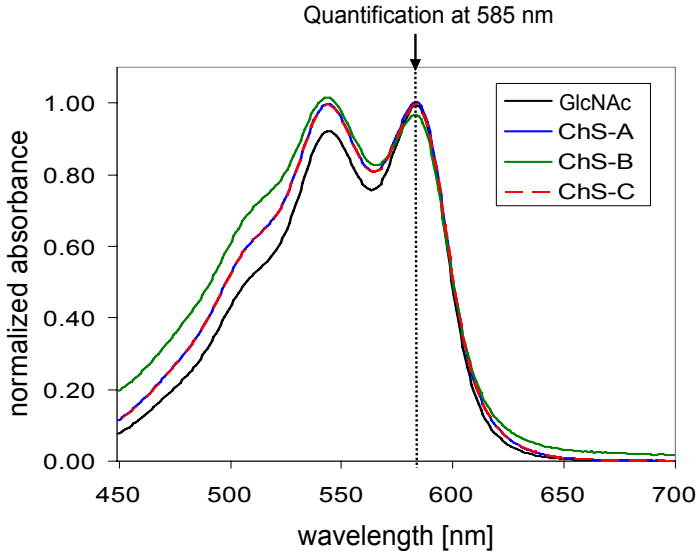


**Fig. 5.24** Normalized absorption spectra of the Morgan-Elson reaction products. The following substances were used for the Morgan-Elson reaction: GlcNAc (black), ChS A degraded by chondroitinase ABC (blue), ChS B degraded by chondroitinase ABC (green) and ChS C degraded by chondroitinase ABC (red).

Although the spectra of the Morgan-Elson products differ at shorter wavelengths (< 570 nm), the shape of the maximum at 585 nm, the quantification wavelength of the colorimetric activity assay, is nearly identical for all products (**Fig. 5.24**). Therefore, absorbance values determined in the Morgan-Elson assay with different substrates were compared to enable the determination of enzymatic activity relative to the activity on the natural substrate, HA, under optimum conditions (maximum enzymatic activity).

It should be noted, however, that the reaction catalyzed by chondroitinase ABC, the enzyme used for these reference measurements, is an elimination reaction creating Δ4,5-unsaturated disaccharide units (Yamagata et al. 1968). Human hyaluronidases catabolize HA in a hydrolysis reaction creating saturated disaccharide units and are expected to perform a similar reaction with the alternative substrates.

5.3.7.2. pH-dependent degradation of ChS by Hyal-1

Hyal-1, expressed by DS-2 cells, was tested for its ability to degrade ChS A, B and C at pH values 2.0 – 9.0 in the turbidimetric and in the colorimetric activity assay. Based on the considerations described above the results were converted into % of maximum enzymatic activity, i.e. the activity at the pH optimum of the HA degradation in the respective assay (cf. **Fig. 5.11**) was set as 100 %.

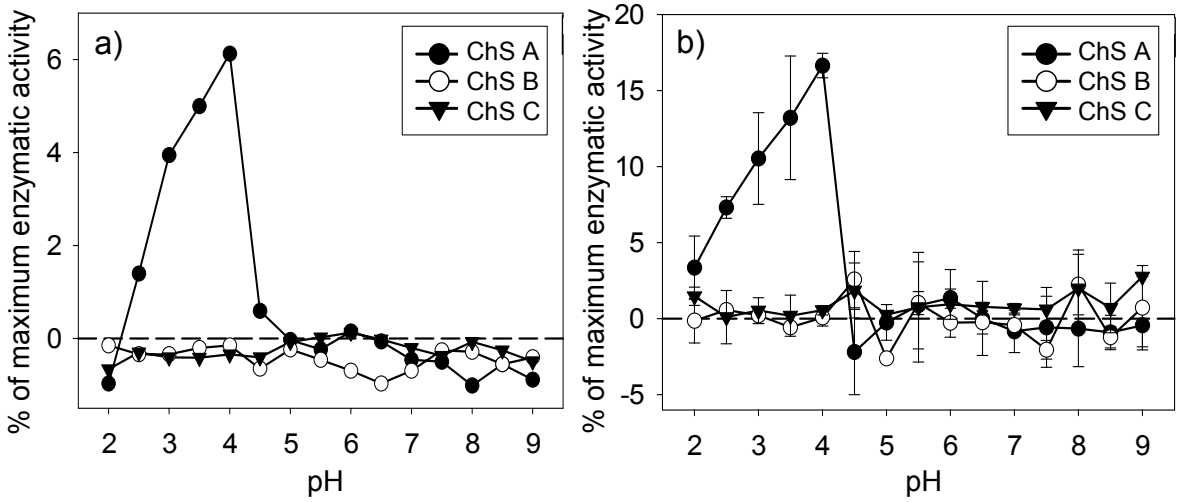


**Fig. 5.25** pH-dependent degradation of ChS A, B and C by human Hyal-1 expressed in DS-2 cells. pH-profiles were measured in the colorimetric activity assay (Morgan-Elson assay, incubation mixture B) (a) and in the turbidimetric activity assay (incubation mixture B) (b). 100 % enzymatic activity was determined at pH 3.5 with HA used as a substrate.

Both assays revealed the degradation of ChS A by Hyal-1/DS-2, but did not show any detectable activity of the enzyme on ChS B and C. Maximum activity on ChS A was measured at pH 4.0 with the pH profile closely resembling the pH dependent activity determined with HA as a substrate (**Fig. 5.11** and **Fig. 5.25**).

It should be noted that the relative activities (% of maximum enzymatic activity) in the colorimetric assay were significantly lower than the activities determined in the turbidimetric assay. This phenomenon was observed for other hyaluronidase derivatives as well and is discussed in Chapter 6.

The recognition of ChS A as a substrate, but not of ChS C, revealed the tolerance of a charged, spacious group like the sulfate group in position 4 of the GlcNAc residue, but not in

position 6. Furthermore, a change of the position of the carboxylic group of GlcUAc into axial position in addition to the sulfate group in position 4 resulted in a complete loss of the recognition of the substance as a substrate for Hyal-1/DS-2. Interestingly, the 4-sulfated ChS (ChS A) is known to be a worse substrate for all other hyaluronidases than the 6-sulfated derivative (ChS C) (Stern and Jedrzejas 2006).

## 5.4. Summary and conclusions

In DS-2 cells the human hyaluronidase Hyal-1 was expressed as a long (Hyal-1/L) and short variant (Hyal-1/S) into the medium by the use of pMT/Hygro, a special expression vector constructed for the selection of cells and expression of recombinant proteins into the medium.

Hyaluronidases have been described in the venoms of arthropods and insects, but in the extracellular matrix of *D. melanogaster* no hyaluronan has been found (Toyoda 2002). Furthermore, no sequences with any significant similarity to hyaluronidase genes were found in the genome of *D. melanogaster*. *Drosophila* Schneider-2 cells are undifferentiated, embryonic cells growing at high densities (up to $20 \cdot 10^6$ cells/mL) in serum-free medium (Schneider 1972, Deml and Wagner 1998). Both, the absence of endogenous hyaluronidases, and the continuous growth at high densities, was well suited for the expression of human hyaluronidases.

While Hyal-1/L was identified as a homogenous, enzymatically active protein of 54 kDa in the medium of transiently and stably transfected DS-2 cells, Hyal-1/S with a molecular weight of 50 kDa exhibited no enzymatic activity at all. The expression of Hyal-1/L in stably transfected DS-2 cells was optimized in respect to the cell culture conditions during induction. The maximum activity gained in the cell medium was 450 nmol GlcNAc $\cdot$ $min^{-1}$ $\cdot$ $mL^{-1}$ cell medium.

Purification of Hyal-1/L was optimized using various column materials and purification steps until finally highly pure enzyme (specific activity 8 - 10 U/mg) was obtained after a combination of ammonium sulfate precipitation, cation exchange chromatography and Ni-IMAC. Purification was complicated by the binding of insect cell proteins to the Ni-IMAC and the tendency of Hyal-1/L to adhere to surfaces, e.g. column materials and filter membranes. Adhesion could be minimized by including a non-ionic detergent, Triton X-100,

in the buffer systems. Previous studies also described the necessity of detergents during the purification of human Hyal-1 (Frost et al. 1997).

Comparison of Hyal-1, expressed in *E. coli* (cf. Chapter 4) and in a DS-2 cell system, clearly revealed the advantages and problems of each expression system. While the bacterial system is definitely the simplest and fastest one to achieve high amounts of protein, insect cells grow slower with much lower yields, but produce protein with a glycosylation pattern similar to mammalian proteins. Although both expression systems yielded enzymatically active Hyal-1, a comparison of yields as well as specific activities clearly shows the superiority of the insect cell system (**Tab. 5.2**).

**Tab. 5.2** Comparison of the characteristics of Hyal-1, expressed in a prokaryotic (*E. coli*) and in a eukaryotic (DS-2 cell) system.

| **Expression system** | ***E. coli*** | **DS-2 cells** |
|---|---|---|
| Time of induction | 3 – 4 h | 10 – 12 d |
| Molecular mass | 48 kDa | 54 kDa |
| Glycosylation | none | N-glycosylation (4 kDa) |
| Total protein yield | 10 mg / g bacterial pellet<br>(5 g / 6 L culture volume) | 2.3 µg / mL medium<br>(14 mg / 6 L culture volume) |
| Active protein yield | up to 1.0 mU/mL of folding buffer | up to 450 mU/mL of medium |
| Specific activity | 0.1 U/mg | 8 - 10 U/mg |

HA was catabolized by both enzymes, Hyal-1/*E. coli* and Hyal-1/DS-2, with pH activity profiles similar to the one detected with human plasma hyaluronidase (pH optimum 3.5 – 4.0). However, the absolute activity seems to be influenced by the glycosylation, which is only present in Hyal-1, expressed by DS-2 cells. The decrease in activity observed in the course of deglycosylation of Hyal-1/DS-2 can be explained either as a consequence of increased aggregation or surface adhesion of the enzyme or by a direct effect on the enzymatic activity.

The sensitivity of Hyal-1 to NaCl concentrations > 100 mM has been reported previously (Gold 1982) and was observed for the recombinant enzymes as well. However, it remains unclear if NaCl influences the structure of the substrate, HA, or exerts a direct effect on the

enzyme. As the sensitivity of Hyal-1, expressed in *E. coli* and Hyal-1, expressed in DS-2 cells, against NaCl differ, it can be assumed that in the relevant concentration range NaCl does not significantly affect the structure of HA. Among different metal ions only $Cu^{2+}$, $Fe^{2+}$ and $Fe^{3+}$ show significant inhibition of the enzymatic activity of Hyal-1, expressed in DS-2 cells. The necessity of any common metal ion as co-factor of the enzyme can thus be excluded.

An additional feature of Hyal-1/L from both expression systems is its extraordinarily high sensitivity towards GdmCl as denaturing agent in contrast to a rather high stability in the presence of urea. This observation is in agreement with the phenomena observed during *in vitro* folding of Hyal-1 (cf. Chapter 4).
Disulfide bridges were shown to influence the activity as well as the electrophoretic mobility of Hyal-1/DS-2 on the SDS-PAGE significantly. The appearance of two protein bands exhibiting activity against HA on zymography gels could be explained by partial reduction of the enzyme in the sample. The purified, recombinant enzyme was proven to contain a single N-terminal sequence in contrast to Hyal-1 isolated from urine (Csoka et al. 1997).

Since no crystal structure has been obtained yet, the CD-spectroscopic data represent the first experimentally obtained structural information on the human hyaluronidase Hyal-1. The data are consistent with the predicted $(\beta/\alpha)_7$ barrel fold and the structural model reported in literature (Jedrzejas and Stern 2005).

Hyal-1, expressed in DS-2 cells, exhibited low activity against ChS A, the 4-sulfated chondroitin sulfate derivative, but no activity against the 6-sulfated derivative (ChS C) and ChS B. Degradation of ChS A observed in a modified colorimetric and turbidimetric hyaluronidase activity assay revealed a similar pH dependency (pH optimum at pH 3.5 – 4.0) as detected previously for the degradation of HA.

Taken together, Hyal-1, expressed in DS-2 cells, was found to be superior to Hyal-1, expressed in *E. coli*, and can be used for enzymological studies (cf. Chapter 8), crystallization and the development of specific inhibitors.

## 5.5. References


Aboughalia A.H. (2006). Elevation of Hyaluronidase-1 and Soluble Intercellular Adhesion Molecule-1 Helps Select Bladder Cancer Patients at Risk of Invasion. *Arch. Med. Res.* **37**: 109-116.

Afify A., Stern M., Guntenhoner M., Stern R. (1993). Purification and characterization of human serum hyaluronidase. *Arch. Biochem. Biophys.* **305**: 434-441.

Böhm, G., Muhr, R., Jaenicke, R. (1992). Quantitative analysis of protein far UV circular dichroism spectra by neuronal networks. *Protein Engin.* **5**: 191-195.

Botzki A. (2004). Structure-based design of hyaluronidase inhibitors. *Doctoral thesis*. University of Regensburg. http://www.opus-bayern.de/uni-regensburg/volltexte/2004/378/

Cherr G.N., Meyers S.A., Yudin A.I., VandeVoort C.A., Myles D.G., Primakoff P., Overstreet J.W. (1996). The PH-20 Protein in Cynomolgus Macaque Spermatozoa: Identification of Two Different Forms Exhibiting Hyaluronidase Activity. *Dev. Biol.* **175**: 142-153.

Csoka T.B., Frost G.I., Wong T., Stern R. (1997). Purification and microsequencing of hyaluronidase isozymes from human urine. *FEBS Lett.* **417**: 307-310.

Deml L., Wagner R. Stable transfected Drosophila Schneider-2 cells as a novel tool to produce recombinant antigens for diagnostic, therapeutic, and preventive purposes. *in: Molecular diagnosis of infectious diseases.* U. Reischl ed. Totowa. (1998). **13**: 185-200.

Edman P., Begg G. (1967). A protein sequenator. *Eur. J. Biochem.* **1**: 80-91.

Franzmann E., Schroeder G., Goodwin W., Weed D., Fisher P., Lokeshwar V. (2003). Expression of tumor markers hyaluronic acid and hyaluronidase (HYAL1) in head and neck tumors. *Int. J. Cancer* **106**: 438-445.

Frost G.I., Csoka T.B., Wong T., Stern R. (1997). Purification, Cloning, and Expression of Human Plasma Hyaluronidase. *Biochem. Biophys. Res. Commun.* **236**: 10-15.

Gold E.W. (1982). Purification and properties of hyaluronidase from human liver. *Biochem. J.* **205**: 69-74.

Hoechstetter J. (2005). Characterisation of bovine testicular hyaluronidase and a hyaluronate lyase from Streptococcus agalactiae. *Doctoral thesis*. University of Regensburg. http://www.opus-bayern.de/uni-regensburg/volltexte/2005/519/

Hoechstetter J., Oettl M., Asen I., Molz R., Bernhardt G., Buschauer A. (2001). Discrepancies in apparent enzymatic activity of bovine testicular hyaluronidase depend on the type of assay. *Arch. Pharm. Med. Chem.* **334**: 37.

Hosoe S., Shigedo Y., Ueno K., Tachibana I., Osaki T., Tanio Y., Kawase I., Yamakawa K., Nakamura Y., Kishimoto T. (1994). Detailed deletion mapping of the short arm of chromosome 3 in small cell and non-small cell carcinoma of the lung. *Lung Cancer* **10**: 297-305.

Jedrzejas M.J., Stern R. (2005). Structures of vertebrate hyaluronidases and their unique enzymatic mechanism of hydrolysis. *Proteins.* **61**: 227-238.

Julenius K., Molgaard A., Gupta R., Brunak S. (2005). Prediction, conservation analysis and structural characterization of mammalian mucin-type-O-glycosylation sites. *Glycobiology* **15**: 153-164.

Lokeshwar V.B., Cerwinka W.H., Lokeshwar B.L. (2005). HYAL1 Hyaluronidase: A Molecular Determinant of Bladder Tumor Growth and Invasion. *Cancer Res.* **65**: 2243-2250.

Lokeshwar V.B., Rubinowicz D., Schroeder G.L., Forgacs E., Minna J.D., Block N.L., Nadji M., Lokeshwar B.L. (2001). Stromal and epithelial expression of tumor markers hyaluronic acid and HYAL1 hyaluronidase in prostate cancer. *J. Biol. Chem.* **276**: 11922-11932.

Lokeshwar V.B., Schroeder G.L., Carey R.I., Soloway M.S., Iida N. (2002). Regulation of Hyaluronidase Activity by Alternative mRNA Splicing. *J. Biol. Chem.* **277**: 33654-33663.

Mio K., Stern R. (2002). Inhibitors of the hyaluronidases. *Matrix Biol.* **21**: 31-37.

Muckenschnabel I., Bernhardt G., Spruss T., Dietl B., Buschauer A. (1998). Quantitation of hyaluronidases by the Morgan-Elson reaction: comparison of the enzyme activities in the plasma of tumor patients and healthy volunteers. *Cancer Lett.* **131**: 13-20.

Ni X., Canuel M., Morales C.R. (2006). The sorting and trafficking of lysosomal proteins. *Histol. Histopathol.* **21**: 899-913.

Oettl M. (2000). Biochemische Charakterisierung boviner testikulärer Hyaluronidase und Untersuchungen zum Einfluß von Hyaluronidasen auf das Wachstum von Tumoren. *Doctoral thesis*. University of Regensburg.

Posey J.T., Soloway M.S., Ekici S., Sofer M., Civantos F., Duncan R.C., Lokeshwar V.B. (2003). Evaluation of the Prognostic Potential of Hyaluronic Acid and Hyaluronidase (HYAL1) for Prostate Cancer. *Cancer Res.* **63**: 2638-2644.

Schneider I. (1972). Cell lines derived from late embryonic stages of Drosophila melanogaster. *J. Embryol. Exp. Morphol.* **27**: 353-365.

Smith P.K., Krohn R.I., Hermanson G.T., Mallia A.K., Gartner F.H., Provenzano M.D., Fujimoto E.K., Goeke N.M., Olson B.J., Klenk D.C. (1985). Measurement of protein using bicinchoninic acid. *Anal. Biochem.* **150**: 76-85.

Soldatova L.N., Crameri R., Gmachl M., Kemeny D.M., Schmidt M., Weber M., Mueller U.R. (1998). Superior biologic activity of the recombinant bee venom allergen hyaluronidase expressed in baculovirus-infected insect cells as compared with Escherichia coli. *J. Allergy Clin. Immunol.* **101**: 691-698.

Stern R. (2005). Hyaluronan metabolism: a major paradox in cancer biology. *Pathol. Biol.* **53**: 372-382.

Stern R., Jedrzejas M.J. (2006). Hyaluronidases: Their Genomics, Structures, and Mechanism of Action. *Chem. Rev.* **106**: 818-839.

Taylor K.R., Gallo R.L. (2006). Glycosaminoglycans and their proteoglycans: host-associated molecular patterns for initiation and modulation of inflammation. *FASEB* **20**: 9-22.

Toyoda H. (2002). Glycosaminoglycans in Drosophila melanogaster. http://www.glycoforum.gr.jp/science/word/proteoglycan/PGC02E.html

Triggs-Raine B., Salo T.J., Zhang H., Wicklow B.A., Natowicz M.R. (1999). Mutations in HYAL1, a member of a tandemly distributed multigene family encoding disparate hyaluronidase activities, cause a newly described lysosomal disorder, mucopolysaccharidosis IX. *Proc. Natl. Acad. Sci. U. S. A.* **96**: 6296-6300.

Vercruysse K.P., Ziebell M.R., Prestwich G.D. (1999). Control of enzymatic degradation of hyaluronan by divalent cations. *Carbohydr. Res.* **318**: 26-37.

Wei M., Latif F., Bader S., Kashuba V., Chen J., Duh F., Sekido Y., Lee C., Geil L., Kuzmin I., Zabarovsky E., Klein G., Zbar B., Minna J., Lerman M. (1996). Construction of a 600-kilobase cosmid clone contig and generation of a transcriptional map surrounding the lung cancer tumor suppressor gene (TSG) locus on human chromosome 3p21.3: progress toward the isolation of a lung cancer TSG. *Cancer Res.* **56**: 1487-1492.

Wessel D., Flügge U.I. (1984). A method for the quantitative recovery of protein in dilute solution in the presence of detergents and lipids. *Anal. Biochem.* **138**: 141-143.

Yamagata T., Saito H., Habuchi O., Suzuki S. (1968). Purification and properties of bacterial chondroitinases and chondrosulfatases. *J. Biol. Chem.* **243**: 1523-1535.

Zacharius R.M., Zell T.E., Morrison J.H., Woodlock J.J. (1969). Glycoprotein staining following electrophoresis on acrylamide gels. *Anal. Biochem.* **30**: 148-152.

# Chapter 6

# Purification and characterization of human PH-20 expressed by DS-2 cells

## 6.1. Introduction

PH-20 (sperm adhesion molecule 1, SPAM1) was first described by its function as an egg's zona pellucida binding protein of the sperm before its similarity to BVH revealed its function as a hyaluronidase (Gmachl and Kreil 1993).
On the surface of the sperm head PH-20 is anchored in the membrane (Lathrop et al. 1990, Sabeur et al. 1997) and facilitates penetration of the egg through the cumulus extracellular matrix (ECM) (for review see Primakoff and Myles 2002). Upon contact with the zona pellucida the acrosome reaction is triggered, possibly supported by intracellular signaling, mediated by the HA binding region of PH-20 (Cherr et al. 2001). During the acrosome reaction PH-20 anchored in the inner acrosomal membrane (IAM) is released and acts as a soluble, acid active hyaluronidase (**Fig. 6.1**) (Hunnicutt et al. 1996, Yudin et al. 2001).

Variations in the molecular weight and in the pH-dependent activity of PH-20 indicate several steps of modifications during maturation of the sperm and fertilization: a 2 – 3 kDa reduction in the molecular weight of PH-20 was described during maturation in the epididymis (Cherr et al. 2001), sperm surface PH-20 shows activity at both acid and neutral pH with maximum activity at pH 7.0 (Li et al. 1997, Sabeur et al. 1997), while IAM PH-20 was described to have a pH optimum at both neutral and acidic pH (Yudin et al. 2001). Membrane-anchored PH-20 was described as a 64 kDa protein, which is reduced in its molecular weight by 9 kDa upon liberation from the membrane after the acrosome reaction. This soluble, low molecular weight form of PH-20 is probably generated by endoproteolytic cleavage of the high molecular

weight form, resulting in a shift of the pH optimum of the enzyme towards acid pH values (Cherr et al. 1996, Sabeur et al. 1997). The variety of pH optima is assumed to be due to the presence of two different regions involved in the catalytic activity of the enzyme (Cherr et al. 2001).

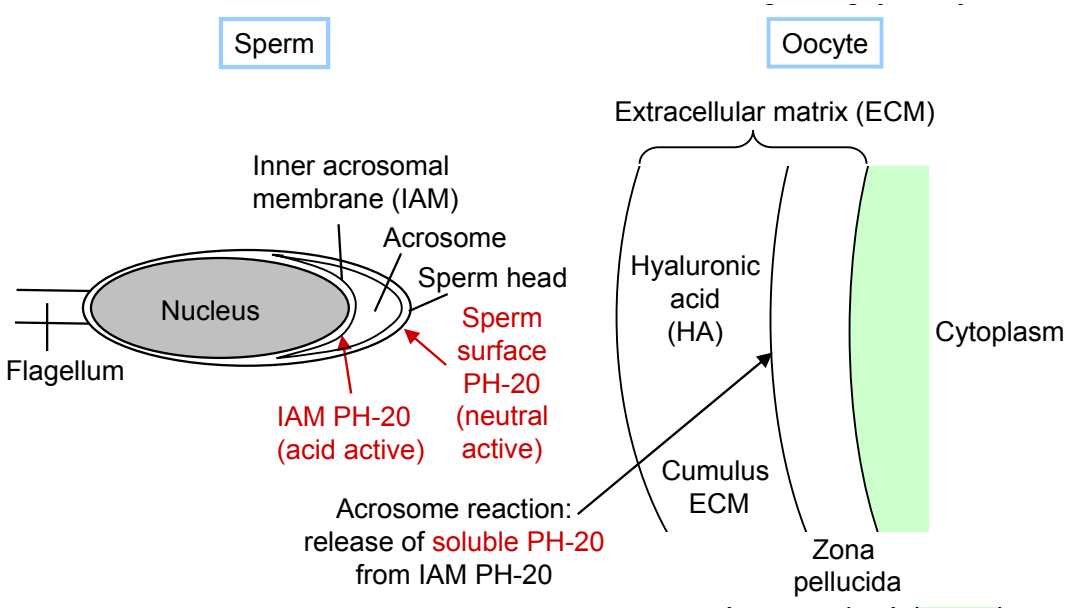


**Fig. 6.1** Role of PH-20 in fertilization. Membrane-anchored PH-20 is located on the surface of the sperm head, exhibiting activity at neutral pH, and in the inner acrosomal membrane (IAM). IAM-anchored PH-20 is released as a soluble protein after the acrosome reaction was triggered by contact of the sperm head with the zona pellucida.

PH-20 was found to be conserved in mouse, bull, macaque and human and was investigated in sperm and testicular preparations of different animals. Recently, an additional hyaluronidase, Hyal-5, was identified in mouse sperm acting in concert with PH-20 (Kim et al. 2005). As this hyaluronidase gene is not present in humans the results from animal studies should be interpreted carefully before transferring the results to human PH-20.

Preparations of bovine testicular hyaluronidase (BTH), e.g. Hylase® „Dessau“, Neopermease® and Wydase®, were for many years therapeutically applied as spreading factors, degrading the glycosaminoglycans of the extracellular matrix (Baumgartner and Moritz 1988, Menzel and Farr 1998). A common field of application of BTH is its addition to local anesthetic agents for ophthalmic anesthesia, as it is known to improve the rapidity of onset, dispersion, depth and duration of the local anesthesia (Kallio et al. 2000). In the course of systemic oncological therapies with vinca alkaloids hyaluronidase is the only highly effective antidote to the extravasation of these antineoplastic agents, especially vinblastine, as it prevents local necrosis by improving the absorption of the paravasate (Albanell and Baselga 2000, Bertelli et al. 1994).

Replacement of the bovine PH-20 preparations by a recombinant human enzyme for therapeutical applications would be preferable in terms of the immune response, the homogeneity and the purity of the product. In 2006 the first recombinant human PH-20 produced in CHO cells was suggested for the enhancement of the interstitial transport of therapeutics (Bookbinder et al. 2006) and for the use in *in vitro* fertilization (Taylor et al. 2006).

The following chapter describes the production of human PH-20 by *Drosophila* Schneider-2 (DS-2) cells for enzymological studies and the development of specific inhibitors. The pH-dependent activity of human PH-20 towards different GAGs was compared to BTH.

## 6.2. Materials and Methods

### *6.2.1. Materials and chemicals*

For subcloning all materials were purchased from the same suppliers as described in Chapter 3. *Drosophila* Schneider-2 cells (DS-2 cells), pCoHygro and pMT/BiP/V5-HisA were kindly provided by V. Runza (Institute of Immunology, Faculty of Medicine, University of Regensburg, Germany). Hyaluronic acid from *Streptococcus zooepidemicus* was purchased from Aqua Biochem GmbH, Dessau, Germany. Chondroitin 4-sulfate (A) from bovine trachea, chondroitin 6-sulphate (C) from shark cartilage and chondroitin sulfate B from porcine intestinal mucosa were purchased from Sigma, Munich, Germany. ChS A and ChS C contained impurities of the respective other GAG of up to 30 % as indicated by the supplier.

Triton X-100 was from Roth, Karlsruhe, Germany. Hygromycin was from A.G. Scientific Inc., San Diego, USA. All other chemicals were of HPLC or analytical grade and were purchased from Merck, Darmstadt, Germany.

### *6.2.2. Construction of the expression vector pMT/Hygro/ph-20*

Human *ph-20* cDNA was amplified by PCR from the I.M.A.G.E. clone vector IMAGp998N2310771 using 5'-ACGCCTAGATCTCTGAATTTCAG-3' as forward primer generating an additional *Bgl*II cleavage site and 5'-TAAATTGGGCCCAGATAGTGTGGA-3' as reverse primer with an additional *Apa*I cleavage site. Amplification was achieved after 30 cycles with an annealing temperature of 53 °C in the presence of 3.0 mM $MgSO_4$. Both, the PCR product and the vector pMT/Hygro (cf. Chapter 5), were digested with *Apa*I and *Bgl*II. The insert restriction digest mixture contained 40 µl of purified PCR product, 2 µL of *Apa*I and 4.7 of µL TANGO$^{TM}$ buffer (Fermentas, St. Leon-Rot, Germany). After incubation

for 1 h at 37 °C, 5.2 µL of TANGO™ buffer and 1 µL of *Bgl*II were added, and the mixture was incubated for 3 h at 37 °C. For digestion of the vector 1 µL of pMT/Hygro (1 mg/mL) were incubated with 2 µL of *Apa*I, 2 µL of TANGO™ buffer and 15 µL of water for 1 h at 37 °C. Then, 2.5 µL of TANGO™ buffer and 1 µL of *Bgl*II were added, and the mixture was incubated for 3 h at 37 °C. Additionally, the vector was dephosphorylated (cf. Chapter 3). Restriction enzymes and the phosphatase were inactivated by heating at 80 °C for 20 min. After ligation and transformation of pMT/Hygro/*ph-20* into *E. coli* Top10 the insertion was confirmed by sequencing (Entelechon, Regensburg, Germany) using a T7 promoter primer and a BGH primer. If not otherwise indicated all cloning procedures were performed as described in Chapter 3.

### *6.2.3. Expression of PH-20 by Drosophila Schneider-2 cells (DS-2 cells)*

DS-2 cells were cultured as described in Chapter 5. DS-2 wildtype cells were transfected with pMT/Hygro/*ph-20* using Lipofectamin™ (Invitrogen, Karlsruhe, Germany) and FuGENE® 6 (Roche Applied Sciences, Mannheim, Germany) as transfection reagents. Transient and stable expression of PH-20 was performed as described for Hyal-1 (Chapter 5).

Aliquots of the medium were taken 3 and 10 d after induction, and the medium was directly used for determination of hyaluronidase activity.

### *6.2.4. Purification of PH-20 from the medium of stably transfected DS-2 cells*

The cell-free medium was supplemented with 0.1 % (v/v) Triton X-100, and the pH was carefully adjusted to 6.7. Before loading the column, the sample was clarified completely by centrifugation (30 min, 8,000 g, 4 °C). PH-20 containing a C-terminal His-tag was bound via the $Cu^{2+}$ ions present in the medium to a HiTrap® Chelating Column (CV 5 ml, GE Healthcare Bio-Sciences AB, Uppsala, Sweden) equilibrated in 50 mM Na-phosphate, 0.5 M NaCl, 0.1 % (v/v) Triton X-100, pH 6.5. After application of the sample the column was washed with 2 CV of equilibration buffer before PH-20 was eluted with 6 CV of 50 mM Na-phosphate, 0.5 M NaCl, 0.1 % (v/v) Triton X-100, pH 4.5. Fractions of 1 mL were collected and analyzed for their protein content and their enzymatic activity.

All buffers used during the purification process were vacuum-degassed and filtrated through a 0.45 µm filter (Millipore, Eschborn, Germany).

### *6.2.5. SDS-PAGE, Western blot and zymography*

SDS-PAGE, Western blot and zymography were performed as described in Chapter 3 and Chapter 5, respectively. For zymography McIlvaine's buffer, pH 4.0, was used as an

incubation buffer. McIlvaine's buffer was adjusted to the desired pH by mixing solution A (0.2 M $Na_2HPO_4$, 0.1 M NaCl) and solution B (0.1 M citric acid, 0.1 M NaCl).

### *6.2.6. Detection of glycoproteins by PAS staining*

For detection of glycoproteins SDS-PA gels were stained by the periodic acid – Schiff (PAS) technique with Schiff's reagent purchased from Sigma, Munich, Germany, following the procedure described by Zacharius et al. (Zacharius et al. 1969). Samples were prepared as described in Chapter 5.

### *6.2.7. Colorimetric hyaluronidase activity assay (Morgan-Elson assay)*

The assay was performed as described in Chapter 4. The following incubation mixture was used: 150 µL of water, 100 µL of BSA solution (0.2 mg/mL), 100 µL of McIlvaine's buffer of various pH (cf. 6.2.5), 50 µL of HA solution (5 mg/mL), 50 µL of sample.
When chondroitin sulfate derivatives were used as substrates, HA was exchanged with an equal volume of chondroitin sulfate solution (5 mg/mL).

### *6.2.8. Turbidimetric hyaluronidase activity assay*

The assay was performed as described in Chapter 3. The turbidity was detected at 355 nm. When chondroitin sulfate derivatives were used as substrates, HA was exchanged against an equal volume of a chondroitin sulfate solution (2 mg/mL).

## 6.3. Results

### *6.3.1. Construction of the expression vector pMT/Hygro/ph-20*

As PH-20 is primarily a membrane-anchored, extracellular protein it was truncated at its N- and C-terminus to yield a soluble protein, which is secreted by the insect cells into the culture medium.

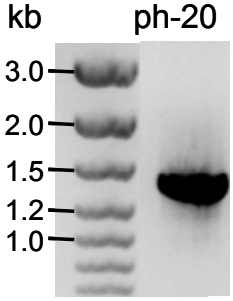


**Fig. 6.2** Agarose gel electrophoresis of the PCR amplification product of *ph-20* with the expected length of 1.40 kb. The gel was loaded with 10 µl of PCR product and 2 µl of 10 x PCR loading buffer.

At the N-terminus the human signal peptide was replaced with the BiP signal sequence encoded on pMT/Hygro. At the C-terminus the GPI-anchoring signal peptide comprising aa 492-512 was excluded from the PCR amplification product (**Fig. 6.2**). Thus, pMT/Hygro/*ph-20* coded for a 502 aa precursor protein with a C-terminal V5 epitope and a His-tag (**Fig. 6.3** and Appendix 2).

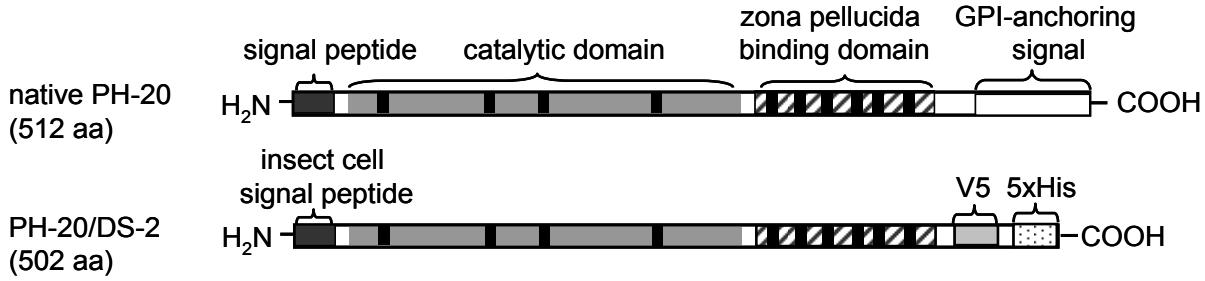


**Fig. 6.3** Schematic view of the primary structure of native human PH-20 (above) and recombinant human PH-20 expressed by DS-2 cells (below). Black boxes indicate the presence of C residues presumably all linked by disulfide bridges.

Due to the absence of activity in the truncated form of Hyal-1 (Hyal-1/S, cf. Chapter 5) PH-20 was merely expressed as a full length protein including both the catalytic and the zona pellucida binding region. Previous experiments by Arming et al. with PH-20 expressed in HeLa cells had shown that a C-terminal truncation of 133 aa, i.e. the GPI-anchoring signal and the zona pellucida binding region, resulted in a complete loss of activity (Arming et al. 1997).

### *6.3.2. Expression of PH-20 in DS-2 cells*

DS-2 wildtype cells were transfected with pMT/Hygro/*ph-20* using varying DNA/transfection reagent ratios. As observed previously for the transfection of DS-2 cells with pMT/Hygro/*hyal-1*, the activity in the medium after transient expression of PH-20 was much lower than after stable expression.

Passaging of transfected DS-2 cells for several weeks in the presence of hygromycin resulted in the stable integration of the expression vector into the genome. Expression of PH-20 was confirmed after 3 and 10 d of growth in the absence and in the presence of the inducing agent $CuSO_4$ by Western blot analysis (**Fig. 6.4**) and the detection of enzymatic activity in the culture medium (**Fig. 6.5**).

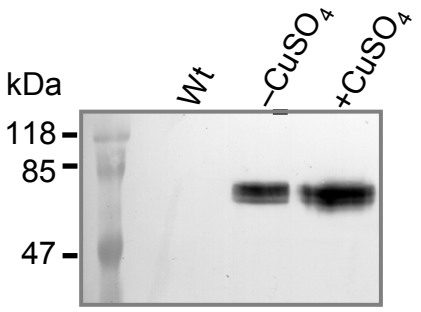


**Fig. 6.4** Western blot analysis of DS-2 cell medium from wild type cells (Wt), DS-2/pMT/Hygro/*ph-20* cells in the absence (-$CuSO_4$) and in the presence (+$CuSO_4$) of $CuSO_4$ as inducer. Each lane contained 30 µl of medium after 10 d of induction. Anti-V5-IgG was used as primary antibody, biotinylated anti-mouse-IgG as secondary antibody and detection of the antibody binding was achieved by HRP/DAB staining.

Recombinant PH-20 was detected by the use of an anti-V5-antibody in the medium of both, induced and uninduced cells, as single band of ca. 60 kDa. However, a quantitative comparison of the expression rates and the exact calculation of the molecular weight were impossible in the Western blot.

Therefore, the enzymatic activity of PH-20 was determined in a colorimetric hyaluronidase activity assay at acid and neutral pH (**Fig. 6.5**) revealing a superior hyaluronidase activity at acidic pH.

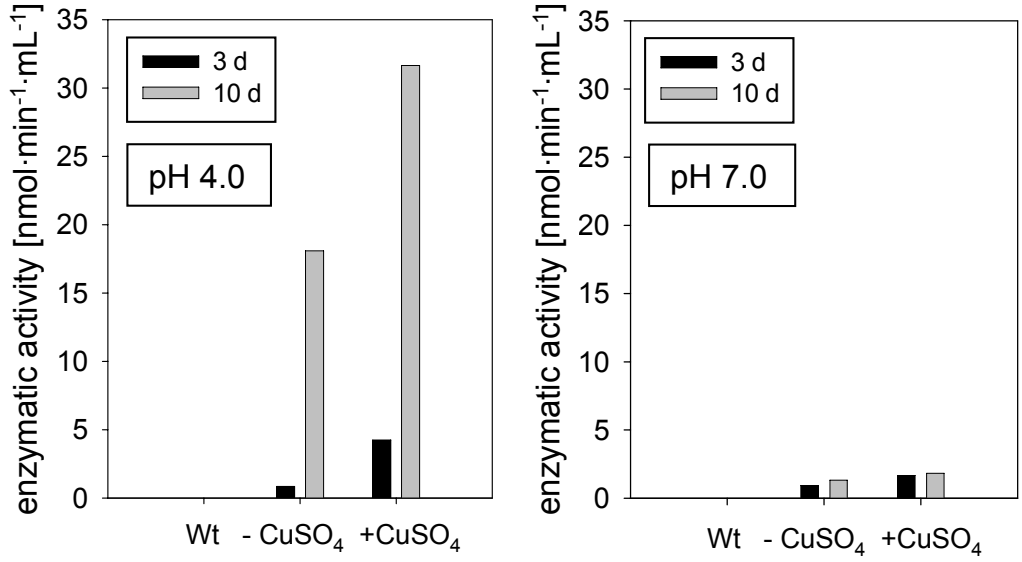


**Fig. 6.5** Hyaluronidase activity in the medium of DS-2 cells, stably transfected with pMT/Hygro/*ph-20*. DS-2 wildtype cells induced with $CuSO_4$ were used as a control (Wt), the medium of transfected cells was analyzed in the presence (+$CuSO_4$) and in the absence of $CuSO_4$ (-$CuSO_4$). Enzymatic activity was determined in the colorimetric activity assay at pH 4.0 (left panel) and pH 7.0 (right panel) 3 and 10 d after induction of expression.

The expression of catalytically active PH-20 was found to increase significantly with prolongued cell growth. Induction of expression with $CuSO_4$ caused a 1.7fold increase in the yield of enzymatic activity 10 d after induction, i.e. at the time of harvesting of the culture medium.

### *6.3.3. Purification of PH-20 by chelating IMAC*

Purification of recombinant human PH-20 from the medium of stably transfected DS-2 cells was achieved by chelating IMAC. The His-tagged, recombinant protein was bound to chelating column material employing the $Cu^{2+}$ ions present in the medium for the induction of the metallothionein promoter. Elution was achieved by a decrease in pH to pH-value of 4.5 for at least 6 CV due to a strong binding affinity of PH-20 to the column material (**Fig. 6.6**).

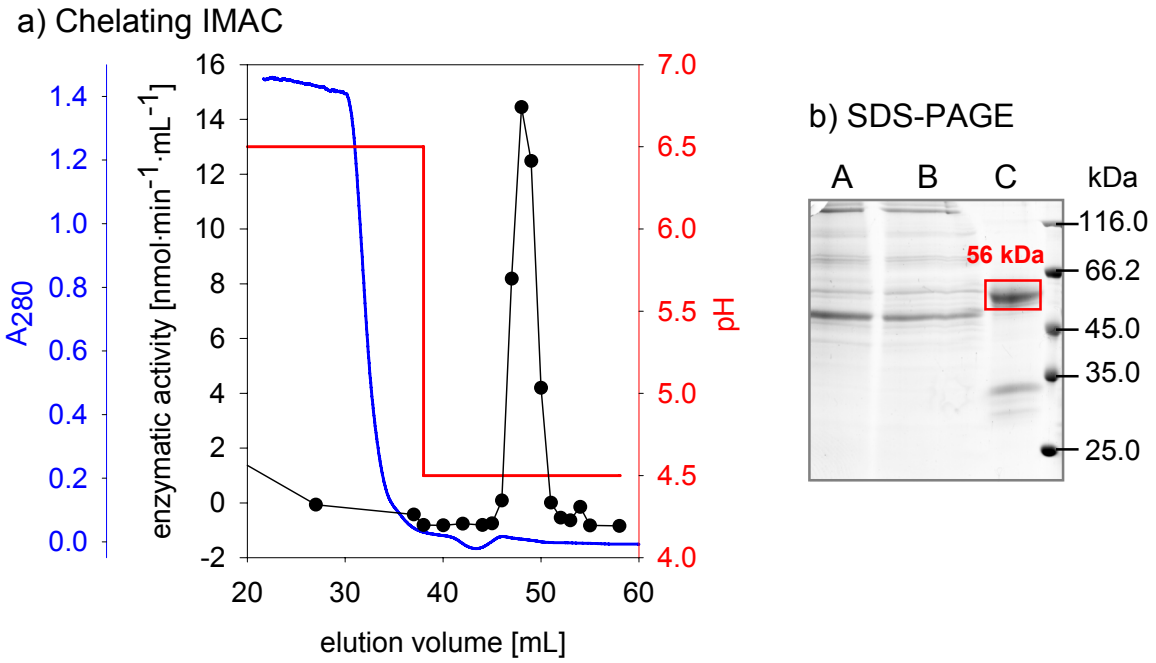


**Fig. 6.6** Purification of PH-20 from the medium of stably transfected DS-2 cells 10 d after induction of expression with $CuSO_4$. Chelating IMAC (a) was monitored by the absorbance at 280 nm (solid, blue line) and by the determination of hyaluronidase activity of the fractions in the colorimetric activity assay (black circles). The decrease in pH at the beginning of the elution of the protein is indicated by the red line. The SDS-PAGE (b) shows the culture medium before application to the column (A), the flow-through (B) and the concentrated elute comprising volume 45 – 53 mL (C).

Measurement of the enzymatic activity at pH 4.0 showed that 91 % of the recombinant PH-20 present in the medium were bound to the column. 127 % of the bound activity was eluted, indicating an increase in the enzymatic activity after purification. The specific enzymatic activity determined in the colorimetric activity assay after purification was 0.5 U/mg, which was 16-fold higher than in the medium. SDS-PAGE analysis after purification revealed a 56 kDa protein as the major protein present in the chelating IMAC elute (**Fig. 6.6.b**), differing only marginally from the molecular weight calculated from the amino acid sequence of PH-20 (55 kDa). Some impurities of lower molecular weight were detected, but zymography revealed the existence of only one catalytically active fraction (ca. 60 kDa) in the medium of DS-2 cells expressing PH-20 (6.3.5). The yield of PH-20 with a specific activity of 0.5 U/mg was ca. 2 µg/mL of culture medium.

Thus, the specific activity of recombinant human PH-20 was ca. 10-fold lower than the activity of BTH (Neopermease®: 50,000 IE/mg referring to 5 U/mg, according to the supplier). This discrepancy is probably due to a lower degree of purification of PH-20 compared to BTH. Furthermore, the removal of the GPI-anchoring signal could cause a decrease in the enzymatic activity as described for the C-terminally truncated forms of PH-20 by Arming et al. (Arming et al. 1997).

### *6.3.4. Analysis of protein glycosylation*

As the calculated molecular weight of PH-20 expressed in DS-2 cells was very similar to the molecular weight determined experimentally (cf. 6.3.3), the protein was checked for the presence of glycosidic residues by PAS staining (**Fig. 6.7**). The amino acid sequence of PH-20 contains seven potential N-glycosylation sites (cf. Chapter 1).

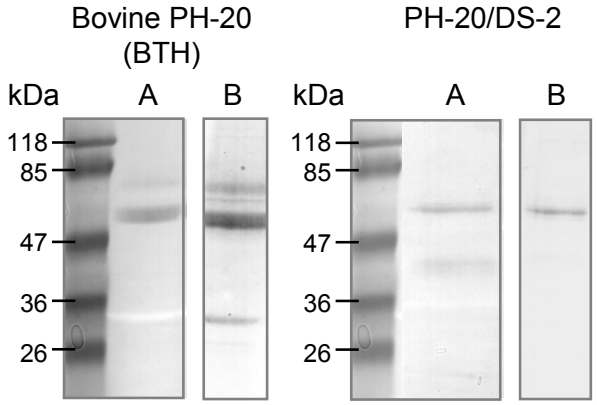


**Fig. 6.7** Analysis of the glycosylation of BTH and human PH-20 by PAS staining (A) of a SDS-PA gel. For comparison the same samples were also stained with Coomassie to visualize the protein components (B).

Out of the three catalytically active fractions of BTH (Hoechstetter 2005) only the 77 kDa and the 58 kDa fraction showed a reaction with PAS. The 33 kDa fraction is not glycosylated as described previously. Human PH-20, expressed by DS-2 cells, was found to be glycosylated, however, the glycosylation seems to have only minor influence on the molecular weight.

### *6.3.5. Stability towards reducing agents*

To investigate the presence of disulfide bridges in PH-20 and the stability of the protein, the activity of PH-20 was determined by zymography under different conditions. Obviously, PH-20 was expressed as a single protein exhibiting a molecular weight of ca. 60 kDa in the absence of DTT on the SDS-PA gel (**Fig. 6.8**).

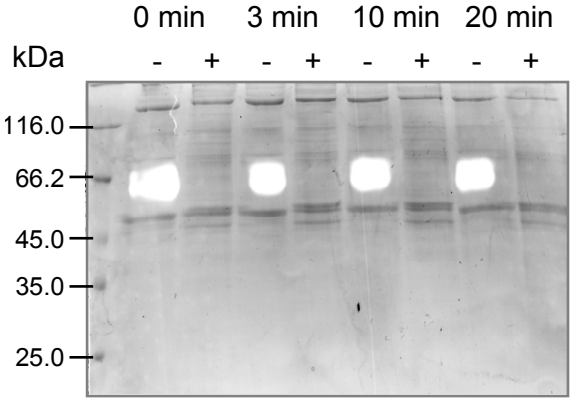


**Fig. 6.8** Zymography of human PH-20 expressed by DS-2 cells in the presence (+) and in the absence of reducing agents (-). Samples contained the culture medium of DS-2 cells collected 10 d after the induction of PH-20 expression. All samples were mixed with SDS sample buffer with or without DTT to achieve a final SDS concentration of 2 % and boiled for the time periods indicated on top of each lane. The gel was stained with Alcian blue and Coomassie.

The presence of disulfide bridges seems to be essential for the activity of PH-20 since the catalytic activity was lost even without boiling of the sample. When the disulfide bridges were present in the protein, PH-20 regained enzymatic activity even after boiling for 20 min with 2 % SDS (**Fig. 6.8**).

### *6.3.6. pH-dependent hyaluronidase activity of PH-20 in comparison to BTH*

Previous experiments in our laboratory had revealed a difference in the pH activity profiles of BTH in dependence on the type of activity assay (Hoechstetter 2005) (**Fig. 6.9.a**). Therefore, it was of interest to investigate the pH profiles of recombinant human PH-20. As shown in **Fig. 6.9.b** the pH dependent degradation of HA by human PH-20 exhibited a maximum located at neutral pH (pH 5.5) in the turbidimetric assay, while this maximum was shifted to acidic pH (pH 4.5) in the colorimetric assay. Thus, the resulting pH profiles of human PH-20 were similar to the profiles of bovine PH-20 (BTH) with respect to the inverse shape of the profiles and the location of the maxima.

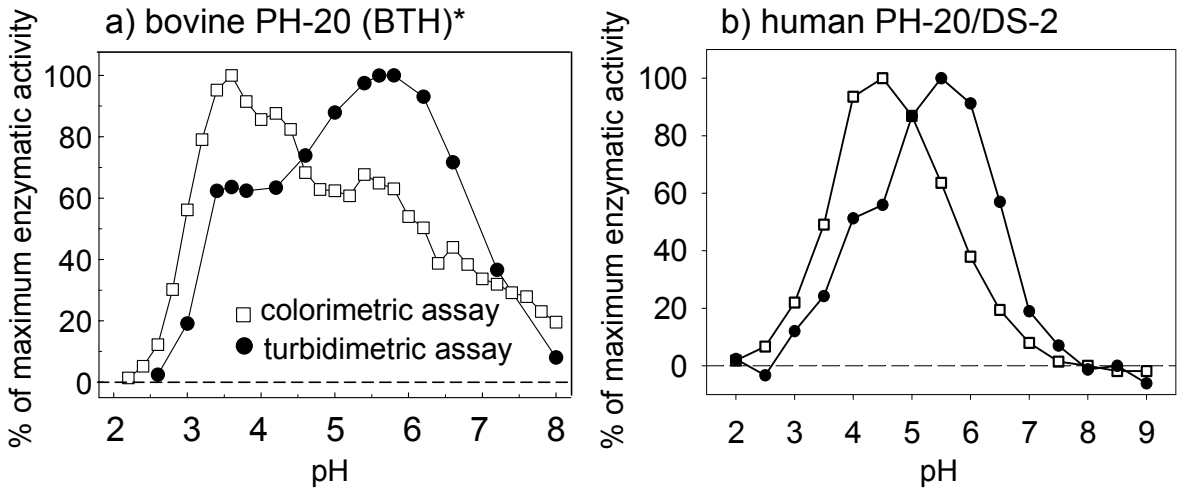


**Fig. 6.9** pH activity profiles of BTH (a) and human PH-20 expressed by DS-2 cells (b) determined in the colorimetric activity assay (white squares) and in the turbidimetric activity assay (black circles).
* The pH profile of BTH was adopted from Hoechstetter 2005.

The difference between the activity maxima in the turbidimetric and in the colorimetric assay was more pronounced for BTH than for human PH-20 (**Tab. 6.1**). A possible explanation could be the presence of three different active species in BTH with different activity profiles (Oettl et al. 2003, Hoechstetter 2005), while human PH-20 expressed in DS-2 cells was merely a single active species in the zymographic analysis (**Fig. 6.8**).

**Tab. 6.1** pH of maximum activity of bovine and human PH-20, determined in the colorimetric and in the turbidimetric hyaluronidase activity assay.

| | **Bovine PH-20 (BTH)** | **Human PH-20/DS-2** |
|---|---|---|
| Colorimetric assay | pH 3.5 | pH 4.5 |
| Turbidimetric assay | pH 5.5 – 6.0 | pH 5.5 |

The phenomenon of the inverse pH profiles was discussed in detail by Hoechstetter (Hoechstetter 2005). The existence of inverse pH profiles for human PH-20 indicates variations in the catalytic process with respect to high and low molecular weight HA fragments at acidic and neutral pH. A thorough discussion of the differences between the enzymatic reactions at acidic and neutral pH is given in Chapter 8.

### *6.3.7. pH-dependent degradation of ChS by PH-20 and BTH*

As described in Chapter 5 the colorimetric and the turbidimetric hyaluronidase activity assays were both found to be suitable for the determination of chondroitin sulfate degradation. To investigate the substrate specificities of the enzyme preparations the pH-dependent activities of BTH and human PH-20 on chondroitin sulfate derivatives were measured in both assay systems.

BTH degraded ChS A and ChS C at a pH range from pH 3.5 to 7.0 with a maximum in enzymatic activity at pH 5.5 for ChS C degradation and at pH 4.0 – 5.0 for ChS A degradation. ChS B was not degraded by BTH (**Fig. 6.10**). Both assay systems showed very similar results concerning the pH dependency of the degradation, but the relative enzymatic activity determined at each pH value varied significantly: in the turbidimetric assay the relative enzymatic activity was generally about twice as high as in the colorimetric assay. This phenomenon was also observed for the degradation of ChS degradation by Hyal-1 (Chapter 5) and human PH-20 (see below).

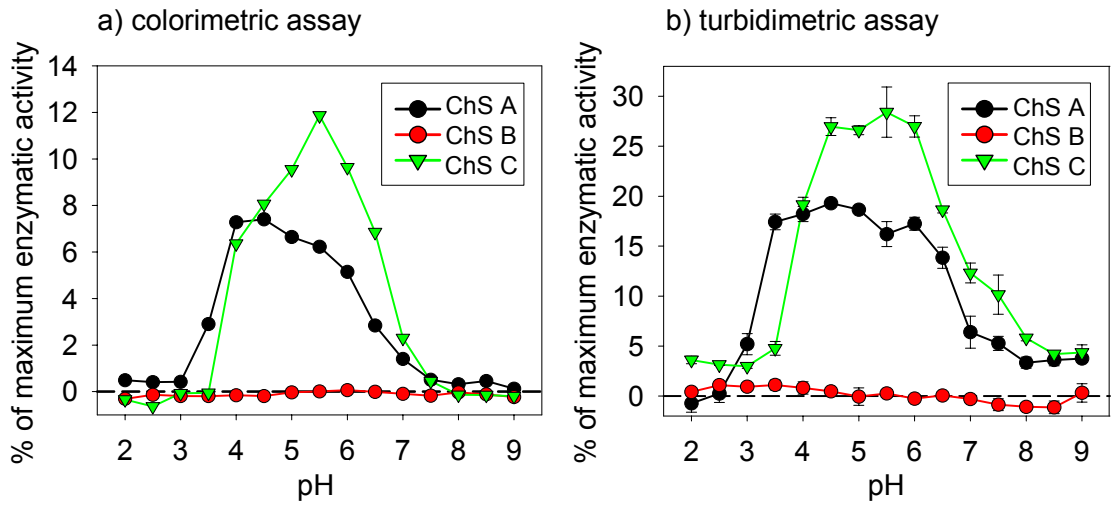


**Fig. 6.10** pH-dependent degradation of chondroitin sulfates by BTH determined in the colorimetric (a) and in the turbidimetric activity assay (b). 100 % enzymatic activity was determined with HA as substrate at pH 3.5 in the colorimetric assay and at pH 5.5 in the turbidimetric assay, respectively.

Recombinant human PH-20 was compared to BTH with respect to its pH-dependent degradation of ChS A and ChS C (**Fig. 6.11**). ChS B was excluded from the experiments with PH-20 due to the absence of any catalytic activity of BTH towards this chondroitin sulfate derivative. ChS B, also known as dermatan sulfate, differs from ChS A merely in the exchange of GlcUAc against IdoUAc. This change in the position of the carboxyl group (equatorial in GlcUAc, axial in IdoUAc) seems to disturb the recognition of the substrate essentially, i.e. no degradation occurs.

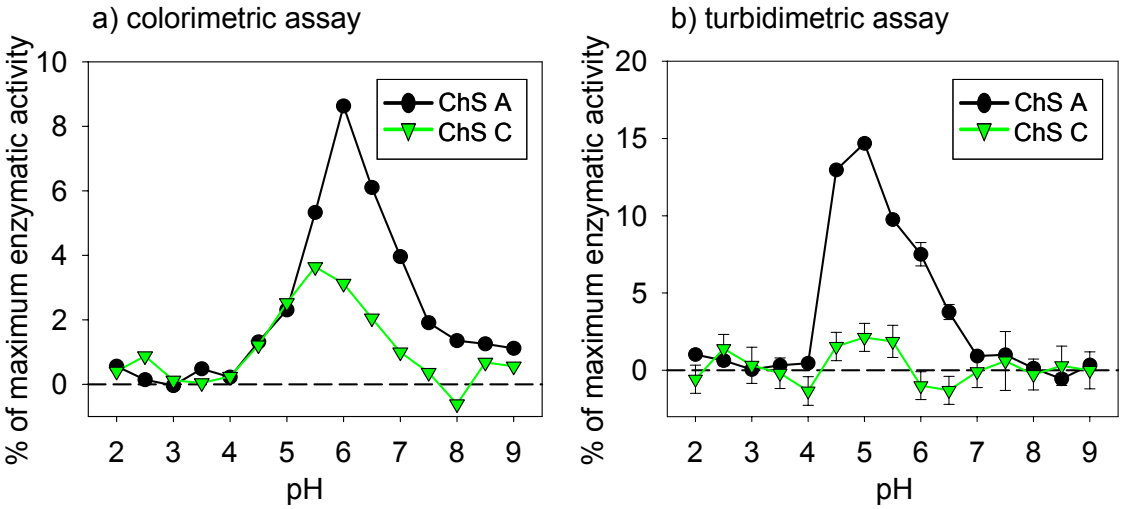


**Fig. 6.11** pH-dependent degradation of chondroitin sulfates by recombinant human PH-20 determined in the colorimetric (a) and in the turbidimetric activity assay (b). 100 % enzymatic activity was determined with HA as a substrate at pH 4.5 in the colorimetric assay and at pH 5.5 in the turbidimetric assay, respectively.

In contrast to the substrate specificity of BTH, ChS A was a better substrate for recombinant human PH-20 than ChS C. The pH-optima were generally narrower than those measured with

BTH. However, the pH-optima were also in the range between pH 5.0 and 6.0. A 2-fold increase in the relative enzymatic activity values determined in the turbidimetric assay compared to the values calculated from the colorimetric assay was also found for PH-20.
This difference in the two assay systems was independent of the type of hyaluronidase and of the type of substrate used (cf. Chapter 5), indicating a general phenomenon in the degradation of these alternative substrates.
The main difference between the colorimetric and the turbidimetric assay is the fact, that in the turbidimetric assay only the degradation of high molecular weight substrate molecules (> 8 kDa) is detected, while the colorimetric assay is independent of fragment size. Thus, if the turbidimetric assay yields higher relative enzymatic activities than the colorimetric assay, this is indicative for a faster degradation of high molecular weight substrates compared to smaller substrate molecules with molecular weights, which are not precipitated in the turbidimetric assay.

## 6.4. Summary and conclusions

Human PH-20 was expressed by DS-2 cells as a soluble protein with a molecular weight of 56 kDa. The protein was glycosylated, however, the molecular weight differed only by about 1 kDa from the molecular weight calculated from the amino acid sequence.
Although human PH-20, expressed on the surface of HeLa cells, was reported to be glycosylated to a higher higher degree (65 kDa) (Arming et al. 1997), PH-20, expressed by DS-2 cells, was catalytically active. Thus, the presence of glycosidic modifications seems to be essential to gain enzymatically active PH-20 (cf. Chapter 4), but the exact pattern of glycosylation seems to be of minor importance. Similar results were previously obtained with Hyal-1 (cf. Chapter 5), indicating a role of N-linked glycans in the stability or solubility of human hyaluronidases.
In accordance with the data on macaque sperm PH-20 reported in literature (Li et al. 1997), the activity of recombinant human PH-20 was completely eliminated after reduction of the disulfide bridges. Otherwise, the protein exhibited a high stability even after extended periods of boiling.

A comparison of PH-20, expressed in DS-2 cells, to BTH revealed a similar pH-dependent degradation of HA with the typically inverse pH profiles in the colorimetric and in the turbidimetric hyaluronidase activity assay (Hoechstetter 2005). The alternative substrates ChS

A and ChS C were degraded to a much lower extent by BTH and recombinant human PH-20 than HA with a pH optimum at pH 5.0 – 6.0. Surprisingly, PH-20, expressed by DS-2 cells, showed a higher activity towards ChS A, while BTH degraded ChS C more efficiently than ChS A. As the sequence identity of human and bovine PH-20 is rather high (65 %), a possible explanation for the differing behavior towards ChS A and ChS C might be the presence of three catalytically active protein fractions in BTH, each exhibiting an unknown activity against the chondroitin sulfates.
Furthermore, the determination of the pH-dependent activity against chondroitin sulfates indicated a preferential degradation of higher molecular weight chondroitin sulfates.

Taken together, recombinant human PH-20 exhibited a similar catalytic behavior against HA, but differed in its activity against alternative substrates compared to BTH. PH-20, expressed in DS-2 cells, was not purified to homogeneity, but the achieved purity was sufficient for the development of specific inhibitors and the characterization of catalytic properties (cf. Chapter 8).

## 6.5. References

Albanell, J., Baselga, J. (2000). Systemic therapy emergencies. *Semin. Oncol.* **27**: 347-361.

Arming S., Strobl B., Wechselberger C., Kreil G. (1997). In vitro mutagenesis of PH-20 hyaluronidase from human sperm. *Eur. J. Biochem.* **247**: 810-814.

Baumgartner G., Moritz A. *Hyaluronidase: Anwendungen in der Onkologie.* Springer-Verlag. Wien, Berlin, Heidelberg. (1988).

Bertelli, G., Dini, D., Forno, G.B., Gozza, A., Silvestro, S., Venturini, M., Rosso, R., Pronzato, P. (1994). Hyaluronidase as an antidote to extravasation of Vinco alkaloids: clinical results. *J. Cancer Res. Clin. Oncol.* **120**: 505-506.

Bookbinder L.H., Hofer A., Haller M.F., Zepeda M.L., Keller G.A., Lim J.E., Edgington T.S., Shepard H.M., Patton J.S., Frost G.I. (2006). A recombinant human enzyme for enhanced interstitial transport of therapeutics. *J. Controlled Release* **114**: 230-241.

Cherr G.N., Meyers S.A., Yudin A.I., VandeVoort C.A., Myles D.G., Primakoff P., Overstreet J.W. (1996). The PH-20 Protein in Cynomolgus Macaque Spermatozoa: Identification of Two Different Forms Exhibiting Hyaluronidase Activity. *Dev. Biol.* **175**: 142-153.

Cherr G.N., Yudin A.I., Overstreet J.W. (2001). The dual functions of GPI-anchored PH-20: hyaluronidase and intracellular signaling. *Matrix Biol.* **20**: 515-25.

Gmachl M., Kreil G. (1993). Bee venom hyaluronidase is homologous to a membrane protein of mammalian sperm. *Proc. Natl. Acad. Sci. U. S. A.* **90**: 3569-3573.

Hoechstetter J. (2005). Characterisation of bovine testicular hyaluronidase and a hyaluronate lyase from Streptococcus agalactiae. *Doctoral thesis*. University of Regensburg. http://www.opus-bayern.de/uni-regensburg/volltexte/2005/519/

Hunnicutt G., Primakoff P., Myles D. (1996). Sperm surface protein PH-20 is bifunctional: one activity is a hyaluronidase and a second, distinct activity is required in secondary sperm-zona binding. *Biol. Reprod.* **55**: 80-86.

Kallio, H., Paloheimo, M., Maunuksela, E.L. (2000). Hyaluronidase as an adjuvant in bupivacaine-lidocaine mixture for retrobulbar/peribulbar block. *Anesth. Analg.* **91**: 934-937

Kim E., Baba D., Kimura M., Yamashita M., Kashiwabara S., Baba T. (2005). Identification of a hyaluronidase, Hyal5, involved in penetration of mouse sperm through cumulus mass. *Proc. Natl. Acad. Sci. U. S. A.* **102**: 18028-18033.

Lathrop W.F., Carmichael E.P., Myles D.G., Primakoff P. (1990). cDNA cloning reveals the molecular structure of a sperm surface protein, PH-20, involved in sperm-egg adhesion and the wide distribution of its gene among mammals. *J. Cell Biol.* **111**: 2939-2949.

Li M., Cherr G.N., Yudin A.I., Overstreet. J.W. (1997). Biochemical characterization of the PH-20 protein on the plasma membrane and using acrosomal membrane of cynomolgus macaque spermatozoa. *Mol. Reprod. Dev.* **48**: 356-366.

Menzel E.J., Farr C. (1998). Hyaluronidase and its substrate hyaluronan: biochemistry, biological activities and therapeutic uses. *Cancer Lett.* **131**: 3-11.

Oettl M., Hoechstetter J., Asen I., Bernhardt G., Buschauer A. (2003). Comparative characterization of bovine testicular hyaluronidase and a hyaluronate lyase from Streptococcus agalactiae in pharmaceutical preparations. *Eur. J. Pharm. Sci.* **18**: 267-277.

Primakoff P., Myles D.G. (2002). Penetration, Adhesion, and Fusion in Mammalian Sperm-Egg Interaction. *Science* **296**: 2183-2185.

Sabeur K., Cherr G.N., Yudin A.I., Primakoff P., Li M.W., Overstreet J.W. (1997). The PH-20 protein in human spermatozoa. *J. Androl.* **18**: 151-158.

Taylor T.H., Elliott T., Colturato L.F., Straub R.J., Mitchell-Leef D., Nagy Z.P. (2006). Comparison of bovine- and recombinant human-derived hyaluronidase with regard to fertilization rates and embryo morphology in a sibling oocyte model: a prospective, blinded, randomized study. *Fertil. Steril.* **85**: 1544-1546.

Yudin A.I., Li M.W., Robertson K.R., Cherr G.N., Overstreet J.W. (2001). Characterization of the active site of monkey sperm hyaluronidase. *Reproduction* **121**: 735-743.

Zacharius R.M., Zell T.E., Morrison J.H., Woodlock J.J. (1969). Glycoprotein staining following electrophoresis on acrylamide gels. *Anal. Biochem.* **30**: 148-152.

# Chapter 7

# Characterization of human hyaluronidase Hyal-2 expressed by DS-2 cells

## 7.1. Introduction

Hyal-2, formerly termed LUCA-2 (Wei et al. 1996), was first described by Lepperdinger et al. (Lepperdinger et al. 1998) as an acid-active, lysosomal hyaluronidase present in all tissues except brain. However, since then, the few publications on the localization and catalytic activity of Hyal-2 have been rather inconsistent.

Hyal-2 was found as a GPI-anchored protein on the surface of some cultured cells (Rai et al. 2001, Müllegger and Lepperdinger 2002b, Miller 2003), but was also located intracellularly in lysosomes (Lepperdinger et al. 1998, Chow et al. 2006a, Chow et al. 2006b). It was identified as the cell surface receptor for Jaagsiekte sheep retrovirus (JSRV) (Miller 2003) and was suggested to be responsible for the strong oncogenic potential of the retrovirus, which, itself, contains no oncogenes (Rai et al. 2001, Liu et al. 2003). While Lepperdinger et al. speculated that Hyal-2 might be targeted to lysosomes by re-uptake of formerly membrane-anchored Hyal-2 (Lepperdinger et al. 2001), Chow et al. suggested the localization of Hyal-2 primarily in lysosomes with a fraction of the expressed protein being transferred to a membrane-anchor and occurring at the cell surface (Chow et al. 2006b).

Data about the catalytic activity of Hyal-2 are even more contradictory. Hyal-2 was described to degrade high molecular weight HA from different sources to fragments of ca. 20 kDa (Lepperdinger et al. 1998, Lepperdinger et al. 2001), but also to low molecular weight HA fragments, albeit at a much slower rate (Vigdorovich et al. 2005). The detected hyaluronidase

activity was considerably lower than the activity of other hyaluronidases (PH-20, Hyal-1), and some authors could not detect any hyaluronidase activity at all (Rai et al. 2001). Degradation of HA by Hyal-2 was observed at pH 3.5 – 4.0 (Lepperdinger et al. 1998, Chow et al. 2006a), but was also described at nearly neutral pH (Müllegger and Lepperdinger 2002a, Vigdorovich et al. 2005).
The variety of properties described for Hyal-2 possibly results from interferences with intrinsic hyaluronidases present in many cell types (Lepperdinger et al. 1998, Rai et al. 2001). Detection of the extremely low Hyal-2 activity might therefore be a problem in transfected cells. Moreover, the detected activity of Hyal-2 seems to be species as well as tissue specific due to a differential distribution of Hyal-2 (intracellular and membrane-anchored).

Due to the absence of hyaluronan (Toyoda 2002) and hyaluronidase-like genes in *Drosophila melanogaster*, DS-2 cells present a suitable system for the production of Hyal-2. Hyal-2 was expressed as a soluble protein in the medium of DS-2 cells by analogy with PH-20 (cf. Chapter 6) since the aim of this study was the characterization of the catalytic properties of Hyal-2 and the supply of the enzyme for inhibitor assays.

A variety of hyaluronidase assays has been developed over the years ranging from the classical methods (Meyer and Rapport 1952) to electrophoretic (Guntenhoner et al. 1992, Mio et al. 2001), chromatographic (Cramer et al. 1994, Vercruysse et al. 1994), fluorescent (Krupa et al. 2003, Nagata et al. 2004) and ELISA-like assays (Stern and Stern 1992, Nawy et al. 2001). The classical methods comprise biological techniques like the observation of the "spreading effect" of a dye in the tissue of animals (Meyer and Rapport 1952), chemical methods including the colorimetric activity assay (Morgan-Elson assay) (Reissig et al. 1955, Takahashi et al. 2003) and physicochemical methods. Viscosimetric (Vercruysse 1995) and turbidimetric activity assays (Di Ferrante 1956) utilize changes in the physicochemical properties of HA dependent on the chain length for the detection of hyaluronidase activity.
Since the detection of Hyal-2 activity is complicated by its unusual substrate specificity described in literature (Lepperdinger et al. 2001), a range of activity assays (colorimetric, turbidimetric, viscosimetric assays, electrophoretic techniques) was applied to detect the activity of Hyal-2 expressed in DS-2 cells.

## 7.2. Materials and Methods

### *7.2.1. Vectors, cells, enzymes and chemicals*

Drosophila Schneider-2 cells (DS-2 cells), pCoHygro and pMT/BiP/V5-HisA were kindly provided by V. Runza (Institute of Immunology, Faculty of Medicine, University of Regensburg, Germany). Materials for subcloning were described in Chapter 3, materials used for DS-2 cell culture, protein expression and purification were identical to those described in Chapter 5.

Hyaluronic acid from *S. zooepidemicus* was purchased from Aqua Biochem GmbH, Dessau, Germany, HA from umbilical cord from Serva, Heidelberg, Germany. BTH (Neopermease®) was a gift from Sanabo, Vienna, Austria. Chondroitin 4-sulfate (A) from bovine trachea and chondroitin 6-sulfate (C) from shark cartilage were from Sigma, Munich, Germany. All other chemicals were from Merck, Darmstadt, Germany.

### *7.2.2. Construction of the expression vector pMT/Hygro/hyal-2*

Human *hyal-2* cDNA was amplified by PCR from the IMAGE clone vector IMAGp958H01139Q2 using 5'-TACTACCCGGGATGGAGCTCAAGCCCAC-3' as forward primer generating an additional *Sma*I cleavage site and 5'-TTAACTAAGCGGCCGCCCTCCAGCTGCC-3' as reverse primer with an additional *Not*I cleavage site. Amplification was achieved after 30 cycles and an annealing temperature of 77 °C in the presence of 2.5 mM $MgSO_4$. Both, the PCR product and the vector pMT/Hygro (cf. Chapter 5), were cleaved sequentially with *Sma*I and *Not*I. The insert restriction digest mixture contained 40 µL of purified PCR product, 1 µL of *Sma*I and 4.5 µL of TANGO™ buffer (Fermentas, St. Leon-Rot, Germany). After an incubation time of 2 h at 30 °C 5.2 µL of TANGO™ buffer and 2 µL of *Not*I were added and the mixture was incubated for 2 h at 37 °C. For digestion of the vector 1 µL of pMT/Hygro (1.0 mg/mL) was incubated with 1 µL of *Sma*I, 2 µL of TANGO™ buffer and 16 µL of water for 1 h at 30 °C. Then 2.5 µL of TANGO™ buffer and 2 µL of *Not*I were added and the mixture was incubated for 1 h at 37 °C. The vector was additionally dephosphorylated (cf. Chapter 3). Restriction enzymes and the phosphatase were inactivated by heating at 80 °C for 20 min. After ligation and transformation of pMT/Hygro/*hyal-2* into *E. coli* Top10 the insertion was confirmed by sequencing using a T7 promoter primer and a BGH primer.

If not indicated otherwise all cloning procedures were performed as described in Chapter 3.

### *7.2.3. Tranfection of DS-2 cells with pMT/Hygro/hyal-2 and expression of Hyal-2*

DS-2 cells were cultivated and transfected with pMT/Hygro/*hyal-2* as described previously for Hyal-1 (Chapter 5) using Lipofectamin$^{TM}$ 2000 CD (Invitrogen, Karlsruhe, Germany) as transfection reagent. Hyal-2 was expressed in DS-2 cells according to the protocol for Hyal-1 expression described in Chapter 5.

### *7.2.4. Western blot*

Principally, the protocol described in Chapter 4 was followed for the preparation of Western blots. Anti-V5-IgG (Sigma-Aldrich, Munich, Germany) diluted 2000-fold in 10 mL washing buffer was used as primary antibody and the secondary antibody was identical to the one used in Chapter 4.

For analysis of HA binding properties native PA-gels were prepared by analogy with the procedure for the preparation of SDS-PA gels, but without SDS. To achieve gel retardation the gels were supplemented with 67 µg/mL of HA. All gels were used for Western blotting after electrophoresis. DS-2 cell medium samples were mixed with 0.2 volumes of 5 x SDS sample buffer without DTT (cf. Chapter 3). Some samples were mixed with 5 x SDS sample buffer without SDS and DTT.

### *7.2.5. Purification of Hyal-2 by Ni-IMAC*

DS-2/pMT/Hygro/*hyal-2* cells were incubated for 10 d at 27 ± 1 °C and 135 rpm with an initial cell density of $1.5 \cdot 10^6$ cells/mL. The cell-free medium was supplemented with 0.1 % (v/v) Triton X-100, 20 mM imidazole and the pH was carefully adjusted to pH 7.8. Before application to the column the sample was clarified completely by centrifugation (30 min, 4 °C, 8,000 g). Hyal-2 containing a C-terminal His-tag was bound to a Ni-IMAC Column (CV 5 mL, GE Healthcare Bio-sciences AB, Uppsala, Sweden) equilibrated in 50 mM Na-phosphate, 0.5 M NaCl, 0.1 % (v/v) Triton X-100, pH 7.8. After loading the column was washed with 2 CV equilibration buffer before Hyal-2 was eluted with 1 CV of 50 mM Na-phosphate, 0.5 M NaCl, 0.1 % (v/v) Triton X-100, pH 4.5 and with 1 CV of 50 mM Na-phosphate, 0.5 M NaCl, 0.1 % (v/v) Triton X-100, pH 3.5. Fractions of 1 mL were collected and analyzed for their protein content (Bradford assays, cf. Chapter 4) and their enzymatic activity.

All buffers used during the purification process were vacuum-degassed and filtrated through a 0.45 µm filter (Millipore, Eschborn, Germany).

### *7.2.6. Turbidimetric and colorimetric hyaluronidase activity assay*

The turbidimetric and colorimetric hyaluronidase activity assays were described in detail in Chapter 3 and 4, respectively. For determination of BTH activity McIlvaine's buffer, pH 4.0, was used as an incubation buffer, for examination of Hyal-2 activities McIlvaine's buffer, pH 4.0 – 7.0, and 0.1 M Na-formate/formic acid, 0.1 M NaCl, pH 3.5, were used. If indicated the buffers were also used in absence of NaCl.

### *7.2.7. Agarose gel electrophoresis of hyaluronic acid (HA)*

HA digestion mixtures were analyzed by agarose gel electrophoresis as described previously (Rai et al. 2001, Vigdorovich et al. 2005). In brief, incubation mixtures were prepared consisting of 25 µL of HA solution (5 mg/mL), 10 µL of BSA (0.2 mg/mL), 10 µL of incubation buffer and 10 µL of sample. After incubation for 24 h and 5 d, respectively, at 37 °C the samples were mixed with 10 µL of HA loading buffer (40 mM Tris/HOAc, 1 mM EDTA, pH 8.0, 85 % (v/v) glycerol). 30 µL of these samples were immediately loaded on a 0.5 % agarose gel (for preparation cf. Chapter 3). Electrophoresis was performed with ca. 20 mA for 4 h. Then the gel was stained for 1 – 2 h in 0.5 % (w/v) Alcian blue in 7 % HOAc, pH 2.5, and subsequently destained by incubation with 7 % HOAc until bands of hyaluronic acid became visible.

Gels were analyzed with a Bio-Rad gel detection system (GS-710 Imaging Densitometer) using a "Stains All" filter set and Quantity One quantification software, version 4.0.3. (Biorad, Munich, Germany). GeneRuler$^{TM}$ DNA Ladder Mix (Fermentas, St. Leon-Rot, Germany) was used as molecular weight marker and was visualized after incubation of the agarose gel slice containing the marker in 1 x TBE (cf. Chapter 3) supplemented with 1 µg/mL ethidium bromide. DNA bands were detected as described in Chapter 3. The number of base pairs of the DNA marker was converted into Da (1 bp = 660 Da).

### *7.2.8. Pulsed field gel electrophoresis (PFGE)*

Pulsed field gel electrophoresis (PFGE) was performed in a Bio-Rad electrophoresis chamber (Bio-Rad, Munich, Germany) using 0.5 x TBE buffer (cf. Chapter 3) and a 0.5 % (w/v) agarose gel. Samples were prepared in twice the volume described in 7.2.7 and 90 µl of each sample were applied to the gel. As DNA standards a mixture of phage lambda DNA and GeneRuler$^{TM}$ DNA Ladder Mix (Fermentas, St. Leon-Rot, Germany) was used. Electrophoresis was performed by a clamped-homogeneous-electric-field technique for 10.5 h

at 4 °C and 6 V/cm with an automatic program adapted for DNA fragments of 2 – 100 kb. The initial switch time was 0.1 s and the final switch time 21.8 s at a switching angle of 120 °.

### *7.2.9. Viscosimetric detection of HA degradation*

Based on the official method for standardization of hyaluronidase preparations (European Pharmacopoeia, 2002) the hyaluronidase activity was measured as described by Hoechstetter (Hoechstetter 2005) in an Ubbelohde capillary viscosimeter (Schott-Geräte, Mainz, Germany). A micro-Ubbelohde viscosimeter (Ref. No. 53713, capillary diameter 0.53 mm) was clamped into an AVS measurement tripod connected to an AVS automated measuring device. The viscosimeter was immersed in a waterbath with a tripod at 37 °C.

Incubation mixtures containing 1 mL of incubation buffer, 1 mL of BSA (0.2 mg/mL), 1.5 mL of HA solution (5 mg/mL), 0.5 mL of $H_2O$ and 0.5 mL of enzyme solution were incubated at 37 °C for 24 h and 5 d, respectively, and filled into the viscosimeter. Due to the long incubation periods the outflow time during measurement of the viscosity was neglected for the calculation of incubation times.

The relative viscosity $\eta_{rel}$ was calculated according to the following equations:

$$\eta_{rel} = \frac{\nu}{\nu_{ref}} = \frac{K \cdot t}{K \cdot t_{ref}} = \frac{t_M - t_{HC}}{t_{ref} - t_{HC}} \qquad \text{Eq. 7.1}$$

with ν being the kinetic viscosity of the sample and $\nu_{ref}$ of the reference substance. K is the viscosimeter constant (0.03082 mm²/s²). The outflow times $t_M$, measured for the sample and $t_{ref}$ for the reference substance, were both corrected by the Hagen-Couette correction time ($t_{HC}$) according to the manufacturer's recommendation.

References were prepared by replacement of HA by $H_2O$ in the incubation mixtures. Incubation buffers were identical to those specified in 7.2.6. Enzyme samples were prepared from the medium of DS-2 cells expressing Hyal-2 (10 d after induction of expression) by dialysis (MWCO 14,000, 4 °C) against PBS supplemented with 1 mM EDTA. As negative control DS-2 wild type cells were treated in an identical way as DS-2 cells transfected with pMT/Hygro/*hyal-2*.

## 7.3. Results

### *7.3.1. Construction of the expression vector pMT/Hygro/hyal-2*

Hyal-2 is presumably a membrane-anchored, extracellular protein similar to PH-20. Therefore, the *hyal-2* cDNA was truncated during subcloning into pMT/Hygro (**Fig. 7.1**) at its N- and C-terminus to yield a soluble protein transported into the medium of the insect cells (cf. Chapter 6).

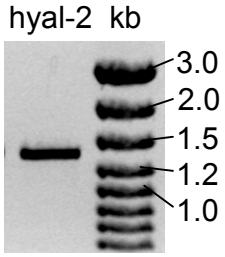


**Fig. 7.1** Agarose gel electrophoresis of the PCR amplification product *hyal-2*, showing the expected length of 1.3 kb. The lane contained a mixture of 5 µl of PCR product and 1 µl of 10 x PCR loading buffer.

At the N-terminus the human signal peptide was replaced by the BiP signal sequence encoded on pMT/Hygro and at the C-terminus the GPI-anchoring signal peptide comprising aa 449-473 was excluded from the PCR amplification product. Thus, pMT/Hygro/*hyal-2* coded for a 485 aa precursor protein with a C-terminal V5 epitope and His-tag (Appendix 2).

### *7.3.2. Stable expression of Hyal-2 in DS-2 cells*

DS-2 cells were transfected with pMT/Hygro/*hyal-2* and selected for the presence of hygromycin resistance. These stably transfected cells were found to express a ca. 54 kDa protein reacting specifically with anti-V5-IgG into the medium (**Fig. 7.2**). In the Western blot analysis no significant difference could be found in the Hyal-2 expression rate of induced and non-induced cells.

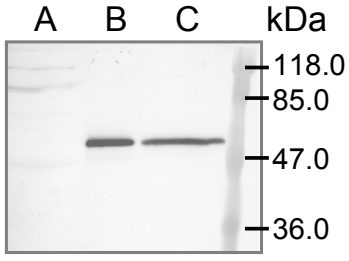


**Fig. 7.2** Western blot analysis of 30 µl of cell medium 10 d after induction of stable expression. Lane A contained induced wild type DS-2 cell medium, lane B uninduced DS-2/pMT/Hygro/*hyal-2* cell medium and lane C induced DS-2/pMT/Hygro/*hyal-2* cell medium. Anti-V5-IgG was used as primary antibody, biotinylated anti-mouse-IgG as secondary antibody and detection of the antibody binding was achieved by HRP/DAB staining.

The molecular mass of Hyal-2 expressed in DS-2 cells was consistent with the mass calculated from the amino acid sequence (53.7 kDa) indicating a low level of glycosylation.

### *7.3.3. Purification of Hyal-2 by Ni-IMAC*

Since the expression of Hyal-2 in the medium of DS-2 cells did not reveal a significant difference between induced and non-induced cell medium (7.3.2) purification of Hyal-2 was performed using non-induced DS-2/pMT/Hygro/*hyal-2* cell medium to avoid interferences of $CuSO_4$ with the purification procedure (**Fig. 7.3**).

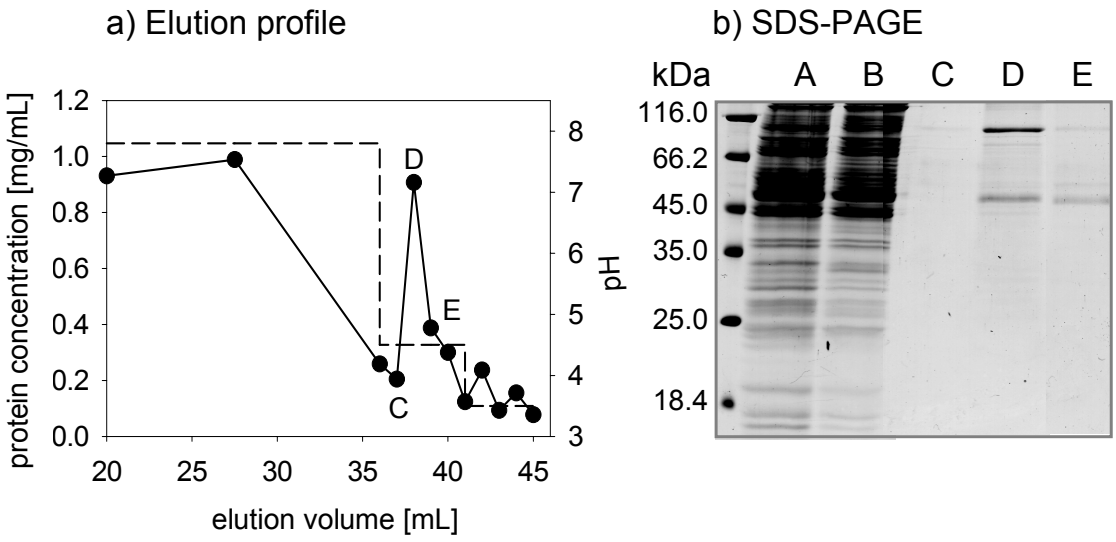


**Fig. 7.3** Ni-IMAC purification of Hyal-2 from DS-2 cell medium after 10 d of incubation. a) Elution profile detected by the protein concentration; b) SDS-PAGE of the Hyal-2 purification process: A) DS-2/pMT/Hygro/*hyal-2* cell medium, B) flow-through, C) – E) elution fractions at pH 4.5.

At pH 4.5 a 54 kDa protein was eluted from the Ni-IMAC column, which was identified as Hyal-2 by Western blot analysis. Although the elute contained protein impurities further purification was abandoned due to the absence of any enzymatic activity (see below).

### *7.3.4. Colorimetric and turbidimetric activity assays*

The standard hyaluronidase activity assays used for detection of the catalytic activity of BTH, Hyal-1 and PH-20 (cf. Chapter 5 and 6) failed to detect any hyaluronidase activity for Hyal-2 purified from the medium of stably transfected DS-2 cells. Although a range of pH values (pH 3.5 – 7.0), different substrate molecules (HA from *S. zooepidemicus*, HA from umbilical cord, chondroitin sulfate A and C) and extended incubation times (24 h – 7 d) were used, no activity could be detected in the colorimetric and the turbidimetric hyaluronidase activity assay, respectively. Therefore, alternative hyaluronidase activity assays were explored for their ability to detect the degradation of HA through the action of Hyal-2.

### *7.3.5. Agarose electrophoresis of HA digestion mixtures*

Hyal-2 activity was in most cases detected by the increase in the electrophoretic mobility of HA fragments of lower size in an agarose gel (Lepperdinger et al. 1998, Rai et al. 2001, Vigdorovich et al. 2005). As the colorimetric and the turbidimetric activity assays failed to detect HA degradation by Hyal-2 expressed by DS-2 cells HA degradation mixtures were separated on an agarose gel to visualize decreases in the size of high-molecular weight HA fragments.

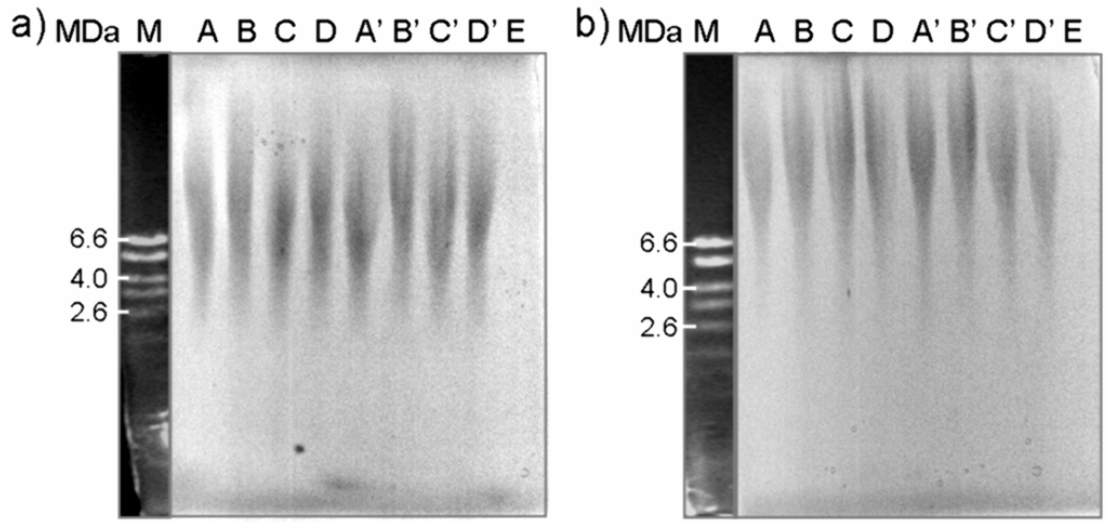


**Fig. 7.4** Agarose gel electrophoresis of HA digestion mixtures (24 h) with HA from human umbilical cord (a) and HA from *S. zooepidemicus* (b). M) standard DNA molecular weight marker, A) cell-free medium, B) induced wild type cell medium, C) uninduced DS-2/pMT/Hygro/*hyal-2* medium, D) induced DS-2/pMT/Hygro/*hyal-2* medium. Samples A) – D) were incubated using 0.1 M Na-formate/formic acid, pH 3.5, samples A') – D') containing the analogous samples were incubated with McIlvaine's buffer without NaCl, pH 5.5. Sample E) was a control using BTH as sample and McIlvaine's buffer, pH 4.5.

As shown in **Fig. 7.4** HA fragments were not distinctly separated by electrophoresis, but formed a broad band consistent with the polydisperse nature of HA in the incubation mixtures. This observation confirms the previously described results of this assay (Lepperdinger et al. 1998, Rai et al. 2001).

The increased propagation of umbilical cord HA compared to HA from *S. zooepidemicus* indicates a lower molecular weight of HA from umbilical cord. According to the suppliers' declarations the molecular weight of HA from *S. zooepidemicus* is 1 – 2 MDa and 200 – 800,000 Da for HA from umbilical cord. However, a comparison of the molecular weight given by the suppliers with the molecular weight observed on the agarose gel reveals a large discrepancy, probably due to the different electrophoretic mobilities of DNA and HA.

If HA was degraded during the incubation period a shift of the HA band towards lower molecular masses should occur. The positive control (lane E in **Fig. 7.4**) contained no visible

HA fragments due to complete degradation of HA to low molecular weight fragments by the action of BTH. The residual incubation mixtures revealed no changes in the size of the HA fragments compared to the negative controls containing cell-free medium. Neither after 24 h (**Fig. 7.4**) nor after 5 d (data not shown) of incubation any hyaluronidase activity was observed for the Hyal-2 samples in the agarose gel electrophoresis.

### *7.3.6. Pulsed field gel electrophoresis (PFGE)*

To improve the separation of HA fragments in the agarose gel electrophoresis PFGE was performed. PFGE is generally used for the separation of macromolecular DNA fragments with up to 5 Mb (Lottspeich and Zorbas 1998). However, the high molecular weight HA fragments present in the incubation mixtures were not separated distinctly by this technique (**Fig. 7.5**).

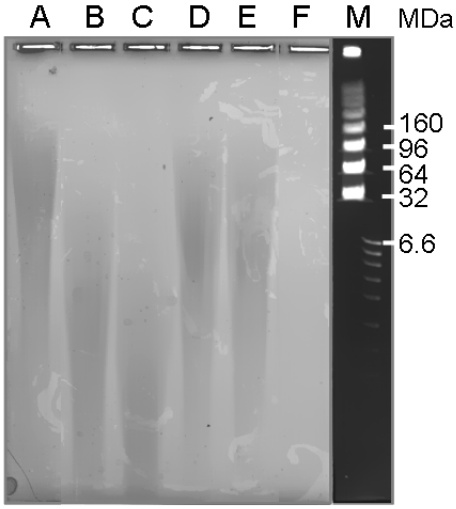


**Fig. 7.5** Pulsed field gel electrophoresis (PFGE) of HA from *S. zooepidemicus*. A) HA solubilized in water, B) HA, sonicated for 3 min, C) HA, sonicated for 5 min, D) incubation mixture (24 h) with purified Hyal-2 and 0.1 M Na-formate/formic acid, pH 3.5, as incubation buffer, E) incubation mixture (24 h) with purified, heat-inactivated Hyal-2 and 0.1 M Na-formate/formic acid, pH 3.5, as incubation buffer, F) incubation mixture (24 h) with BTH and McIlvaine's buffer, pH 4.5 as incubation buffer, M) DNA ladders with bp transformed into MDa.

Although a reduction in the molecular weight of HA was observed upon ultrasonication (lane B and C in **Fig. 7.5**) no changes in the HA fragment sizes were observed in the incubation mixtures containing purified Hyal-2 (lane D and E in **Fig. 7.5**).

### *7.3.7. Viscosimetric determination of HA degradation*

7.3.7.1. Principle of hyaluronidase detection by viscosimetry

The degradation of high molecular weight HA through the action of hyaluronidases can be followed by the decrease in the viscosity of the incubation mixture. The kinetic viscosity ν can be determined by the volume (V) passing a capillary with an inner radius R during the time t as follows:

$$\nu = t \cdot \frac{\pi R^4 g h_m}{8LV} = t \cdot K \qquad \text{Eq. 7.2}$$

The geometric parameters of the capillary (R, $h_m$, L, V) can be summarized in the viscosimeter constant K. Due to loss of pressure at the ends of a capillary the real flow time $t_M$ is increased compared to the ideal flow time t, thus a correction time $t_{HC}$ (Hagen-Couette-correction time) has to be substracted from $t_M$:

$$t = t_M - t_{HC} \qquad \text{Eq. 7.3}$$

The difference between the real and the ideal flow time decreases with increasing $t_M$. The $t_{HC}$ values can be inferred from instrument specific calibration tables (Wilke et al.). Thus, the relative viscosity $\eta_{rel}$ of a HA degradation mixture was determined as given in Eq. 7.1 using a solution without HA as reference. Maximum relative viscosities were determined at zero enzymatic activity in the presence of HA.

7.3.7.2. Sensitivity of viscosimetry compared to the colorimetric and turbidimetric hyaluronidase activity assays

To allow for a comparison of the different hyaluronidase activity assays the change in the detected parameter, i.e. relative viscosity, $A_{585}$ or $OD_{355}$, was observed in dependence of the enzymatic activity of BTH in the stock solution (IE/mL) after an incubation period of 24 h ( **Fig. 7.6** and **Fig. 7.7**).

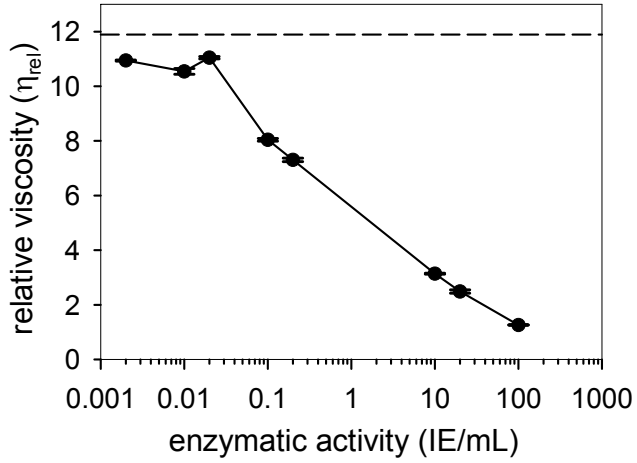


**Fig. 7.6** Decrease in the relative viscosity of HA digestion mixtures through the action of BTH. The digestion mixtures were prepared with McIlvaine's buffer, pH 4.0, as incubation buffer and were incubated for 24 h at 37 °C. The viscosity of each sample was determined three times. The relative viscosity values are mean values ± SEM.

Enzymatic activities of ca. 0.1 IE/mL were already detected by a decrease in the viscosity of the incubation mixture, while the formation of Morgan-Elson products in the colorimetric assay was observed at activities > 2 IE/mL (**Fig.7.7.a**). The turbidimetric assay performed in microtiter-plates was found to be slightly less sensitive than the colorimetric assay with ca. 5 IE/mL being the minimum hyaluronidase activity detected after 24 h of incubation time (**Fig.7.7.b**).

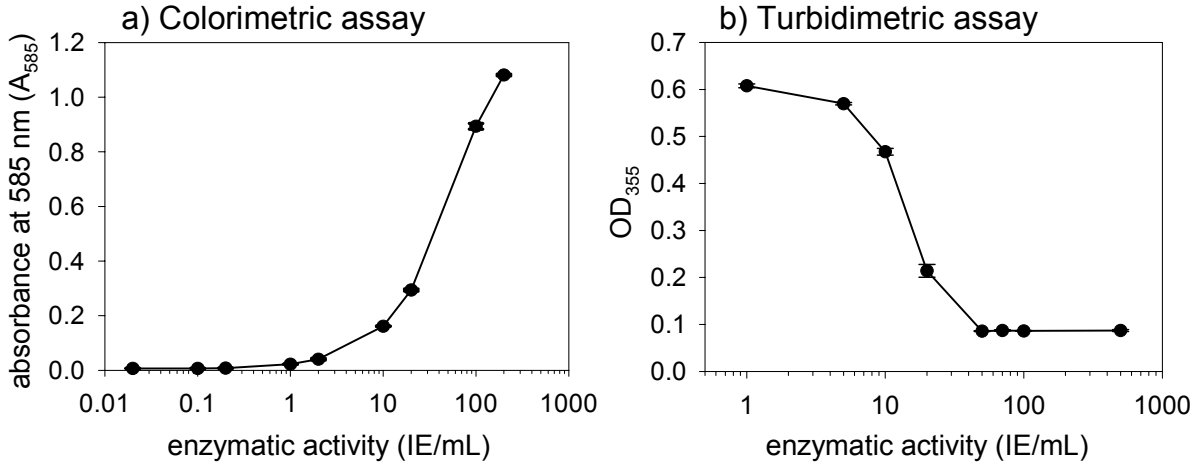


**Fig. 7.7** Sensitivity of the colorimetric (a) and turbidimetric activity assay (b) for the degradation of HA through the action of BTH after 24 h of incubation in McIlvaine's buffer, pH 4.0.

When all assays were performed according to the standard procedures the decrease in viscosity was the most sensitive method to determine degradation of HA by the action of hyaluronidases. Compared to the colorimetric and turbidimetric assay viscosimetry was ca. 10-fold more sensitive.

7.3.7.3. Viscosimetric analysis of Hyal-2 in DS-2 cell medium

Incubation mixtures containing HA from *S. zooepidemicus* and the dialyzed medium of wild type DS-2 cells or of DS-2 cells expressing Hyal-2 were incubated for 24 h and 5 d, respectively, at acidic and nearly neutral pH. Strikingly, the viscosity determined at pH 3.5 was significantly higher than the viscosity determined at pH 5.5, as shown in **Fig.7.7**.

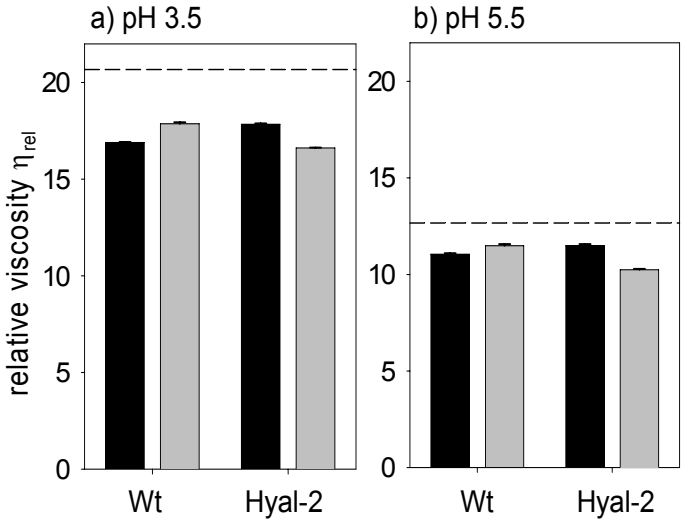


**Fig. 7.8** Viscosimetry of HA digestion mixtures incubated at 37 °C for 24 h (black bars) and 5 d (grey bars) at pH 3.5 (a) and pH 5.5 (b), respectively. The HA was of microbiological origin (*S. zooepidemicus*). Incubation mixtures contained the induced medium of DS-2 wild type (Wt) cells or of DS-2 cells expressing Hyal-2 (Hyal-2). The reference lines (dashed) indicate the maximum relative viscosity measured with PBS at the beginning of the incubation period.

Furthermore, a decrease in viscosity was observed in all incubation mixtures incubated at 37 °C for ≥ 24 h in comparison to the reference with maximum viscosity (t = 0) (**Fig. 7.8**). However, the incubation mixtures containing the medium from DS-2 cells expressing Hyal-2

did not differ in the reduction of viscosity compared to the DS-2 wild type cell medium, neither after 24 h nor after 5 d.

The activity of Hyal-2 described in literature was often determined with HA from human umbilical cord (Rai et al. 2001). Therefore, the viscosity was also measured after incubation of HA from human umbilical cord to assure that the absence of hyaluronidase activity was not dependent on the source of HA used in the assay.

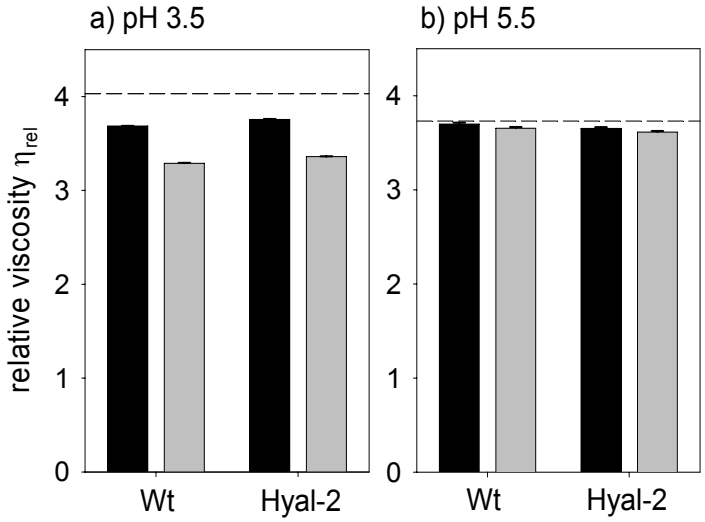


**Fig. 7.9** Viscosimetry of HA digestion mixtures incubated at 37 °C for 24 h (black bars) and 5 d (grey bars) at pH 3.5 (a) and pH 5.5 (b), respectively. The HA was a preparation from human umbilical cord. Incubation mixtures contained the induced medium of DS-2 wild type (Wt) cells or of DS-2 cells expressing Hyal-2 (Hyal-2). The reference lines indicate the relative viscosity measured with PBS at the beginning of the incubation period (t = 0).

As already described previously (Hoechstetter 2005), the viscosity of human umbilical cord HA was significantly lower than that of HA derived from *S. zooepidemicus* (**Fig. 7.8** and **Fig. 7.9**) due to a reduced HA chain length of umbilical cord HA. Additionally, the difference between the viscosity at acid and nearly neutral pH was much more significant for HA from *S. zooepidemicus* than for HA from umbilical cord. Possibly, the pH-dependent differences in viscosity originate from the formation of HA secondary or tertiary structures occurring through interactions of high molecular weight HA chains at higher pH values. An increased chain length as present in HA from *S. zooepidemicus* might facilitate the formation of these interactions in contrast to the lower molecular weight chains in HA from umbilical cord.

### *7.3.8. HA binding properties of Hyal-2*

As no hyaluronidase activity of Hyal-2 expressed in DS-2 cells could be detected, the question arose if Hyal-2 might merely be a receptor for HA, i.e. if Hyal-2 could bind hyaluronan without catabolizing it.

Therefore, the primary sequences of human Hyal-1, Hyal-2, Hyal-4, PH-20 and BVH were analyzed for the presence of HA binding motifs (Yang et al. 1994). The HA binding motif $B(X)_7B$, with B being a basic amino acid and X being any amino acid except an acid one, was

found 1 – 3 times in all hyaluronidases. In Hyal-2 the motif was found twice, but not in close proximity to the active site. RR, another sequence motif causing binding of HA in peptides (Amemiya et al. 2005), was also identified a few times in the human hyaluronidases. However, Hyal-2 did not exhibit any extraordinary sequence motifs compared to the other hyaluronidases. A BLAST search (Altschul et al. 1990) of human Hyal-2 revealed only Hyal-2 from other species, other human hyaluronidases and hypothetical proteins without any identified function as proteins with any reasonable sequence similarity (BLAST score > 300). The sequence identity of Hyal-2 with the other human hyaluronidases comprises ca. 35 – 40 %.

Although the sequence of Hyal-2 did not reveal any extraordinarily high number of HA binding motifs compared to other human hyaluronidases, Hyal-2 was tested for its ability to bind HA. Previous studies on HA binding proteins revealed a retardation of these proteins on SDS-PA gels containing HA (Hrkal et al. 1996). To test for HA binding properties of Hyal-2 the electrophoretic mobility of unpurified Hyal-2 was observed in the absence and in the presence of HA integrated in a PA-gel and visualized by Western blotting (**Fig. 7.10**). The use of SDS-PA gels did not alter the running behavior of Hyal-2 on the Western blot (data not shown).

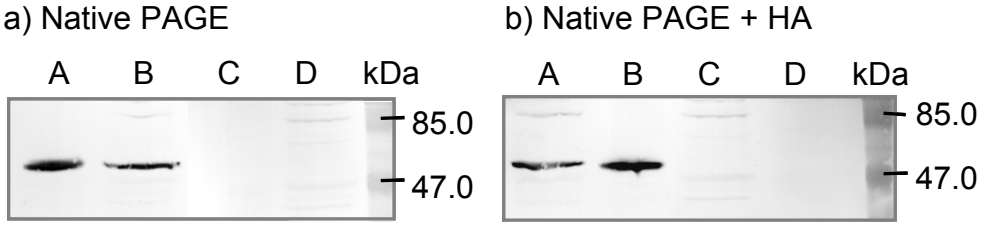


**Fig. 7.10** Western blot analysis of Hyal-2 on a native PAGE (a) and a native PAGE supplemented with HA (b). DS-2 cell medium 10 d after induction of expression was mixed with sample buffer with or without SDS, the gels were blotted after electrophoresis and the antibody reaction was achieved with Anti-V5-IgG as primary antibody, biotinylated anti-mouse-IgG as secondary antibody and subsequent HRP/DAB staining. A) DS-2/pMT/Hygro/*hyal-2* medium without SDS, B) DS-2/pMT/Hygro/*hyal-2* medium with SDS, C) DS-2 wild type medium without SDS, D) DS-2 wild type medium with SDS.

Since the HA binding properties had to be retained during electrophoresis PA-gels without SDS were used for the Western blot analysis. However, the electrophoretic mobility of Hyal-2 was not decreased in the presence of HA in the PA-gel (**Fig. 7.10**) indicating the absence of strong HA binding properties. Addition of SDS to the sample buffer did not influence the electrophoretic mobility of Hyal-2.

## 7.4. Summary and conclusions

By analogy with the human hyaluronidases Hyal-1 and PH-20 (cf. Chapter 5 and 6) Hyal-2 was expressed into the medium of stably transfected DS-2 cells and partially purified by Ni-IMAC. The presence of Hyal-2 was proven by Western blot analysis, but the detection of hyaluronidase activity failed. Since Hyal-2 is known to degrade mainly high molecular weight HA to fragments of ca. 20 kDa (50 disaccharide units), a variety of assays was evaluated for the detection of HA degradation through the action of Hyal-2.

Absence of Hyal-2 activity in the colorimetric hyaluronidase activity assay was reported previously (Lepperdinger et al. 1998). Furthermore, the suitability of the turbidimetric activity assay for the detection of HA degradation products of ca. 20 kDa must be put into question. Nevertheless, both assays were tested for the detection of Hyal-2 activity, but failed to give positive results. To investigate if insufficient sensitivity of these standard hyaluronidase activity assays was the reason for the absence of Hyal-2 activity, degradation of HA was analyzed by agarose gel electrophoresis of HA and by viscosimetry. Agarose gel electrophoresis assays, although often employed for the detection of Hyal-2 degradation products, did not reveal any decrease in the molecular weight of HA even after extended incubation periods (up to 5 d) with Hyal-2. As the agarose gel electrophoresis exhibited some disadvantages in handling, e.g. high background staining of the agarose with Alcian blue, viscosimetry was used to detect the activity of Hyal-2. The significant decrease in HA viscosity, particularly at the beginning of the degradation reaction (Hoechstetter 2005), favors viscosimetry for the detection of Hyal-2 activity. As the viscosity of mixtures incubated for up to 5 d did not decrease compared to the negative control (DS-2 wildtype cells), Hyal-2 expressed in DS-2 cells was considered as a protein without any hyaluronidase activity.

Heterologous expression of proteins can cause a loss of protein function due to wrong or missing post-translational modifications or the combination with sequence tags. However, Vigdorovich et al. (Vigdorovich et al. 2005) expressed human Hyal-2 as a soluble protein linked to a C-terminal His-tag in a baculovirus system. In this insect cell system, Hyal-2, lacking the GPI-anchor signal peptide, was excreted into the culture medium of Sf9 cells. Thus, the resulting recombinant Hyal-2 was very similar to Hyal-2 expressed in DS-2 cells. Vigdorovich et al. observed Hyal-2 activity over a broad pH range (Vigdorovich et al. 2005), but revised their observations due to an intrinsic hyaluronidase activity of the Sf9 cells (Vigdorovich et al. 2007). Very recently, recombinant Hyal-2 was described as an acid-active

enzyme with very weak hyaluronidase activity (Vigdorovich et al. 2007). However, in consideration of the extremely weak activity it seems problematic to discriminate between endogenous hyaluronidase and Hyal-2.

No matter if the activity of Hyal-2 is extremely low or not detectable at all, the biological function of Hyal-2 as a hyaluronidase has to be questioned. Up to now it could not be proven that Hyal-2 binds hyaluronic acid, although this could explain the function of Hyal-2 as a HA receptor as postulated by Csoka et al. (Csoka et al. 2001). For Hyal-2 expressed in DS-2 cells there was no retardation of the protein in a PA-gel as a consequence of HA binding. However, HA binding can not be completely excluded based on this assay and further investigations are necessary to confirm the results.

In summary, the recombinant expression of Hyal-2 in DS-2 cells showed that the hyaluronidase activity of Hyal-2 described in literature has to be evaluated very carefully with respect to impurities affecting hyaluronidase activity and concerning the assay systems used for the detection of HA degradation products. Hemopexin, a serum-heme binding protein, provides an example for a protein, first described as a hyaluronidase (Zhu et al. 1994), while further investigations revealed only HA binding properties and no catalytic activity (Hrkal et al. 1996). Serum hyaluronidase impurities within the hemopexin samples had feigned the existence of hyaluronidase activity. If Hyal-2 is only an extremely weak or no hyaluronidase at all, the biological function of the enzyme has to be reviewed as well.

## 7.5. References

Altschul S.F., Gish W., Miller W., Myers E.W., Lipman D.J. (1990). Basic local alignment search tool. *J. Mol. Biol.* **215**: 403-410.

Amemiya K., Nakatani T., Saito A., Suzuki A., Munakata H. (2005). Hyaluronan-binding motif identified by panning a random peptide display library. *Biochim. Biophys. Acta* **1724**: 94-99.

Chow G., Knudson C.B., Knudson W. (2006a). Expression and cellular localization of human hyaluronidase-2 in articular chondrocytes and cultured cell lines. *Osteoarthritis Cartilage* **14**: 849-858.

Chow G., Knudson C.B., Knudson W. (2006b). Human hyaluronidase-2 is localized intracellularly in articular chondrocytes and other cultured cell lines. *Osteoarthritis Cartilage* **14**: 1312-1314.

Cramer J.A., Bailey L.C., Bailey C.A., Miller R.T. (1994). Kinetic and mechanistic studies with bovine testicular hyaluronidase. *Biochim. Biophys. Acta* **1200**: 315-21.

Csoka A.B., Frost G.I., Stern R. (2001). The six hyaluronidase-like genes in the human and mouse genomes. *Matrix Biol.* **20**: 499-508.

Di Ferrante N. (1956). Turbidimetric measurement of acid mucopolysaccharides and hyaluronidase activity. *J. Biol. Chem.* **220**: 303-306.

Guntenhoner M.W., Pogrel M.A., Stern R. (1992). A substrate-gel assay for hyaluronidase activity. *Matrix* **12**: 388-396.

Hoechstetter J. (2005). Characterisation of bovine testicular hyaluronidase and a hyaluroniate lyase from Streptococcus agalactiae. *Doctoral thesis*. University of Regensburg. http://www.opus-bayern.de/uni-regensburg/volltexte/2005/519/

Hrkal Z., Kuzelova K., Muller-Eberhard U., Stern R. (1996). Hyaluronan-binding properties of human serum hemopexin. *FEBS Lett.* **383**: 72-74.

Krupa J.C., Marie Butler A., Mort J.S. (2003). Quantitative bead assay for hyaluronidase and heparinase I. *Anal. Biochem.* **319**: 280-286.

Lepperdinger G., Mullegger J., Kreil G. (2001). Hyal2 -- less active, but more versatile? *Matrix Biol.* **20**: 509-514.

Lepperdinger G., Strobl B., Kreil G. (1998). HYAL2, a human gene expressed in many cells, encodes a lysosomal hyaluronidase with a novel type of specificity. *J. Biol. Chem.* **273**: 22466-22470.

Liu S., Duh F., Lerman M., Miller A.D. (2003). Role of virus receptor Hyal2 in oncogenic transformation of rodent fibroblasts by sheep betaretrovirus env proteins. *J. Virol.* **77**: 2850-2858.

Lottspeich F., Zorbas H. *Bioanalytik.* Spektrum Akademischer Verlag GmbH. Heidelberg, Berlin. (1998).

Meyer K., Rapport M.M. (1952). Hyaluronidases. *Adv. Enzymol. Relat. Areas Mol. Biol.* **13**: 199-236.

Miller A.D. (2003). Identification of Hyal2 as the cell-surface receptor for jaagsiekte sheep retrovirus and ovine nasal adenocarcinoma virus. *Curr. Top. Microbiol. Immunol.* **275**: 179-199.

Mio K., Csoka A.B., Nawy S.S., Stern R. (2001). Detecting hyaluronidase and hyaluronidase inhibitors. Hyaluronan-substrate gel and -inverse substrate gel techniques. *Methods Mol. Biol.* **171**: 391-397.

Müllegger J., Lepperdinger G. (2002a). Degradation of hyaluronan by a Hyal2-type hyaluronidase affects pattern formation of vitelline vessels during embryogenesis of Xenopus laevis. *Mech. Dev.* **111**: 25-35.

Müllegger J., Lepperdinger G. (2002b). Hyaluronan is an abundant constituent of the extracellular matrix of Xenopus embryos. *Mol. Reprod. Dev.* **61**: 312-316.

Nagata H., Kojima R., Sakurai K., Sakai S., Kodera Y., Nishimura H., Inada Y., Matsushima A. (2004). Molecular-weight-based hyaluronidase assay using fluorescent hyaluronic acid as a substrate. *Anal. Biochem.* **330**: 356-358.

Nawy S.S., Csoka A.B., Mio K., Stern R. (2001). Hyaluronidase activity and hyaluronidase inhibitors. Assay using a microtiter-based system. *Methods Mol. Biol.* **171**: 383-389.

Rai S.K., Duh F.-M., Vigdorovich V., Danilkovitch-Miagkova A., Lerman M.I., Miller A.D. (2001). Candidate tumor suppressor HYAL2 is a glycosylphosphatidylinositol (GPI)-anchored cell-surface receptor for jaagsiekte sheep retrovirus, the envelope protein of which mediates oncogenic transformation. *Proc. Natl. Acad. Sci. U. S. A.* **98**: 4443-4448.

Reissig J., Strominger J., Leloir L. (1955). A modified colorimetric method for the estimation of N-Acetylamino sugars. *J. Biol. Chem.* **217**: 959-966.

Stern M., Stern R. (1992). An ELISA-like assay for hyaluronidase and hyaluronidase inhibitors. *Matrix* **12**: 397-403.

Takahashi T., Ikegami-Kawai M., Okuda R., Suzuki K. (2003). A fluorimetric Morgan-Elson assay method for hyaluronidase activity. *Anal. Biochem.* **322**: 257-263.

Toyoda H. (2002). Glycosaminoglycans in Drosophila melanogaster. http://www.glycoforum.gr.jp/science/word/proteoglycan/PGC02E.html

Vercruysse K.P., Lauwers A.R., Demeester J.M. (1994). Kinetic investigation of the degradation of hyaluronan by hyaluronidase using gel permeation chromatography. *J. Chromatogr. B. Biomed. Appl.* **656**: 179-190.

Vercruysse K.P., Lauwers, A. R., Demeester, J. M. (1995). Absolute and empirical determination of the enzymatic activity and kinetic investigation of the action of hyaluronidase on hyaluronan using viscosimetry. *Biochem. J.* **306**: 153-160.

Vigdorovich V., Miller A.D., Strong R.K. (2007). Ability of hyaluronidase-2 to degrade extracellular hyaluronan is not required for its function as a receptor for jaagsiekte sheep retrovirus. *J. Virol.* doi: 10.1128/JVI.02177-06.

Vigdorovich V., Strong R.K., Miller A.D. (2005). Expression and characterization of a soluble, active form of the Jaagsiekte sheep retrovirus receptor, Hyal2. *J. Virol.* **79**: 79-86.

Wei M., Latif F., Bader S., Kashuba V., Chen J., Duh F., Sekido Y., Lee C., Geil L., Kuzmin I., Zabarovsky E., Klein G., Zbar B., Minna J., Lerman M. (1996). Construction of a 600-kilobase cosmid clone contig and generation of a transcriptional map surrounding the lung cancer tumor suppressor gene (TSG) locus on human chromosome 3p21.3: progress toward the isolation of a lung cancer TSG. *Cancer Res.* **56**: 1487-1492.

Wilke J., Kryk H., Hartmann J., Wagner D. *Theorie und Praxis der Kapillarviskosimetrie. Eine Einführung.* SCHOTT-Geräte GmbH. Hofheim.

Yang B., Yang B.L., Savani R.C., Turley E.A. (1994). Identification of a common hyaluronan binding motif in the hyaluronan binding proteins RHAMM; CD44 and link protein. *EMBO J.* **13**: 286-296.

Zhu L., Hope T.J., Hall J., Davies A., Stern M., Muller-Eberhard U., Stern R., Parslow T.G. (1994). Molecular cloning of a mammalian hyaluronidase reveals identity with hemopexin, a serum heme-binding protein *J. Biol. Chem.* **269**: 32092-32097.

# Chapter 8

# Isozyme-specific differences in the degradation of HA and HA oligosaccharides by BTH, human PH-20 and human Hyal-1

## 8.1. Introduction

Bovine testicular hyaluronidase (BTH) has been extensively studied with respect to its catalytic behavior at various pH values, dependency on salt concentrations and the formation of reaction products (Gorham et al. 1975, Takagaki et al. 1994, Oettl 2000, Hoechstetter 2005). In contrast to BTH, the HA degradation products of human Hyal-1 and human PH-20 have not been studied in detail yet. Due to the availability of the human enzymes in very low quantities up to now information on their enzymatic properties has been restricted to a few elementary properties, such as the pH profiles and the nature of the reaction products (Gold 1982, Afify et al. 1993, Gmachl et al. 1993, Frost et al. 1997, Sabeur et al. 1997). The production of pure, recombinant human Hyal-1 (cf. Chapter 5) and partially purified, recombinant human PH-20 (cf. Chapter 6) enabled the detailed investigation of Hyal-1 and PH-20 in comparison to BTH.

Bovine testicular hyaluronidase (BTH) and, presumably, all mammalian hyaluronidases catalyze the hydrolysis as well as the transglycosylation of hyaluronan fragments (Weissmann 1955) (cf. Chapter 1). For BTH hydrolysis is favored at acidic pH values, while transglycosylation occurs preferentially at neutral pH values and at low NaCl concentrations (Gorham et al. 1975, Saitoh et al. 1995).

The complex reactions catalyzed by hyaluronate hydrolases and the polymeric structure of the substrate severely complicate the analysis of enzymological characteristics by means of Michaelis-Menten kinetics. Although $K_M$ and $v_{max}$ values for hyaluronidase-catalyzed degradation of the high molecular weight substrate HA can be found in literature (Cramer et al. 1994, Vercruysse et al. 1995, Asteriou et al. 2006), the determination of exact Michaelis-Menten kinetics is impeded by the steady increase in the substrate concentration during the cleavage of the HA chains. Therefore, small oligosaccharides have been employed enabling an exact analysis of the reactions catalyzed by BTH (Cramer et al. 1994).

Due to the negatively charged groups present in GAG oligosaccharides capillary zone electrophoresis (CZE) is often applied in the analysis of GAGs in biological or biopharmaceutical preparations (Mao et al. 2002). CZE has been used for the separation of HA digestion products from various biological samples, e.g. for vitreous humor HA (Grimshaw et al. 1994), synovial fluid HA (Grimshaw et al. 1996) and for the analysis of HA fragments produced by venom hyaluronidases (Pattanaargson and Roboz 1996). A wide variety of CZE conditions is described in literature for the separation of HA fragments, e.g. migration with normal polarity (Grimshaw et al. 1994, Pattanaargson and Roboz 1996), migration with reverse polarity (Hayase et al. 1997), the use of ion-pairing reagents (Payan et al. 1998) and polymers (Kakehi et al. 1999) to improve the separation of high molecular weight HA fragments.
The analysis of unmodified HA degradation products in biological samples is hampered by the absence of a suitable chromophore in the HA degradation products of hydrolases. If detection is performed by absorbance at low wavelengths (200 – 210 nm) buffer substances as well as protein impurities interfere with the GAG detection. Grimshaw et al. (1994) employed a capillary zone electrophoresis method with an alkaline phosphate-borate buffer and SDS for the separation of protein impurities from the HA fragments. As described in the following chapter this method was optimized for the qualitative and quantitative analysis of hydrolase digestion products formed by the catalysis of pure enzyme samples.

The CZE method was utilized to analyze the formation of degradation products of high molecular weight HA and of hyaluronan oligosaccharides produced through the action of BTH, recombinant, human PH-20 and recombinant, human Hyal-1. The hyaluronan hexasaccharide ($n_3$) is known to be the minimum substrate for BTH (Highsmith et al. 1975, Cramer et al. 1994), and is supposed to be the minimum substrate of the human

hyaluronidases as well (Stern and Jedrzejas 2006). BTH was shown to exhibit differences in its catalytic activity at acidic and neutral pH (Hoechstetter 2005). Therefore, the investigations performed with BTH were focused on the comparison of the HA fragments produced at acidic and around neutral pH.

While the degradation kinetics of high molecular weight HA was followed qualitatively in a colorimetric hyaluronidase activity assay and by CZE, the degradation kinetics of $n_3$ and $n_4$ at different substrate concentrations was quantified in the CZE.

## 8.2. Materials and Methods

### *8.2.1. Chemicals*

Hyaluronic acid (HA) from *S. zooepidemicus* was purchased from Aqua Biochem GmbH, Dessau, Germany. Neopermease® was a gift from Sanabo, Vienna, Austria, Hyal-1 and PH-20 were produced by DS-2 cells and purified as described in Chapter 5 and 6. BSA was purchased from Serva, Heidelberg, Germany, cetyltrimethylammonium bromide (CTAB) from Roth, Karlsruhe, Germany, *p*-Dimethylaminobenzaldehyde (DMAB) from Sigma, Munich, Germany. All other chemicals were from Merck, Darmstadt, Germany. Water was purified by a Milli-Q system (Millipore, Eschborn, Germany).

### *8.2.2. Preparation of HA oligosaccharides*

High molecular weight HA was exhaustively digested by BTH (Neopermease®) for 48 h at 37 °C. One mL of BTH (50,000 IE/mL, according to the supplier, dissolved in BSA solution (0.2 mg/mL)) was added to an incubation mixture containing 50 mL of incubation buffer (0.1 M HOAc/NaOAc, 0.1 M NaCl, pH 4.0), 50 mL of HA solution (5 mg/mL), 25 mL of BSA solution (0.2 mg/mL) and 74 mL of water. At the end of the incubation period the solution was boiled for 10 min and centrifuged for 20 min at 5,000 g. The supernatant was lyophilized, and the residual oligosaccharides dissolved in Milli-Q water to gain a concentration of 40 mg/mL. The oligosaccharides were filtered (GH Polypro membrane disc filter, 0.45 µm, Pall Life Sciences, Dreieich, Germany) and separated on a Superdex™ Peptide 10/300 GL (GE-Healthcare Bio-sciences AB, Uppsala, Sweden) at a flow rate of 0.5 mg/mL, using 0.1 M $NH_4OAc$ as mobile phase. The maximum sample volume was 200 µL.

For large-scale preparation of HA oligosaccharides a HiLoad 16/60 Superdex™ 30 prep grade (GE-Healthcare Bio-Sciences AB, Uppsala, Sweden, formerly Pharmacia Biotech) was used at a flow rate of 1 mL/min with a maximum sample volume of 1.5 mL. Both columns were

operated by a Millipore® Waters solvent delivery module, Model 590, connected to a Merck Hitachi L-4000 UV detector. Detection was carried out at 210 nm, and fractions were collected manually. Di- and tetrasaccharides were sufficiently pure after one separation step, while hexa- and octasaccharides had to be purified twice on the Superdex 30 column. Fractions were pooled, lyophilized and dissolved in Milli-Q water. Purity and identity of the fractions was determined by mass spectrometry and capillary zone electrophoresis, respectively. Oligosaccharide solutions were stored at -20 °C.

All buffers used during the preparation process were vacuum-degassed and filtrated through a 0.45 µm filter (Millipore, Eschborn, Germany).

### *8.2.3. ESI-MS*

HA oligosaccharides were analyzed by ESI-MS on a ThermoQuest Finnigan TSQ 7000 spectrometer (Thermo Electron GmbH, Dreieich, Germany). Lyophilized oligosaccharide samples were dissolved in a 1:10 mixture of water and methanol containing 10 mM $NH_4OAc$, and were manually injected into the ion source. Analysis was performed in the negative ion mode with a spray voltage of 3 kV and a capillary temperature of 200 °C.

### *8.2.4. Capillary zone electrophoresis (CZE)*

8.2.4.1. Qualitative analysis of high molecular weight HA degradation products

High molecular weight HA was incubated for different time periods in the following incubation mixtures:

BTH, pH 4.5: 100 µL of BSA solution (0.2 mg/mL), 100 µL of incubation buffer (0.1 M HOAc/NaOAc, 0.1 M NaCl, pH 4.5), 50 µL of HA solution (5 mg/mL), 10 µL of BTH (2,000 IE/mL, according to the supplier). Water was added to reach a total volume of 450 µL.

BTH, pH 5.5: analogous to BTH, pH 4.5, but using 0.1 M HOAc/NaOAc, 0.1 M NaCl, pH 5.5 as incubation buffer and 23 µL of BTH (2,000 IE/mL, according to the supplier).

PH-20, pH 4.5: analogous to BTH, pH 4.5, but using 40 µL of PH-20 instead of BTH (20 IE/mL, as determined by the Morgan-Elson assay at pH 5.0).

PH-20, pH 5.5: analogous to BTH, pH 5.5, but using 40 µL of PH-20 instead of BTH (20 IE/mL, as determined by the Morgan-Elson assay at pH 5.0).

Hyal-1: analogous to BTH, pH 4.5, but using 0.1 M formic acid/Na-formate, pH 3.5 as incubation buffer and 10 µL of Hyal-1 instead of BTH (6,300 IE/mL, as

determined by the Morgan-Elson assay at pH 3.5). Additionally, the mixture was supplemented with 5 µL of NaCl solution (1 M).

After incubation at 37 °C for various time periods the enzymatic reaction was stopped by addition of 900 µL of cold acetonitrile. The samples were dried in the Speed Vac (Savant speed-vac Plus SC110A, Divebid, Cambridge, USA), dissolved in 225 µL of 10-fold diluted CZE operating buffer (cf. 8.2.4.4) and centrifuged for 10 min at 12,000 g. The supernatant was used for CZE analysis.

8.2.4.2. Quantitative analysis of oligosaccharide degradation products

Various concentrations of HA hexasaccharides ($n_3$) and octasaccharides ($n_4$), isolated as described in 8.2.2, were incubated with BTH, Hyal-1 and PH-20. Incubation mixtures containing the following components were used:

BTH, pH 4.0: 44 µg/mL BSA, 22 mM HOAc/NaOAc, pH 4.0, 22 mM NaCl, 61 IE/mL BTH (as determined by the Morgan-Elson reaction at pH 4.0; 100 IE/mL according to the supplier).

BTH, pH 6.0: analogous to BTH, pH 4.0, but using 22 mM HOAc/NaOAc, pH 6.0, and 122 IE/mL BTH (as determined by the Morgan-Elson reaction at pH 4.0; 200 IE/mL according to the supplier).

Hyal-1: analogous to BTH, pH 4.0, but using 22 mM formic acid/Na-formate, pH 3.5, and 100 IE/mL Hyal-1 instead of BTH (as determined by the Morgan-Elson reaction at pH 3.5).

PH-20: analogous to BTH, pH 4.0, but using 60 IE/mL PH-20 instead of BTH (as determined by the Morgan-Elson reaction at pH 4.0).

For calculation of the NaCl concentration in the incubation mixture it was considered that Hyal-1 and PH-20 were both dissolved in 50 mM Na-phosphate, 0.5 M NaCl, 0.1 % Triton X-100, pH 4.5. Hyaluronidase activity was determined directly before the kinetic measurement in the Morgan-Elson assay using incubation mixtures analogous to the CZE mixtures.

For each oligosaccharide concentration an incubation mixture was pre-incubated for 5 min at 37 °C, then the enzyme was added and samples of 25 – 100 µL were taken at defined time points (0 – 60 min). The enzymatic reaction was stopped by mixing the sample with twice the volume of ice-cold acetonitrile. All samples were then dried in the SpeedVac at low drying rate and re-dissolved in 100 µL of 10-fold diluted CZE operating buffer (cf. 8.2.4.4). After centrifugation for 10 min at 12,000 g the supernatant was analyzed by CZE.

8.2.4.3. CZE calibration curves

After determination of the concentration by the Morgan-Elson assay, $n_1$, $n_2$, $n_3$ and, if necessary, $n_4$ were mixed in the respective buffer system, used for the particular kinetic measurement (cf. 8.2.4.2). The calibration mixtures were treated in an identical way as the samples, i.e. they were mixed with twice the volume of acetonitrile, dried in a Speed Vac and solubilized in 10-fold diluted CZE operating buffer (cf. 8.2.4.4).

8.2.4.4. CZE conditions

All CZE experiments were carried out with a Biofocus 3000 capillary electrophoresis system (Biorad, Munich, Germany) equipped with an uncoated fused silica capillary (75 cm x 50 µm, Chrompack). Buffer conditions were adapted from Grimshaw et al. (Grimshaw et al. 1994). The CZE operating buffer contained 50 mM $Na_2HPO_4$, 20 mM $Na_2B_4O_7$, pH 9. Samples were dissolved in 10-fold diluted CZE operating buffer in Milli-Q water. The sample was injected by pressure (20 psi · s), and electrophoresis was performed in the normal polarity mode at a capillary temperature of 15 °C with a run voltage of 15 kV. HA fragments were detected by their absorption at 200 nm. The capillary was washed after each run with 0.1 M NaOH (200 s), Milli-Q water (200 s) and the operating buffer (300 s).

### *8.2.5. Morgan-Elson assay (colorimetric hyaluronidase activity assay)*

The Morgan Elson assay, also termed colorimetric hyaluronidase activity assay (cf. Chapter 3), was used for the quantification of HA oligosaccharides as well as for the detection of time-dependent HA degradation by Hyal-1, PH-20 and BTH.

For quantification of HA oligosaccharides 0.05 – 0.1 µmol of GlcNAc were dissolved in 450 µL of water to obtain a calibration curve. Unknown oligosaccharide concentrations were determined in triplicate.

When HA was enzymatically degraded to completion by BTH, PH-20 or Hyal-1, the incubation mixtures were identical to those used for the investigation of the HA degradation products by CZE (8.2.4). The enzymatic reaction was stopped after different incubation periods by addition of alkaline borate solution (cf. Chapter 3), and the samples were stored at 4 °C until analysis. The detection of reducing GlcNAc ends was performed as described in Chapter 3.

### *8.2.6. Theoretical calculation of HA fragment patterns*

Calculation was performed by a C-program ("bth.c") written by Dr. H.-J. Wittmann, Faculty of Chemistry and Pharmacy, University of Regensburg, Germany. Hydrolysis and transglycosylation were defined for a HA fragment containing n disaccharide units as follows:

| | | | |
|---|---|---|---|
| Hydrolysis: | $n_i \rightarrow n_j + n_k$ | with i = j + k | Eq. 8.1 |
| Transglycosylation: | $n_i + n_j \rightarrow n_k + n_m$ | with i + j = k + m | Eq. 8.2 |

All fragments were assumed to be converted at random, i.e. cleavage was allowed to occur at any site with the same probability, independent of the size of the fragment and the position of the cleavage site within the fragment. Di- ($n_1$) and tetrasaccharides ($n_2$) were excluded from further hydrolysis reactions due to the low binding affinity observed for these fragments with respect to the binding site of BTH (Highsmith et al. 1975). The smallest fragment allowed to be transferred during transglycosylation was one disaccharide unit ($n_1$).

### *8.2.7. Calculation of Michaelis-Menten kinetics*

Initial degradation velocity was obtained by plotting the substrate concentration determined in the CZE against incubation time and fitting the initial part of each degradation curve to a linear equation. For determination of the maximum velocity ($v_{max}$) and the Michaelis-Menten constant ($K_M$) the initial degradation velocity (v) was plotted against the substrate concentration ([S]). Curves were fit to the data points according to the Michaelis-Menten equation (Eq. 8.3.) using SigmaPlot 9.0 (Systat Software Inc., San Jose, USA).

$$v = \frac{v_{max} \cdot [S]}{K_M + [S]} \qquad \text{Eq. 8.3}$$

The turnover-number ($k_{cat}$) was determined by deviding the maximum velocity ($v_{max}$) by the number of enzyme molecules present in the sample.

## 8.3. Results

### *8.3.1. Determination of enzyme kinetics by CZE: optimization of the parameters*

For the quantification of BTH activity McIlvaine's buffer (McIlvaine 1921) was routinely used (Oettl 2000, Hoechstetter 2005). However, for CZE a volatile incubation buffer was necessary to avoid interference with the CZE buffer system. As Gorham et al. reported an inhibitory effect of acetate on the enzymatic activity of BTH (Gorham et al. 1975), hyaluronidase activity was measured in HOAc/NaOAc and formic acid/Na-formate buffer. In

a standard Morgan-Elson assay the volatile buffer systems showed no inhibition of the activity of BTH in comparison to the enzymatic activity in McIlvaine's buffer (**Fig. 8.1.a**).

To assure a fast and complete stop of the enzymatic reaction after a defined period of incubation the addition of acetonitrile to the incubation mixture was investigated as an alternative to boiling, which is often used to stop hyaluronidase reactions (Holmbeck and Lerner 1993, Mahoney et al. 2001, Tawada et al. 2002). Stopping of the enzymatic reaction by addition of acetonitrile was shown to be more efficient than boiling, due to the faster denaturation of the protein by the organic solvent compared to inactivation by heat (**Fig. 8.1.b**).

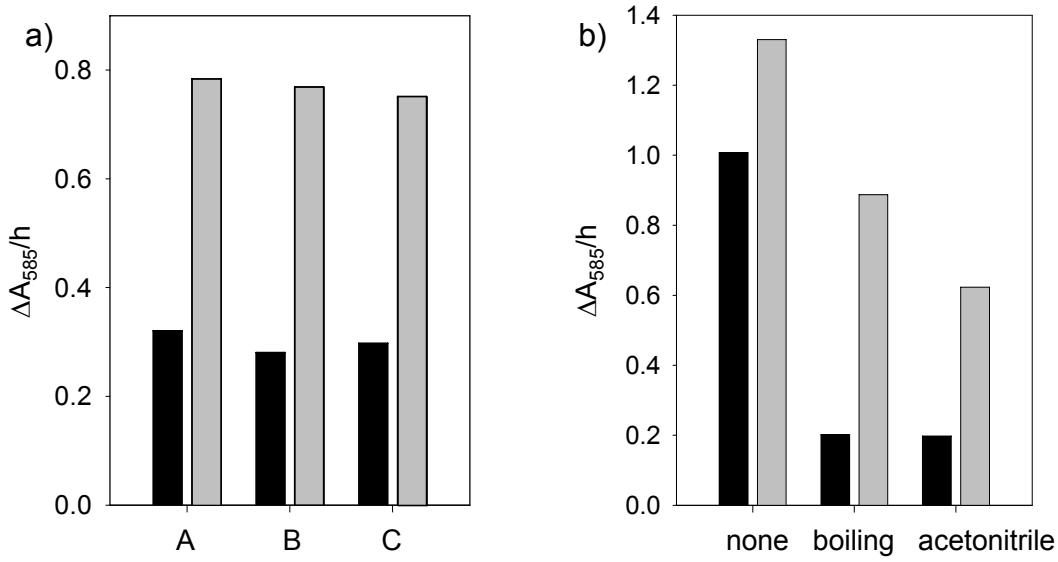


**Fig. 8.1** Choice of a buffer system (a) and evaluation of the denaturing conditions for CZE analysis (b). Morgan-Elson incubation mixtures with 5 IE (black) and 20 IE (grey) of BTH (as declared by the supplier) were incubated for one hour. a) BTH was incubated at pH 4.0 with McIlvaine's buffer (0.2 M $Na_2HPO_4$/0.1 M citric acid) (A), 0.1 M NaOAc/HOAc (B) and 0.1 M Na-formate/formic acid (C). All buffers were supplemented with 0.1 M NaCl. b) Stopping of the reaction was investigated by incubation of BTH with buffer B. The samples were not stopped at all, boiled for 10 min or stopped by addition of twice the sample volume of acetonitrile. Then, the samples were incubated overnight at 37 °C, dried in the SpeedVac, re-dissolved in the original sample volume of water. GlcNAc at the reducing ends was determined by the Morgan-Elson reaction.

### *8.3.2. Degradation of high molecular weight HA*

#### 8.3.2.1. Degradation of high molecular weight HA by BTH at pH 4.5

The formation of GlcNAc residues from high molecular weight HA through the activity of a hyaluronidase is assumed to increase linearly with time, providing the basis for the determination of hyaluronidase activity in the Morgan-Elson assay (colorimetric hyaluronidase activity assay). The increase in absorbance at the absorption maximum (585

nm) of the Morgan-Elson reaction product per time is used for the definition of hyaluronidase activity units (U).

However, the observed increase in absorbance in the Morgan-Elson assay over extended incubation periods revealed a non-linear proportionality for the formation of GlcNAc at the reducing ends during digestion of HA by BTH at pH 4.5 (**Fig. 8.2**).

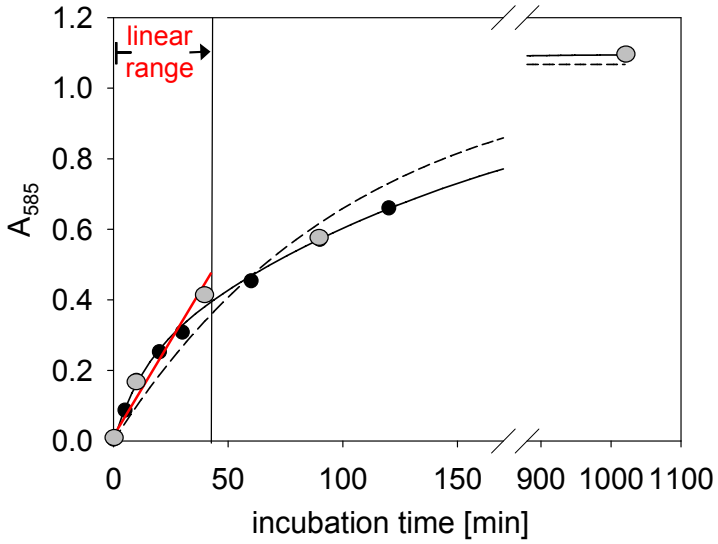


**Fig. 8.2** Formation of GlcNAc residues at the reducing ends during digestion of HA with BTH (44 IE/mL, as declared by the supplier) at pH 4.5 followed over an incubation period of 1,000 min by the Morgan-Elson assay. Data were fit to an exponential equation with 4 parameters ($A_{585}$ = a $(1\text{-}e^{-bt})$+c$(1\text{-}e^{-dt})$). The dashed line shows the fit to a mono-exponential equation ($A_{585}$ = a $(1\text{-}e^{-bt})$), the linear range is used for the determination of hyaluronidase activity. Grey data points were additionally obtained by CZE (**Fig. 8.3**).

Obviously, reducing GlcNAc end groups were liberated with the highest velocity at the beginning of the reaction, i.e. high molecular weight HA was degraded with the highest efficiency. Thus, high molecular weight HA seems to be hydrolyzed faster than lower molecular weight HA with a steady decrease in the cleavage velocity with decreasing chain length. Consequently, the range between 0.1 and 0.4 $A_{585}$ was used for the quantification of enzymatic activities, which can be approximated by a linear equation (**Fig. 8.2**).

The description of the time-dependent formation of GlcNAc end groups by a double-exponential model is consistent with the results obtained by Vincent et al. (Vincent et al. 2003), who speculated about an effect of the HA chain length on the mode of hyaluronidase action.

To gain a more detailed insight into the time-dependent degradation processes, the HA digestion products were analyzed by CZE in parallel with the determination of reducing GlcNAc end groups with the Morgan-Elson reaction. High molecular weight HA forms a single peak in CZE (Grimshaw et al. 1994) due to the low difference in the charge to mass ratio between the polydisperse HA. As shown in **Fig. 8.3** high molecular weight HA ($n_{2500}$ – $n_{5000}$, $1 - 2 \cdot 10^6$ Da, according to the supplier) was degraded at pH 4.5 continuously into smaller fragments of di- ($n_1$) to octasaccharides ($n_4$) accumulating as final products.

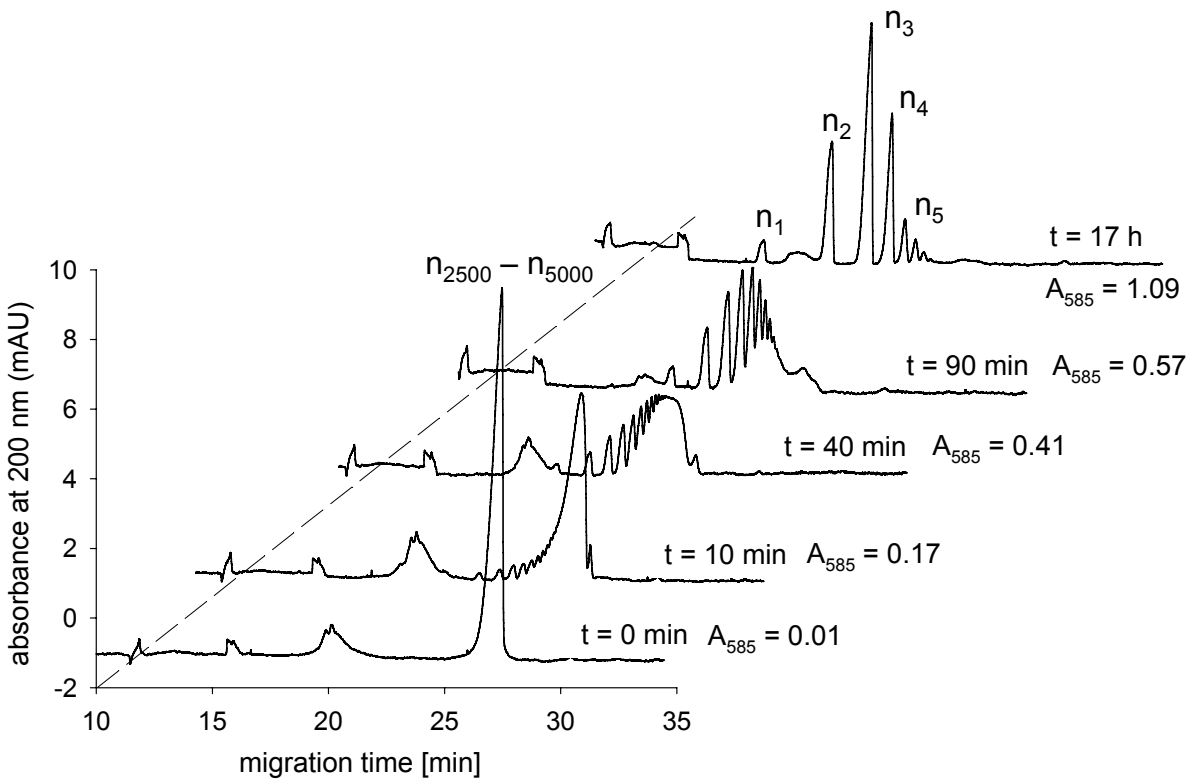


**Fig. 8.3** CZE analysis of different stages of HA digestion by BTH (44 IE/mL, according to the supplier) at pH 4.5. The enzymatic reactions were stopped after 0, 10, 40, 90 min and 17 h by mixing with acetonitrile. Each sample was additionally analyzed by the Morgan-Elson reaction ($A_{585}$) as shown in **Fig. 8.2**. Exhaustive digestion products $n_1$ – $n_5$ were identified by mean differences in migration times (**Tab. 8.2**).

8.3.2.2. Degradation of HA by BTH at pH 5.5

Previous investigations by Hoechstetter (Hoechstetter 2005) indicated a change in the kinetics of HA degradation by BTH dependent on the pH. These observations were mainly based on differences in the pH profiles measured in the turbidimetric and the colorimetric hyaluronidase activity assay (Hoechstetter et al. 2001) and on the detection of HA degradation products by HPLC (Hoechstetter 2005). In the HPLC experiments HA digestion products were separated from the protein by filtration, thus excluding high molecular weight HA (MW > 10 kDa) from the HPLC analysis. The CZE procedure developed for the analysis of HA digestion products enables the analysis of HA digests without separation of reaction products and avoids possible modifications of the HA fragments as observed, e.g. during boiling. Therefore, BTH degradation products formed at pH 5.5 were analyzed by CZE by analogy with the measurements at pH 4.5 described above.

As observed at pH 4.5, the increase in reducing GlcNAc residues during digestion of HA at pH 5.5 showed an exponential rise to a maximum value of ca. 1.2 $A_{585}$ (**Fig. 8.4**). The time-

dependent increase in reducing GlcNAc residues at pH 5.5 could be described by a double-exponential equation as shown in **Fig. 8.2** for the degradation at pH 4.5.

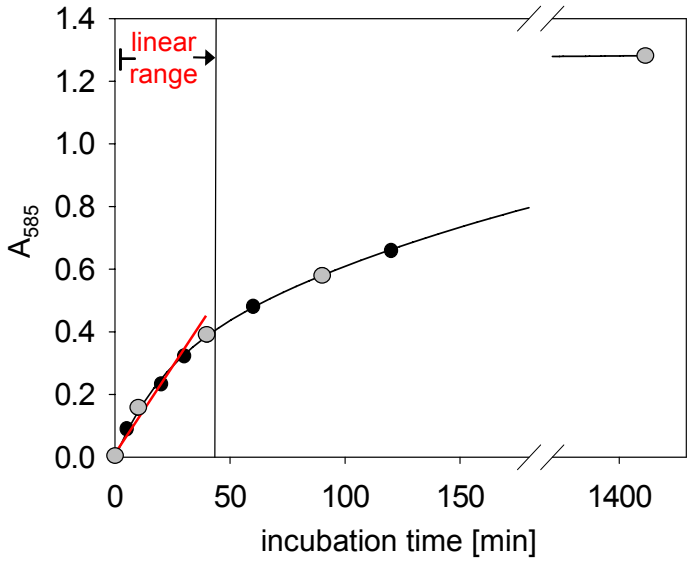


**Fig. 8.4** Formation of GlcNAc residues during digestion of HA with BTH (102 IE/mL, as declared by the supplier) at pH 5.5 followed over an incubation period of 1500 min by the Morgan-Elson assay. Data were fit to an exponential equation with 4 parameters ($A_{585}$ = a $(1\text{-}e^{-bt})$ + c$(1\text{-}e^{-dt})$), the linear range is used for the determination of hyaluronidase activity. Grey data points were additionally analyzed by CZE (**Fig. 8.5**).

However, CZE analysis of the HA fragments produced at pH 5.5 revealed a different size distribution of HA degradation products than observed at pH 4.5: high molecular weight HA was degraded to small oligosaccharides ($n_1$ – $n_4$), but with higher molecular weight fragments remaining in the incubation mixture (marked with an arrow in **Fig. 8.5**). The exact size of the higher molecular weight HA fragments could not be determined since no separation of the fragments was achieved at these charge to mass ratios. A very small fraction of the higher molecular weight HA fragments could also be observed during degradation of HA by BTH at pH 4.5 (**Fig. 8.3**).

It should be noted that the peaks of the HA degradation products, especially of the HA oligosaccharides, at pH 5.5, were broadened compared to the digestion products at pH 4.5. Hoechstetter (Hoechstetter 2005) previously observed the formation of odd-numbered HA oligosaccharides at pH 5.0 – 6.0 carrying GlcUAc at both ends. Due to the different separation principles of CZE and HPLC HA fragments, carrying the same charge, but a slightly reduced molecular mass, might result in a broadening of peaks in CZE, while anion exchange HPLC was capable of separating even- and odd-numbered HA fragments.

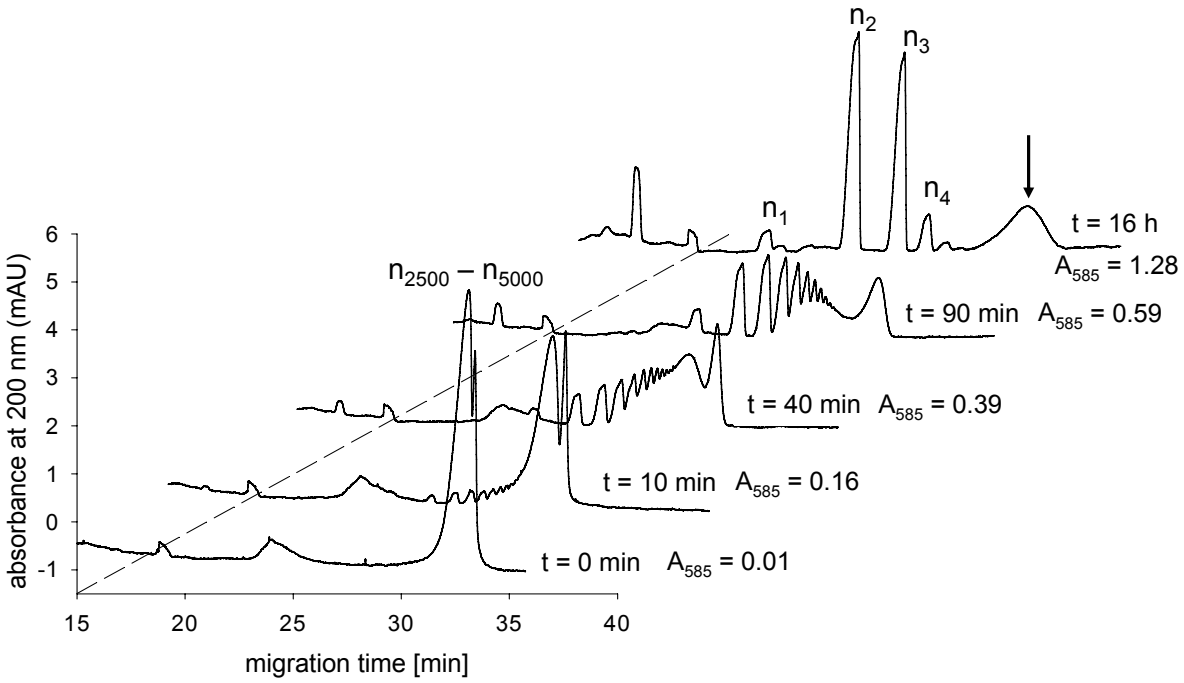


**Fig. 8.5** CZE analysis at different stages of HA digestion by BTH (102 IE/mL, according to the supplier) at pH 5.5. Enzymatic reactions were stopped after 0, 10, 40, 90 min and 16 h by mixing with acetonitrile. Each sample was additionally analyzed with the Morgan-Elson assay ($A_{585}$) as shown in **Fig. 8.4**. Exhaustive digestion products $n_1 – n_4$ were identified by mean differences in migration times (**Tab. 8.2**).

8.3.2.3. Degradation of HA by recombinant, human PH-20

Partially purified human PH-20 expressed in DS-2 cells exhibited a shift in the pH-dependent activity in the colorimetric and turbidimetric assay similar to BTH. Maximum enzymatic activity was found at pH 4.5 in the colorimetric assay and at pH 5.5 in the turbidimetric assay (cf. Chapter 6).

Due to instability problems during storage the enzymatic activity of PH-20 available for the CZE experiments was significantly lower than the activity used for the degradation of HA by BTH and Hyal-1. The low activity was compensated by extended incubation periods in order to gain similar amounts of reducing GlcNAc groups for each of the time points analyzed with CZE (**Fig. 8.6**). The formation of reducing GlcNAc residues by PH-20 exhibited a similar time-dependent curve as observed for BTH (**Fig. 8.2** and **Fig. 8.4**) with a continuous decrease in the velocity of the liberation of reducing GlcNAc ends (data not shown).

The reaction products formed at both pH optima were analyzed by CZE after varying periods of incubation. As shown in **Fig. 8.6** the degradation products formed at pH 4.5 and at pH 5.5 were nearly identical. The formation of small oligosaccharides in the presence of higher molecular weight HA fragments, as observed with BTH at pH 5.5 (**Fig. 8.5**), was detected at both pH values, but with a significantly smaller fraction of higher molecular weight HA

fragments remaining in the mixture than observed with BTH at pH 5.5 (indicated by arrows in **Fig. 8.6**). The fraction of residual high molecular weight HA seemed to be only slightly increased at pH 4.5 compared to pH 4.5.

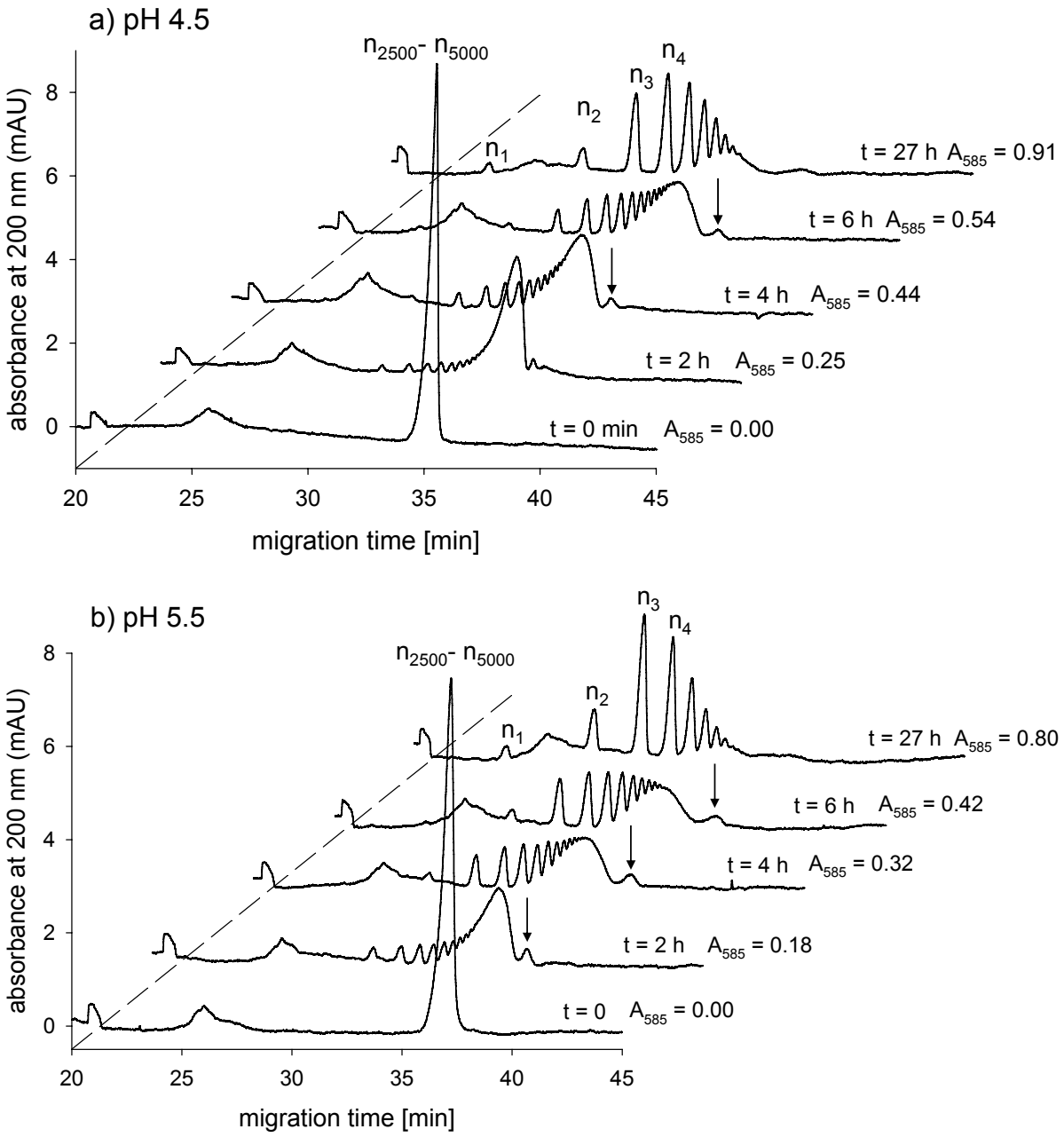


**Fig. 8.6** CZE analysis at different stages of HA digestion by recombinant, human PH-20 (2 IE/mL, as determined by the Morgan-Elson assay at pH 4.5) at pH 4.5 (a) and pH 5.5 (b). Enzyme reactions were stopped after 0, 2, 4, 6 and 27 h by mixing with acetonitrile. Each sample was additionally analyzed in the Morgan-Elson reaction ($A_{585}$). Digestion products $n_1$ – $n_4$ were identified by the mean differences in migration times (**Tab. 8.2**).

However, the enzymatic activity of PH-20 was insufficient to follow the degradation process to completion, i.e. the reaction products observed after 27 h represent not the final oligosaccharides. Nevertheless, the smallest oligosaccharides produced by human PH-20 at both pH values, pH 4.5 and 5.5, were identified as HA disaccharides ($n_1$) and tetrasaccharides

($n_2$). A significant broadening of the peak shape at pH 5.5, as seen with BTH, was not observed. Thus, the formation of odd-numbered oligosaccharides described for BTH around neutral pH might be a phenomenon specific for BTH.

8.3.2.4. Degradation of HA by recombinant human Hyal-1

As described above for BTH and PH-20, the degradation process of high molecular weight HA through the action of Hyal-1 was followed in parallel with the Morgan-Elson assay (**Fig. 8.7**) and by means of CZE (**Fig. 8.8**).

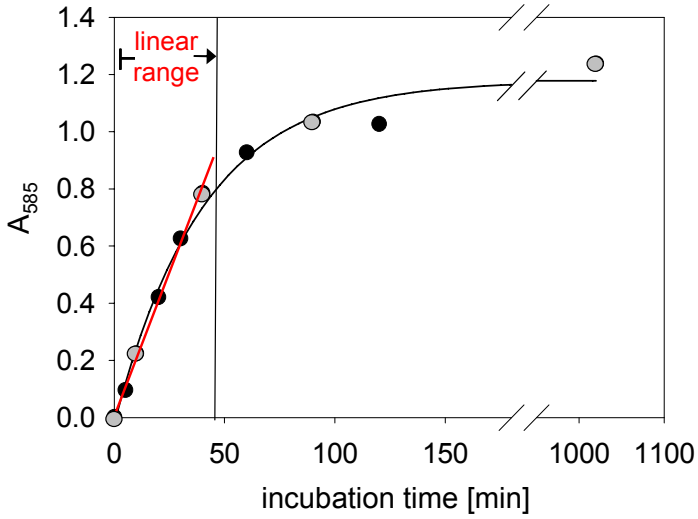


**Fig. 8.7** Formation of reducing GlcNAc residues during digestion of HA with Hyal-1 (35 IE/mL) at pH 3.5 followed over an incubation period of 1,100 min by the Morgan-Elson assay. Data were fit to a mono-exponential equation with 2 parameters ($A_{585}$ = a (1 - $e^{-bt}$)). The linear range was used for the determination of hyaluronidase activity. Grey data points were additionally analyzed by CZE (**Fig. 8.8**).

In contrast to BTH and PH-20, the formation of reducing GlcNAc end groups caused by the action of Hyal-1 exhibited a mono-exponential time-dependency (**Fig. 8.7**). The initial part of the curve showed an extended linear range (0.1 – 0.8 $A_{585}$) suitable for the determination of Hyal-1 activity. Intriguingly, the degradation kinetics of BTH (**Fig.8.2**, **Fig.8.4**) could only be described sufficiently by a double-exponential equation.

The time-dependent formation of GlcNAc end groups through the action of a hyaluronidase following a mono-exponential process can be explained by the following model proposed by Vincent et al. (Vincent et al. 2003):

The degradation of HA chains can be considered as a reaction with each possible cleavage site …- GlcNAc - GlcUAc -… present in the incubation mixture being a substrate moiety:

$$\ldots - GlcNAc - GlcUAc - \ldots \xrightarrow{k_1} \ldots - GlcNAc + GlcUAc - \ldots \qquad \text{Eq. 8.4}$$

The time-dependent degradation of n cleavage sites can thus be assumed as a first-order reaction. The concentration of n cleavage sites at any time t is given by the following equation:

$$[n] = [n_0] \cdot e^{-k_1 t} \qquad \text{Eq. 8.5}$$

Thus, the formation of reducing GlcNAc end groups (…-GlcNAc) measured with the Morgan-Elson reaction via the absorbance at 585 nm is described by a function of exponential growth to a maximum value $A_0$:

$$[...-GlcNAc] = A_0(1-e^{-k_1 t}) \qquad \text{Eq. 8.6}$$

The existence of a single velocity constant $k_1$ for the degradation process thus indicates a constant catalytic activity of Hyal-1 towards all HA fragments, independent of the chain length. CZE analysis of the degradation products confirmed this assumption as a continuous decrease in the molecular weight of the HA chains (**Fig. 8.8**). As final reaction products tetra- ($n_2$), hexa- ($n_3$) and octasaccharides ($n_4$) with traces of disaccharide ($n_1$) accumulated.

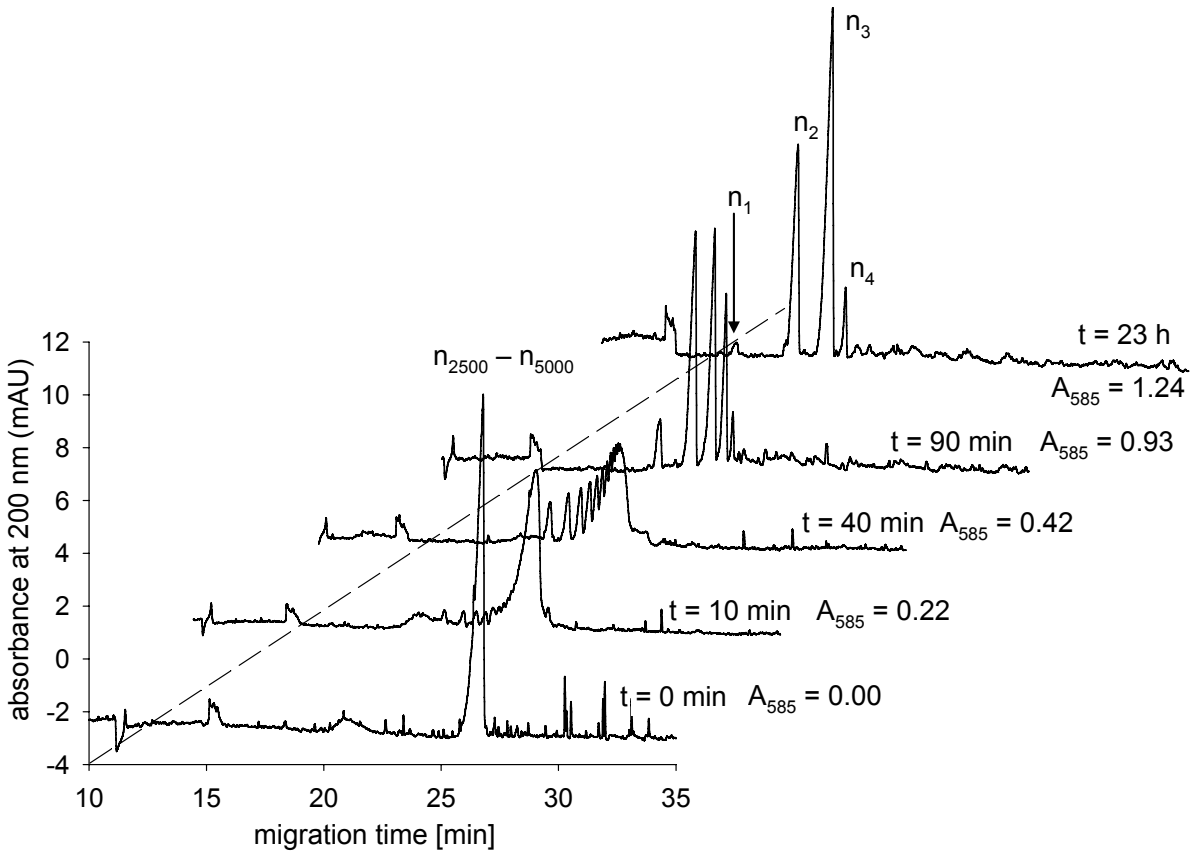


**Fig. 8.8** CZE analysis of different stages of HA digestion by Hyal-1 (35 IE/mL, as determined in the Morgan-Elson reaction at pH 3.5) at pH 3.5. Enzymatic reactions were stopped after 0, 10, 20, 60 min and 23 h by mixing with acetonitrile. Each sample was additionally analyzed in the Morgan-Elson reaction as shown in **Fig. 8.7**. Exhaustive digestion products $n_1$ – $n_4$ were identified by the mean differences in migration times (**Tab. 8.2**).

### 8.3.2.5. Theoretical calculation of the size distribution of HA fragment produced by hydrolysis and transglycosylation

The existence of both, high and low molecular weight HA fragments after digestion of HA by BTH and PH-20, gave rise to the idea that this unusual distribution of HA fragments might be

a result of the transglycosylation activity of these enzymes. Therefore, the distribution of HA fragment sizes was calculated, allowing hydrolysis as well as transglycosylation reactions.
In order to keep the calculation time within a reasonable limit, the HA chain length had to be chosen far below the actual size of high molecular weight HA. Additionally, the number of degradation steps accessible by calculation was limited, especially when considering transglycosylation reactions.
The absorbance at 200 nm can be estimated to be directly proportional to the number of disaccharide units n of a HA fragment. Therefore, a comparison of the calculated relative concentrations to the fragment patterns observed in the CZE was enabled by multiplying the relative concentration of the oligosaccharide fragments by the chain length (n):

$$\text{relative absorbance} = \text{relative concentration} \cdot n \qquad \text{Eq. 8.7}$$

After 5 cleavage steps of a HA chain comprising 20 disaccharide units the relative concentration of fragments produced by hydrolysis only, decreased steadily with increasing chain length (**Fig. 8.9.a**). Di- ($n_1$) and tetrasaccharides ($n_2$) were excluded from further reactions and accumulated as the major products. The highest relative absorbance was observed for the tetrasaccharide ($n_2$). When the calculation was continued, the concentration of longer HA chains decreased further with an accumulation of $n_1$ and $n_2$.

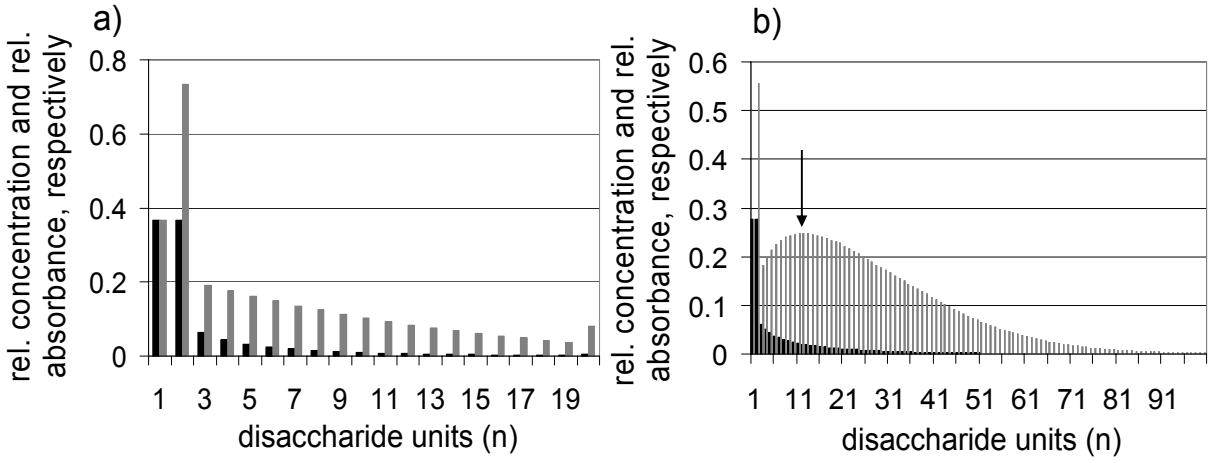


**Fig. 8.9** Calculation of the relative occurrence of HA fragments (black) and the relative absorbances (grey) after 5 conversion steps. The initial HA chain contained 20 disaccharide units with a relative concentration of 1. The following reaction probabilities (P) were chosen for the calculation: a) P(hydrolysis) = 0.6, P(transglycosylation) = 0. b) P(hydrolysis) = 0.3, P(transglycosylation) = 0.3.

In a second approach hydrolysis and transglycosylation reactions were allowed to occur with equal probabilities (**Fig. 8.9.b**). When transglycosylation was allowed to occur at random with fragments of every size, HA fragments of both, higher and lower molecular weight compared to the initial HA fragment, were formed. Thus, a fragment pattern containing much longer HA

fragments than the initial chain length ($n_{20}$) was observed. After 5 steps of conversion the pattern of the relative concentrations of fragments was similar to the one observed after mere hydrolysis, with $n_1$ and $n_2$ accumulating as the final products. However, the relative absorbances revealed the occurrence of a fraction of fragments in the range between $n_{10}$ and $n_{15}$ with an increased relative absorbance compared to shorter HA fragments (marked with an arrow in **Fig. 8.9.b**). Additionally, $n_1$ and $n_2$ accumulated as the major reaction products, exhibiting also the highest relative absorbance values.

Although the calculation was restricted to very few elementary parameters and the initial chain length did not approximate the real situation, the fragment patterns calculated were comparable to the situation experimentally observed during degradation of high molecular weight HA by the action of hyaluronidases.

When only hydrolysis was allowed in the calculation, the fragment pattern resembled roughly the situation observed during degradation of HA by BTH at pH 4.0 and by Hyal-1. The accumulation of hexasaccharides ($n_3$) in addition to tetrasaccharides ($n_2$) as the main fragments in the CZE analysis might indicate that the hexasaccharide ($n_3$) might be a worse substrate than the higher molecular weight HA fragments. Changes in the affinity of very low molecular weight HA chains towards the binding site were not considered in the calculations except for the di- ($n_1$) and tetrasaccharide ($n_2$), but probably contribute to the fragment pattern observed in the real degradation reactions (Highsmith et al. 1975).

The fragment pattern, observed when transglycosylation and hydrolysis were allowed to occur with equal probabilities, showed the characteristic bulk of higher molecular weight HA fragments remaining in the reaction mixture in addition to the low molecular weight oligosaccharides. A similar fragment pattern, but with much larger overall fragment sizes, was observed during degradation of HA by BTH at nearly neutral pH and by PH-20 (**Fig. 8.5** and **Fig. 8.6**).

Although only very few restrictions were introduced in the calculation, the allowance of transglycosylation and hydrolysis reactions could provide a fragment pattern approximating the situation observed in the CZE.

### *8.3.3. Preparation and quantification of HA oligosaccharides*

8.3.3.1. Separation of HA oligosaccharides by size exclusion chromatography (SEC)

After exhaustive digestion at acid pH, high molecular weight HA is degraded by BTH to even-numbered oligosaccharides with tetra- ($n_2$) and hexasaccharides ($n_3$) forming the main reaction products (Hoechstetter 2005). A volatile incubation buffer system ($NH_4OAc$) was chosen to allow for the lyophilization and concentration of the degradation products after digestion.

**Fig. 8.10** shows the elution profile of an exhaustive HA digest separated by size exclusion chromatography (SEC) on a SuperdexPeptide 10/300 GL. The HA fragments were detected at 210 nm due to the lack of a chromophore absorbing at higher wavelength. Detection at this wavelength resulted in a high absorbance of the buffer leading to a low sensitivity in detection.

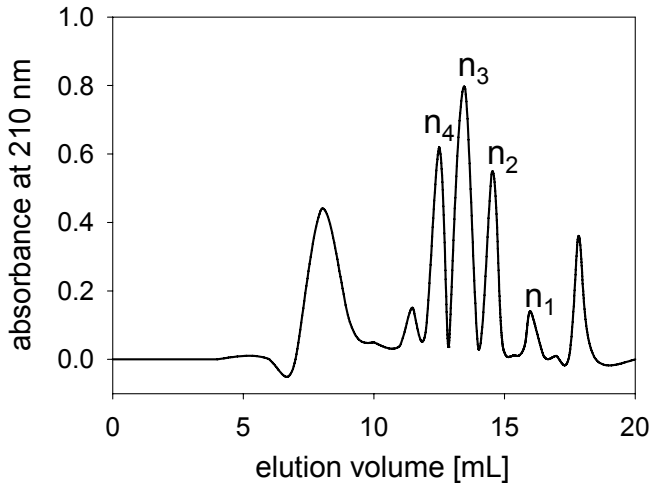


**Fig. 8.10** Elution profile of HA digestion products separated by SEC (Superdex Peptide 10/300 GL). 150 µL of HA digested by BTH for 48 h were applied to the column in a concentration of 30 mg/mL. Separation was performed at 0.5 mL/min in 0.1 M $NH_4OAc$ and monitored by detection of the absorbance at 210 nm. The oligosaccharide peaks were identified by ESI-MS.

HA fragments were exclusively separated by their size, i.e. large fragments were eluted first, followed by oligosaccharides of decreasing size. Since the relative differences in molecular weight increase with decreasing size of the HA fragments, the separation improved with decreasing chain length. Fractions containing di- ($n_1$) to octasaccharides ($n_4$) contained pure oligosaccharides as determined by ESI-MS and CZE (8.3.3.2).

Higher quantities of HA oligosaccharides were separated on a Superdex 30 column with a sample volume of up to 1.5 mL, but the separation of the HA oligosaccharides deteriorated (**Fig. 8.11**). Peaks containing hexa- ($n_3$) and octasaccharide ($n_4$) were not sufficiently pure after the first separation and were therefore pooled, concentrated by lyophilization and separated in a second run on the same column.

Comparison of the mass of the oligosaccharides to the mass of high molecular weight HA used for digestion revealed a yield of < 4 % for $n_1$, 8 % for $n_2$, 44 % for $n_3$ and 12 % for $n_4$.

The overall yield in pure HA oligosaccharides was ca. 68 % of the digested high molecular weight HA. Deficits resulted mainly from intermediate fractions containing mixtures of oligosaccharides, which were not collected. Additionally, higher molecular weight fragments were still present in the incubation mixture, but were not collected.

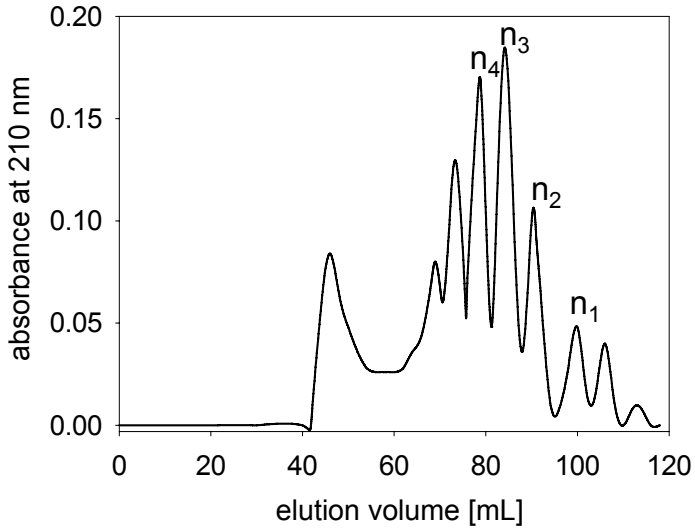


**Fig. 8.11** Elution profile of HA digestion products separated by SEC (Superdex 30). 1.5 mL of HA digested by BTH for 48 h were applied to the column in a concentration of 40 mg/mL. Separation was performed at 1.0 mL/min in 0.1 M $NH_4OAc$ monitored by detection of the absorbance at 210 nm. The oligosaccharides were identified by ESI-MS.

However, when the concentration of the oligosaccharides was determined by the Morgan-Elson reaction (**Fig. 8.12**), it turned out that the yield calculated using the molecular masses depicted in **Tab. 8.1** was much lower than the one calculated from the mass after lyophilization. For $n_1$ a yield of 2 % was determined, for $n_2$ 4 % and for $n_3$ 8 %.

Probably, this discrepancy between oligosaccharide masses determined by direct and indirect measurement via the Morgan-Elson assay was a result of the strong hygroscopicity of HA. While water molecules associated to HA as well as to oligosaccharides were implied during direct weighing, those were not determined by the Morgan-Elson reaction resulting in these extreme discrepancies.

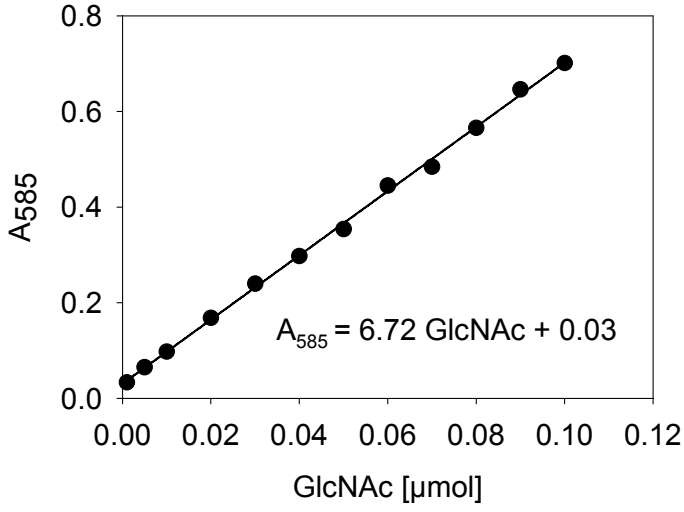


**Fig. 8.12.** Calibration curve for the quantification of HA oligosaccharides by the Morgan-Elson assay. GlcNAc diluted in water was quantified by the absorbance of the Morgan-Elson product at 585 nm. Water was used as a reference.

8.3.3.2. Analysis of HA oligosaccharides by ESI-MS and CZE

After separation by SEC the components of the lyophilized fractions were identified by ESI-MS. In **Tab. 8.1** the molecular masses of the monoisotopic oligosaccharides are given.
The purity of oligosaccharides identified by ESI-MS was confirmed by CZE. As the elution times in the CZE vary from one experiment to another, an identification of SEC fractions by CZE was impossible. However, during separation of HA digestion mixtures (cf. 8.3.2) $n_1$, $n_2$, $n_3$ and $n_4$ were identified by mean differences between the migration times of specific HA oligosaccharides (**Tab. 8.2**).

**Tab. 8.1.** Calculated molecular masses of the monoisotopic oligosaccharides.

| HA oligosaccharide | Molecular formula | Molecular mass (Da) |
|---|---|---|
| disaccharide ($n_1$) | $C_{14}H_{23}NO_{12}$ | 397.33 |
| tetrasaccharide ($n_2$) | $C_{26}H_{44}N_2O_{23}$ | 776.23 |
| hexasaccharide ($n_3$) | $C_{42}H_{65}N_3O_{34}$ | 1155.34 |
| octasaccharide ($n_4$) | $C_{56}H_{86}N_4O_{45}$ | 1534.46 |

**Tab. 8.2** Mean differences in the migration times of HA oligosaccharides in the electropherograms. Distances were calculated from 14 independent experiments using mixtures of pure di- ($n_1$), tetra- ($n_2$), hexa- ($n_3$) and octasaccharides ($n_4$). STD indicates the standard deviations.

| Oligosaccharides | Mean difference ± STD |
|---|---|
| $n_1 - n_2$ | 3.01 ± 0.40 min |
| $n_2 - n_3$ | 1.82 ± 0.25 min |
| $n_3 - n_4$ | 0.87 ± 0.24 min |

Although the standard deviations (STD) of the mean differences were high (up to 27 %) an unambiguous identification of $n_1 - n_4$ was possible for fragments occurring in combination with the neighboring HA fragments.

8.3.3.3. Quantitative analysis of di-, tetra- and hexasaccharides by CZE

The concentration of pure HA oligosaccharides was quantified by the amount of reducing GlcNAc ends by the Morgan-Elson assay and the molecular mass of the respective compound. In the CZE the area/time (A/t) ratio of $n_1$, $n_2$ and $n_3$ correlated linearly to the

concentration of the respective oligosaccharide in a concentration range between 25 µM and ca. 2.0 mM (**Fig. 8.13**).

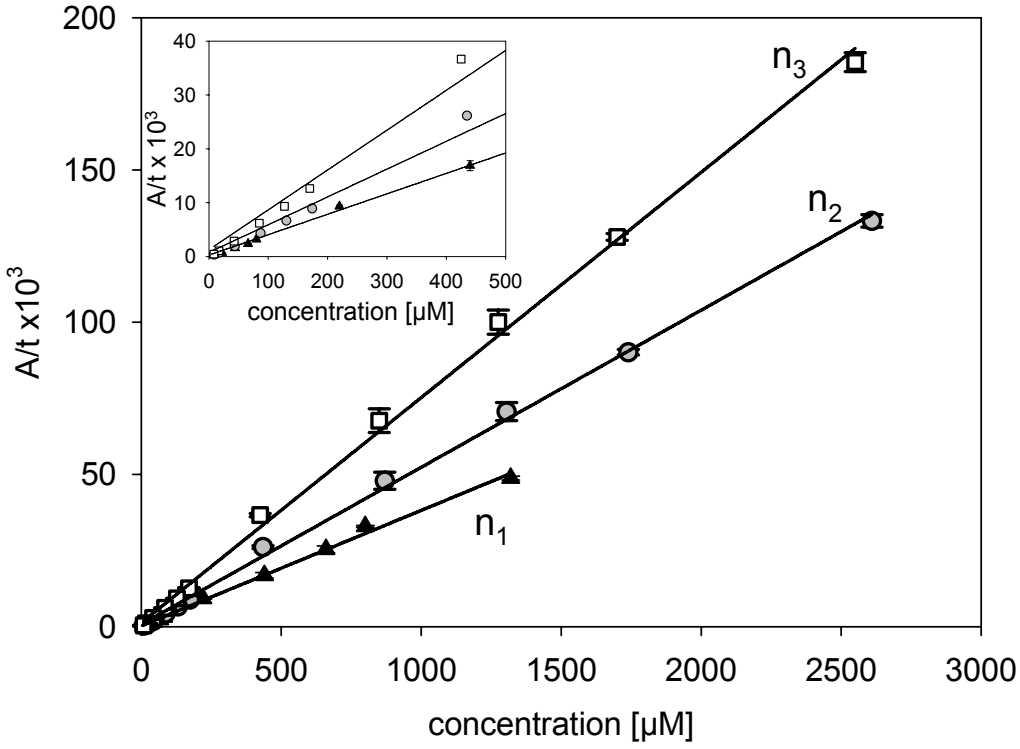


**Fig. 8.13** Calibration curve of di- ($n_1$) (black triangles), tetra- ($n_2$) (grey circles) and hexasaccharides ($n_3$) (open squares) measured by CZE. A/t values are mean values ± SEMs (standard error of means) of 3 injections. The inset shows a magnified view of the concentration range 0 – 500 µM.

Peaks at concentrations > 2 mM showed flattened peak tops, thus concentrations above 2.0 mM were not used for the quantitative analysis. Triple injection of the same sample confirmed a constant sample volume injected automatically by pressure (SEMs ≤ 5 %) (**Fig. 8.13**). Therefore, variations of the injection volume were neglected in the following experiments and all samples were injected only once.

### *8.3.4. Time-dependent degradation of hyaluronan oligosaccharides*

8.3.4.1. Time-dependent degradation of $n_3$ by BTH at pH 4.0

To investigate, if the pH influences BTH with respect to its degradation kinetics as well as its mechanism of HA degradation HA hexasaccharide ($n_3$) was used as a substrate at pH 4.0 and pH 6.0. The conversion of the HA hexasaccharide ($n_3$), the well-known minimum substrate of BTH (Cramer et al. 1994), was monitored over a concentration range (25 µM – 2 mM) to gain information about the catalytic behavior of the hyaluronidase under Michaelis-Menten conditions.

CZE analysis of the conversion of $n_3$ revealed the formation of $n_2$ as the major reaction product, while all other products, $n_1$, $n_4$, $n_5$ and $n_6$, occurred at very low concentrations. Especially, the formation of the transglycosylation products, $n_4$ and $n_5$, was extremely low. **Fig. 8.14** shows as an example the electropherograms after the conversion of 100 µM $n_3$ into $n_1$, $n_2$ and $n_4$ through the action of BTH at pH 4.0.

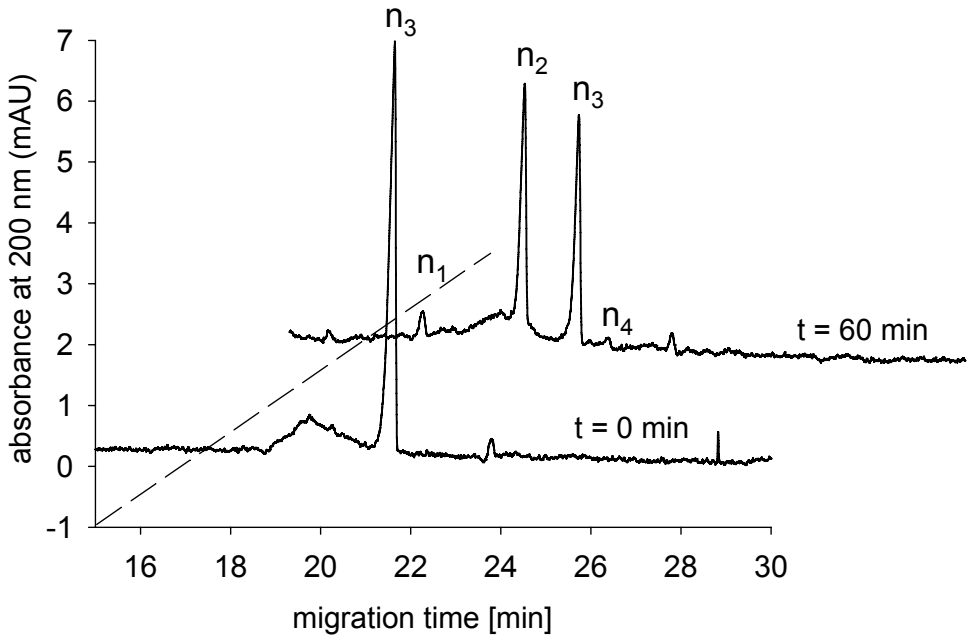


**Fig. 8.14** CZE analysis of the degradation of 100 µM HA hexasaccharide ($n_3$) by BTH (100 IE/mL according to the supplier; 60 IE/mL measured in the Morgan-Elson assay at pH 4.0) at pH 4.0. Samples were incubated for 0 and 60 min, respectively.

Considering $n_5$ as the largest reaction product and omitting hydrolysis reactions of HA fragments larger than $n_3$, the following reactions can be assumed to occur at the initial stage of $n_3$ degradation at pH 4.0:

Hydrolysis: $n_3 \rightarrow n_1 + n_2$ Eq. 8.8

Transglycosylation: $2\ n_3 \rightarrow n_2 + n_4$ Eq. 8.9

$n_4 + n_3 \rightarrow n_2 + n_5$ Eq. 8.10

Previous data (Highsmith et al. 1975) indicate that $n_1$ and $n_2$ are too small to bind to the active site. Removal of $n_1$ was not allowed with the exception of Eq. 8.8, which obviously occurred due to the high concentrations of $n_3$ present in the reaction mixture (**Fig. 8.14**).

Intriguingly, the degradation of $n_3$ slowed down at concentrations > 300 µM and came to a complete halt at concentrations > 500 µM, indicating substrate inhibition of the enzyme at higher concentrations (**Fig. 8.15**). It should be noted that $n_3$ is under physiological conditions the degradation product of high molecular weight HA rather than the substrate. Thus, the inhibition can be described as both, substrate and product inhibition.

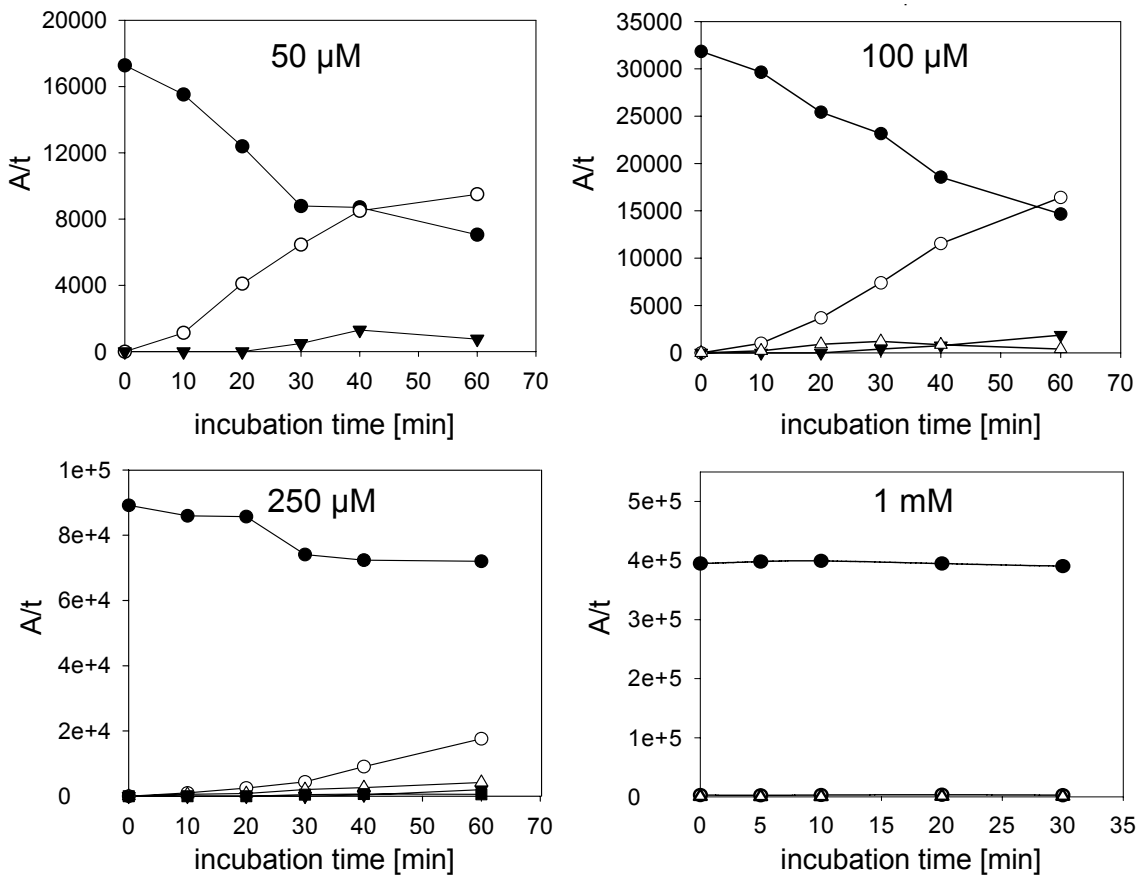


**Fig. 8.15** Time-dependent degradation of different concentrations of $n_3$ followed by the area/time (A/t) ratio of the oligosaccharide in the CZE with $n_1$ represented as filled triangles, $n_2$ as open circles, $n_3$ as filled circles, $n_4$ as open triangles and $n_5$ as filled squares. Digestions were performed by BTH (100 IE/mL according to the supplier; 60 IE/mL as determined by the Morgan-Elson reaction at pH 4.0) at pH 4.0.

Octa- ($n_4$) and decasaccharides ($n_5$) produced by transglycosylation at the initial stage of the reaction were observed to be degraded preferentially in the course of the incubation time even in the presence of a great excess of hexasaccharide ($n_3$) (e.g. 100 µM in **Fig. 8.15**).

The initial linear part of the degradation curve of the hexasaccharide at various concentrations enabled the calculation of initial degradation velocities in dependence on the substrate concentration. The calculation of characteristic enzymatic constants based on the observation of the time-dependent degradation of HA hexa- ($n_3$) and octasaccharides ($n_4$) is summarized in 8.3.4.5.

### 8.3.4.2. Time-dependent degradation of $n_3$ by BTH at pH 6.0

Experiments with high molecular weight HA had shown a difference in the degradation mode of BTH at acidic and neutral pH (cf. 8.3.2). Therefore, the degradation of $n_3$ at pH 6.0 was monitored by analogy with the CZE experiments performed at pH 4.0 (cf. 8.3.4), and the decrease in the concentration of $n_3$ could be quantified by means of a CZE calibration curve.

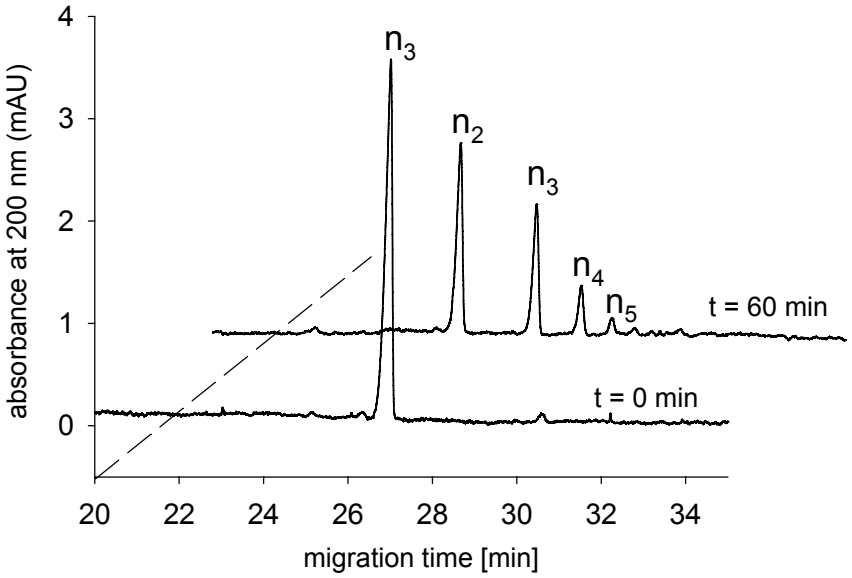


**Fig. 8.16** CZE analysis of the degradation of 100 µM HA hexasaccharide ($n_3$) by BTH (200 IE/mL, as declared by the supplier; 60 IE/mL measured in the Morgan-Elson assay at pH 6.0) at pH 6.0. Samples were incubated for 0 and 60 min, respectively.

The degradation of $n_3$ at pH 6.0 showed a preferential formation of oligosaccharides of higher molecular weight ($n_4$ and $n_5$). Intriguingly, no $n_1$ was produced during the degradation of $n_3$ at pH 6.0 (exemplarily shown for 100 µM $n_3$ in **Fig. 8.16**).

Considering the reactions involved in the degradation process of $n_3$ shown in Eq. 8.8 – Eq. 8.10, the hydrolysis of $n_3$ into $n_1$ and $n_2$ (Eq. 8.8) can therefore be excluded from the processes occurring at pH 6.0. The decrease in $n_3$ at the initial stage of the reaction was thus exclusively caused by the transglycosylation activity of BTH, which is known to occur preferentially at higher pH values (Gorham et al. 1975).

At pH 6.0 an increase in the initial degradation velocity of $n_3$ was observed up to concentrations of ca. 800 µM, then the velocity of degradation decreased fast and at concentrations > 1 mM no conversion of the substrate was observed any more (**Fig. 8.21**). These results are consistent with the substrate/product inhibition observed at pH 4.0. However, at pH 4.0 the inhibition occurred at lower substrate concentrations (> 200 µM). The apparent $K_M$ and $v_{max}$ values of the degradation of $n_3$ by BTH at pH 6.0 were calculated for the low concentration range from the initial velocities of $n_3$ degradation (cf. 8.3.4.5).

8.3.4.3. Time-dependent degradation of $n_3$ and $n_4$ by Hyal-1

Recombinant human Hyal-1 produced by DS-2 cells was incubated with $n_3$ as a substrate at pH 3.5, the optimum pH of Hyal-1 activity (cf. Chapter 5). Surprisingly, the incubation mixtures analyzed after different periods of incubation by CZE revealed no conversion of the HA hexasaccharide (**Fig. 8.17**). Although a wide range of $n_3$ concentrations (20 µM – 6 mM)

similar to those assayed for the digestion with BTH was analyzed, Hyal-1 exhibited no catalytic activity against $n_3$ (**Fig. 8.17.b**).

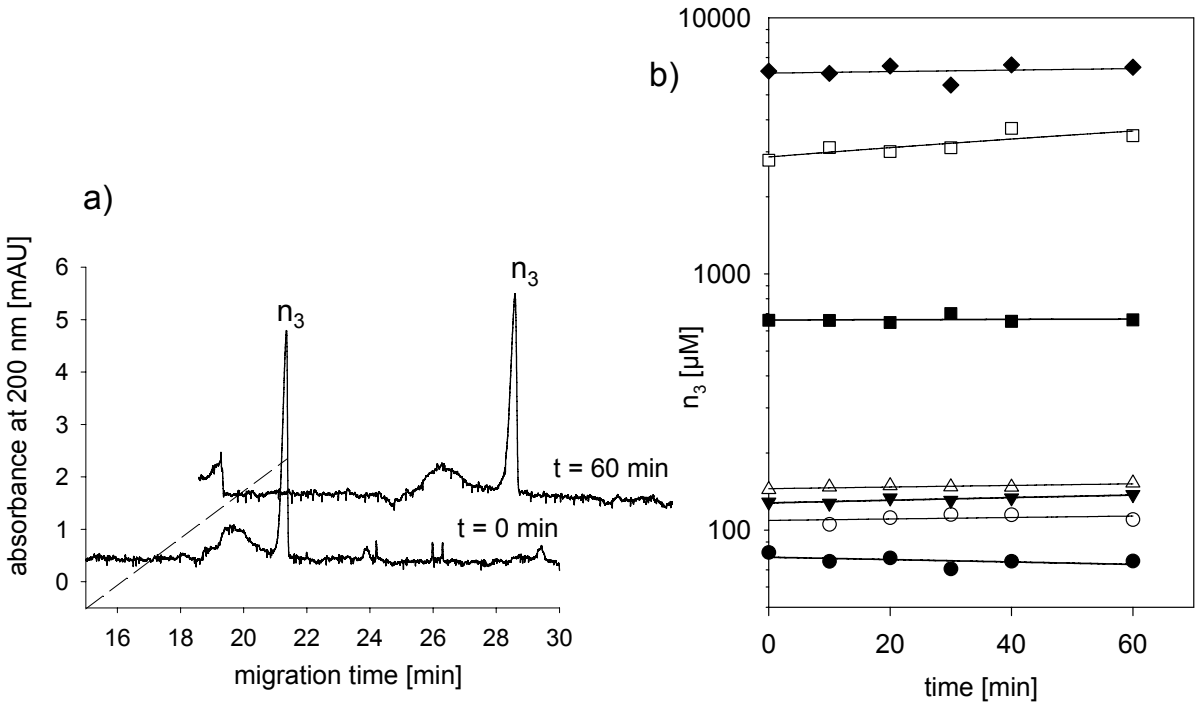


**Fig. 8.17** a) CZE analysis of the incubation of 100 µM HA hexasaccharide ($n_3$) with Hyal-1 (100 IE/mL measured in the Morgan-Elson assay at pH 3.5) at pH 3.5. Samples were incubated for 0 and 60 min, respectively. b) Time-dependent curves of increasing concentrations of $n_3$ incubated with 100 IE/mL Hyal-1 at pH 3.5. $n_3$ concentrations were calculated from CZE peaks by means of a calibration curve.

Thus, the active site of Hyal-1 seems to differ from BTH with respect to the catalytic activity towards small oligosaccharides. The inability of Hyal-1 to degrade $n_3$ indicates either a very low affinity for HA fragments of three disaccharide units or a low catalytic activity towards bound $n_3$. However, two facts hint to a low affinity of $n_3$ towards the binding site: first, BTH is known to exhibit lower affinity towards $n_3$ than $n_4$, suggesting the existence of a site S3' being relevant for binding (Highsmith et al. 1975). Possibly, the importance of this site in the binding pocket of Hyal-1 is even more distinctive. A second hint can be drawn from the observation, that $n_3$ inhibited the degradation of high molecular weight HA by Hyal-1 very weakly (30 % inhibition at 3 mM) (personal communication by M. Spickenreither).

In a second approach various concentrations of HA octasaccharide ($n_4$) were used as substrate of Hyal-1 at pH 3.5. In contrast to the hexasaccharide ($n_3$), the octasaccharide ($n_4$) was converted quickly at substrate concentration between 25 µM and 1 mM. At concentrations higher than 1 mM weak substrate inhibition was observed (**Fig. 8.21.a**). Furthermore, the reaction products formed, varied significantly, depending on the substrate concentration. At

low $n_4$ concentrations (< 500 µM) no transglycosylation products were observed, while at higher $n_4$ concentrations (> 500 µM) fragments larger than the substrate were observed and the disaccharide ($n_1$) occurred at concentrations close to the detection limit of the CZE (**Fig. 8.18**).

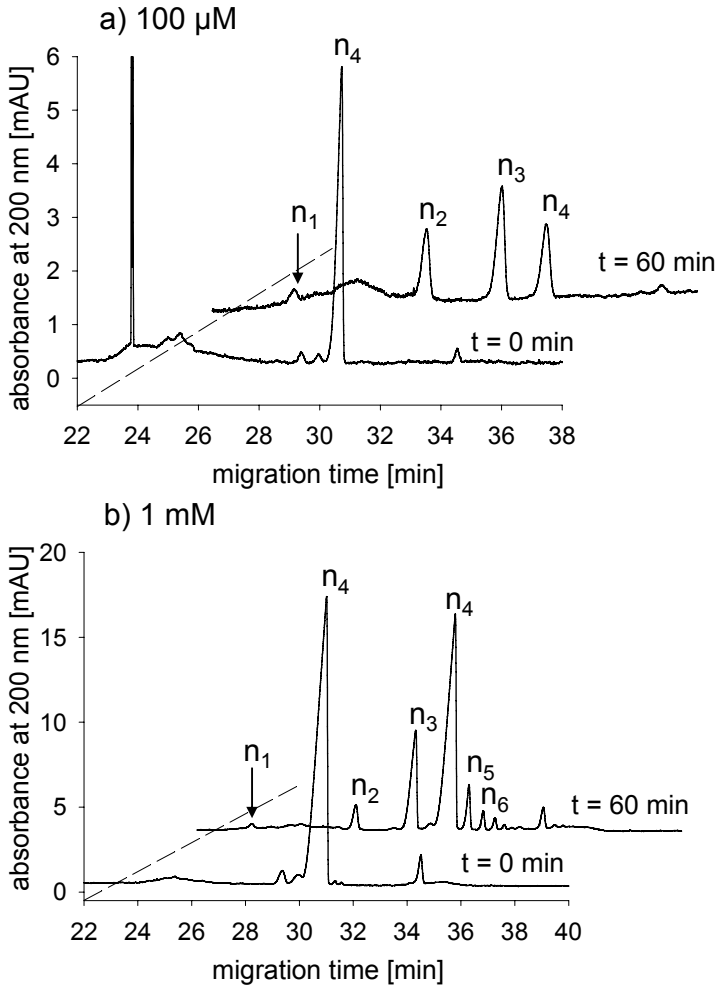


**Fig. 8.18** CZE analysis of the incubation of 100 µM (a) and 1 mM (b) of HA octasaccharide ($n_4$) with Hyal-1 (100 IE/mL measured by the Morgan-Elson assay at pH 3.5) at pH 3.5. Samples were incubated for 0 and 60 min, respectively.

At low substrate concentrations the reactions catalyzed by Hyal-1 seem to be restricted to hydrolysis of the octasaccharide ($n_4$):

$$n_4 \rightarrow n_1 + n_3 \qquad \text{Eq. 8.11}$$

$$n_4 \rightarrow 2\ n_2 \qquad \text{Eq. 8.12}$$

When the substrate concentration increased above ca. 500 µM transglycosylation reactions occurred at a higher frequency than at low substrate concentrations, enabling the production of HA fragments larger than the substrate:

$$2\ n_4 \rightarrow n_3 + n_5 \qquad \text{Eq. 8.13}$$

$$2\ n_4 \rightarrow n_2 + n_6 \qquad \text{Eq. 8.14}$$

Other transglycosylation reactions were omitted due to the occurrence of fragments other than $n_4$ in very low concentrations. Although substrate inhibition was observed at high substrate concentrations (> 1 mM) apparent $K_M$ and $v_{max}$ values were calculated (**Fig. 8.21.b** and **Tab. 8.3**), which were significantly increased compared to the values observed during degradation of the HA hexasaccharide ($n_3$) by BTH.

8.3.4.4. Time-dependent degradation of $n_3$ and $n_4$ by PH-20 at pH 4.5

Partially purified human PH-20, expressed by DS-2 cells (cf. Chapter 6), was analyzed for its degradation behavior in respect of low molecular weight HA oligosaccharides. Although BTH and PH-20 refer to the same hyaluronidase isozymes from different species, recombinant human PH-20 did not recognize the HA hexasaccharide as a substrate molecule. In accordance with the observations described for Hyal-1, increasing concentrations of HA hexasaccharide (25 µM – 2 mM) incubated for various time periods with PH-20 resulted in no conversion of the putative minimum substrate (**Fig. 8.21.a**).

Therefore, the HA octasaccharide ($n_4$) was offered as substrate and was found to be degraded very efficiently. Intriguingly, the conversion of HA octasaccharide ($n_4$) proceeded very quickly, with hexa- ($n_3$) and tetrasaccharides ($n_2$) forming the major final reaction products (**Fig. 8.19**, t = 60 min).

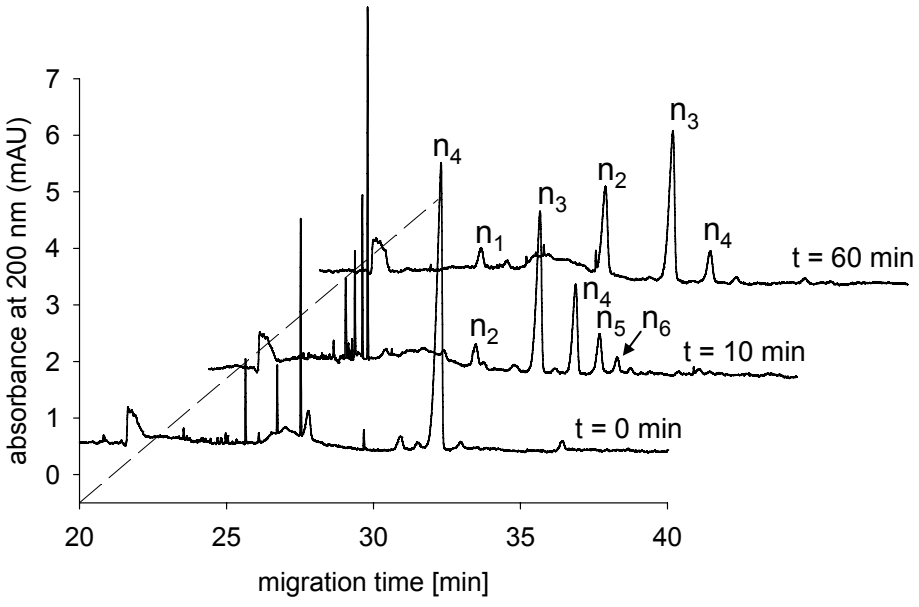


**Fig. 8.19** CZE analysis of the incubation of 100 µM of HA octasaccharide ($n_4$) with PH-20 (94 IE/mL determined by the Morgan-Elson assay at pH 4.5) at pH 4.5. Samples were incubated for 0, 10 and 60 min, respectively.

In the course of the degradation significant amounts of HA fragments larger than the octasaccharide ($n_4$) were formed, indicating the occurrence of transglycosylation reactions. Yet these deca- ($n_5$) and dodecasaccharides ($n_6$) were obviously preferred as substrate

molecules since they were hydrolyzed again during the incubation period (**Fig. 8.19**, t = 10 min and 60 min).

Thus, the reactions occurring during degradation of $n_4$ by PH-20 are generally identical to those catalyzed by Hyal-1, but with a much stronger influence of the transglycosylation reactions. The hydrolysis of $n_4$ (Eq. 8.11 and Eq. 8.12) seems to be of minor importance as concluded from the formation of low concentrations of $n_1$ and $n_2$ during the initial phase of degradation (**Fig. 8.19**, t = 10 min). Moreover, the transglycosylation reactions shown in Eq. 8.13 and Eq. 8.14 seem to account for the major decrease in the concentration of $n_4$, as the reaction products observed after 10 min of incubation were $n_3$ and $n_5$, and only to a minor extent $n_6$ and $n_2$. At elevated substrate concentrations (> 500 µM) higher molecular weight oligosaccharides (up to $n_8$) were detected, confirming the preference of transglycosylation reactions catalyzed by PH-20. The formation of HA disaccharide ($n_1$) was observed during the conversion process of the octasaccharide ($n_4$) only in very low concentrations as shown in **Fig. 8.19** or not at all.

Since no significant difference was observed between the kinetics of the degradation of high molecular weight HA catalyzed by PH-20 at pH 4.5 and pH 5.5, i.e. at the pH optima of the colorimetric and the turbidimetric hyaluronidase activity assays (8.3.2.3), the conversion of $n_4$ was merely observed at pH 4.5.

8.3.4.5. Calculation of kinetic parameters

The time-consumption curves of the hexasaccharide ($n_3$) and the octasaccharide ($n_4$) by the action of the hyaluronidases exhibited linear parts at the initial stage the reactions, referring to the steady-state conditions of the Michaelis-Menten kinetics. Quantification of the substrate was performed by CZE calibration curves (8.3.3.2). As an example, the degradation kinetics of the hexasaccharide ($n_3$) by BTH at pH 4.0 is shown in **Fig. 8.20**. The slope of the time-consumption curves represents the initial degradation velocity of the substrate molecule.

**Fig. 8.21** shows the initial reaction velocity at various substrate concentrations for BTH at pH 4.0 and 6.0, for Hyal-1 at pH 3.5 and for PH-20 at pH 4.5. Both, BTH and Hyal-1, were inhibited by the substrate at increasing concentrations: BTH was inhibited by $n_3$ concentrations above 200 µM at pH 4.0 and at pH 6.0 by $n_3$ concentrations above 800 µM, Hyal-1 was inhibited by $n_4$ concentrations above 1 mM. In contrast to the other hyaluronidases, PH-20 was not inhibited by the HA octasaccharide ($n_4$) at concentrations up to 2 mM reaching a maximum degradation velocity of 1.9 nmol/min.

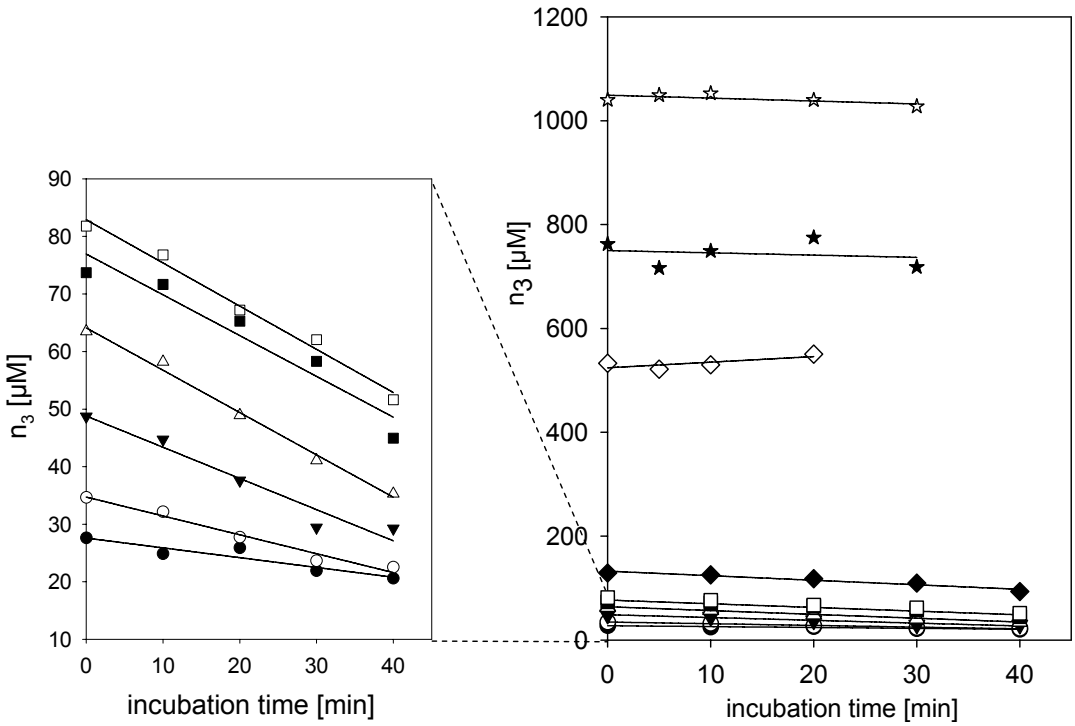


**Fig. 8.20** Linear part of the time-consumption curves of the digestion of increasing concentrations of $n_3$ with 60 IE/mL BTH at pH 4.0. $n_3$ concentrations were calculated from CZE peak area/time ratios using a calibration curve. The left graph shows a zoomed section of the $n_3$ concentration range 0 – 90 µM, the right graph shows the whole concentration range up to 1 mM $n_3$ as substrate.

Due to the occurrence of substrate inhibition at higher concentrations only the region not influenced by the inhibitory effects of the substrate was used for the calculation of apparent Michaelis-Menten kinetics (**Fig. 8.21.b**).

For BTH the apparent $K_M$ values determined at the acid and the pH optimum around neutral were very similar (100 – 150 µM), but the maximum velocity ($v_{max}$) differed by a factor of 4 (**Tab. 8.3**). The $K_M$ value of $n_4$ degradation by PH-20 was found to be very similar to the $K_M$ values of $n_3$ cleavage by BTH, though the maximum degradation velocity ($v_{max}$) of the minimum substrate of PH-20 outnumbered $v_{max}$ of BTH by a factor of 10 at acid pH conditions. The $v_{max}$ and $K_M$ values calculated for Hyal-1 were significantly increased compared to BTH.

Using the molecular mass of the main fraction of BTH (58 kDa) (Hoechstetter 2005) and a specific enzymatic activity of 50,000 IE/mg (according to the supplier) the turnover-number ($k_{cat}$) as well as the catalytic efficiency $k_{cat}/K_M$ could be calculated. For the calculation of $k_{cat}$ of Hyal-1 a molecular mass of 54 kDa and a specific enzymatic activity of 10 U/mg (100,000 IE/mg) were assumed (cf. Chapter 5). Since PH-20 was only partially purified (cf. Chapter 6) the catalytic efficiency $k_{cat}$ of PH-20 (56 kDa) was estimated using the specific enzymatic activity of BTH (50,000 IE/mg).

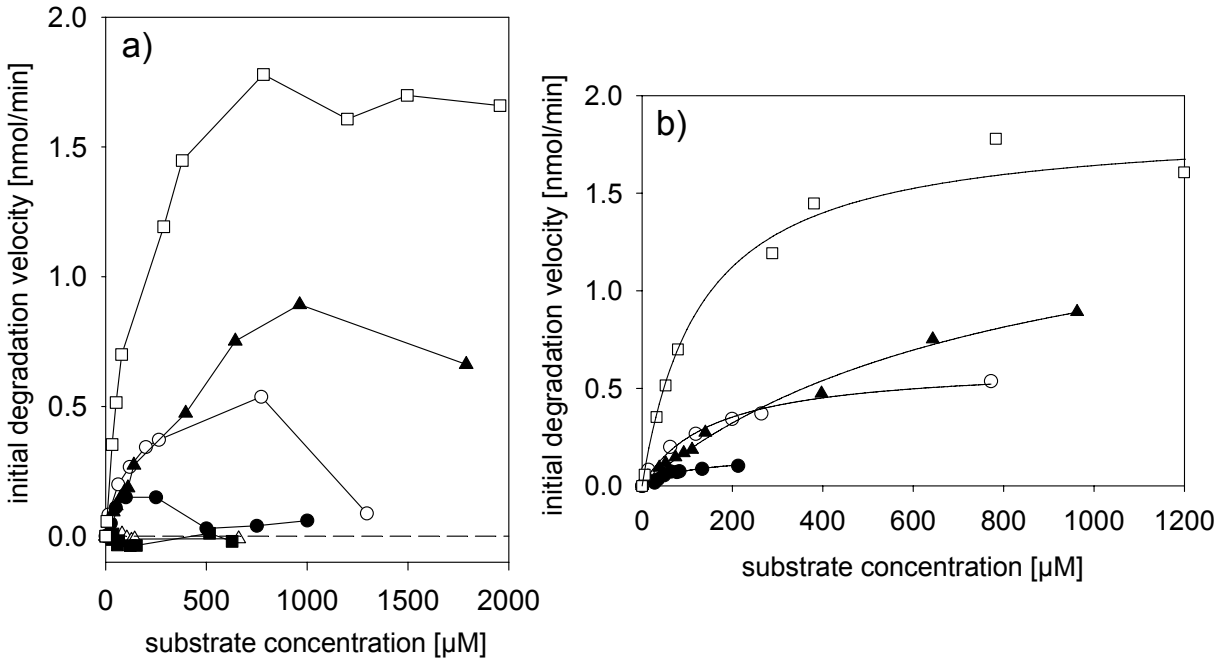


**Fig. 8.21** Initial degradation velocity plotted against the substrate concentration for the degradation of $n_3$ and $n_4$, respectively, by different hyaluronidases: degradation of $n_3$ by BTH at pH 4.0 (filled circles) and at pH 6.0 (open circles), degradation of $n_3$ (filled squares) and $n_4$ (open squares) by PH-20 at pH 4.5 and degradation of $n_3$ (open triangles) and $n_4$ (filled triangles) by Hyal-1 at pH 3.5. a) Complete curves showing the inhibition of the reaction velocity at higher substrate concentrations for BTH and Hyal-1. b) Calculation of apparent $K_M$ and $v_{max}$ values by curve fitting.

**Tab. 8.3** Comparison of apparent $K_M$, $v_{max}$, $k_{cat}$ and $k_{cat}/K_M$ values calculated from the time-dependent degradation of HA oligosaccharides by BTH, Hyal-1 and PH-20.

| Enzyme (pH) | Substrate | Apparent $K_M$ [µM] | Apparent $v_{max}$ [nmol/min] | $k_{cat}$ [$s^{-1}$] | $k_{cat}/K_M$ [$min^{-1}M^{-1}$] |
|---|---|---|---|---|---|
| BTH (4.0) | $n_3$ | 103 ± 33 | 0.16 ± 0.03 | 0.76 | $0.44 \cdot 10^6$ |
| BTH (6.0) | $n_3$ | 154 ± 24 | 0.63 ± 0.04 | 1.5 | $0.59 \cdot 10^6$ |
| PH-20 (4.5) | $n_3$ | - | - | - | - |
| PH-20 (4.5) | $n_4$ | 130 ± 18 | 1.9 ± 0.06 | 9.3 # | $4.3 \cdot 10^6$ # |
| Hyal-1 (3.5) | $n_3$ | - | - | - | - |
| Hyal-1 (3.5) | $n_4$ | 824 ± 150 | 1.6 ± 0.17 | 14.4 | $1.0 \cdot 10^6$ |

Obviously, PH-20 and Hyal-1 turn over their minimum substrate, $n_4$, about ten times faster than BTH turns over the hexasaccharide ($n_3$). The turnover-number ($k_{cat}$) can be considered as a rate constant for the velocity of substrate cleavage once it is bound to the enzyme, i.e. PH-

# values including an estimation of the specific enzymatic activity.

20 and Hyal-1 catalyze the cleavage of a bound octasaccharide ($n_4$) much faster than BTH catalyzes the cleavage of a bound hexasaccharide ($n_3$). Additionally, the catalytic efficiency $k_{cat}/K_M$ of Hyal-1 and PH-20 towards $n_4$ is increased compared to the catalytic efficiency of BTH towards $n_3$ indicating a faster binding of the substrate moiety to the binding pocket ($k_{cat}/K_M$).

## 8.4. Discussion

### *8.4.1. Degradation of high molecular weight HA*

The degradation of high molecular weight HA by different hyaluronidase isoenzymes was qualitatively characterized using a colorimetric assay for the detection of reducing GlcNAc ends and a CZE method for separation of the HA fragments. In the CZE high molecular weight HA ($n_{2500} - n_{5000}$, MW 1 – 2 Mio Da) migrated as a single, broad peak (Grimshaw et al. 1994, Grimshaw et al. 1996), but fragments consisting of less than 9 disaccharide units were detected as separate peaks.

When high molecular weight HA was degraded by BTH at pH 4.5, the formation of reducing GlcNAc ends decreased continuously with incubation time following double-exponential kinetics. In CZE a continuous decrease in the molecular weight of the substrate could be observed. At pH 5.5 the formation of GlcNAc residues followed a similar time course as observed at pH 4.5. However, as detected by CZE high molecular weight HA was only degraded partially to low molecular weight oligosaccharides with higher molecular weight HA fragments remaining in the incubation mixture.
Obviously, the velocity of GlcNAc formation slows down steadily indicating a faster hydrolysis of high molecular weight HA chains compared to low molecular weight HA. The fact that the formation of GlcNAc residues can not be described by a mono-exponential equation as in the case of Hyal-1 (cf. 8.3.2.4) is an indication of the existence of several factors influencing the degradation process, e.g. transglycosylation and changes in the affinity for high and low molecular weight HA fragments.
The simultaneous occurrence of higher molecular weight HA chains and HA oligosaccharides around neutral pH could be a consequence of an increased transglycosylation activity of the enzyme at higher pH (Gorham et al. 1975, Takagaki et al. 1994). The transfer of HA fragments comprising at least one disaccharide unit from one non-reducing HA chain end to another (Weissmann 1955, Highsmith et al. 1975) was mainly shown for low molecular

weight oligosaccharides (Highsmith et al. 1975, Takagaki et al. 1994, Saitoh et al. 1995) up to now. However, Bystricky et al. (Bystricky et al. 2002) described the formation of higher molecular weight HA chains as a result of transglycosylation under specialized conditions. A theoretical calculation of the HA fragments formed by hydrolysis and transglycosylation reactions showed an approximation to the fragment pattern observed by degradation of HA through the action of BTH at approximately neutral pH. However, these results must be considered as a mere hint, as several simplifications were necessary for the simulation.
In fact, the observed differences in the degradation products of hyaluronan produced at acidic and at neutral pH provide an explanation for the shift in the pH optima in the turbidimetric and in the colorimetric assay. While the number of GlcNAc residues produced during the incubation period is larger at pH 4.5 than at pH 5.5, the amount of fragments falling below the detection limit (< 8 kDa) of the turbidimetric assay is larger around neutral pH. As only fragments of sizes > 8 kDa, i.e. comprising more than 20 disaccharide units, are detected in the turbidimetric assay, most fragments separated by CZE fall below the level of detection. Apparently, the high molecular weight HA is degraded faster to a size of < 8 kDa at nearly neutral pH than at acid pH, thus resulting in a pH optimum of pH 6.0 in the turbidimetric assay.

The situation observed during degradation of high molecular weight HA by recombinant, human PH-20 was similar to BTH, but with the difference between the two pH optima at pH 4.5 and pH 5.5 being much less pronounced. Thus, the shift in the pH optima measured in the two hyaluronidase activity assays (cf. Chapter 6) can be explained by the same principle as described for BTH. However, the existence of different enzymatically active isoforms in BTH preparations (Oettl et al. 2003) seems to facilitate the pH dependent changes in the degradation mechanism of HA.
Though all results were obtained by *in vitro* experiments, it can be speculated if the specific pattern of hyaluronan fragments observed at pH 5.5 might be of any biological importance. Intriguingly, pH values > 5.3 were found during mammalian fertilization in the environment of the sperm before and after the acrosome reaction (Nakanishi et al. 2001). Possibly, the sperm hyaluronidase generates a pathway through the cumulus extracellular matrix of the oocyte by degradation of high molecular weight HA chains without complete destruction of the HA network, i.e. with higher molecular weight HA chains remaining as observed *in vitro*.

The situation observed with Hyal-1 was much simpler than in the case of the PH-20 isoenzymes: the time-dependent liberation of reducing GlcNAc ends during the degradation of high molecular weight HA could be described by a first-order reaction. The size of the produced HA fragments decreased sequentially until HA di- ($n_1$) to hexasaccharides ($n_3$) accumulated as the final products. The observed degradation kinetics might thus be explained by cleavage of the HA chains in a random fashion without any preferences for high or low molecular weight HA.

Although the HA fragment pattern produced by Hyal-1 showed no residual higher molecular weight HA and roughly resembled the situation calculated by sole random hydrolysis of an HA chain, the occurrence of transglycosylation in addition to hydrolysis can not be excluded.

### *8.4.2. Degradation of HA oligosaccharides*

Much more specific insight into the catalytic mechanism of BTH, Hyal-1 and PH-20 was gained from the quantitative analysis of the time-dependent conversion of defined pure HA oligosaccharides.

BTH converted its well-known minimum substrate, the HA hexasaccharide ($n_3$), mainly by hydrolysis at acidic pH (pH 4.0). Around neutral pH the preferential formation of fragments larger than the substrate indicated a higher frequency of transglycosylation events. In contrast to the degradation at pH 4.0, no HA disaccharide ($n_1$) was detected as reaction product at pH 6.0. Thus, hydrolysis of the hexasaccharide ($n_3$) was excluded.

Due to the lack of crystal structures, information about the active site of mammalian hyaluronidases is only available from the x-ray structure of the mammalian-type BVH (Markovic-Housley et al. 2000). Based on experimental data of the reactions catalyzed by BTH, specific sites of binding and catalysis were postulated (Highsmith et al. 1975, Takagaki et al. 1994). The current view of the catalytic site of BTH comprises a E residue acting as an acid/base catalyst (cf. Chapter 1) and several binding sites (S) on both sides of the cleavage site, each occupied by one disaccharide unit of the HA chain. Highsmith et al. (Highsmith et al. 1975) proposed a site S2 – S1 – S1’ – S2’ – S3’ according to the terminology of Schechter and Berger (Schechter and Berger 1966) with the reducing terminus of the sugar chain located on the right hand side, and the cleavage occurring between S1 and S1’. Based on the observation, that at pH 5.0 HA tetrasaccharides ($n_2$) are insufficient substrate molecules for BTH, hexasaccharides ($n_3$) are the minimum substrate moieties and octasaccharides ($n_4$) are

better substrates than hexasaccharides differential affinities of the disaccharide binding sites were proposed: weak binding affinity of the sites S1 and S1', high affinity of S2' in contrast to a very weak binding affinity of S2 and an important, but not essential binding affinity of S3' (Highsmith et al. 1975) (**Fig. 8.22**).

Binding of $n_3$ encompasses the sites S1 – S1' – S2' with $n_1$ leaving the site S1 and $n_2$ the sites S1'-S2' after hydrolysis at pH 4.0. At pH 6.0, however, $n_1$ does not, or only to a minor extent, leave the site S1, but remains bound until transglycosylation to another acceptor molecule like $n_3$ has occurred. Therefore, the increased transglycosylation activity around neutral pH might be explained by an increase in the affinity of the site S1 at pH 6.0 compared to pH 4.0.

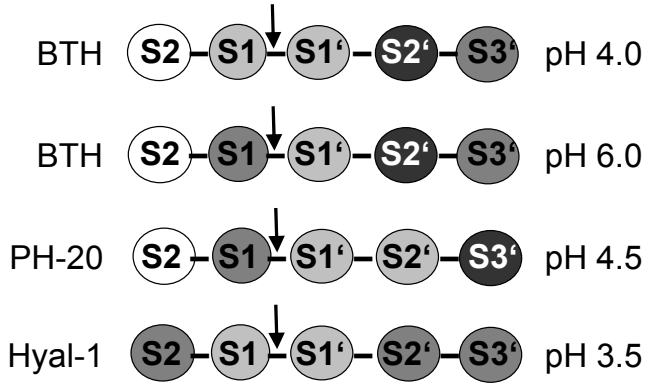


**Fig. 8.22** HA binding site model adapted from Highsmith et al. (Highsmith et al. 1975). Each subsite S binds one disaccharide unit, the cleavage site is marked by an arrow. The affinity of the subsites towards the substrate moieties as concluded from kinetic measurements are marked by the grey circles. An increase in affinity is represented by a darker shade of grey.

The degradation of HA oligosaccharides by BTH or ovine testicular hyaluronidase has often been observed before. However, the reaction products as well as the kinetic parameters determined differ significantly due to the use of various detection methods and buffer conditions. The formation of the HA disaccharide ($n_1$) as reaction product was reported by some authors (Weissmann 1955, Takagaki et al. 1994, Saitoh et al. 1995), while others could not detect any $n_1$ (Highsmith et al. 1975, Cramer et al. 1994, Kinoshita et al. 2001). As all the results were obtained in buffer systems at pH 5.0 – 5.3 other factors such as the nature of the buffering ions as well as the overall salt concentrations seem to influence the degradation behavior of BTH (Saitoh et al. 1995, Asteriou et al. 2006).

Asteriou et al. (Asteriou et al. 2006) described substrate inhibition for the degradation of high molecular weight HA at low ionic strengths, but no substrate inhibition was described up to now for the degradation of low molecular weight HA oligosaccharides (Gorham et al. 1975, Highsmith et al. 1975, Cramer et al. 1994). The recording of CZE kinetics at higher salt concentrations (> 0.1 M) had to be abandoned due to interferences with the CZE method at increased salt concentrations.

The recombinant human enzymes PH-20 and Hyal-1 exhibited a completely different catalytic behavior than BTH with respect to HA oligosaccharides as substrates. Both enzymes were not able to catalyze any conversion or degradation of the supposed minimum substrate, the HA hexasaccharide ($n_3$). Although experimental evidence for the identity of the minimum substrate of human hyaluronidases was missing, the HA hexasaccharide ($n_3$) was generally believed to be the smallest substrate moiety for all mammalian-type hyaluronidases (Stern and Jedrzejas 2006). However, the HA octasaccharide ($n_4$) could be proven to be the minimum substrate for both, recombinant, human PH-20 and Hyal-1.
In terms of the substrate binding site model the hexasaccharide, occupying the sites S1 – S1' – S2', seems to exhibit insufficient affinity towards the binding site of PH-20 and Hyal-1. Thus, the affinity of the subsite S2', which provides the essential affinity for binding of the hexasaccharide to BTH (Highsmith et al. 1975), is significantly decreased in PH-20 and Hyal-1 (**Fig. 8.22**).

The conversion of the octasaccharide by PH-20 can be explained by assuming a shift of the essential binding site from position S2' to position S3' (**Fig. 8.22**). The site S1 seems to exhibit considerable affinity since transglycosylation reactions were preferentially catalyzed by PH-20 (cf. BTH at pH 6.0). However, the model can not provide a satisfactory explanation for the formation of $n_2$ and $n_3$ as the major reaction products, but $n_1$ in extremely low concentrations. Presumably, the enzyme catalyzed mainly the transglycosylation reaction shown in Eq. 8.13 as concluded from the occurrence of the decasaccharide ($n_5$) as the main transglycosylation product. The fast degradation of the decasaccharide in the course of time indicated a preferential hydrolysis of $n_5$, which could provide the major reaction products $n_2$ and $n_3$.

The following binding site model is proposed to explain the reactions catalyzed by Hyal-1: the octasaccharide ($n_4$) was degraded to di-, tetra- and hexasaccharides, thus suggesting the binding of the octasaccharide in two different position, one covering the sites S2 – S1 – S1' – S2' (Eq. 8.12) and the other one covering the sites S1 – S1' – S2' – S3' (Eq. 8.11). Assuming that the affinity of the hexasaccharide is insufficient for binding (cf. 8.3.4.3), the binding affinity of the octasaccharide might be dependent on the occupation of at least two binding sites with medium affinity, i.e. two of the sites S2, S2' and S3' (**Fig. 8.22**).
Hyal-1 is able to catalyze transglycosylation of the HA octasaccharide ($n_4$), albeit only in the presence of high substrate concentrations ($n_4$ > 500 μM). In contrast to Hyal-1 the

transglycosylation activity of BTH was pH dependent without any significant effect of the substrate concentration.

An explanation for the concentration-dependent changes in the catalytic process might be provided by the affinity of the disaccharide unit occupying the subsite S1 (and S2). For transglycosylation at least the site S1 has to stay occupied while the product on the other side of the cleavage site leaves the site S1' – S2' – S3' and a new acceptor molecule is bound. Thus, if the rate constant for the release of the disaccharide unit in position S1 ($k_{off}$) is in the same time range as the diffusion-controlled encounter and binding of enzyme and acceptor molecule, the occurrence of concentration-dependent transglycosylation events might be explained as follows: at low substrate concentrations (< 500 µM) the position S1 releases the disaccharide unit before a new acceptor molecule is bound; at high substrate concentrations (> 500 µM), however, the probability for the encounter and binding of another acceptor molecule within the time-range of $k_{off}$ is increased, resulting in transglycosylation.

Interestingly, the maximum concentration of HA fragments, i.e. disaccharide units, present in the incubation mixture* during observation of the degradation of high molecular weight HA by Hyal-1 (8.3.2.4) was in the low concentration range (139 µM). Provided that the results observed with the HA oligosaccharide can be transferred to the catabolism of high molecular weight HA, the occurrence of transglycosylation events during the degradation of HA observed in the Morgan-Elson assay and in the CZE can be excluded. This hypothesis is supported by the kinetics of the GlcNAc formation through the action of Hyal-1 as described previously.

If the concentration-dependent shift from mere hydrolysis to higher transglycosylation activity has any biological importance in the catabolism of hyaluronan is questionable. The main function of Hyal-1 seems to be the hydrolysis of high molecular weight hyaluronan to low molecular weight oligosaccharides at acid pH values.

The analysis of the degradation of high molecular weight HA as well as of HA oligosaccharides provided new insights into the catalytic mechanism of different hyaluronidase isozymes within the family of mammalian hyaluronan hydrolases. The differences between the hyaluronidase isoenzymes were much more pronounced than

* concentration of disaccharide units = 55 µg/mL (concentration of high molecular weight HA)/397 g/mol (molecular weight of one disaccharide unit) = 139 µM.

expected. Obviously, the different hyaluronidase isozymes have evolved into very specialized enzymes with respect to their mechanism of HA degradation.

## 8.5. References


Afify A., Stern M., Guntenhoner M., Stern R. (1993). Purification and characterization of human serum hyaluronidase. *Arch. Biochem. Biophys.* **305**: 434-441.

Asteriou T., Vincent J.-C., Tranchepain F., Deschrevel B. (2006). Inhibition of hyaluronan hydrolysis catalysed by hyaluronidase at high substrate concentration and low ionic strength. *Matrix Biol.* **25**: 166-174.

Bystricky P., Machova E., Kolarova N. (2002). Effect of Gluco-Monosaccharides and Different Conditions on Digestion of Hyaluronan by Testicular Hyaluronidase. *Gen. Physiol. Biophys.* **21**: 463-469.

Cramer J.A., Bailey L.C., Bailey C.A., Miller R.T. (1994). Kinetic and mechanistic studies with bovine testicular hyaluronidase. *Biochim. Biophys. Acta* **1200**: 315-321.

Frost G.I., Csoka T.B., Wong T., Stern R. (1997). Purification, Cloning, and Expression of Human Plasma Hyaluronidase. *Biochem. Biophys. Res. Commun.* **236**: 10-15.

Gmachl M., Sagan S., Ketter S., Kreil G. (1993). The human sperm protein PH-20 has hyaluronidase activity. *FEBS Lett.* **336**: 545-548.

Gold E.W. (1982). Purification and properties of hyaluronidase from human liver. *Biochem. J.* **205**: 69-74.

Gorham S.D., Olavesen A.H., Dodgson K.S. (1975). Effect of ionic strength and pH on the properties of purified bovine testicular hyaluronidase. *Conn. Tissue Res.* **3**: 17-25.

Grimshaw J., Kane A., Trocha-Grimshaw J., Douglas A., Chakravarthy U., D. A. (1994). Quantitative analysis of hyaluronan in vitreous humor using capillary electrophoresis. *Electrophoresis* **15**: 936-940.

Grimshaw J., Trocha-Grimshaw J., Fisher W., Rice A., Smith S., Spedding P., Duffy J., Mollan R. (1996). Quantitative analysis of hyaluronan in human synovial fluid using capillary electrophoresis. *Electrophoresis* **17**: 396-400.

Hayase S., Oda Y., Honda S., Kakehi K. (1997). High-performance capillary electrophoresis of hyaluronic acid: determination of its amount and molecular mass. *J. Chromatogr. A* **768**: 295-305.

Highsmith S., Garvin J.H., Jr, Chipman D.M. (1975). Mechanism of action of bovine testicular hyaluronidase. Mapping of the active site. *J. Biol. Chem.* **250**: 7473-7480.

Hoechstetter J. (2005). Characterisation of bovine testicular hyaluronidase and a hyaluronate lyase from Streptococcus agalactiae. *Doctoral thesis*. University of Regensburg. http://www.opus-bayern.de/uni-regensburg/volltexte/2005/519/

Hoechstetter J., Oettl M., Asen I., Molz R., Bernhardt G., Buschauer A. (2001). Discrepancies in apparent enzymatic activity of bovine testicular hyaluronidase depend on the type of assay. *Arch. Pharm. Med. Chem.* **334**: 37.

Holmbeck S., Lerner L. (1993). Separation of hyaluronan oligosaccharides by the use of anion-exchange HPLC. *Carbohydr. Res.* **239**: 239-244.

Kakehi K., Kinoshita M., Hayase S., Oda Y. (1999). Capillary electrophoresis of N-acetylneuraminic acid polymers and hyaluronic acid: correlation between migration order reversal and biological functions. *Anal. Chem.* **71**: 1592-1596.

Kinoshita M., Okino A., Oda Y., Kakehi K. (2001). Anomalous migration of hyaluronic acid oligomers in capillary electrophoresis: correlation to susceptibility to hyaluronidase. *Electrophoresis* **22**: 3458-3465.

Mahoney D.J., Aplin R.T., Calabro A., Hascall V.C., Day A.J. (2001). Novel methods for the preparation and characterization of hyaluronan oligosaccharides of defined length. *Glycobiology* **11**: 1025-1033.

Mao W., Thanawiroon C., Linhardt R.J. (2002). Capillary electrophoresis for the analysis of glycosaminoglycans and glycosaminoglycan-derived oligosaccharides. *Biomed. Chromatogr.* **16**: 77-94.

Markovic-Housley Z., Miglinerini G., Soldatova L., Rizkallah P., Müller U., Schirmer T. (2000). Crystal Structure of Hyaluronidase, a Major Allergen of Bee Venom. *Structure* **8**: 1025-1035.

McIlvaine T.C. (1921). A buffer solution for colorimetric comparison. *J. Biol. Chem.* **49**: 183-186.

Nakanishi T., Ikawa M., Yamada S., Toshimori K., Okabe M. (2001). Alkalinization of Acrosome Measured by GFP as a pH Indicator and Its Relation to Sperm Capacitation. *Develop. Biol.* **237**: 222-231.

Oettl M. (2000). Biochemische Charakterisierung boviner testikulärer Hyaluronidase und Untersuchungen zum Einfluß von Hyaluronidase auf das Wachstum von Tumoren. *Doctoral thesis*. University of Regensburg.

Oettl M., Hoechstetter J., Asen I., Bernhardt G., Buschauer A. (2003). Comparative characterization of bovine testicular hyaluronidase and a hyaluronate lyase from Streptococcus agalactiae in pharmaceutical preparations. *Eur. J. Pharm. Sci.* **18**: 267-277.

Pattanaargson S., Roboz J. (1996). Determination of hyaluronidase activity in venoms using capillary electrophoresis. *Toxicon* **34**: 1107-1117.

Payan E., Presle N., Lapicque F., Jouzeau J.Y., Bordji K., Oerther S., Miralles G., Mainard D., Netter P. (1998). Separation and quantification by ion-association capillary zone electrophoresis of unsaturated disaccharide units of chondroitin sulfates and oligosaccharides derived from hyaluronan. *Anal. Chem.* **70**: 4780-4786.

Sabeur K., Cherr G.N., Yudin A.I., Primakoff P., Li M.W., Overstreet J.W. (1997). The PH-20 protein in human spermatozoa. *J. Androl.* **18**: 151-158.

Saitoh H., Takagaki K., Majima M., Nakamura T., Matsuki A., Kasai M., Narita H., Endo M. (1995). Enzymic Reconstruction of Glycosaminoglycan Oligosaccharide Chains Using the Transglycosylation Reaction of Bovine Testicular Hyaluronidase. *J. Biol. Chem.* **270**: 3741-3747.

Schechter I., Berger A. (1966). The hydrolysis of diastereoisomers of alanine peptides by carboxypeptidase A and leucine aminopeptidase. *Biochemistry* **5**: 3371-3375.

Stern R., Jedrzejas M.J. (2006). Hyaluronidases: Their Genomics, Structures, and Mechanism of Action. *Chem. Rev.* **106**: 818-839.

Takagaki K., Nakamura T., Izumi J., Saito H., Endo M. (1994). Characterization of hydrolysis and transglycosylation by testicular hyaluronidase using ion-spray mass spectrometry. *Biochemistry* **33**: 6503-6507.

Tawada A., Masa T., Oonuki Y., Watanabe A., Matsuzaki Y., Asari A. (2002). Large-scale preparation, purification, and characterization of hyaluronan oligosaccharides from 4-mers to 52-mers. *Glycobiology* **12**: 421-426.

Vercruysse K.P., Lauwers A.R., Demeester J.M. (1995). Kinetic investigation of the action of hyaluronidase on hyaluronan using the Morgan-Elson and neocuproine assays. *Biochem. J.* **310**: 55-59.

Vincent J.-C., Asteriou T., Deschrevel B. (2003). Kinetics of hyaluronan hydrolysis catalysed by hyaluronidase. Determination of initial reaction rate and kinetic parameters. *J. Biol. Phys. Chem.* **3**: 35-44.

Weissmann B. (1955). The transglycosylative action of testicular hyaluronidase. *J. Biol. Chem.* **216**: 783-794.

# Chapter 9

# Summary

Hyaluronidases and their substrate, hyaluronic acid, are known to play a role in signal transduction events directly correlated with tumor growth and cell migration. Yet correlations with disease progression are controversial due to scarce information on enzymatic properties and the lack of specific inhibitors as pharmacological tools. Therefore, the aim of this thesis was the establishment of recombinant expression systems for the human hyaluronidase subtypes, purification of the enzymes and their characterization with respect to biochemical and catalytic properties.

In a first approach the human hyaluronidase subtypes PH-20, Hyal-1, Hyal-2 and Hyal-4 were efficiently expressed in *E. coli*. All human hyaluronidases formed inclusion bodies in the cytoplasm of *E. coli* due to the presence of disulfide bridges in the native proteins. Only Hyal-1 could be re-folded *in vitro* into an enzymatically active protein with the folding yields strongly depending on the kind of denaturing agent used, the disulfide shuffling system and the presence of arginine in the folding buffer. However, both the yield of active protein and the specific enzymatic activity of Hyal-1, purified by Ni-IMAC under denaturing conditions, were extremely low.

As *in vitro* folding of the human hyaluronidases posed major problems, the human hyaluronidases Hyal-1, PH-20 and Hyal-2 were alternatively expressed into the culture medium of *Drosophila* Schneider-2 cells (DS-2 cells) enabling the correct formation of disulfide bonds and mammalian-like glycosylation.

Native Hyal-1 was expressed by DS-2 cells and purified by ammonium sulfate precipitation, cation exchange chromatography and Ni-IMAC. During purification the use of detergents was

required because of the extraordinarily high adsorbance of the protein to surfaces. Highly pure, homogeneous Hyal-1 (54 kDa with 4 kDa comprising glycosidic residues) with a specific enzymatic activity comparable to human plasma hyaluronidase was isolated in quantities sufficient for biophysical characterization studies. Although characteristic features such as the pH profile showed a similar catalytic behavior of Hyal-1, expressed in the prokaryotic and the eukaryotic system, the glycosylation of Hyal-1 was shown to improve the catalytic efficiency of the enzyme in solution. A truncation of Hyal-1 by the C-terminal domain failed to yield enzymatically active protein in both expression systems.

Human PH-20 (56 kDa) was stably expressed by DS-2 cells and purified by chelating-IMAC. As determined previously for bovine testicular hyaluronidase (BTH), a commercially available hyaluronidase preparation, human PH-20 exhibited the typical assay-dependent shift in the pH activity optimum. Furthermore, recombinant Hyal-1 and PH-20 recognized chondroitin sulfate A and C as alternative substrates with pH-dependent activities similar to the preferred substrate, hyaluronic acid.

In contrast to PH-20 and Hyal-1, no catalytic activity was detected with recombinant human Hyal-2 (54 kDa), expressed by DS-2 cells. Since the hydrolytic activity of human Hyal-2 is discussed controversially in the literature, a variety of hyaluronidase activity assays, including electrophoretic and viscosimetric techniques, was explored. However, none of the methods proved any hyaluronidase or chondroitinase activity of recombinant Hyal-2 under acid, neutral or basic pH conditions.

To gain more detailed insight into the catalytic mechanism of the recombinant human hyaluronidases Hyal-1 and PH-20 in comparison to BTH a capillary zone electrophoresis method was established for the qualitative and quantitative detection of degradation products of hyaluronic acid. BTH and, less significantly, recombinant human PH-20 produced different degradation products of hyaluronic acid at acidic and nearly neutral pH, explaining the assay-dependent shift of the pH activity profiles. Human Hyal-1 was found to degrade high molecular weight hyaluronic acid consecutively into di- to hexasaccharides as final products.
The quantitative analysis of the conversion of hyaluronan hexa- and octasaccharides revealed specific properties of the hyaluronidase subtypes: the minimum substrate of BTH, the hexasaccharide, was not accepted as a substrate by Hyal-1 and PH-20, albeit the octasaccharide; transglycosylation, which was catalyzed to a significant extent by BTH and

PH-20, occurred with Hyal-1 only in the presence of a great excess of substrate. The calculation of enzymatic parameters by Michaelis-Menten kinetics revealed additional features of the hyaluronidase subtypes. A model of an array of disaccharide unit binding sites framing the active site was employed to explain the pH- and subtype-specific properties of the hyaluronidases.

Taken together, the recombinant production of human hyaluronidases provides the basis for enzymological studies, crystallization and the structure-based development of specific inhibitors, which can be used, for example, as pharmacological tools.

# Chapter 10

# Appendix

## Appendix 1: Hyaluronidase cDNA sequences

Bases printed in **bold and underlined** designate mutations in the sequences compared to the reference sequences.

**Hyal-1: RZPD clone I.D. IRAKp961O1779Q2**

Reference sequence: BC035695

```
   1 ggtgcagctg gggtggaatc tggccaggcc ctgcttaggc ccccatcctg gggtcaggaa
  61 atttggagga taaggccctt cagccccaag gttgtcctcg accagtcccg tgccatggca
 121 gcccacctgc ttcccatctg cgccctcttc ctgaccttac tcgatatggc ccaaggcttt
 181 aggggccccc tgctacccaa ccggcccttc accaccgtct ggaatgcaaa cacccagtgg
 241 tgcctggaga ggcacggtgt ggacgtggat gtcagtgtct tcgatgtggt agccaaccca
 301 gggcagacct tccgcggccc tgacatgaca attttctata gctcccagct gggcacctac
 361 ccctactaca cgcccactgg ggagcctgtg tttggtggtc tgccccagaa tgccagcctg
 421 attgcccacc tggcccgcac attccaggac atcctggctg ccatacctgc tcctgacttc
 481 tcagggctgg cagtcatcga ctgggaggca tggcgcccac gctgggcctt caactgggac
 541 accaaggaca tttaccggca gcgctcacgg gcactggtac aggcacagca ccctgattgg
 601 ccagctcctc aggtggaggc agtagcccag gaccagttcc agggagctgc acgggcctgg
 661 atggcaggca ccctccagct ggggcgggca ctgcgtcctc gcggcctctg gggcttctat
 721 ggcttccctg actgctacaa ctatgacttt ctaagcccca actacaccgg ccagtgccca
 781 tcaggcatcc gtgcccaaaa tgaccagcta gggtggctgt ggggccagag ccgtgccctc
 841 tatcccagca tctacatgcc cgcagtgctg gagggcacag ggaagtcaca gatgtatgtg
 901 caacaccgtg tggccgaggc attccgtgtg gctgtggctg ctggtgaccc caatctgccg
 961 gtgctgccct atgtccagat cttctatgac acgacaaacc actttctgcc cctggatgag
1021 ctggagcaca gcctgggggа gagtgcggcc caggggggcag ctggagtggt gctctgggtg
1081 agctgggaaa atacaagaac caaggaatca tgtcaggcca tcaaggagta tatggacact
1141 acactggggc ccttcatcct gaacgtgacc agtggggccc ttctctgcag tcaagccctg
1201 tgctccggcc atggccgctg tgtccgccgc accagccacc ccaaagccct cctcctcctt
1261 aaccctgcca gtttctccat ccagctcacg cctggtggtg ggcccctgag cctgcggggt
1321 gccctctcac ttgaagatca ggcacagatg gctgtggagt tcaaatgtcg atgctaccct
1381 ggctggcagg caccgtggtg tgagcggaag agcatgtggt gattggccac acactgagtt
1441 gcacatattg agaacctaat gcactctggg tctggccagg gcttcctcaa atacatgcac
1501 agtcatacaa gtcatggtca cagtaaagag tacactcagc cactgtcaca ggcatattcc
1561 ctgcacacac atgcatactt acagactgga atagtggcat aaggagttag aaccacagca
1621 gacaccattc attccatgtc catatgcatc tacttggcaa ggtcatagac aattcctcca
1681 gagacactga gccagtcttt gaactgcagc aatcacaaag gctgacattc actgagtgcc
1741 tactctttgc caatccccgt gctaagcgtt ttatgtggac ttattcattc ctcacaatga
1801 ggctatgagg aaactgagtc actcacattg agagtaagca cgttgcccaa ggttgcacag
1861 caagaaaagg gagaagttga gattcaaacc caggctgtct agctccgggg gtacagccct
1921 tgcactccta ctgagtttgt ggtaaccagc cctgcacgac ccctgaatTt gTtgagaggc
```

```
1981 accagtccag caaataaagc agtcatgatt tacttaaaaa aaaaaaaaaa aaaaaaaaaa
2041 aaaaaaaaaa aaaaaaa
```

**Hyal-4: RZPD clone I.D. IMAGp958H01139Q2**

Reference sequence: NM_012269

The 5'-end of the sequence (crossed) is replaced in the RZPD clone by a short nucleotide sequence (ggcacgagg).

```
   1~~cgcccgggca ggtctttatt ttatttatgc tatctatttc ttttcctttt ttttttttt~~
  61~~tttttgagat gaagtcttac tctgttgccc aggctggagt gtagtggtgt gatctcggct~~
 121~~cgctgcagcc actgcctcct gggttcaggt gattctcctg acttagcctc ctgagtggct~~
 181~~gggactgcag gagcatgcca tcatgcccag ctgatttttg tatttttagt agagatgggg~~
 241~~tttcaccgtg ttggccagaa tggtttgcat tcctgacctc aagtgatctg cctgcctcag~~
 301~~cctcccaaaa tgttgggtac aggggtgagc caccgtgcct tgctattaat gccatctatt~~
 361~~tcactgaaga ttccgcctct catttcttga gtcatttttt ttaaatttcc ttaaattgga~~
 421~~cttcacattt tctgatgcct ccttgtttag cttaataact gaccttctga attcttttt~~
 481~~aggaaaatca ggaatttctt cttggtttgg agccattgct ggacatcctt tgccattcaa~~
 541~~cctctgattt gcacaaggtg actaaaggac cagcagcaaa caaaacgttt ggtcttctag~~
 601~~agtgcactaa agcagaagat acgtaacatt tttatcttac catgaaa~~gta ttatctgaag
 661 gacagttaaa gctttgtgtt gttcaaccag tacatctcac ttcatggctc cttatatttt
 721 ttattctaaa gtctatctct tgtctaaaac ctgctcgact tccaatttat caaaggaaac
 781 cttttatagc tgcttggaat gctccaacag atcagtgttt gataaaatat aatttaagac
 841 taaatttgaa aatgtttcct gtgattggaa gcccactggc caaggccagg gggcaaaatg
 901 tcactatatt ttatgtcaac agattgggat actatccgtg gtatacatca ca<u>**a**</u>ggggtcc
 961 ccattaatgg aggtctccca cagaacataa gtttacaagt acatctggaa aaagctgacc
1021 aagatattaa ttattacatc cctgctgaag atttcagtgg acttgctgtt atagattggg
1081 aatattgg<u>**c**</u>g accacagtgg gcccggaact ggaactcaaa agatgtttac agacagaagt
1141 caagaaagct tatttccgat atgggaaaga atgtatcagc taccgatatt gaatatttag
1201 ccaaagtgac ctttgaagaa agtgcaaaag ctttcatgaa ggaaaccatc aaattgggaa
1261 ttaagagccg acccaaaggc ctttggggtt attatttata tcctgattgc cacaattata
1321 acgtttatgc cccaaactac tctgggtcat gcccagaaga cgaagtcttg aggaacaatg
1381 agctctcttg gctctggaac agcagtgctg ctttatatcc ttctatctgt gtctggaaat
1441 cccttggaga cagtgaaaac attttgcgct tctccaaatt tcgggtgcat gaatccatga
1501 ggatctccac catgacatct catgattatg ctctgcctgt atttgtctac acaaggctag
1561 ggtacagaga tgaaccttta tttttccttt ctaagcaaga tctagtcagc accataggag
1621 aaagtgctgc cttgggagct gcaggcattg ttatttgggg agacatgaat ttaactgcat
1681 ccaaggccaa ctgtacaaag gtgaagcagt ttgtgagttc tgatttaggg agctacatag
1741 ccaatgtgac cagagctgct gaggtatgca gccttcacct ctgcaggaac aatggcaggt
1801 gcataaggaa gatgtggaac gcgcccagtt accttcactt gaaccctgca agttaccaca
1861 tagaggcctc tgaggacggg gagtttactg tgaaaggaaa agcatctgat acagacctgg
1921 cagtgatggc agatacattt tcctgtcatt gttatcaggg atatgaagga gctgattgca
1981 gagaaataaa gacggctgat ggctgctctg gggtttcccc ttctcctggt tcactaatga
2041 cactttgtct actgctttta gcaagttatc gaagcattca gttgtgagat aattgagttt
2101 aaagggaatt gtgtggcctc tagcctagtc atttaaagaa ggatgtaact tataacattt
2161 tttttctctt atgaattcta ttgagagata ttataagtag acattatgta tgtcacttaa
2221 cataaacaga aacattattt tatttgcctc cagtctggct aggaaaccag atctggggta
2281 aagtcaatgt acacttcctc cttattggaa tatttaagtt gcatttaaac taaaactagt
2341 ataatttagt cttttcatga atgtacatac ataaaattat acataaaaat attaaattat
2401 tcatttcaaa aaaa
```

## Appendix 2: Recombinant hyaluronidases expressed by DS-2 cells

Amino acid sequences were determined by translation of the DNA sequences, which had been confirmed by sequencing.

Underlined: BiP signal peptide (cleaved off during maturation of the protein)

**Bold**: V5 epitope

**Bold and underlined**: His-tag

### BiP/Hyal-1/L/V5/His

MKLCILLAVVAFVGLSLGRSPWPGFRGPLLPNRPFTTVWNANTQWCLERHGVDVDVSVFDVVANPGQT
FRGPDMTIFYSSQLGTYPYYTPTGEPVFGGLPQNASLIAHLARTFQDILAAIPAPDFSGLAVIDWEAW
RPRWAFNWDTKDIYRQRSRALVQAQHPDWPAPQVEAVAQDQFQGAARAWMAGTLQLGRALRPRGLWGF
YGFPDCYNYDFLSPNYTGQCPSGIRAQNDQLGWLWGQSRALYPSIYMPAVLEGTGKSQMYVQHRVAEA
FRVAVAAGDPNLPVLPYVQIFYDTTNHFLPLDELEHSLGESAAQGAAGVVLWVSWENTRTKESCQAIK
EYMDTTLGPFILNVTSGALLCSQALCSGHGRCVRRTSHPKALLLLNPASFSIQLTPGGGPLSLRGALS
LEDQAQMAVEFKCRCYPGWQAPWCERKSMWRPLESRGPFE**GKPIPNPLLGLDST**RTG**HHHHHH**

### BiP/Hyal-1/S/V5/His

MKLCILLAVVAFVGLSLGRSPWPGFRGPLLPNRPFTTVWNANTQWCLERHGVDVDVSVFDVVANPGQT
FRGPDMTIFYSSQLGTYPYYTPTGEPVFGGLPQNASLIAHLARTFQDILAAIPAPDFSGLAVIDWEAW
RPRWAFNWDTKDIYRQRSRALVQAQHPDWPAPQVEAVAQDQFQGAARAWMAGTLQLGRALRPRGLWGF
YGFPDCYNYDFLSPNYTGQCPSGIRAQNDQLGWLWGQSRALYPSIYMPAVLEGTGKSQMYVQHRVAEA
FRVAVAAGDPNLPVLPYVQIFYDTTNHFLPLDELEHSLGESAAQGAAGVVLWVSWENTRTKESCQAIK
EYMDTTLGPFILNVTSGALLGRPLESRGPFE**GKPIPNPLLGLDST**RTG**HHHHHH**

### BiP/PH-20/V5/His

MKLCILLAVVAFVGLSLGRSLNFRAPPVIPNVPFLWAWNAPSEFCLGKFDEPLDMSLFSFIGSPRINA
TGQGVTIFYVDRLGYYPYIDSITGVTVNGGIPQKISLQDHLDKAKKDITFYMPVDNLGMAVIDWEEWR
PTWARNWKPKDVYKNRSIELVQQQNVQLSLTEATEKAKQEFEKAGKDFLVETIKLGKLLRPNHLWGYY
LFPDCYNHHYKKPGYNGSCFNVEIKRNDDLSWLWNESTALYPSIYLNTQQSPVAATLYVRNRVREAIR
VSKIPDAKSPLPVFAYTRIVFTDQVLKFLSQDELVYTFGETVALGASGIVIWGTLSIMRSMKSCLLLD
NYMETILNPYIINVTLAAKMCSQVLCQEQGVCIRKNWNSSDYLHLNPDNFAIQLEKGGKFTVRGKPTL
EDLEQFSEKFYCSCYSTLSCKEKADVKDTDAVDVCIADGVCIDAFLKPPMETEEPQIFYNASPSTLSG
PFE**GKPIPNPLLGLDST**RTG**HHHHHH**

### BiP/Hyal-2/V5/His

MKLCILLAVVAFVGLSLGRSPWPGMELKPTAPPIFTGRPFVVAWDVPTQDCGPRLKVPLDLNAFDVQA
SPNEGFVNQNITIFYRDRLGLYPRFDSAGRSVHGGVPQNVSLWAHRKMLQKRVEHYIRTQESAGLAVI
DWEDWRPVWVRNWQDKDVYRRLSRQLVASRHPDWPPDRIVKQAQYEFEFAAQQFMLETLRYVKAVRPR
HLWGFYLFPDCYNHDYVQNWESYTGRCPDVEVARNDQLAWLWAESTALFPSVYLDETLASSRHGRNFV
SFRVQEALRVARTHHANHALPVYVFTRPTYSRRLTGLSEMDLISTIGESAALGAAGVILWGDAGYTTS
TETCQYLKDYLTRLLVPYVVNVSWATQYCSRAQCHGHGRCVRRNPSASTFLHLSTNSFRLVPGHAPGE
PQLRPVGELSWADIDHLQTHFRCQCYLGWSGEQCQWDHRQAAGGRPLESRGPFE**GKPIPNPLLGLDST**
RTG**HHHHHH**

## Appendix 3: Abbreviations

| | |
|---|---|
| aa | amino acid |
| Arg | L-arginine · HCl |
| BSA | bovine serum albumin |
| BTH | bovine testicular hyaluronidase |
| BVH | bee venom hyaluronidase |
| CD | circular dichroism |
| ChS | chondroitin sulfate |
| ChS A | chondroitin 4-sulfate |
| ChS B | dermatan sulfate |
| ChS C | chondroitin 6-sulfate |
| CIP | calf intestine alkaline phosphatase |
| CTAB | cetyltrimethylammonium bromide |
| CV | column volume |
| CZE | capillary zone electrophoresis |
| DAB | diaminobenzidine |
| DMSO | dimethylsulfoxide |
| DS-2 | *Drosophila* Schneider-2 |
| DTT | dithiothreitol |
| ECM | extracellular matrix |
| *E. coli* | *Escherichia coli* |
| EDTA | ethylene diamine tetraacetate |
| ER | endoplasmic reticulum |
| ESI-MS | electrospray ionisation mass spectrometry |
| GAG | glycosaminoglycane |
| GdmCl | guanidinium chloride |
| GlcNAc | N-acetyl-D-glucosamine |
| GlcUAc | D-glucuronic acid |
| GPI-anchor | glycosylphosphatidylinositol-anchor |
| GSH | reduced glutathione |
| GSSG | oxidized glutathione |
| HA | hyaluronic acid |
| HOAc | acetic acid |
| HRP | horseradish peroxidase |

| | |
|---|---|
| IAM | inner acrosomal membrane |
| IBs | inclusion bodies |
| IdoAc | idoronic acid |
| IMAC | ion metal affinity chromatography |
| IPTG | isopropylthiogalactoside |
| LB-medium | Luria-Bertani medium |
| MALDI-TOF MS | matrix assisted laser desorption ionization – time-of-flight mass spectrometry |
| MCS | multiple cloning site |
| MW | molecular weight |
| MWCO | molecular weight cut-off |
| NTA | nitrilotriacetic acid |
| $n_x$ | hyaluronic acid oligosaccharide containing x disaccharides units |
| OD | optical density |
| ORF | open reading frame |
| pI | isoelectric point |
| PAGE | polyacrylamide gel electrophoresis |
| PAS | periodic acid – Schiff |
| PBS | phosphate buffered saline |
| PFGE | pulsed field gel electrophoresis |
| PIPES | piperazine-1,4-bis(2-ethanesulfonic acid) |
| SDS | sodium dodecyl sulfate |
| SEC | size exclusion chromatography |
| SEM | standard error of means |
| TCA | trichloro acetic acid |
| Tris | tris(hydroxymethyl)aminomethane |
| UTR | untranslated region |

# Appendix 4: List of publications and poster presentations

Hofinger E.S.A., Spickenreither M., Oschmann J., Rudolph R., Bernhardt G., Buschauer A. (2007). Human hyaluronidase Hyal-1: insect cells versus *E. coli* as expression system and identification of low molecular weight inhibitors. *Glycobiology*, in press. [Epub ahead of print 2007, January 16]

Spickenreither M., Hofinger E.S.A., Bernhardt G., Dove S., and Buschauer A. (2007). Ascorbic Acid Derivatives with Increased Lipophilicity as Potent Inhibitors of Bacterial and Human Hyaluronidases.
Annual Meeting of the GDCh, Fachgruppe Medizinische Chemie, "Frontiers in Medicinal Chemistry", Berlin, Germany.

Hofinger E., Hoechstetter J., Bernhardt G., Buschauer A. (2006). Recombinant expression, purification and characterization of the human hyaluronidase PH-20.
XIX$^{th}$ International Symposium on Medicinal Chemistry, 2006, Istanbul, Turkey.
Abstract published in: *Drugs of the Future* **31**(Suppl. A): 126

Spickenreither, M., Hofinger, E., Bernhardt, G., Dove, S., Buschauer, A. (2006). L-ascorbic acid derivatives as inhibitors of bacterial and mammalian hyaluronidases.
XIX$^{th}$ International Symposium on Medicinal Chemistry, 2006, Istanbul, Turkey.
Abstract published in: *Drugs of the Future* **31**(Suppl. A):125-126

Hofinger E., Bernhardt G., Buschauer A. (2006) Recombinant expression, purification and characterization of the human hyaluronidase PH-20.
3$^{rd}$ Summer School Medicinal Chemistry, Regensburg, Germany.

Hofinger, E., Bernhardt, G., Oschmann, J., Rudolph, R., Buschauer, A. (2005). Expression of human hyaluronidase Hyal-1 in *E. coli* and Drosophila Schneider-2 cells.
Annual Meeting of the German Pharmaceutical Society (DPhG), Mainz, Germany.

Hofinger, E., Oschmann, J., Bernhardt, G., Rudolph, R., Buschauer, A. (2005). *In vitro* folding and characterization of human hyaluronidase Hyal-1 expressed in *E. coli.*
6$^{th}$ Carbohydrate Bioengineering Meeting, Barcelona, Spain.

Hofinger, E., Bernhardt, G., Parthier, C., Rudolph, R., Buschauer, A. (2004). Expression and *in vitro* folding of recombinant human hyaluronidase Hyal-1.
Annual Meeting of the German Pharmaceutical Society (DPhG), Regensburg, Germany.

Hofinger, E., Bernhardt, G., Parthier, C., Rudolph, R., Buschauer, A. (2004). *In vitro* folding of recombinant human hyaluronidase Hyal-1 expressed in *E. coli*.
2$^{nd}$ Summer School Medicinal Chemistry, Regensburg, Germany.